An investigation of initial retention of stem / progenitor cells following intracoronary injection: implications to cell therapy for the treatment of heart failure

Thesis submitted for the degree of:

Doctor of Philosophy

Niall Gordon Simon Campbell

Queen Mary, University of London

ABSTRACT

Intracoronary injection is a frequently used clinical protocol for stem / progenitor cell therapy to the heart. Initial donor cell retention in the heart is the key to the success of this approach; however, this process has been poorly investigated. I established an original model to quantitatively assess initial donor cell retention after intracoronary cell injection in rats using an ex-vivo heart perfusion system and investigated factors that could affect retention.

The initial retention efficiency of bone marrow mononuclear cells (BMMNC) was 20% after injection into normal hearts. The majority (>90%) of BMMNC loss into the coronary effluent occurred within the first minute of injection. Increased BMMNC dose increased absolute retention with a linear dose-effect relationship, while retention efficiency was unaltered. Retention efficiency increased to 30% in hearts with ischaemia-reperfusion, while flow cytometric studies showed that surface marker expression was unchanged between the pre-injection donor cell population and the population in the coronary effluent in both normal and ischemia-reperfused hearts. This suggests that active interactions between donor cells and coronary endothelium were not critical for donor cell retention using these experimental conditions. Instead, cell size assessment revealed that larger subpopulations of BMMNC were preferentially retained compared to smaller BMMNC in both normal and ischemia-reperfused hearts. Furthermore, a larger cell type, bone-marrow derived mesenchymal stem cells (MSC; median cell size=10.1 μm), had a markedly increased retention efficiency (80%) compared to BMMNC (median cell size=7.0 μm). A greater proportion of MSC with a larger diameter were retained compared to smaller diameter MSC; this enhanced retention plateaued with MSC ≥ 9 μm.

Immunohistochemical analysis using fluorescently labeled donor cells demonstrated that all BMMNC retained in normal and ischaemia-reperfusion hearts were located within the coronary vasculature, without extravasation, up to 60 minutes after injection. Heart

perfusion parameters and histological features exhibited evidence of coronary embolism after intracoronary injection of MSC, but not BMMNC (up to $40x10^6$).

These data collectively suggest that passive mechanical entrapment, and not active endothelial cell-donor cell interactions, is responsible for initial donor cell retention after intracoronary injection. This has important implications for future clinical protocols of intracoronary injection of stem / progenitor cells to the heart.

TABLE OF CONTENTS

List of figures

List of tables

Acknowledgements

This study was funded by a British Heart Foundation Clinical Research Training Fellowship Grant. The project would not have been possible without the wise and thoughtful counsel of Professor Ken Suzuki, my supervisor, Professor Anthony Mathur and Virginia, my wife.

Chapter 1 - INTRODUCTION

1.1. Importance of heart failure

The lifetime risk for developing heart failure is approximately 1 in 5 for a person aged 40 years[1] and most frequently occurs as a consequence of myocardial infarction (MI). Heart failure is associated with a high morbidity and accounts for 5% of all medical and geriatric hospital additions in patients over the age of 65 (a greater proportion than those hospitalized for acute MI [AMI])[2]. This places an enormous burden on health care services and society, accounting for 2% of all health-care spending in European and North American studies[3]. Despite enormous efforts by scientists and clinicians utilizing the available treatment options, heart failure remains the leading cause of death in the Western World[4] and 30-40% of patients die within 1 year of diagnosis[3].

A wide range of emerging therapies have been introduced with the aim of improving survival and quality of life in heart failure patients, including pharmaceutical agents[5], percutaneous coronary intervention[6], coronary artery bypass grafting[7], biventricular pacing[8], implantable cardioverter defibrillators[9] and the use of left ventricular assist devices[10]. None of these approaches, however, overcomes the irreversible loss of cardiomyocytes which fundamentally underpins the aetiology of heart failure following MI[11]. Cardiac transplantation is a more aggressive, radical treatment option which does address cardiomyocyte loss, although due to a shortage of donors, immunosuppression and financial cost, this is not feasible for widespread use[12]. Research attention more recently has been directed towards biological therapies as a potential avenue to explore. Transplantation of stem/progenitor cells is one of the most promising approaches.

1.2. Stem/progenitor cell transplantation for acute myocardial infarction and heart failure

1.2.1. Stem and progenitor cells

Stem cells are defined by their capacity for infinite self-renewal and also for the ability to differentiate into multiple cell types (pluripotency)[13-15]. Progenitor cells and precursor cells are more committed cells which have the ability to differentiate to a limited lineage. These cells are not "stem cells' according to the strict definition, but, in the field of stem cell therapy, these cells are frequently referred to as "stem cells".

"Stem cells" can be divided into two broad categories: pluripotent stem cells and adult stem cells. Currently available pluripotent stem cells for therapeutic purposes include embryonic stem cells (ESC) and induced pluripotent stem cells. Adult stem cells have been found in a number of different tissues in adults and are usually tissue-specific progenitor or precursor cells, the major types of which include mesenchymal stem cells (MSC), endothelial progenitor cells (EPC), haematopoietic stem cells, skeletal myoblasts and cardiac progenitor cells (CPC). The potential of these cell types to be used for cell transplantation is discussed in more detail in section 1.3.

1.2.2. Stem cell transplantation to the heart

In the last two decades, experimental research has demonstrated that injection of stem/progenitor cells is a promising new approach to treat AMI and heart failure[16] and has led to a number of clinical studies using this strategy.

Because of their utility as autografts, adult stem cells do not require immunosuppression after transplantation and are free from the risk of teratoma formation

and from the ethical issues associated with ESC. For these reasons, adult stem cells have been used preferentially in clinical trials, even though these cells have much more limited differentiation abilities than that of ESC. This thesis will focus on adult stem cells, which are currently more clinically relevant.

While early clinical trials of transplantation of adult stem/progenitor cells reported the feasibility, safety and possible therapeutic effectiveness of this innovative strategy[17], improvements in outcome measures[18-23] observed in more recent, large-scale, randomized, controlled studies were not as sizeable as expected. However, pooling of data in meta-analytical studies has shown that bone marrow mononuclear cell (BMMNC) injection is associated with statistical improvements in cardiac function and a tendency towards decreased event rates and improved mortality after AMI (without statistical significance)[24-27]. Overall, this approach is promising, but improvements in our understanding and a refinement of protocols by further laboratory investigation are needed for its future clinical success.

1.2.3. Mechanisms of stem/progenitor cell transplantation for heart disease

The detailed mechanisms underpinning the beneficial effects observed after adult stem/progenitor cell transplantation still need to be determined. Cell transplantation does not necessarily equal regeneration therapy, and it is now rather doubtful whether transdifferentiation and/or cell fusion of donor cells lead to new cardiomyocytes or to vascular cells which then contribute to improvements in cardiac function. In fact, many reports have shown that cardiomyogenic differentiation of adult stem cells is extremely limited following administration to the heart *in vivo*[28-30]. One proposed alternative mechanism is a paracrine effect, whereby growth factors, cytokines, chemokines, and other signalling molecules released from the transplanted cells lead to neovascular formation, fibrosis reduction, activation of endogenous CPC and an increase in viability and function of

host cardiomyocytes[31]. Such changes could have the potential to recover, restore and/or regenerate the damaged myocardium, leading to improvement of cardiac function. These mechanisms are likely to be cell-type dependent[32].

1.3. Types of adult stem cells for transplantation to the heart

Many types of adult stem/progenitor cells have been tested as donor for cell transplantation to the heart. Whether one cell type is superior for heart delivery has not been fully elucidated. It is noteworthy that both experimental and clinical studies have had differing protocols, with variations in donor cell numbers and cell types, injection routes, the time after MI that cells were administered, and outcome measures. Such heterogeneity and complexities make a direct comparison between cell types difficult. Previously and currently promising sources of adult stem/progenitor injection to the heart include skeletal myoblasts, BMMNC, EPC, MSC, and CPC[33,34].

1.3.1. Skeletal myoblasts

Skeletal myoblasts (satellite cells) are undifferentiated precursors for skeletal muscle and were the first cell type administered to heart failure patients[35]. For clinical use, these cells were obtained from skeletal muscle biopsies and propagated *ex vivo* before being administered to the heart[36]. They were initially thought to be an attractive candidate cell type for cell transplantation, based on their muscular (thus contractile) phenotype and their relative resistance to ischaemia[37]. After transplantation into the heart, they have been shown to form myotubes within the heart but are unable to transdifferentiate to cardiomyocytes[38]. Despite this observation, they still improve cardiac function in animal models, presumably

due to their paracrine effects. Subsequent initial clinical studies showed that skeletal myoblast injection was feasible and possibly improved cardiac function but led to an increase of incidence of critical ventricular arrhythmias[39,40]. Parallel research has demonstrated the inability of skeletal myoblasts to integrate electrically with host cardiomyocytes, which would increase arrhythmia risk[41].

The largest clinical study of skeletal myoblast transplantation reported to date is the Myoblast Autologous Grafting in Ischaemic Cardiomyopathy (MAGIC) Trial[42]. In this double-blinded study, patients with previous MI, poor left ventricular (LV) function and a requirement for coronary artery bypass grafting (CABG) were randomized to receive epicardial intramyocardial (IM) injection of autologous skeletal myoblasts (at a cell dose of 400 or 800×10^6) or placebo. All patients were required to undergo implantation of an implantable cardioverter defibrillator. After 6 months follow-up, no statistically significant benefit of myoblast transplantation over CABG alone was observed for measures of LV regional or global function. There was a higher incidence of arrhythmic events observed in the myoblast-treated patients, although there were no deaths attributable to arrhythmias. Since then, the focus of research attention regarding cell transplantation to the heart has been mostly directed at other cell types.

1.3.2. Bone marrow mononuclear cells (BMMNC)

Bone marrow-derived cells are currently the most frequent cell source used in clinical trials. In the majority of trials, these cells are used as unfractionated BMMNC. Their administration has been shown to be safe and feasible, although long-term follow-up data is lacking[18-23,43-46]. Bone marrow is a complex environment containing heterogeneous subpopulations of multipotent cells. BMMNC include haematopoietic stem cells (2%), EPC and MSC (<0.05%), all of which could be beneficial for cardiac repair or regeneration.

The main advantage of BMMNC in clinical use is that BMMNC fraction can be isolated relatively quickly from bone marrow aspirate without need for further *ex-vivo* purification, sorting or expansion. Cells can be injected directly after isolation (at the same day). Preclinical studies have suggested that BMMNC have superior survival 6 weeks after intramyocardial injection, compared with MSC, skeletal myoblasts and fibroblasts[47]. To date, several large-scale, randomized, controlled studies using BMMNC have reported significant therapeutic benefits, however, the degree of the improvement of cardiac function has not been as sizeable as previously anticipated (please refer to 1.5.2 and 1.5.3)[18-23].

BMMNC are a heterogeneous cell population and have been sub-classified by cluster of differentiation (CD) surface marker expression[48]. Some of these markers appear to be functionally important in leukocyte – endothelial cell interactions, and may therefore contribute to donor cell – coronary endothelium interactions after intracoronary (IC) injection into the heart (please refer to 1.8.2).

CD11b and CD18*:* Integrins are transmembrane proteins which mediate interactions between adhesion molecules and adjacent cells and/or the extracellular matrix. They are heterodimers consisting of two distinct alpha and beta subunits. CD11b, otherwise known as macrophage antigen-1 (MAC-1), complement receptor-3 or integrin alpha M is one chain of the $\alpha_M\beta_2$ integrin, the other being the common β_2 subunit, CD18. The $\alpha_M\beta_2$ integrin is expressed on monocytes, granulocytes, macrophages and natural killer cells[49]. The CD11b subunit is involved in the adhesion and spreading of cells, but cell migration also requires the presence of CD18. Its central role is the regulation of leukocyte adhesion and chemotaxis as well as phagocytosis and cell mediated cytotoxicity[49]. The role of $\alpha_M\beta_2$ is dependent on its ability to recognise intercellular adhesion molecule-1 (ICAM-1), fibrinogen and complements.[50]

CD29*:* Integrin alpha-4-beta-1 (very late antigen 4, VLA-4) is an integrin dimer composed of CD29 (beta) and CD49a (alpha). Vascular cell adhesion molecule-1 (VCAM-1) binds to

VLA-4 which is constitutively expressed on leukocyte plasma membranes (predominantly lymphocytes, monocytes and eosinophils[51]), but this adherence does not occur until the leukocytes are stimulated by chemotactic agents. Once this occurs, the integrins undergo the necessary conformational change to confer a high binding affinity. In mice, depletion of VLA-4 in adult haematopoietic stem cells impaired homing to the bone marrow in haematopoietic stem cell transplantation studies[52]. It is also used as an identification marker in MSC.

CD31*:* CD31, also known as platelet endothelial adhesion molecule-1 (PECAM-1), is found on most leukocyte subtypes, platelets and at the intercellular junctions of endothelial cells. 34% of mouse BMMNC have been shown to express CD31 and flow cytometry study has shown that all >99% of $CD31^+$ cells also express CD45[53] indicating that they are haematopoietic cells. Transendothelial migration of leukocytes is partly regulated by PECAM-1. Blocking antibodies to PECAM-1 attenuate leukocyte transmigration and reduce injury to myocardium and coronary endothelium following ischaemia-reperfusion injury. It is thought that the major ligand for PECAM-1 is PECAM-1[54].

CD34*:* CD34 is a primitive marker for early haematopoietic and so-called endothelial progenitor cells. The biological functions of CD34 are largely unknown. $CD34^+$ cells are mobilized into the blood following AMI and it has been postulated that these cells contribute to endothelial and myocardial repair post MI. However, in patients with cardiovascular disease, the number of circulating $CD34^+$ cells are reduced[55].

CD44*:* CD44 is a ligand of E-selectin (CD62E)[56,57] and cooperates with PSGL-1 and E-selectin ligand 1 (ESL-1) to control rolling velocities of leukocytes on the walls of inflamed venules[58]. Intravital microscopy demonstrated that CD44 knock-out mice had dramatically reduced neutrophil recruitment to the cremater muscle following TNF-α administration[58]. In a mouse model of stroke, when CD44 deficiency mice were used, attenuated post-ischaemia recruitment of bone marrow MSC to an ischaemic hemisphere occurred, suggesting CD44

may be a critical ligand for MSC recruitment[59]. 47.7% of unselected isolated BMMNC expressed CD44 in murine samples[60].

***CD45**:* CD45 (previously known as the leukocyte-common antigen) is a transmembrane tyrosine phosphatatase. It is expressed at high levels (>95%) on all nucleated haematopoietic cells and their precursors[61,62]. Red blood cells and plasma cells do not express CD45. The extracellular domain of CD45 is large with a number of alternatively spliced isoforms which are both specific to haematopoietic cell type and differentiation[63]. Despite extensive research effort, target ligands for the different ligands of CD45 have not been conclusively found[64,65].

***CD90**:* CD90 is otherwise known as Thy1 and there are two alleleic forms; Th1.1 and Th1.2. Mice express both forms but rats only express Th1.1[66]. Its expression in rat bone marrow cells has been reported to be 47%[67] and in human bone marrow cells has been reported to be 1-4%[68]. This is also used as an identification marker of MSC. CD90 expressed on endothelial cells mediates adhesion of inflammatory cells *via* interactions with CD11b/CD18[69].

***CD162 (P-selectin glycoprotein ligand -1)**:* PSGL-1 is expressed on myeloid cells and a subset of lymphocytes. This has been shown to contribute to different rates of recruitment from various cell types to atherosclerotic lesions[70,71]. It binds to P-, E- and L-selectin and mediates the interactions of leukocytes with endothelial cells, platelets and other leukocytes. PSGL-1 and its interaction with P-selectin mediates the initial steps of rolling and tethering in the leukocyte recruitment cascade. PSGL-1 therefore contributes to vascular damage after ischaemia-reperfusion injury.

1.3.3. Mesenchymal stem cells

MSC, otherwise known as mesenchymal stromal cells, are isolated by their adherence to plastic and can be extensively expanded in culture[72]. They can be isolated from bone marrow

or adipose tissue, and have been shown to differentiate into adipocytes, osteocytes and chondrocytes (mesenchymal lineages)[73] as well as into cardiomyocytes[74] and endothelial cells[75]. They should be positive for CD90, CD73, CD27, CD29 and CD105, while negative for haematopoietic and endothelial markers (CD45, CD34, CD14, CD11b) as usually measured by flow cytometry[76]. Injection of MSC have been shown to improve cardiac function in animal heart failure models and it has been speculated this is predominantly due to paracrine mechanisms[77]. Clinical feasibility studies have reported that MSC transplantation (with or without[78] co-administration of EPC[79]) is feasible, safe and improves cardiac function. In contrast to BMMNC, this cell type requires *ex vivo* expansion (for usually 3-4 weeks) to obtain the sufficient number of cells for transplantation. On the basis of these results, as of June 2012, there are currently 12 phase I and II active registered ongoing clinical trials being undertaken to assess MSC transplantation for heart disease[80].

Interestingly, experimental evidence suggests that allogenic MSC *in vitro* do not stimulate a T-cell immune response[81,82]. The mechanisms of this immune tolerance remain controversial, but such a phenomenon has encouraged clinicians to transplant allogenic MSC in human subjects with non-cardiac pathology including polymyositis and inflammatory bowel disease[83,84]. There are several registered clinical trials utilizing allogenic MSC for the treatment of heart disease, but these have not yet been reported.

However, concerns remain regarding the observations that late-passage MSC exhibit chromosomal abnormalities[85] and reports regarding heterotopic differentiation such as ossification or tumour formation[86-88]. MSC are also larger in size than BMMNC and have a larger diameter than that of capillaries in average. IC injection of MSC may therefore result in a greater number of cells persisting in the heart by physical entrapment within the vasculature[89-91] although such entrapment could lead to decreased perfusion in the feeding arterial system (coronary embolism)[89] and lead to myocardial injury.

1.3.4. Endothelial progenitor cells (EPC)

The term "EPC" describes a subgroup of multipotent cells incorporating a heterogeneous group of circulating and culture-derived cells[92] which overlap with cells from a haematopoietic lineage in terms of surface markers[93,94]. These cells originate from the bone marrow, and together with mature endothelial cells, are thought to contribute to endothelial regeneration and neovascularization *via* differentiation as well as paracrine ability[95,96]. In addition, endogenous EPC have been reported to play a role in pathogenesis of various types of cardiovascular disease[97]. They can be isolated from the bone marrow or from the peripheral blood, but the identification and characterization of EPC and their contribution to vascular biology *in vivo* remains controversial[92,98,99]. The main disadvantage with the concept of EPC as a source for cell transplantation is that their numbers and function are reduced in patients with cardiovascular disease, limiting the potential effects of autologous EPC transplantation[55].

In clinical settings, so-called EPC have been isolated using particular cell surface markers (such as CD34 or CD133). Clinical studies administering $CD133^+$ cells have shown that this is a feasible approach to improve cardiac function, although this may lead to an increased rate of atherosclerosis in the treated vessel[100-103]. No clinical trial has been performed to date that compares outcomes in EPC against BMMNC although the "Transplantation of Progenitor Cells and Regeneration Enhancement in Acute Myocardial Infarction Study" (TOPCARE-AMI) demonstrated that both BMMNC and circulating progenitor cells (presumed to be similar to circulating EPC) improved cardiac function to a similar degree.

1.3.5. Cardiac progenitor cells (CPC)

Several groups have recently reported that adult hearts contain resident CPC that are able to form functional cardiomyocytes, endothelial cells and vascular smooth muscle cells *in vivo*

and *in vitro*[104,105]. These are thought to contribute to a slow turn-over of cardiomyocytes in normal hearts, but cannot overcome the high degree of cardiomyocyte loss in AMI[106]. It is reportedly possible to isolate, expand *ex vivo*, and inject CPC into the heart, resulting in cardiac functional improvement *via* cardiomyogenic differentiation and/or paracrine mechanisms in animal studies[107,108].

These cells are now undergoing clinical investigation. Preliminary results of a trial using c-kit positive, lineage-negative CPC have been reported using small patient numbers[109]. In the Stem Cell Infusion in Patients with Ischaemic Cardiomyopathy (SCIPIO) trial, patients with left ventricular (LV) impairment post-MI who were undergoing CABG were randomized to receive autologous culture-expanded CPC via IC injection at a mean of 113 days post CABG. The CPC were isolated using the atrial tissue obtained during surgery and approximately 2×10^6 cells could be obtained per patient. Compared to a control group who did not receive cells, LVEF was improved at 4 months post cell transplantation; an effect that was enhanced 1 year post cell injection. Additionally, a phase 1 clinical study using cardiosphere-derived CPC has suggested that IC injection of these cells is safe and may reduce infarct size compared with controls, although no improvement was seen in LVEF[110].

This cell type requires further investigation and validation in both laboratory and clinical studies. One of the main factors limiting the widespread clinical use of CPC is various overlapping CPC types have been reported including c-kit, Sca-1, islet-1, and Cardiosphere-derived cells, the superior type of which has not been clarified[111]. In addition, the reproducibility and reliability of some reported data regarding cardiomyogenic differentiation of CPC remains controversial[112].

1.4. Routes for administering cells into the heart

For the success of cell transplantation to the heart, the choice of the cell delivery route is critically important; this will affect the retention, survival, distribution, integration and functionality of donor cells and will therefore influence the subsequent outcomes of the treatment.

The ideal cell-delivery method would meet a number of criteria[113]: (a) donor cells would be reproducibly and efficiently delivered to the target area(s) of the heart without leakage to other organs; (b) grafted donor cells would persist and survive in the heart, maintaining their important cellular functions; (c) the procedure would not cause damage to the host heart; (d) the procedure would be well tolerated by patients (even in those with severe heart failure) and have a low complication rate; (e) the method could be made available in most hospitals without the need for substantial additional facilities; (f) the method would be technically straightforward and able to be performed by most interventional cardiologists/surgeons after training; (g) the procedure would not be too costly; and (h) cells administered by this route would result in benefits to clinical outcome measures, such as patient mortality and morbidity. In addition, it would be advantageous if the technique were applicable to many types of donor cells and useful in a number of clinical situations, ranging from patients with AMI to chronic heart failure. Different routes for administering cells to the heart are currently available, including intravenous (IV), intramyocardial (IM), and intracoronary (IC) routes, as shown in Figure 1-1.

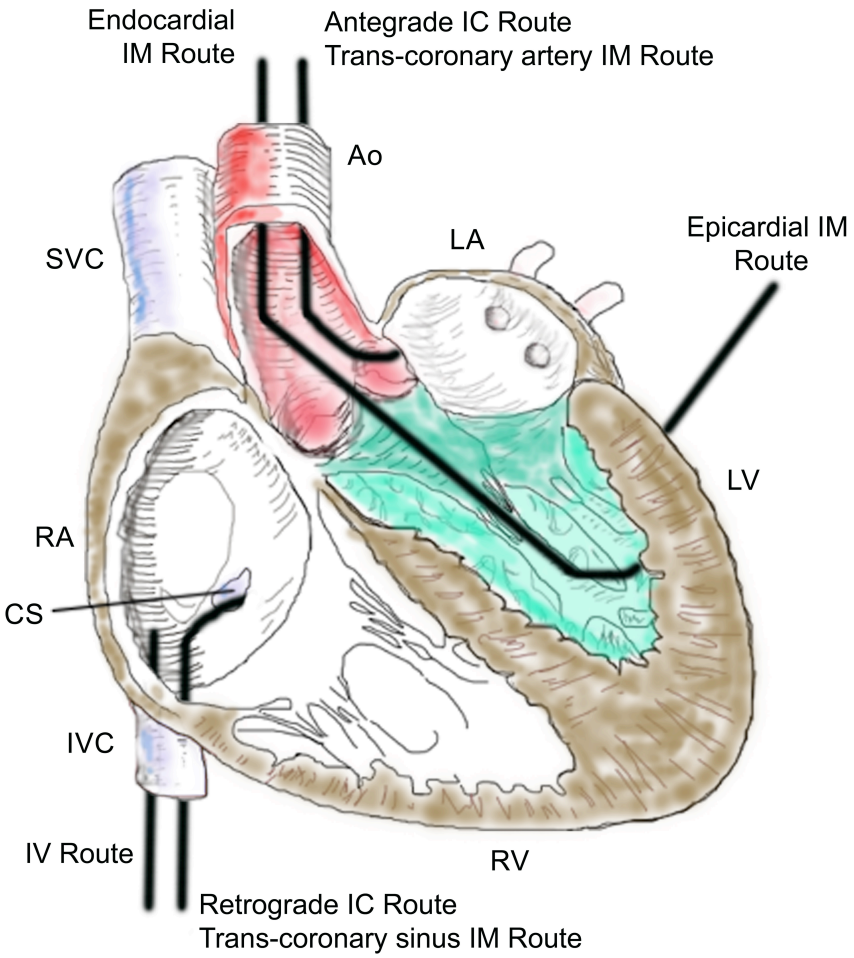

Figure 1-1: Current major routes of delivering stem cells to the heart. LV: left ventricle. RV: right ventricle. LA: left atrium. RA: right atrium. CS: coronary sinus. Ao: aorta. SVC: superior vena cava. IVC: inferior vena cava. IC: intracoronary. IV: intravenous. IM: intramyocardial.

1.4.1. Intravenous (IV) injection

This systemic route is simpler, less invasive and less expensive than other current cell delivery routes. However, injected donor cells' accumulation in the heart ('homing') and retention in the heart using this route are extremely limited. Given that only 4-5% of cardiac output is dedicated to supplying coronary artery flow (with even less through an occluded/stenosed artery)[114,115] and that many cells are entrapped in the lung, it is likely that a very low proportion of IV administered cells actually even pass through the coronary circulation.

In fact, after IV injection of radioactively labelled, *ex vivo* expanded, human circulating EPC into athymic, nude rats following MI, only a small amount of radioactivity (a proportion of about 2 %) was detected in the heart after 24–96 hours[116]. Most of the radioactivity was found in the lungs, spleen and liver[116,117]. This finding has been replicated using BMMNC[118], peripheral blood mononuclear cells[117] and purified $CD34^+$ cells[119]. A Positron Emission Tomography (PET) study in three human subjects failed to detect any cell uptake in the heart following IV injection of 18F-FDG-labelled cells[120]. Therefore, the IV route is less frequently used in clinical trials using these cell types. However, this method may be useful for MSC injection[121], based on the data that homing of this particular cell type to the damaged heart appears to be higher than other cells[122,123].

1.4.2. Intramyocardial (IM) injection

IM injection is by far the most frequently used cell injection method in small animal studies due to its technical feasibility, since reliable *in-vivo* models for IC injection in small rodents have not been established. The IM injection method can deliver cells into a specific target area, irrespective of the patency of its vascular supply, and results in a higher initial retention of cells within the heart compared with IC or IV injection[117,124,125]. The two most frequent approaches of IM injection in the clinical setting are performed (1) epicardially by direct injection after thoracotomy and (2) endocardially *via* a percutaneous catheter inserted into the LV cavity (targeted using electromechanical mapping)[126].

IM cell injection is associated with mechanical injury and a subsequent acute inflammatory response, which damages the host myocardium as well as the injected donor cells[127]. In addition, cells injected by this method are known to form islet-like cell clusters within the myocardium, resulting in limited interaction with host cells and therefore limited integration into the host myocardium. Formation of such intramyocardial heterogeneity has been postulated to lead to the development of reentrant ventricular arrhythmias observed in

previous experimental and clinical studies of IM injection of skeletal myoblasts[41]. Our group has also reported that IM injection of BMMNC, but not IC injection, was associated with an increased rate of ventricular arrhythmias following transplantation in a rat model of ischaemic cardiomyopathy[128].

The feasibility, safety and efficiency of IM injection of BMMNC have been investigated in clinical settings. A meta-analysis has been undertaken of six reported studies (with a total of 179 patients) examining epicardial IM injection of autologous BMMNC performed at the same time as CABG[129]. Patients who received cells in addition to CABG exhibited greater improvement in LV function and a greater reduction in cardiac dimensions, compared with those who underwent CABG only. There were no major complications detected in these studies.

Epicardial IM injection is usually carried out in conjunction with other open-heart procedures, such as CABG[130] or left ventricular assist device (LVAD) implantation[131], because using this approach in isolation may be too invasive and associated with a higher financial cost. Endocardial IM injection requires specialized electromechanical mapping equipment and is both a time consuming and technically challenging procedure.

To reduce the invasiveness of epicardial IM injection (along with the requirement for open chest procedures), several attempts to utilize trans-coronary IM injection have been made in small animals, large animals and patients[132-134]. Trans-coronary IM injection can be achieved *via* a percutaneous catheter introduced into the coronary sinus or the coronary artery; injection of donor cells into the myocardium is performed using a specific needle catheter penetrating through the vessel wall into the target territory[135-137]. These methods, however, require further investigations to establish their safety and efficacy in the delivery of stem cells into the heart.

1.4.3. Intracoronary (IC) injection

IC injection is a method of injecting donor cells into coronary circulation and can be achieved by two routes; injection into the coronary artery (antegrade IC injection) and injection into the cardiac vein (retrograde IC injection). With both methods, donor cells are administered into the vessel cavity using an over-the-wire balloon catheter. In clinical trials, antegrade IC injection is the most commonly used technique[138]. This procedure is thought to be a physiological method of delivering cells to the heart which enables cells to be more homogenously disseminated into target areas (without forming cell-clusters and with less myocardial damage) than is the case with the IM approach[128]. One reason for the popularity of this method is that most interventional cardiologists are familiar with the percutaneous technique to access the coronary arteries. IC injection is less invasive to patients compared to the epicardial IM approach and requires only standard equipment in the cardiac catheterization laboratory. Although this technique cannot deliver cells to an area in which the arterial supply is occluded, IC cell transplantation can be applied once the artery is reopened by intervention. A disadvantage of IC cell injection is a risk of coronary embolism[139] and this risk may be particularly important when larger cell types, such as MSC[91], are injected into the coronary arteries.

This approach was first reported in humans in 2001 in a feasibility study of BMMNC transplantation after primary PCI for AMI[140]. Since then, the majority of clinical studies have been performed using this approach, particularly when injecting smaller cells such as BMMNC, and a sizable evidence base has been built up. However, there is a lack of appropriate small rodent models for this cell delivery approach, which partly explains why there is only a limited understanding of donor cell physiology and dynamics after IC injection.

The retrograde IC approach has been reported to be a successful technique to administer stem/progenitor cells to the heart in both animals and human. This method is theoretically associated with a lower risk of coronary embolism and can deliver cells to

avascular areas. Suzuki and colleagues have developed an original model of retrograde IC cell injection in rat and shown that BMMNC[128] and skeletal myoblasts[128] could be satisfactorily administered to the heart *via* this method. The rates of donor cell survival, improvements in LV function, increased neovascular formation, and reduction in cardiac hypertrophy / fibrosis obtained by this treatment were similar after epicardial IM injection of the same number of cells. Small clinical studies have suggested that this approach is feasible and safe for delivery of BMMNC[141].

1.4.4. Other approaches

There are several other emerging technologies for cell delivery to the heart using novel biomedical engineering. These include the transplantation of stem cells or stem cell-derived cardiomyocytes as tissue-engineered constructs[142]. The cell sheet technique is one of the most promising new approaches. Okano and colleagues have developed a novel bioengineering technology to generate scaffold-free cell-sheets using unique culture dishes[143] where cells are detached from the dish as a free cell-sheet, in response to temperature changes. These sheets can then be layered onto the epicardial surface of the heart under direct visualisation. Following successful preclinical studies in small and large animals[144], a hospital-led clinical trial of skeletal myoblast sheet therapy for treating heart failure has started in Japan, which has provided positive preliminary results. Further investigation is needed to confirm the safety and efficacy of these methods, if they are to become clinically established.

1.5. Clinical studies of intracoronary (IC) injection of adult stem cells

IC injection is technically feasible by most interventional cardiologists in a standard cardiac catheter laboratory and is less invasive compared to the other major injection method; epicardial IM injection. The IC method is applicable to a range of clinical settings including AMI, post-MI heart failure, and dilated cardiomyopathy. Donor cells injected by this method do not form isolated cell-clusters, which may cause critical ventricular arrhythmias that can occur following IM injection. In fact, the vast majority of previous large-scale clinical trials have utilised IC injection, particularly antegrade IC route, and these clinical studies have proven the feasibility and safety of this method. For all these reasons, and especially because antegrade IC injection is the most widely used protocol in clinical trials, this project will focus on the investigation of antegrade IC injection. When described in this thesis henceforth, 'IC injection' will refer to antegrade IC injection.

1.5.1. Therapeutic outcomes of clinical trials of IC cell transplantation

There are an increasing number of randomized, blinded, multi-centre clinical trials using the IC route for cell therapy for heart disease (summarized in Table 1-1). The majority of these studies have administered autologous BMMNC shortly following cell isolation, utilizing the antegrade IC approach. Typically, 1-100 $\times 10^6$ BMMNC were injected, with the procedure proven to be feasible and safe. There is no evidence that rates of atherosclerotic disease, in-stent restenosis, ventricular arrhythmias or neoplasia increase following cell administration. The majority of studies have been performed delivering cells early after MI (0-7 days), but some reports have investigated cell administration in chronic cardiomyopathy.

A recent Cochrane database meta-analysis has examined the effects of IC administration of BMMNC after MI[27]. 33 randomized controlled trials with 1765 subjects were included. After short-term follow-up, cell treatment in addition to standard care was shown to significantly improve LVEF, an effect that was maintained after follow-up of up to 61 months. The weighed mean difference of LVEF% after long-term follow-up was 3.75. This is comparable to the LVEF improvement observed when ACE-inhibitors in isolation are given to patients with LV impairment[145]. There were also beneficial effects on cardiac dimensions and a correlation was observed between the donor cell dose and improvements in LVEF, suggesting that cell therapy exhibits a dose-response effect. However, these improvements did not translate into a reduction in mortality.

To date, the largest multi-centre, double blind, randomized controlled trial with the longest reported follow-up time was the Reinfusion of Enriched Progenitor Cells and Infarct Remodelling in Acute Myocardial Infarction (REPAIR-AMI) trial[46,146]. 204 patients with AMI treated with primary PCI were randomized to receive antegrade IC injection of $>230\times10^6$ autologous BMMNC or placebo into the infarct artery, 3-7 days post MI and PCI. After 2 years, the cumulative end-point of death, MI, or revascularization was significantly reduced in the BMMNC group compared to the placebo group. This was also associated with a significant improvement in LV function, cardiac dimensions and infarct size.

Although most of the clinical trials using antegrade IC injection have investigated acute or subacute MI, there are also an increasing number of studies of IC cell injection for chronic heart failure, (in both post-MI ischaemic cardiomyopathy and dilated cardiomyopathy). The ABCD (Autologous Bone Marrow Cells in Dilated Cardiomyopathy) trial randomized 44 dilated cardiomyopathy patients with normal coronary arteries to receive either autologous BMMNC by antegrade IC injection, or medical treatment only[147]. Two thirds of the cells were administered into the left coronary artery and one third were administered into the right coronary artery. After a 3 year follow-up period, there was a significant improvement in LV function in the treatment group.

The majority of clinical trials of antegrade IC injection have utilized BMMNC, although other cell types have also been studied. Chen and colleagues[78] performed a study whereby patients with AMI after coronary angiography ± PCI underwent bone marrow harvesting, and bone marrow-derived MSC were expanded for 10 days[148]. The patients were randomized to either receive antegrade IC injection of 8-10×10^9 MSC or placebo. It was reported that LV dimensions and perfusion defects decreased in the MSC group after 3 months follow-up and LV function improved after 6 months follow-up. No deaths occurred in the 6 month follow-up[78]. More recently, CPC - either c-kit^+/Lin^- cardiac cells or cardiosphere-derived cells - have been transplanted into human hearts *via* the antegrade IC route[109,110], but these approaches require further validation in larger scale studies and comparison with other established cell types.

Table 1-1. Major clinical trials utilizing the IC injection route for adult stem cell therapy to the heart

Outcomes are expressed as significant changes in the test group versus the control group, or as absolute changes when no control group was used. RCT, randomized controlled trial; NYHA, New York Heart Association; STEMI, ST segment elevation myocardial infarction.

AUTHOR	STUDY TYPE	PATIENT POPULATION	CELL GROUP	CONTROL GROUP	OUTCOMES	FOLLOW-UP TIME
Strauer[149] (2002)	Case Control Study	STEMI & balloon PCI	n=10 Autologous BMMNC	n=10 declined cell therapy	Infarct region ↓	3 months
Schachinger[150] (2004) TOPCARE-AMI	Non-randomized trial	STEMI & PCI	n=59 Autologous BMMNC or cultured peripheral MNC	No controls	LVEF ↑ Infarct size ↓	1 year
Chen[78] (2004)	RCT (? blinding)	AMI ± PCI	n=34 BM cultured MSC	n=35 placebo	LVEF ↑ LV dimensions ↓	3-6 months
Wollert[43] (2004) BOOST	Open Label RCT	AMI & PCI	n=30 Autologous BMMNC	n=30 no injection	LVEF ↑	6 months
Ruan[151] (2005)	RCT (? blinding)	AMI & PCI	n=9 Autologous BMMNC	n=11 control serum	LVEF ↑ Cardiac dimensions ↓	6 months
Strauer[152] (2005) IACT	Case-Control Study	Chronic MI	n=18 Autologous BMMNC	matched controls no injection	LVEF ↔ VO_2 max ↑ Myocardial perfusion ↑	3 months
Ge[153] (2006) TCT-STAMI	Double-blind RCT	AMI & PCI	n=10 Autologous BMMNC	n=10 BM supernatant	LVEF ↑ LV dimensions ↓ Myocardial perfusion ↑	6 months
Janssens[45] (2006) LEUVEN-AMI	Double-blind RCT	AMI & PCI	n= 33 Autologous BMMNC	n= 34 placebo injection	LVEF ↑ Myocardial perfusion ↑	4 months
Lunde[154] (2006) ASTAMI	Open Label RCT	AMI & PCI	n=47 Autologous BMMNC	n=50 no injection	LVEF ↔ LV dimensions ↔	6 months
Schachinger[46] (2006) Assmus[146] (2010) REPAIR-AMI	Double blind RCT	AMI & PCI	n=101 Autologous BMMNC	n=103 placebo	↓ combined endpoint (death, MI, repeat revascularization)	2 year

Assmus[155] (2006) TOPCARE-CHD	Randomized Controlled Crossover Study	AMI & PCI	n=75 Autologous BMMNC or cultured Peripheral MNC	No control	LVEF ↑ in initial BMMNC group and in cross-over to BMMNC group	3 months
Kang[156] (2006) MAGIC Cell-3 DES	Open Label RCT	AMI & PCI	n=25 G-CSF & Autologous BMMNC	n=25 no injection	LVEF ↑ LV dimensions ↓	6 months
		Chronic MI	n=16 G-CSF & Autologous BMMNC	n=16 no injection	LVEF ↔ LV dimensions ↔	6 months
Penicka[157] (2007)	Open Label RCT	AMI & PCI	n=17 Autologous BMMNC	n=10 no injection	LVEF ↔ LV dimensions ↔ Wall motion ↔ Infarct size ↔	4 months
Li[158] (2007)	Open Label RCT	AMI ± PCI	n=35 Autologous BMMNC	n=35 no injection	LVEF ↑ Wall motion ↑	6 months
Tatsumi[159] (2007)	Open Label RCT	AMI & PCI	n= 18Autologous Peripheral MNC	n=36 no injection	LVEF ↑ Perfusion ↑	6 months
Suarez de Lezo[160] (2007)	Double blind RCT	AMI, thrombolysis and PCI LVEF<45%	n=10 Autologous BMMNC	n=10 G-CSF and n=10 no injection	LVEF↑ in cell group, but not in G-CSF group	3 months
Huikuri[20] (2008) FINCELL	Double-blind RCT	AMI, thrombolysis & then PCI	n=40 Autologous BMMNC	n=40 placebo injection	LVEF ↑	6 months
Ang[161] (2008)	Double-blind RCT	CABG with myocardial scar	n=21 Autologous BMMNC	n=20 placebo n=21 IM Autologous BMMNC	LVEF ↔	6 months
Meluzin[162] (2008)	Open Label RCT	AMI	n=40 Autologous BMMNC at high and low doses	n=20 no injection	LVEF ↑ in high cell dose group	12 months
Plewka[163] (2009)	Open label RCT	AMI & PCI EF<40%	n=40 Autologous BMMNC	n=20 no injection	LVEF ↑ Major adverse events ↓	2 years
Cao[164] (2009)	Double-blind RCT	AMI & PCI	n=41 Autologous BMMNC	n=45 placebo injection	LVEF ↑ Myocardial viability ↔ Adverse events ↔	4 years
Tendera[21] (2009) REGENT	Open Label RCT	AMI & PCI	n=80 unselected BMMNC or n=80 $CD34^+$ $CXCR4^+$ BMMNC	n=40 no injection	LVEF / LV dimensions ↔ unselected *vs.* selected cells ↔	6 months

Yao[165] (2009)	RCT Participants not blinded	AMI & PCI LVEF 29-39%	n=27 Autologous BMMNC Day 3-7 post MI ± 3 months post MI	n=12 placebo (1 dose)	LVEF ↑ Myocardial perfusion ↑ (repeated doses > 1 dose)	12 month
Yousef[166] (2009) BALANCE	Case-Control Study	AMI & PCI	n=62 agreed to Autologous BMMNC	n=62 declined cell therapy	Infarct size ↓ Survival ↑	5 years
Grajek[167] (2010)	Single blinded RCT	AMI & PCI	n=31 Autologous BMMNC	n=14	LVEF ↔ Myocardial perfusion ↑	6 months
Strauer[168] (2010) STAR-heart	Case-Control Study	Chronic MI	n=191 agreed to Autologous BMMNC	n=200 declined cell therapy	LVEF ↑ LV dimensions ↓ Symptoms ↓ Exercise capacity ↑ O_2 uptake ↑ Mortality ↓	3-5 months
Piepoli[169] (2010)	Open Label RCT	AMI & PCI early LVEF<40%	n=19 autologous BMMNC	n=19 no injection	LVEF ↑ O2 uptake ↑ Myocardial perfusion ↑ Death / clinical events ↔	12 months
Seth[147] (2010) ABCD	Open Label RCT	Non-ischaemic dilated cardiomyopathy	n=41 Autologous BMMNC	n=40 no injection	Functional status ↑ LVEF ↑ LV dimensions ↓	3 years
Wohrle[170] (2010)	Double Blinded RCT	AMI & PCI	n=29 Autologous BMMNC	n=13 placebo	LVEF ↔ LV dimensions ↔ Infarct size ↔	6 months
Hirsch[171] (2011) HEBE	Open Label RCT	AMI & PCI	n=69 Autologous BMMNC or n=66 Autologous peripheral MNC	n=65 placebo	LVEF in both cells ↔ BMMNC *vs*. circ. MNC ↔	4 months
Roncalli[172] (2011) BONAMI	Open Label RCT	AMI & PCI early LVEF<45% & ↓viability	n=52 Autologous BMMNC	n=49 no injection	Myocardial viability ↑	3 months
Traverse[173] (2011) LateTIME	Double blind RCT	2-3 weeks post AMI and PCI	n=55 Autologous BMMNC	n=26 placebo	LVEF / LV dimensions ↔ wall motion ↔	6 months
Quyyumi[174] (2011)	Open Label RCT	AMI & PCI	n=16 CD34+ Autologous BMMNC at 3 different doses	n=15 no injection	LVEF ↔ Infarct size ↓ (medium / high dose groups)	6 months
Bolli[109] (2011) SCIPIO	Unblinded RCT	EF≤40% after CABG	n=16 c-kit$^+$ lineage –ve Cardiac Stem Cells.	n=7 no injection	LVEF ↑ Infarct size ↓ NYHA class ↓	12 months
Makkar[110](2012) CADUCEUS	Unblinded RCT	AMI & PCI LVEF 25-45%	n=17 cardiosphere-derived cells	n=8 no injection	↓ Infarct size LVEF / LV dimensions ↔	6 months

1.5.2. Poor donor cell retention/presence after IC injection observed in clinical studies

In parallel to studying the safety and therapeutic effect of IC cell transplantation, some clinical studies have attempted to quantify the donor cell persistence/survival in the heart after IC injection (Table 1-2). Although these studies have only used small numbers of patients and different approaches of quantification, the results collectively suggest that very few donor cells are retained and survive in the heart after IC injection.

Goussetis *et al.* assessed donor cell numbers persisting in the heart in patients with chronic ischaemic cardiomyopathy[175]. $CD133^+$ and $CD133^-/CD34^+$ cells were immunomagnetically isolated from the bone marrow of the patients, labelled with ^{99m}Tc-hexamethylpropylenamineoxime (99mTc-HMPAO) and infused into the infarct coronary artery after PCI. Scintigraphic images obtained at 24 hours in 4 patients demonstrated a mean 6.8% donor cell uptake in the heart. Images obtained in a single patient at 1 hour showed an uptake of 9.2%.

Hofmann *et al.* examined transplanted cells retained in the heart of AMI patients treated with stenting of the infarct artery[115]. Unselected BMMNC (n=3) or $CD34^+$ BMMNC (n=3) were labelled with [^{18}F]-fluoro-2-deoxy-D-glucose (^{18}F-FDG) and injected into the infarct artery. Fifty to seventy-five minutes after cell administration, the patients underwent PET imaging and only 1.3-2.6% of labelled BMMNC were found in the heart, a proportion that increased to 14-39% in patients receiving $CD34^+$ BMMNC. The remaining radioactivity was found mainly in the liver and spleen. This study suggests that there may be subpopulations of BMMNC which are preferentially retained in the heart.

Kurpisz and colleagues, using a similar approach, examined donor cell retention in 3 patients with a recent MI treated with stenting[176]. Autologous $CD34^+$ BMMNC were radiolabelled with Indium and the labelled cells were injected into the infarct artery. Twenty-four hours after injection, SPECT imaging showed that 2.6-11.0% of donor cells persisted in the heart.

As was observed in the other reports, the majority of donor cells were found in the liver and the spleen.

Schachinger and colleagues studied donor cell retention in 17 patients with MI treated with either stenting or CABG[177]. Mononuclear cells were isolated from peripheral blood and then subjected to *ex-vivo* culture. These cells (described as circulating progenitor cells by the authors) were then radiolabelled with ^{18}F-FDG and administered *via* IC injection. When assessed by PET, a mean of 7% of the injected donor cells persisted in the heart 1 hour after cell injection, which further declined to 2% after 3-4 days.

Kang and colleagues examined retention in 17 post MI patients undergoing planned PCI, 5 of whom had chronic ischaemic cardiomyopathy[120]. Isolated peripheral mononuclear cells were mobilized with granulocyte colony-stimulating factor (G-CSF). These cells (described by the authors as peripheral haematopoietic stem cells) were labelled with ^{18}F-FDG and 2 hours post IC injection, the patients were assessed with PET. A mean of 1.5% of injected cells were found in the myocardium. A single patient underwent 2 PET studies that demonstrated myocardial activity of 3.3% at 2 hours and 1.5% at 20 hours.

Penicka *et al.* investigated donor cell retention in 5 patients with AMI and 5 patients with chronic MI[178]. Unselected BMMNC radiolabelled with 99mTc-HMPAO were injected into the left anterior descending artery after PCI. At 2 hours after injection, radioactivity was detected in the hearts of all patients with AMI though only 1-5% of the total radioactivity. This further decreased by 20 hours post injection. In the chronic MI patients, activity was detected (1-3%) in 4 of 5 patients after 2 hours, but no activity was detected after 20 hours.

Schots *et al.* assessed cell retention in 8 patients with chronic MI (>12 months)[179]. Selected CD133^{+} cells were radiolabelled with 111-Iridium and administered *via* IC injection. In each patient, serial nuclear imaging was obtained at 2, 12, 36 and 60 hours post-injection. This demonstrated a mean retention efficiency in the heart of 7.4, 2.8, 1.6 and 1.2%, at each time point respectively.

Table 1-2: Clinical studies which have assessed donor cell retention and presence after IC injection of adult stem cells

	Species	*Cell Type*	*Cell Number Injected*	*Timing of Cell Delivery post MI*	*Timing of measurement post delivery*	*Measurement method*	*Cell retention results*
Kang (2006)[120]	Human (n=17)	Circulating mononuclear cells	Not stated	3-300 days	2 hours	FDG labelled cells PET/CT of heart	1.5% retention
Blocket (2006)[180]	Human (n=6)	Circulating $CD34^+$ mononuclear cells	$4x10^6$	7-21 days	1 hour	FDG-labelled cells PET of heart	5.5% retention
Schachinger (2008)[177]	Human (n=17)	Circulating mononuclear cells, expanded *ex-vivo*	$1x10^6$	5 days – 17 years	1 hour & 2-3 days	FDG labelled cells PET of heart	6.9% retention at 1 hour 2% retention at 2-3 days.
Goussetis (2006)[175]	Human (n=1)	Bone Marrow $CD133^+$ & $CD133^-$ $CD34^+$	$1.5x10^7$	>9 months	1 hour	^{99m}Tc labelled cells Scintigraphic imaging	9.2% retention at 1 hour (n=1)
Hofmann (2005)[115]	Human (n=6)	Unselected BMMNC & BM $CD34^+$	$2.5x10^8$	5-10 days	50-75 mins	FDG labelled cells PET of heart	1.3-2.6% retention unselected BMMNC 14-39% retention BM $CD34^+$ cells
Schots (2007)[179]	Human (n=8)	Peripheral blood $CD133^+$	5 - 50 $x10^6$	>12 months	2 and 12 hours	111-In-oxine cell labelling Scintigraphic imaging	6.9-8.0% retention at 2 hours 2.3-3.2% at 12 hours
Penicka (2007)[178]	Human (n=10)	BMMNC	2.4 - 5.7 $x10^9$	Not specified	2 and 20 hours	^{99m}Tc labelled cells Scintigraphic imaging	1.3-5.1% retention at 2 hours. 1.0-1.3% retention at 20 hours
Penicka (2005)[181]	Human (n=1)	BMMNC	$2.7x10^9$	9 days	2 and 18 hours	^{99m}Tc labelled cells Scintigraphic imaging	5% retention at 2 hours 1% retention at 18 hours
Kurpisz (2007)[176]	Human (n=3)	$CD34^+$ BMMNC	$2\text{-}4x10^6$	4-7 days	24 hours	Indium-labelled cells SPECT	2.6-11.0% retention

1.5.3. Poor donor cell retention with IC injection observed in animal studies

Clinical studies have suggested that there is a poor presence of donor stem/progenitor cells in the heart after IC injection (please refer to 1.5.2). However, these results were based on studies utilizing a small number of heterogeneous patients with varying injection protocols. Several groups have provided further supporting evidence regarding the low retention rate of donor cells after IC injection by using large animal models. This approach enabled standardized procedures to be applied to more homogeneous subjects in a more reproducible manner.

Forest *et al.* assessed retention of autologous BMMNC labelled with either a fluorescent marker or a radioactive tracer in a day 7 porcine MI model[118]. Cells were injected either *via* the IC or IV routes. Radioactivity analysis measurements demonstrated that only 6.0 ± 1.7% of cells were still retained in the heart after 24 hours of IC injection. After IV injection, no donor cells were detected in the heart and the majority of donor cells were found in the lungs.

Doyle *et al.* dynamically tracked the fate of ^{18}F-FDG labelled circulating EPC following IC injection in a porcine AMI model[182]. The location of labelled cells was determined every minute for 1 hour using PET. A balloon was placed in the infarct artery and cells were injected using cycles of balloon occlusion / reperfusion. Peripheral blood was drawn at 1-minute intervals and 18F-FDG activity was also recorded from these samples. After each balloon deflation following injection, there was a loss of 80% of peak myocardial activity, which mostly occurred in the first 2 minutes following deflation. This abrupt drop in myocardial radioactivity with each balloon deflation was associated with a transient spike of peripheral cell-bound (>90%) activity, indicating that the administered cells rapidly pass into the systemic circulation.

Tossios and colleagues also tracked the retention of BMMNC utilizing a pig AMI model and compared cell retention between two IC injection protocols; in group 1, BMMNC

were delivered during balloon inflation, followed by subsequent balloon deflation whereas in group 2, the same number of cells were delivered without an intracoronary balloon.[183] Group 1 injections resulted in a higher immediate retention of cells than group 2, but in group 1, the cells were rapidly lost during balloon deflation (reflow). In group 2, there was a more steady loss of cells. As a result, there was no difference between the retained cell number at 1 hour or 24 hours between the groups, leading the authors to conclude that balloon inflation is not necessary for IC cell injection. Dynamic scintigraphic imaging showed that donor cell loss from the heart occurred within minutes following IC injection.

Freyman *et al.* utilized a pig model of AMI to compare the number of donor MSC (a larger cell type than BMMNC) remaining in the heart, after delivery either *via* the IC, IM and IV routes[89]. Iridium-labelled cells were delivered 75 minutes after the initiation of AMI and the organs were harvested following cell delivery for quantification of iridium-particle number. 14-days following IC and IM injection, 6% and 3% of the administered cells were still located in the heart respectively ($p<0.01$). No detectable cells were found after IV administration and a high proportion were located in the lungs

These results of large animal and human studies have consistently shown that donor cell retention, survival, and/or engraftment are extremely poor after IC injection. In particular, following antegrade IC injection of BMMNC (the most frequently used clinical protocol), only 1-5% of injected donor cells are still found in the heart around 24 hours after transplantation. Furthermore, it is suggested that such poor donor cell presence at 24 hours is the consequence of poor donor cell presence (as poor as 1-10%) at much earlier time points (1-2 hours) after IC injection. A high proportion of injected cells are found in extra-cardiac organs, such as the lungs, liver or spleen. Such poor donor cell presence in the heart is a critical weakness of IC injection of stem/progenitor cells, which limits the therapeutic effects of this approach.

1.6. Initial donor cell Retention following IC injection

When a new pharmaceutical agent is developed for market, rigorous preclinical testing and understanding of the underlying mechanisms mostly occur prior to clinical studies. In the field of stem cell therapy to the heart, however, I believe that these normal translational processes have not properly occurred. In the rush to introduce stem cell therapy into clinical studies, these fundamental preclinical investigations have not occurred to any great degree. As a result, there is still a poor understanding of many of the critical processes that occur following IC cell injection.

Given the consistent results from clinical and large animal studies (see 1.5.1 and 1.5.2), it is clear that initial retention of donor cells in the heart is poor after IC cell injection. This results in limited mid/long-term donor cell engraftment and consequently in limited therapeutic effects of the treatment. There remains little understanding of the mechanisms that affect donor cell retention after IC injection. Further understanding and enhancement of retention of donor cells is key to the future clinical success of IC cell injection.

1.6.1. Definition of "initial retention" of donor cells after IC injection

The words that describe the state of transplanted donor cells within the heart after IC injection need to be carefully defined. In the literature, the word 'engraftment' is often used to describe donor cells within the heart at any time point[184], although this is linguistically erroneous. In general, successful 'engraftment' of organs or tissues is understood to mean that the donor organ/tissue has formed functional connections with adjacent structures[185]. The word 'engraftment' when applied to cell transplantation, should be used similarly – functional integration of surviving donor cells with the host myocardium.

At least three major factors influence "engraftment" of IC injected cells: "initial retention" within the heart, subsequent "survival", and functional "integration" into the host myocardium. Intramyocardial migration and proliferation may also influence "engraftment" in some cases. Initial retention encompasses the processes of adhesion of donor cells to the endothelium or physical entrapment in the intravascular lumen. Initial retention may also include subsequent transendothelial migration into the myocardial interstitium, and/or migration into the vascular wall. Importantly, as discussed above, poor longer term "survival or presence" and "engraftment" following IC cell injection is predominantly due to poor "initial retention", which should occur within minutes after injection.

1.6.2. Importance of "initial retention" of donor cells after IC injection

As discussed in section 1.5, clinical studies have suggested that the retention rate after IC injection is below 10% after 1-2 hours. Such a poor retention rate at 1-2 hours is likely to be determined by low retention rates at an even earlier time point: within minutes after injection ("initial retention"). However, the quantitative time-course of initial retention of adult stem/progenitor cells in the heart following IC transplantation and its underlying mechanisms remain largely unknown. Elucidation of these and improvement of these low initial retention rates are required if this cell administration route is to enter standard clinical practice.

This thesis aims to characterise the retention in the heart, with a particular focus on the "initial retention", of adult stem/progenitor cells after IC injection, in a quantitative and systemic manner.

1.6.3. Current experimental models to assess initial retention of donor cells after IC injection

To elucidate the detailed time course of retention of different stem/progenitor cells in a range of conditions, a reproducible, cost-effective small rodent model is required. However, there is currently a lack of established small animal models to mimic IC injection and to evaluate donor cell retention. To date, the majority of quantitative analyses of donor cell presence/retention in the heart after IC injection have utilized large animal models or clinical subjects, in which IC injection protocols are well-established. However, due to the extensive resources required, large animal models were not suitable for my study. Possible methods of quantitative measurement of initial donor cell retention in small and large animals are discussed below:

Histological detection of donor cells: Histological techniques offer the potential to track injected cells in the heart, to examine their numerical frequency and location in relation to blood vessels, and to determine their fate. Various methods to label donor cells are available including labelling with fluorescent dyes[186,187] or quantum dots[188]. Alternatively, the use of genetically-modified cells to express markers such as GFP, and immune-detection of donor cell specific antigen (such as species-specific or sex-specific antigens) can be used[189]. However, histological techniques that involve the counting of cells in the host heart only provide a semi-quantitative assessment of the number of cells in the heart unless the whole heart is fully investigated. Other limitations are that animals need to be euthanized for the heart to be examined and longitudinal cell fate cannot be assessed in the same animal. Additionally, fluorescent markers are also subject to decay in the heart, dye leakage into adjacent cells/tissues and fusion events. These may all interfere with histological interpretation.

Donor cell detection in digested hearts: One of the methods to quantitatively measure donor cell retention is chemical/molecular assessment of marker molecules contained in the heart after injection of cells labelled with these markers. Here, after IC injection of pre-labelled

donor cells, the heart is digested, and quantity/activation of marker molecules contained in the heart homogenate is measured. Possible markers include radioactive substrates (assessed by nuclear assessments[89,119,127], ß-galactosidase (by enzymatic activity)[139,190], firefly luciferase (by chemiluminescence), and male specific genes (quantitative Polymerase Chain Reaction after transplantation of male cells into female hearts)[127]. This method is applicable in small animals; however, it requires euthanasia of the animals at each study point and does not enable longitudinal cell fate tracking in the same sample. The method is prone to overestimating the cell retention, because signals from particles after cell death that persist in the cardiac tissue or which are taken up by tissue macrophages will be misinterpreted as representing cell presence.[191] Also, some marker molecules may affect the cellular integrity of donor cells[192].

Detection of living donor cells: Radiolabelling of donor cells in large animals and patients is one approach to assess the persistence of cells in the heart. Radioactivity measurements using Single Photon Emission Tomography (SPECT) or Positron Emission Tomography (PET) are used to estimate the donor cell number retained in the heart[89,116,117,120,175,177,180,182,193]. One major advantage of these techniques are that the quantification of donor cell presence can be determined at several different time points in the same subject. Long-term presence can only be utilized when the half-life of tracers is sufficiently long (for examples in the cases of ^{111}In which is used with SPECT or ^{64}Cu-PTSM which is used with PET)[194]. However, unfortunately, these methods are not easy to apply to small animals, resulting in insufficient sensitivity and resolution. In addition, several reports have shown that radiolabelling is toxic to blood cells, haematopoietic stem cells or MSC, and it is possible that radioactivity could damage functions of donor cells[119,123,195]. Furthermore, this method is associated with a risk of release of tracer from dead cells, which may be retained in cardiac tissue and therefore lead to misleading conclusions regarding cell presence. Recently an approach using a reporter gene coupled to a systemically injected radiotracer with nuclear assessment by PET has been utilized to

quantify cells[196]. This technique could avoid some of these problems with direct radiolabelling of cells but quantification is not straightforward and the need for systemic injection of tracer increases background signal and decreases the contrast.

Donor cell labelling with iron particles for magnetic resonance imaging (MRI) visualization is another approach that has been used to assess donor cell presence *in vivo*. Aspects of this technique which are appealing include the fact that MRI provides high quality anatomical localization of tissues, does not require ionizing radiation and that iron has been reported to be non-toxic for cells[197,198]. However, iron nano-particles released by dead cells may be taken up by tissue macrophages and persist in the heart for 5 weeks[199-201]. In addition, this method will have insufficient sensitivity and resolution to detect low numbers of donor cells when applied to small animals.

1.7. New models to assess retention following IC injection in small animals

Clinical studies and large animal experiments have provided proof-of-concept that poor initial retention of donor stem/progenitor cells occurs after IC injection. Small animal models are required for a large-scale mechanistic study to assess initial retention of donor cells quantitatively in a number of experimental conditions at multiple time points. However, there are two hurdles that must be overcome; lack of a model of IC injection and lack of a method to assess early retention in small animals serially (please refer to 1.6). Previously, injection of cells into the aortic root (with simultaneous snaring of the ascending aorta and pulmonary artery)[108], injection into the LV cavity[186] or IV injection[122] have all been used in small rodents as a model of IC injection. However, these approaches cannot deliver cells into the coronary artery in a reproducible manner and therefore are unsuitable for a quantitative study of donor cell retention. Possible methods to overcome these issues in small animals are described as follows;

1.7.1. Intravital microscope model

Intravital microscopy is a widely used technique for studying the microvasculature in animals *in situ*. It utilizes thin tissues that can be trans-illuminated including bat wing, tadpole tail, and externalized mesentery of the bowel and externalized cremaster muscle in small rodents. This sophisticated method has been used to characterize the complex multi-step processes which occur during leukocyte adhesion and migration by real-time and time-lapse observation, monitoring, and recording of leukocyte-endothelial interactions[202]. Target cells (either endogenous cells or injected cells from the responsive artery) can be tracked to determine their location in relation to the vasculature (intra-luminal, trans-luminal or transendothelial migration) under pulsatile blood flow in a semi-quantitative manner[203]. It can also help elucidate the effects of cell surface molecules on either the cells to be injected or the recipient endothelium, with or without the use of genetically-modified animals. Using the externalized cremaster muscle, it is also possible to inject cells selectively[204] and to induce localized ischaemia-reperfusion injury[205].

Toma *et al.* have recently utilized intravital microscopy to track the fate of intraarterially-delivered, fluorescently labelled-MSC in rat cremaster muscle[204]. They found that 92% of MSC arrested within the vasculatures and interrupted flow during the first pass at the pre-capillary level, resulting in decreased flow in the feeding arteriole. At 3 days post MSC injection, the donor cell number decreased to 14% of its initial peak, mainly due to cell death. Labelling of the basement membrane confirmed that at day 1, MSC were sited on the luminal side of the basement membrane but by day 3, they had integrated into the microvascular wall.

Using this approach, intravital microscopy could potentially provide a technique of obtaining a semi-quantitative assessment of retention[202] in small animal models. However, it would not provide a fully quantitative assessment of retention. In addition, an important limitation of this method is that it investigates non-cardiac tissue, which may exhibit different endothelial properties or different mechanisms of donor cell retention.

1.7.2. Bioluminescence imaging

Bioluminescence imaging may be useful to measure donor cell retention in small animals[47,201,206-208], once a reproducible IC injection model is established. Genetically engineered cells overexpressing firefly luciferase are administered, and the animals are then injected with the substrate of luciferase D-luciferin. Anaesthetized animals are imaged and light is detected using a highly sensitive camera. Only viable cells generate a signal, which is advantageous, but this is totally dependent on the sensitivity of the chemiluminescence analyser. Furthermore, only surface images can be obtained and results are sensitive to the depth of cardiac imaging (cells in the anterior wall will generate a higher signal than those in the posterior wall). Additionally, because it can be difficult to obtain a baseline signal intensity, there may be a wider variation between sample measurements compared to other techniques.

1.7.3. The use of a Langendorff isolated heart perfusion model

The Langendorff -perfused mammalian heart model was established by Oscar Langendorff in 1897[209]. The general principle of this method is that crystalloid perfusate is delivered to the heart through a cannula secured in the ascending aorta. Retrograde flow in the aorta, driven by pressure and volume load, closes the leaflets of the aortic valve and as a result, all the perfusate enters the coronary arteries *via* the coronary ostia at the aortic root, enabling the heart to be continuously perfused and beat. The perfusion pressure of the coronary arteries is kept constant by maintaining a constant perfusate hydrostatic pressure or regulating the flow by a pump[210]. Most studies use a physiological crystalloid solution (*e.g.* Krebs and Henseleit buffer) to mimic the ionic constituents of plasma[211]. Although a small number of groups have reported the utility of a blood-perfusion model in rodents[212], this has not become a widely-used model because of technical and practical difficulties maintaining heart stability.

The main overall advantage of using the Langendorff crystalloid-perfused heart is that we can easily and reproducibly achieve IC cell injection in small rodents. It is possible to inject a target number of cells into the coronary arteries *via* the aorta from a side port of the aortic cannula while the heart beats normally. Using this approach, our group has proposed a model to measure the quantitative frequency and pattern of donor cells in the heart following IC injection in mice[213]. In this model, a known number of cells are delivered by injection into the aorta and the coronary effluent is continuously collected following injection. Knowledge of the initial donor cell number and counts of donor cells within the coronary effluent enable the calculation of the proportion of donor cells that are retained within the heart (see 4.3 for details). An additional advantage of this model is that we could directly and reproducibly inject antibodies or pharmacological substances to inhibit or stimulate adhesion molecules/ligands into the heart *via* the coronary tree, which would enable us to study the molecular mechanisms of retention. It should be noted that intravenous or intraperitoneal administration of such agents that affect donor cell retention are not guaranteed to reach the heart in a reproducible manner. A further advantage of this model is that it is also easy to induce ischaemia-reperfusion (I-R) injury, by halting and restarting perfusion (global I-R injury), or by ligation of left coronary artery (LCA) followed by ligature release for reperfusion (regional I-R injury).

Limitations of this Langendorff-based model may include the lack of blood components (cytokines, growth factors, and blood cells such as neutrophils and platelets) in the perfusate. However, I believe that this potential limitation will not be significant for my project. It is important to note that donor cell retention in the usual clinical procedure takes place under almost complete crystalloid perfusion conditions, where donor cells are suspended with non-blood, serum-free solution/buffer and injected into the coronary artery while occluding the proximal portion of the coronary artery and thereby preventing pulsatile blood flow[45,154]. Hence, most blood components are flushed out with crystalloid solution, and thus the intravascular space of my interest is almost blood-free under a non-pulsatile

condition. Although the Langendorff model cannot be used for long-term studies, various reports have indicated that the Langendorff-heart perfused with crystalloid buffer confers a stable circulation without any damage to the coronary endothelium or myocardium for at least 2 hours[214-217]. It has been reported that 2 hour normoxic crystalloid perfusion does not increase the expression of adhesion molecules such as P-selectin[217,218]. Consistent with this, our group have previously confirmed with histological analyses that 1 hour crystalloid perfusion did not influence expression of major adhesion molecules including P-selectin, ICAM-1 and VCAM-1 on the coronary endothelium[213].

In this thesis, the Langendorff-based model in rat will be used to further investigate initial retention of donor adult stem/progenitor cells after IC injection.

1.8. Potential mechanisms responsible for initial donor cell retention

To date, the underlying mechanisms of the initial retention of any type of stem/progenitor cells following IC injection remain largely unknown. It could be speculated that there are at least two different mechanisms. One could be a physical, mechanical entrapment of injected donor cells within the vascular lumen ("passive retention"). The other responsible mechanism may be similar to that of leukocyte-endothelial adhesion, with a specific group of adhesion molecules and their ligands playing an important role (defined as "active retention"). The balance between active and passive cell retention may depend on injection conditions (including injection pressure and / or volume), the condition of the donor cells and the environment of the recipient coronary vessels.

1.8.1. Passive retention (mechanical entrapment)

Donor stem/progenitor cells injected into the coronary arteries may settle within the lumen of coronary vasculature by mechanical (passive) entrapment. This mechanism of retention may dominate when cells are injected into hearts with normal, intact coronary endothelium (without significant expression of adhesion molecules). Typical examples for this could include injection into chronic ischaemic or dilated cardiomyopathic hearts. For this passive retention, it could also be speculated that the size of donor cells may have an impact on the initial donor cell retention. In a semi-quantitative study using a porcine AMI model, Ly and colleagues used *in-vivo* open-chest bioluminescence imaging to determine cell retention for the first 60 minutes after IC injection of the same number of BMMNC or MSC[90]. As a result, they showed that a greater number of MSC, which have a larger cell size, were found in the heart at all time points measured, compared to BMMNC. This difference in retention

at 60 minutes after IC injection is likely to be a consequence of enhanced initial retention, minutes after injection.

1.8.2. Active retention (adhesion molecule-related mechanism)

Leukocyte-endothelial interaction is a multistep cascade of sequential molecular processes, which have been determined using techniques such as intravital microscopy and *in-vitro* flow models with genetic knock-out/-in transgenic models, with or without antibody neutralization[203]. In the normal condition (i.e. absence of inflammation), leukocytes rarely interact with the vessel wall but after an inflammatory stimulus is applied, the leukocyte-endothelial cascade occurs in the post-capillary venules. Upon the initiation of acute inflammation, leukocytes roll along the vessel walls at a reduced velocity; this step is mediated by the selectin family of adhesion molecules. A few minutes later, some rolling cells arrest and undergo a change in their conformational shape. This step, known as adhesion, is influenced by the integrin-family including the β2-integrins, such as lymphocyte-function associated-antigen 1 (LFA-1) and MAC-1[219,220]**.** Extravasation of cells crossing the endothelial barrier and migration into the extravascular tissue then follows, requiring activation or upregulation of a specific distinct set of adhesion molecules such as Intercellular adhesion molecule-2 (ICAM-2), junctional adhesion molecule – A (JAM-A) and PECAM-1 which have a distinct and sequential role in mediating neutrophil transmigration[202].

In several types of stem/progenitor cells, it has been shown that selectins are involved in the active retention (donor cell-endothelial adhesion) processes[221-223]. Ryzhov *et al.* showed the importance of the P-selectin/PSGL-1 axis on retention of embryonic EPC within the heart. They showed using mouse models that short-term stimulation of adenosine receptors rapidly enhanced EPC adhesion to cardiac endothelial cells *in vitro*, and increased retention using DiI-labelled cells injected into a Langendorff perfused heart (assessed only

semi-quantitatively using immunohistochemistry of collected heart specimens; a different model from our new method). These effects of adenosine on EPC adhesion *in vitro* could be partially attenuated by the application of either a P-selectin inhibitor or a blocking agent against PSGL-1[223]. Oh *et al.* examined the effects of E-selectin on retention, by investigating the homing of EPC to an ischaemic limb in mice after intracardiac injection. EPC obtained from $GFP^{+/+}$ mice underwent intracardiac injection into wild-type mice and showed that administration of E-selectin enhanced EPC homing to an ischaemic hindlimb (semi-quantitatively assessed by immunohistochemistry) and that EPC injection into E-selectin knockout mice impaired homing, although this could be rescued by local E-selectin treatment[221]. Vajkoczy and colleagues have reported that blocking P-selectin, E-selectin and PSGL-1 impaired donor embryonic EPC arrest in the tumour microcirculation, using a murine intravital microscopy model[222]. It has also been shown that human cells do not express E-selectin but that *ex-vivo* engineering of human MSC, can convert CD44 into a E-selectin/L-selectin ligand which enhances the retention of such engineered cells into mouse bone marrow[224].

The importance of integrin interactions in stem/progenitor cell retention under several specific conditions has been demonstrated. Wu and colleagues used mouse models to investigate ICAM-1-integrin interactions on retention. They reported that EPC attachment to endothelial cells *in vitro* was diminished by the blockade of CD18; ICAM-1's ligand on donor cells. After the administration of DiI labelled EPC — with or without a CD18 antagonist — into the LV cavity of 3-day-post-MI animals, the CD18 antagonist was found to almost completely abolish EPC retention in the heart, assessed by whole heart digestion/cell counting and immunohistochemistry[225]. Segers *et al.* showed that VCAM-1 which interacts with α4-integrins may have an important role in MSC retention, using rat *in vivo* and *in vitro* models. They demonstrated that pre-treating donor cells and the endothelium with TNF-α and IL1-β enhanced adhesion of DiI labelled MSC to cardiac microvascular endothelial cells in both static and dynamic flow conditions and also

increased retention in the normal heart after left ventricular cell injection. The increased adherence observed *in vitro* after inflammatory cytokine administration was completely abolished by the administration of anti-VCAM-1 antibodies, but not anti-ICAM-1 antibodies[226].

Although none of these studies are appropriately quantitative and they did not examine IC injection directly, taken together they suggest that adhesion molecules may play an important role in initial retention of stem/progenitor cells in the heart following IC injection. This concept requires further clarification.

1.8.3. Timescale of endothelial adhesion molecule expression during ischaemia-reperfusion (I-R)

For studying the role of adhesion-molecules involved in the mechanisms of donor cell retention after IC injection, it is essential to understand the timescale and degree of adhesion molecule expression on coronary endothelium after I-R. In summary based on the following data, after 30 minutes of ischaemia and 30 minutes of reperfusion - the condition that will be used in this study - it is expected that P-selectin would be upregulated and detectable, but that ICAM1, VCAM1 or E-selectin would not be upregulated/detectable in the coronary endothelium.

P-selectin: P-selectin is synthesized constitutively in endothelial cells and stored intracellularly but it is mobilized rapidly to the cell surface after stimulation[227]. In Langendorff I-R studies in guinea pigs[218] and rats[228], P-selectin was not detected after 30 minutes ischaemia by immunohistochemistry, but was detectable after 15 minutes reperfusion. P-selectin upregulation after 30 minutes reperfusion has also been confirmed in a mouse Langendorff model[213]. The time course of P-selectin upregulation after reperfusion was also determined in a rat open-chest model with 45minutes of transient LCA ligation and reperfusion up to 6 hours. It was found that immunohistochemical expression of P-selectin

occurred at 5 minutes of reperfusion (2-fold expression *vs.* controls) and increased further at 30 minutes (3 fold expression *vs*. controls), tailing off thereafter[229]. Similar findings were reported in a cat LCA ligation model with 90 minutes of myocardial ischaemia followed by reperfusion up to 270 minutes; P-selectin was immunohistochemically detected at 20 minutes post reperfusion and gradually declined thereafter[230] with no detectable expression after 270 minutes of reperfusion[231].

ICAM-1: Immunohistochemistry in a cat LCA ligation model of 90 minutes ischaemia and 270 minutes reperfusion demonstrated that ICAM-1 was expressed at a low level in control myocardium. The ICAM-1 level slowly progressively increased through 0, 10, 20 and 60 minutes reperfusion with a significant increase at 150 minutes and a greater increase at 270 minutes[230]. Supporting these findings, a Langendorff I-R model with 30 minutes reperfusion found that ICAM1 was not upregulated when assessed by immunohistochemistry[213] and a rat LAD ligation study reported that ICAM-1 was upregulated after 120 minutes reperfusion[232]. Furthermore, a mouse open-chest I-R study found that a low level of ICAM-1 was present in sham operated mice but that this was upregulated after 60 minutes ischaemia and 60 minutes reperfusion[233]. However, these timings of ICAM-1 upregulation following reperfusion have not been universally repeated. In a dog I-R study with reperfusion for 1 hour, 3 hours or 24 hours, no differences in ICAM-1 immunohistolabelling could be observed between normal or reperfusion hearts. The authors, however, found that ICAM-1 mRNA increased 10-fold from 1 hour to 24 hours post-reperfusion[234]. Bowden and colleagues also failed to demonstrate immunohistochemical ICAM-1 staining at 3 or 24 hours post reperfusion in a mouse left coronary artery ligation model[235].

VCAM-1: Upregulation of VCAM-1 occurs at a later time point post-reperfusion, as shown in a mouse LCA ligation study in which few VCAM-1 vessel were seen in control animals by immunohistochemistry but after 24 hours of reperfusion there was a increase in the number of VCAM-1 positive cells. This increase was not observed at 3 hours post reperfusion[235]. In a mouse model, VCAM-1 was not observed by immunohistochemistry

after 30 minutes of reperfusion[213]. Osborn and colleagues found that VCAM-1 mRNA was barely detectable in normal HUVEC or HUVEC stimulated by TNF-α. However, the mRNA levels greatly increased by 2 hours after stimulation and remained high for 72 hours[236].

PECAM-1: PECAM-1 is found at the intercellular junction of endothelial cells. It is generally thought that the major ligand for PECAM-1 is PECAM-1 on leukocytes[237]. The expression of PECAM-1 has been confirmed in normal and I-R hearts in a monkey closed LCA balloon occlusion model[116].

E-selectin: E-selectin (CD62E) on endothelial cells is a ligand of CD44 on leukocytes[56,57]. A feline LCA-ligation model with 90 minutes of ischaemia with 0, 10, 20, 60, 150 and 270 minutes of reperfusion did not demonstrate immunohistochemical E-selectin expression[230]. A study in monkeys also failed to detect E-selectin in normal hearts or in a closed chest LCA-balloon occlusion MI model with 30-50 minutes ischaemia and 3-5 hours reperfusion[238]. E-selectin is not expressed in unstimulated endothelial cells; it is observed only after *de novo* synthesis 4-6 hours following cytokine or bacterial endotoxin stimulation[239].

Chapter 2 - AIMS AND HYPOTHESES

Transplantation of adult stem/progenitor cells is a promising approach for the treatment of heart disease, but there is a need for further understanding and refinement of the protocol if it is to enter widespread clinical use. One of the major issues facing this emerging treatment is the choice and/or optimization of cell-delivery routes. Antegrade IC injection has important advantages in that it leads to physiological dissemination of donor cells, that it could be utilized in many hospitals without significant additional investment, and that it is less invasive compared to other techniques. In fact, this is the route which has been most commonly used in current clinical trials and its safety and feasibility has been proven in a wide range of clinical settings.

However, poor initial retention of donor stem/progenitor cells is an important limitation of this method, which will have a significant impact on therapeutic outcomes. The aims of this thesis intend to characterise initial donor cell retention in a quantitative, comprehensive manner and also to investigate the mechanisms responsible for initial retention, using an original rat *ex-vivo* Langendorff-perfused heart model. I will mainly study BMMNC, which are the most frequently used donor cell type in current clinical trials. The clinical effects of IC injection of autologous BMMNC, although small, have been proven by recent studies including a Cochrane database meta-analysis[27]. Specific hypotheses/aims in this project include:

1. Our original model using Langendorff-perfused rat beating hearts will provide reproducible and quantitative information about initial retention of donor cells after IC injection.
2. Initial donor cell retention will occur as a result of passive physical entrapment within the vasculature and/or active adhesion to the vascular endothelium *via* adhesion molecule-mediated cell-cell interactions. Therefore, the frequency, pattern

and underlying mechanisms of retention of stem/progenitor cells will vary between donor cell-types, which have different cell size and different expression profiles of endothelial adhesion-related molecules.

3. The pattern and frequency of initial retention of donor cells will also be affected by the condition of recipient hearts, including the impact of prior I-R injury that will alter the expression profile of adhesion molecules on endothelial cells.
4. The frequency and pattern of initial retention of IC injected donor cells will be affected by the cell number injected. Injection of a higher cell number will result in superior retention, but administration of too many cells introduces the risk of coronary embolism. The result obtained will suggest the optimal cell number for IC injection that achieves the greatest retention without coronary embolization. The optimal cell number will be dependent on donor cell-types and the host heart condition.
5. There will be a different frequency of donor cell retention among the different anatomical areas of the left ventricular wall (i.e. endocardial *vs*. epicardial areas).
6. BMMNC are a heterogeneous cell population containing several distinct stem cell populations, including EPC, MSC and haematopoietic stem cells. Within this mixed population, certain subpopulations will show a greater ability to be retained in the heart than others. Identification of such subpopulations will be important in understanding BMMNC transplantation.
7. Initially retained (adhered or entrapped) donor cells to the vascular endothelium will subsequently undergo transendothelial migration into the myocardial interstitium or integration into the vascular walls. The time scale and frequency of these events will be clarified.

The information obtained in this project will be translatable to clinical application of stem cell therapy and valuable for refining clinical protocols for IC injection of stem/progenitor cells.

Chapter 3 - METHODS

3.1. Introduction to the methods

This chapter describes the materials and methods that were utilized in this project. All experiments were performed in the Translational Medicine and Therapeutics Laboratory, the Biological Sciences Unit and the Flow Cytometry Laboratory in the John Vane Building, Charterhouse Square Campus, Queen Mary University of London.

All animal procedures were carried out in accordance with the Home Office Licence (PPL 70/7254). All animals were housed in the Biological Sciences Unit at Charterhouse Square Campus, Queen Mary University of London in identical constant conditions (ambient temperature 19^{o}C, humidity 55%, 12 hours light/day). They were fed a standard rat pellet diet with water *ad libitum*. After arrival, animals were allowed to acclimatise for a minimum of two days in an appropriate room before any experimental (non-recovery) procedure was performed. Animals subjected to recovery surgery were allowed to acclimatise for 7 days after arrival, prior to surgery.

The experiments described in this thesis were all performed using rats. During the initial research for this thesis, a substantial effort was made to utilize mice and to optimize the experimental protocols using this species. One of the reasons for initially pursuing research in mice was because of the availability of house keeping GFP $^{+/+}$ transgenic animals in our institution, which would have assisted with the immunohistochemistry experiments. However, generating the mouse ex-vivo Langendorff model proved extremely challenging and it was not possible to reproducibly generate mouse MSC linages. Therefore the decision

was made to transfer the research to rat; a species in which consistent reproducible data was obtained.

All the experiments and statistical analyses were performed by me, with the exception of animal recovery surgery that was performed by Dr Masahiro Kaneko (see 3.8.2). Dr Chiho Ikebe provided some assistance with MSC passaging steps, on occasion (see 3.4.1). Some assistance for fixation of some hearts in Paraformaldehyde after Langendorff perfusion (see 3.8.1) was provided by Dr Kenta Yasahiro, Dr Yasunori Shintani, Dr Chiho Ikebe, Dr Takuya Narita and Dr Masahiro Kaneko. All these colleagues were members of Professor Ken Suzuki's laboratory at the William Harvey Research Institute. Dr Patrick Campbell provided invaluable assistance with presentation of the immunohistochemical analyses.

3.2. Buffers and solutions

The following solutions were generated and utilized in this project as follows:

Alizarin red:

Alizarin red was prepared by adding 2g Alizarin Red (Fluka, Catalogue: 05600)) to 100 ml double distilled H_2O (ddH_2O; machine: Purelab Ulta, Elga). The pH was adjusted to 4.1-4.3 by the addition of 1M HCl (Sigma-Aldrich, Catalogue 320331), using an Orion 210A meter (ThermoFisher Scientific, UK). The solution was then was manually filtered by hand injection through a 0.45 µl filter (Minisart, Sartorius Stedim) and was stored at room temperature until use.

Bovine serum albumin (0.5%):

0.25 g Bovine Serum Albumin (Sigma, A4503) was added to distilled H_2O. This was allowed to dissolve at room temperature, with the aid of agitation (Roller Mixter, Stuart, Catalogue: SRT6). The solution was then filtered by hand under aseptic conditions through a 0.45 μm filter (Minisart, Sartorius Stedim) and stored at 4°C.

Flow cytometry (FACS) buffer:

40 ml of FACS buffer was manufactured by 37.84 ml HBSS (Sigma, catalogue H6648) with the addition of 2 ml of 0.5% bovine serum albumin (see above) and 160 μl of 0.5M EDTA (final concentration 2 mM; Gibro, catalogue: 15575-038).

Immunohistochemistry blocking solution:

10% goat serum (Gibco, Catalogue: 16210-064) was diluted in PBS / 0.025% triton X-100 (Sigma, Catalogue: T8787).

Modified Krebs-Henseleit (K-H) buffer:

1980 ml ddH_2O was added to a 2 liter glass bottle. The following ingredients were added: NaCl 14.026g, NaHCO3: 3.360g, Glucose: 3.603g (Sigma, Catalogue: G7528). This was then stirred with a magnetic stirrer (Bibby Scientific, UK). The following stock solutions were then added: 4 ml stock solution of KCl and $KHPO_4$ (see below), 4 ml stock solution of $MgSO_4$ (see below) and 2 ml stock solution of $CaCl_2$ (see below). The final concentration of the buffer was NaCl 120 mM, KCl 4.5 mM, $MgSO_4$ 1.2 mM, KH_2PO_4 1.2 mM, $CaCl_2$ 2 mM, $NaHCO_3$ 20 mM, Glucose 10.0 mM in 2L ddH_2O)[240] . The $CaCl_2$ stock solution was added last to avoid precipitation. The solution was then stirred again as above and vacuum filtered into another 2 liter glass bottle through a 0.2 μm filter (PALL life sciences Supor 200, P/N 66236) to remove particulate matter. The buffer was always used within 24 hours.

Stock solution of KCl and $KHPO_4$ (×250):

KCl 41.934g and $KHPO_4$ 20.414g were added to 500 ml ddH_2O. The solution was vacuum filtered through a 0.45 µm filter (Nalge Nunc MF75) into a 500 ml sterile filter bottle (Nunc) and stored at room temperature.

Stock solution of $MgSO_4$ (×250):

18.056g $MgSO_4$ was added to 500 ml ddH_2O. The solution was vacuum filtered through a 0.45 µm filter (Nalge Nunc MF75) into a 500 ml sterile filter bottle (Nunc) and stored at room temperature.

Stock solution of $CaCl_2$: 0.625M

34.684g $CaCl_2$ was dissolved in 500 ml ddH_2O. The solution was vacuum filtered through a 0.45 µm filter (Nalge Nunc MF75) into a 500 ml sterile filter bottle (Nunc) and stored at room temperature.

Oil–red-O stain stock solution:

The Oil-red-O stain stock solution was prepared by adding 150 mg Oil Red O (Sigma, catalogue O0625) to 50 ml 100% Isopropanol (2-propanol) (Sigma, catalogue: I9516), agitated for 10 minutes and stored at room temperature This stock solution was then diluted with distilled water to form a 60 % solution, subjected to filtration by hand injection through a 0.45 µm filter (Minisart, Sartorius Stedim) and used within 2 hours.

Paraformaldehyde (4%):

2g of Paraformaldehyde powder (Sigma-Aldrich; catalogue 6148) was added to 50 ml of PBS and warmed in a microwave (Mx95tcHinari Lifestyle) to approximately 60-70^oC, covered by a paraffin film (Parafilm M, Sigma-Aldrich, Catalogue: P7793-1EA). 200 µl aliquots of 1M NaOH (Sigma-Aldrich, Catalogue: S8045) were then added until the powder had completely dissolved. The same volume of 1M HCl (Sigma-Aldrich, Catalogue 320331) was then added to neutralize the solution. The flask was placed immediately on ice to cool,

was manually filtered by hand injection through a 0.45 µl filter (Minisart, Sartorius Stedim) and was stored at -20^{o}C until use.

Phosphate buffered saline (PBS):

10 PBS tablets (Oxoid, Thermo-fisher scientific, BR0014G) were added to 1L ddH_2O. For ex-vivo and in-vitro protocols, the PBS solution was filtered and autoclaved at 121^{o}C for 7 minutes (Boxer Laboratory Equipment, Ware, UK).

Sodium citrate buffer:

Sodium citrate buffer was prepared by adding 2.94g sodium citrate trisodium salt dehydrate ($C_6H_5Na307•2H_2O$; from Sigma,-Aldrich, Catalogue: S4641) to 1L dH_2O. The pH was adjusted to 6.0 by the addition of 1M citric acid (Sigma-Aldrich, Catalogue: C8, 315-5), using an Orion 210A meter (ThermoFisher Scientific, UK).

Sucrose (30%):

Sucrose 30% solution was prepared by adding 75mg Sucrose (Sigma, Catalogue: 84097) to 250mls ddH_20. The solution was then vacuum filtered through a 0.45 µm filter (Nalge Nunc MF75) into a 250 ml sterile filter bottle (Nunc) and stored at -4^{o}C.

3.3. Bone Marrow Mononuclear Cells (BMMNC)

3.3.1. BMMNC isolation

Male Sprague Dawley rats (aged approximately 6-8 weeks) were purchased from Charles River (UK), sacrificed by cervical dislocation following isofluorane anaesthesia (Abbot, Catalogue B506) using an inhalation anaesthesia unit (Vet Tech Solutions Ltd with Fluorovac Harvard Solutions). The femurs and tibias were dissected, carefully cleaned of adherent soft tissue and transported in sterile PBS (without antibiotics) on ice. The epiphyses were removed with a rongeur, and the marrow was harvested by inserting a syringe needle (19 gauge; BD Microlance 3, Catalogue number 301700) into one end of the bone whilst flushing with PBS into a 50 ml tube (Star Lab; catalogue: E1450-0200). Then, the bones were cut longitudinally using a rongeur and adherent bone marrow tissue was flushed with PBS into the tube. The 50 ml tube was centrifuged at 400 g for 5 minutes (Centrifuge machine: Universal 320, Hettich Zentrifugen) and the supernatant was aspirated and removed. The bone marrow cell pellet was resuspended, filtered through a 100μm filter (BD Falcon, catalogue number 352360) and centrifuged at 400 g for 5 minutes in a 15 ml Falcon tube. The supernatant was removed and the bone marrow cells were resuspended in 5 ml PBS (without antibiotics). The cell suspension was then carefully layered by pipette onto 7 ml Ficoll (Sigma) using cut 1000 μl pipette tips (TipOne, Lot number Z107468R) and subjected to gradient centrifugation at 1040 g for 30 minutes with no brake.[241] Cells at the interface were collected as BMMNC and washed three times in PBS. For washing, the cells were resuspended in PBS and centrifuged as above, followed by supernatant removal as also described above.

3.3.2. Efficiency of BMMNC isolation

The number of BMMNC per animal isolated using the above protocol was determined by counting the number of living cells obtained (n=5 animals) using a haemocytometer (Hawksky, UK) or a Countess Automated Cell Counter (Invitrogen, UK). The viability of isolated BMMNC was determined by quantifying the proportion of unstained cells with Trypan Blue solution (Invitrogen, UK, final concentration 0.2%), viewed with light microscopy (Nikon TMS) utilizing a haemocytometer (Hawksky, UK). For cell counting with the haemocytometer, the number of cells in the four outer quadrants was counted.

3.3.3. Morphology of collected BMMNC

The general cell morphology of freshly isolated BMMNC was examined using a cell smear under a phase-contrast microscope (BZ8000, Keyence). To generate a cell smear, 10 µl of BMMNC suspended in PBS was dropped onto one end of a Polylysine slide glass (Thermo Scientific). A coverslip (22×50mm, VWR International) was then placed at a 45^{o} angle against the droplet on the opposite side to the slide glass end, until capillary motion spread the cell suspension along the coverslip. The coverslip was then pushed along the slide in a rapid motion which dragged the cell suspension along the slide glass[242]. The slide was then allowed to air dry for 30 minutes at room temperature.

3.3.4. Red blood cell contamination of BMMNC samples

There was a concern that isolated BMMNC might be contaminated with red blood cells (RBC). To assess this possibility, isolated cells were dropped onto a Polylysine slide glass (Thermoscientific), smeared using a cover slip and allowed to air dry for 30 minutes as described in 3.3.3. The slides were fixed with 4% Paraformaldehyde for 15 minutes at room temperature and washed with PBS containing 0.025% triton X-100 (Sigma) by adding the slides into Coplin Jars for 5 minutes, 3 times. Cells were stained with DAPI (Roche; 1:1000

in PBS / 0.025% Triton X-100 (Sigma)) for 5 minutes and washed as above. The slides were mounted with fluorescence mounting medium (DAKO, catalogue: S3023) and viewed using a phase contrast microscope (BZ8000, Keyence). RBC proportions were determined by the ratio of non-nucleated (DAPI negative) cells to the total cell number.

3.3.5. Cell size of BMMNC

Collected BMMNC were suspended in PBS and analysed for cell size using a Countess Automated Cell Counter (Invitrogen, UK). The Countess Automated Cell Counter provides a measurement of cell size (diameter) in μm. The BMMNC suspension was added to a slide glass specific to the cell counter machine (Countess Cell Counting Chamber Slides / Invitrogen, UK, C10228). Cells smaller than 5 μm were not included in the final analysis, as they were deemed to be debris and the manufacturers recommend the Automated Cell Counter is used for cell analysis in the size range of 5 – 60 μm. The following settings for analysis were used (Sensitivity: 85.0, Min Cell Size 5 μm, Max Cell Size: 60μm, Circularity 80).

BMMNC from n=11 animals were independently analysed. For each sample, up to 8 measurements were taken of cell size. Each measurement was imported into the Countess Automated Cell Counter software (Invitrogen, UK) and exported using a .csv file a spread-sheet. This file format provides the total number of cells in each measurement subdivided by cell size. The sum of the number of cells per cell size was determined for each sample and this enabled the mean distribution of each cell size (%) to be calculated for each sample. The cell size distribution (%) was used as a measure of cell size, instead of the absolute cell number subdivided by cell size, because the cell numbers were different in each sample. Using the mean cell size distributions per sample, the overall mean sample size for the 11 samples was calculated.

3.3.6. Flow cytometric characterisation of BMMNC

Flow cytometry was performed to determine the expression of relevant cell surface markers on isolated BMMNC prior to cell injection. Surface marker characterisation of donor cells in the coronary effluent was also performed to determine whether cell populations with particular cell surface markers were preferentially retained.

Based on previous reports (see Introduction), this project examined CD11b, CD18, CD29, CD31, CD34, CD44, CD45 and CD90. For each analysis, 1×10^6 BMMNC were placed in separate 1.5 ml eppendorf tubes and suspended in 100 µl of FACS buffer (see 3.2). The relevant primary antibody at an optimised concentration was added to each eppendorf tube and incubated on ice for 30 minutes. The antibodies used with their relevant controls are also described in Table 3-1. The eppendorf tubes were washed three times with FACS buffer; this was performed by aspirating the solution down to the pellet, resuspending in 1000 µl FACS buffer and resuspended in 100 µl of FACS buffer. When the primary antibodies were not conjugated with fluorescent markers, the appropriate secondary antibody was added (see Table 3-1), incubated on ice for 30 minutes and the samples were again washed three times with FACS buffer prior to analysis. To minimize background signal from secondary antibody administration, samples were treated with 5 µg/ml anti rat FAB antibody (Polyclonal goat FAB anti rat Ig (H+L), Southern Biotech, USA, Catalogue Number 3000-01) for 30 minutes, followed by 3 times washing with FACS buffer, before secondary antibody administration. The samples were then incubated with 0.5 µg/ml Propidium Iodide (BD Pharmingen Catalogue number 55646) at room temperature for 15 minutes[243] and analysis was then performed on a DAKOcyan using Summit 4.3 software.

For data analysis, cells were included in the analysis if they were viable and within the main population of cells. Viability was first determined using Propidium Iodide (PI) staining using the PE-Cy5 (or FL3) channel. The proportion of dead cells measured by Propidium Iodide in all the staining protocols was >90%, a level which is deemed to be acceptable for flow cytometry protocols[244]. Viable cells were then gated and the main

population of cells were selected based on observed using histograms using Forward Scatter (FS) and Side Scatter (SS) on logarithmic scales (Figure 3-1).

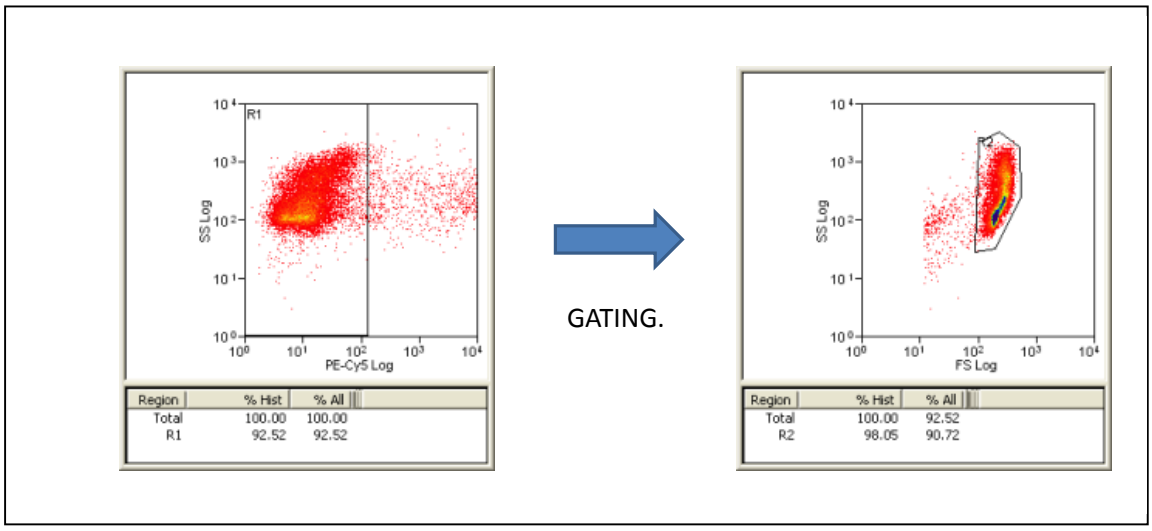

Figure 3-1: Example of selection of BMMNC for flow cytometry using viability, cell size and cell granularity. Unselected BMMNC were incubated with PI and viability (R1) was determined by flow cytometry (DakoCyan flow cytometer and Summit 4.3 software). Viable cells were not stained with PI. Viable cells were then gated and the main population of viable cells were then gated again (R2), according to cell size (forward scatter: FS) and cell granularity (side scatter: SS). In this analysis, 92.5% of cells were viable and 90.7% of the total cells were included in the final analysis.

Analyses for FITC- and PKH67-positivity were analysed on the FITC (or FL1) channel. Alexa-647 labelled cells were analysed on the APC (or FL4) channel. Voltage gating was determined from relevant negative controls. Histograms were generated with the channel of interest plotted against SS (refer to Figure 3-2).

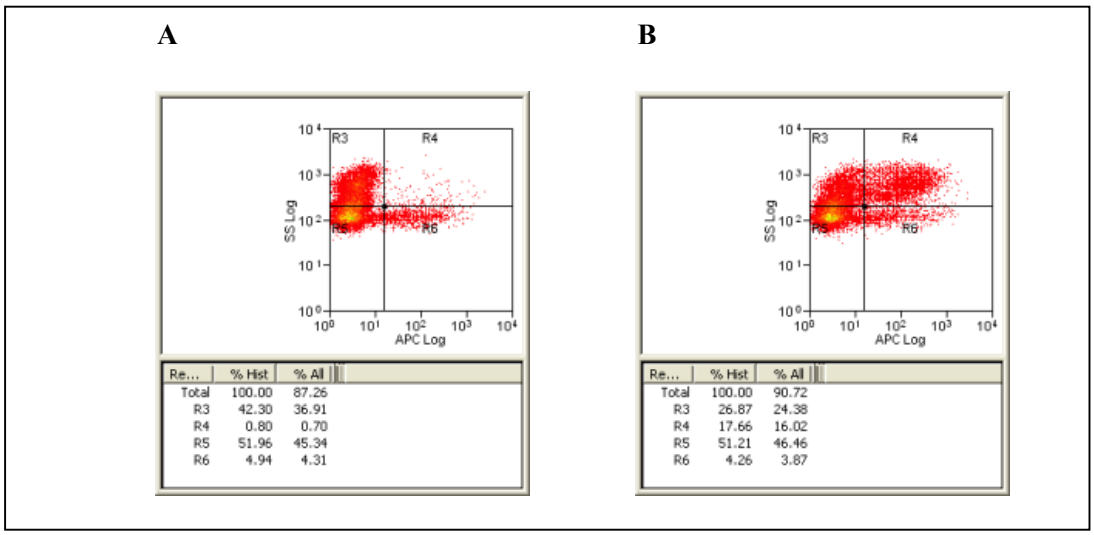

Figure 3-2: Example of quantification of BMMNC surface marker using flow cytometry. A control BMMNC sample was stained with IgA primary antibody and Alexa-647 secondary antibody (A). A separate BMMNC sample was incubated with anti CD11b primary antibody and Alexa-647 secondary antibody (B). Analysis using Dakocyan flow cytometer and Summit 4.3 software. There was a low level (4.9%) of non-selective staining in the control sample (lower right quadrant: R6) and the proportion of this staining was the same (4.3%) in the CD11b sample. Cells in the upper right quadrant (R4) were therefore deemed to represent positivity for CD11b. The proportion of positive cells after CD11b incubation was 16.0% and 0.7% in the control sample. For this sample therefore, CD11b positivity was deemed to be 15.3%.

Table 3-1: Antibodies used for flow cytometry protocols to assess surface markers on BMMNC

	Fluorescent-conjugated	Isotype	Manufacturer	Working Concentration	Control Antibody	Secondary antibody
Primary Antibodies						
CD11b	No	purified monoclonal mouse IgA_k anti-rat CD11b (MAC-1 α chain)	BD Pharmingen, Catalogue: 554980	5µg/ml	IgA	Alexa-647
CD18	No	purified monoclonal mouse $IgG1_k$ anti-rat CD18 (WT.3)	BD Pharmingen, Catalogue: 554977	5µg/ml	IgG	Alexa 647
CD29	Alexa Fluor 647	conjugated monoclonal Armenian Hamster IgG anti mouse and rat (Clone HMβ1-1)	Biolegend Inc., CA, USA, Catalogue 102215	5µg/ml	IgG Alexa 647	N/A
CD31	No	purified monoclonal mouse $IgG1_k$ anti-rat CD31 (TLD-3A12)	BD Pharmingen, Catalogue: 555025	5µg/ml	IgG	Alexa 647
CD34	No	purified monoclonal mouse IgG1 anti rat and human CD34 (ICO115)	Santa Cruz, CA, USA, Catalogue: sc7324	10µg/ml	IgG	Alexa 647
CD44	No	purified monoclonal mouse IgG1 anti rat CD44 (clone OX50).	AbD Serotec, Catalogue: MCA643GA	10µg/ml	IgG	Alexa 647
CD45	No	purified monoclonal mouse $IgG1_k$ anti-rat CD90 (LCA, clone OX-1)	BD Pharmingen Catalogue: 554875	5µg/ml	IgG	Alexa 647
CD90	No	purified monoclonal mouse $IgG1_k$ anti-rat CD90 (clone OX-7)	BD Pharmingen, Catalogue: 554895	5µg/ml	IgG	Alexa 647
Secondary Antibodies						
Anti-mouse IgG Alexa-647		Goat anti-mouse IgG (H+L) highly cross-adsorbed	Invitrogen A21235	20µg/ml		
Control Antibodies						
IgA_k	No	purified mouse IgA_k isotype control Clone M18-254	BD Pharmingen Catalogue 553476	5µg/ml		Alexa 647
IgG_k1	No	purified mouse IgG_k1 isotype control Clone MOPC-31C	BD Pharmingen Catalogue 557273	5µg/ml		Alexa 647
IgG	Alexa Fluor 647	Armenian Hamster IgG isotype control USA (clone ebio299arm)	ebioscience Catalogue 50-4888	2µg/ml		N/A

3.4. Mesenchymal Stem Cells (MSC)

3.4.1. Isolation, culture and passaging of MSC

MSC were isolated from bone marrow of adult Sprague Dawley rats (6-8 week old males; purchased from Charles River, UK) as previously described[73] with modifications. Whole bone marrow cells were isolated as described for BMMNC above (refer to 3.3.1), excluding the gradient centrifugation steps. Collected whole bone marrow cells were placed in 25cm^2 flasks (Nunc) with an initial plating concentration of approximately 1×10^6 cells/cm^2, cultured in αMEM (Gibco) with 20% inactivated fetal bovine serum (FBS) containing L-glutamine (200 mM), penicillin (100 U/ml) and streptomycin (100 mg/ml); (Sigma, catalogue T3924), at 37°C in a humidified atmosphere containing 95% air / 5% CO_2. (incubator: Binder, Germany).The culture medium was aspirated and changed every 48-72 hours without additional washing. When cell confluency reached 80-90%, cells were passaged by detachment using 0.25% Trypsin / 0.2% EDTA (Sigma, catalogue T3924). Plating concentrations for subsequent passages were approximately 2.5×10^4 cells/cm^2.

3.4.2. Morphology of MSC

The morphology of cultured MSC was assessed using phase contrast light microscopy (Nikon TMS) over progressive passaging. Images were acquired with a Nikon Coolpix 2500 x4 magnification at passage 0, passage 1, passage 2 and passage 3.

3.4.3 Cell size of collected MSC

Collected MSC were suspended in PBS and analysed for cell size using a Countess Automated Cell Counter (Invitrogen, UK) as described (refer to 3.3.5). Cells smaller than 5 μm were not included in the final analysis, as they were deemed to be debris and the Automated Cell Counter is recommended by the manufacturers for cell analysis in the size range of 5 – 60 μm. The following settings for analysis were used (Sensitivity: 85.0, Min Cell Size 5 μm, Max Cell Size: 60μm, Circularity 80).

For cell size analysis of passage 2 cells, n=17 separate 175cm^2 flasks, in which MSC were cultured, were analysed. For passage 3 cells, 7 different 175cm^2 flasks were analysed. For passage 4 cells, 9 different 175cm^2 flasks were analysed. Each measurement was imported into the Countess Automated Cell Counter software (Invitrogen, UK) and analysed as described (refer to 3.3.5) for each passage.

3.4.3. Cell surface marker expression of MSC

Expression of CD29, CD34, CD45, and CD90[245] (refer to 1.3.3) in collected MSC were assessed by flow cytometry[246]. 3×10^5 MSC at passage 5 were placed in Protein Lobind 1.5 ml eppendorf tubes (Sigma, Dorset, England); it was found that this led to a lower rate of MSC loss following centrifugation. MSC were subjected to the same antibody staining conditions as described for BMMNC (refer to 3.3.6) using the antibodies described in Table 3-2. Following staining, all cells were stained with Propidium Iodide for 15 minutes prior to analysis (final concentration 0.5μg/ml; BD Pharmingen). Analysis was performed as described for BMMNC (refer to 3.3.6).

Table 3-2: Antibodies used for flow cytometry to assess the surface expression of proteins on cultured MSC

	Fluorescent-conjugated	Isotype	Manufacturer	Working Concentration	Control Antibody	Secondary antibody
Primary Antibodies						
CD29	Alexa Fluor 647	conjugated monoclonal Armenian Hamster IgG anti mouse and rat (Clone HMβ1-1)	Biolegend Inc., CA, USA, Catalogue 102215	5µg/ml	IgG Alexa 647	N/A
CD34	No	purified monoclonal mouse IgG1 anti rat and human CD34 (ICO115)	Santa Cruz, CA, USA, Catalogue: sc7324	10µg/ml	IgG_k1	Alexa 647
CD45	FITC	Conjugated purified monoclonal mouse IgG anti-rat CD45	chemicon international Catalogue: cb1502f	5µg/ml	IgG	N/A
CD90	FITC	Conjugated purified monoclonal mouse IgG1 anti-rat CD90/thy1 (OC-7 clone)	Abcam, Catalogue: ab226-100	1µg/ml	IgG	N/A
Secondary Antibodies						
Anti-mouse IgG Alexa-647		Goat anti-mouse IgG (H+L) highly cross-adsorbed	Invitrogen A21235	20µg/ml		
Control Antibodies						
IgG	Alexa Fluor 647	Armenian Hamster IgG isotype control USA (clone ebio299arm)	ebioscience	2µg/ml		N/A
IgG_k1	No	purified mouse IgG_k1 isotype control Clone MOPC-31C	BD Pharmingen Catalogue 557273	5µg/ml		Alexa 647
IgG1	FITC	Conjugated mouse IgG1 negative control	Abd serotec mca928a488f	5µg/ml		N/A

3.4.4. Differentiation capacity of MSC

At passage 3, the differentiation potential of MSC into adipocytes and osteocytes was examined to confirm the identity of the cells. Adipogenic differentiation assays were performed with cells plated[246,247] at 2×10^4 cells/cm^2 in a base medium (α-MEM containing with15 % FBS and penicillin (100 U/ml) and streptomycin (100 mg/ml), supplemented with 100 μM isobutyl methylxanthine (Sigma-Aldrich I7018), 60 μM indomethacin (Sigma-Aldrich, I7378), 1 μg/ml human insulin (Sigma, catalogue: I9278) and 0.5 μM hydrocortisone (Sigma-Aldrich, H0135)[73]. Osteogenic differentiation assays were performed with plated cells[246,247] at 3×10^3 cells/cm^2 in a base medium supplemented with 0.1 μM dexamethasone (Sigma-Aldrich, D4902), 10 mM B-glycerophosphate (Sigma-Aldrich, G9422) and 0.05 mM ascorbic acid (Sigma-Aldrich, A4403)[248]. Immediately following plating of passage 3 cells, cells were incubated with the differentiation media. Controls were set up using MSC plated with the same cell concentration in a base medium without supplementation. Assays were performed in 6 well plates (Nunc). The medium was changed every 48-72 hours and differentiation was analysed by the methods described below on day 21. The controls were also cultured for 21 days and subjected to the same staining procedures.

Adipogenic differentiation was assessed by Oil-Red-O staining with counterstaining using haematoxylin. Oil–red-O staining solution was prepared (see 3.2) and used within 2 hours. The cells were washed with PBS twice and fixed with 4% PFA for 10 minutes at room temperature. They were further washed three times with PBS and the cells were then incubated with 60% isopropanol solution for 1 minute. That solution was discarded and the cells were then incubated with the Oil-O-Red solution for 10 minutes at room temperature. The cells were washed once with 60% isopropanol (Sigma, catalogue: I9516) and then three times with double distilled water. The cells were then counterstained with haematoxylin

1g/L (Sigma-Aldrich catalogue MHS16) for 5 minutes, rinsed in distilled water and then observed by a microscope (BZ7000, Keyence).

Osteocyte differentiation was confirmed by co-localization of alkaline phosphatase staining with Alizarin Red (for calcium deposition). The cells were washed twice with PBS, fixed with 4% PFA for 10 minutes and washed with distilled water for a further 3 times. To detect alkaline phosphatase, BM Purple (No 11442074001, Roche) was added to the cells and incubated at room temperature for 1 hour. The cells were then washed again with double distilled water three times. The cells were then incubated in Alizarin Red solution (refer to 3.2) until the colour became visualized (for 30 seconds – 5 minutes). The cells were further washed with double distilled water, counter stained with haematoxylin for 5 minutes and then observed by a microscope (BZ7000, Keyence).

3.5. Labelling of donor cells

3.5.1. Choice of PKH67 for donor cell labelling

Labelling of donor stem/progenitor cells is required for their clear discrimination from recipient heart cells after transplantation, particularly in histological studies. PKH67 was chosen among various types of commercially available dyes based on its high-efficiency and strong labelling of a range of cell types, sufficiently-long half-life (10-12 days), low cell-toxicity[249], utility for fluorescent microscope studies[250] and previous reports using it for tracking cell fate following IC injection in vivo[183,251].

3.5.2. PKH67 staining of BMMNC

The labelling condition for BMMNC using a PKH67 labelling kit (Sigma; MIDI67) was optimized as follows. Freshly isolated BMMNC were washed in PBS and re-suspended in 1 ml Diluent C (Sigma) at a concentration of 2×10^7 cells/ml. Then 1 ml of double the final required concentration of PKH67 was added to the cell suspension and mixed gently with a pipette. Final concentrations of 0 μM (control), 2 μM for 5 minutes and 2 μM for 10 minutes were tested (2 μM is the final concentration recommended by the manufacturers). 2 ml FBS (Sigma-Aldrich, Dorset, UK) was then added and incubated for 2 minutes to stop the staining reaction. The cell-dye mixture was then centrifuged at 400g for 10 minutes and resuspended in 10 ml PBS. The solution was transferred to a new tube (to remove residual dye bound to the tube walls) and washed in PBS. All reactions were performed at room temperature with the cells shielded from light. Then, the viability of the cells was assessed with trypan blue staining (Sigma). For this, cells were counted using a haemocytometer (Hawksky, UK); the number of cells in the four outer quadrants was counted and the percentage of non-blue (viable) cells to total cells was calculated. The efficiency of PKH67

staining was determined by fluorescent microscopy and bright field imaging (BZ7000, Keyence); the proportion of PKH positive cells to the total number of cells was calculated.

3.5.3. Possible changes in BMMNC surface marker expression by PKH staining

PKH67 is a cell-membrane labelling dye, and this might affect the surface marker expression of BMMNC. To assure that this was not the case, PKH67-stained cells and unstained cells were subjected to flow cytometric analysis as described above (refer to 3.3.6).

3.5.4. PKH staining of MSC

For optimization of PKH staining of MSC, passage 3 MSC were obtained in a similar fashion to cell passaging using trypsinization. The labelling condition for MSC using a PKH67 labelling kit (Sigma; MIDI67) was optimized as follows. Cultured MSC were washed in PBS and re-suspended in 1 Diluent C (Sigma) at a concentration of 2×10^7 cells/ml. Then 1 ml of double the final required concentration of PKH67 was added to the cell suspension and mixed gently with a pipette. Final concentrations of 0 μM (control), 2 μM for 5 minutes and 2 μM for 10 minutes were tested (2 μM is the final concentration recommended by the manufacturers). 2 ml FBS (Sigma-Aldrich, Dorset, UK) was then added and incubated for 2 minutes to stop the staining reaction. The cell-dye mixture was then centrifuged at 400g for 10 minutes and resuspended in 10 ml PBS. The solution was transferred to a new tube (to remove residual dye bound to the tube walls) and washed in PBS. All reactions were performed at room temperature with the cells shielded from light. Then, the viability of the cells was assessed with trypan blue staining (Sigma). For this, cells were counted using a haemocytometer (Hawksky, UK); the number of cells in the four outer quadrants was counted and the percentage of non-blue (viable) cells to total cells was

calculated. The efficiency of PKH67 staining was determined by fluorescent microscopy and bright field imaging (BZ7000, Keyence); the proportion of PKH positive cells to the total number of cells was calculated.

3.6. The isolated Langendorff-perfused heart model – normal rat heart model

The Langendorff-based, isolated, perfused heart model is a popular, well-established model in cardiovascular research, which has been used for several decades[209,210,240]. Use of an isolated *ex-vivo* heart ensures the absence of confounding effects from other organs and circulating factors such as clotting factors and neurohormonal substances. I applied this method for quantitative measurement of initial donor cell retention after IC cell injection in rats. This section describes the Langendorff perfusion technique using normal rat hearts.

3.6.1. Langendorff apparatus assembly

A photograph of the glassware, thermometer, 3-way tap and clips are shown in Figure 3-3.

Figure 3-3: Langendorff equipment utilized for the project. (A) large warming reservoir for warming and oxygenating K-H buffer, (B) example of a clip to secure glassware, (C) small warming reservoir for warming K-H buffer, (D) warming jacket around heart, used for I-R protocols (E) oxygenator placed within A, (F) Three-way tap, (G) example of large clip to secure glassware.

Water-jacketed glassware was utilized to form the reservoir to warm the buffer; the inner lumen contained the buffer for heart perfusion, whereas the outer lumen was subjected to a continuous flow of warmed double distilled H_2O. Three pieces of glassware were used and positioned in series; a 35cm large upper reservoir which contained a volume of buffer of approximately 400 ml was sited at the highest point (Figure 3-4). Perfusate in this reservoir was supplied with oxygen/CO2 via an oxygenator. This was connected via nylon tubing to a 30cm lower reservoir with a narrower diameter (with an inner lumen volume of approximately 50mls). Below the lower reservoir, a three way tap was connected with further tubing. A three-way cannula was attached to this tubing and a 14 gauge ridged cannula (Harvard) was connected to the lower aspect of this. Sited below the cannula, a

double lumen water jacked was placed which could be raised upwards to the level of the cannula. This was used to submerge the heart and maintain its stable temperature during ischaemia-reperfusion.

A waterbath and pump (Techne TE10A tempette) was used to heat and circulate the double distilled water continuously. The water circuit and pump were connected to the outer lumens of the reservoirs and the water jacket in series. The set-up of the equipment is shown in Figure 3-4. A graphical representation of the Langendorff apparatus is shown in Figure 3-5.

A

B

C

Figure 3-4: Photographs of set-up of Langendorff equipment. (A) The upper reservoir is seen at the top of the image held by two clamps. The lower reservoir is seen at the bottom aspect of the image also supported by one of two clamps. Plastic tubing connects the two reservoirs. (B) The lower reservoir, the three way tap and the water jacket were lined up in series. Below the lower reservoir, the three way tap (C) was sited. This was used to administer donor cells via the side port.

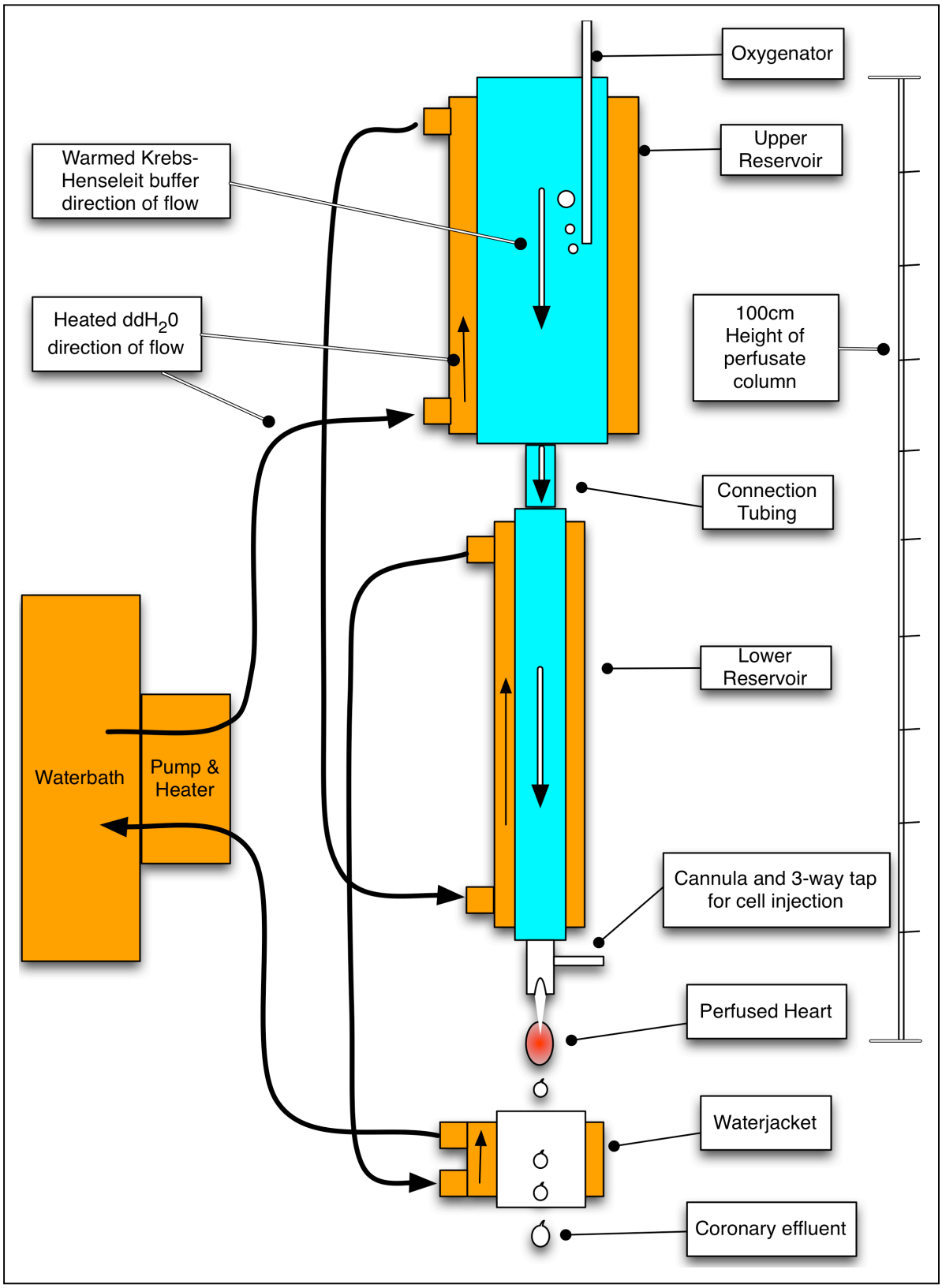

Figure 3-5: Diagrammatic representation of ex-vivo Langendorff apparatus.

3.6.2. Krebs-Henseleit buffer

Under the Langendorff unit, the isolated hearts were perfused with modified Krebs-Henseleit buffer (refer to 3.2)[240]. This was utilized within 24 hours after generation. The buffer was gassed with continuous 95% O_2 /5% CO_2 (BOC) and maintained at 37^{o}C. pH analysis using pH strips (VWR, Catalogue: 1.09584.1111) confirmed that the buffer pH was 7.4 at the cannula tip.

3.6.3. Dissection, cannulation and perfusion of the rat heart using a Langendorff unit

Male Sprague-Dawley rats (200-300g) were purchased from Charles River, UK and weighed using a set of high precision scales (KERN PCB 1000-1, Ballingen, Germany). Rats were anaesthetized with isoflurane anaesthesia (Isoflo 100%, Abbott, USA) and administered with heparin via the intraperitoneal approach (Leo Pharma, FL, USA: 100 iU/kg). After 5 minutes (by which time the anticoagulant was macroscopically effective), cervical neck dislocation was performed, and a median sternotomy was performed. The heart was excised, placed immediately in ice-cold modified Krebs-Henseleit buffer and taken for immediate cannulation. A careful incision of the aorta was made at the level of the aortic arch enabling the ascending aorta to be cannulated with a blunt ended 14-gauge needle (Harvard) with the use of microscopy angled forceps. The aorta was temporarily clipped to the cannula and, once appropriate perfusion was confirmed, the aorta was secured to the cannula with a 5-0 silk suture (Bear, Japan). A small cut was made in the proximal pulmonary artery to ensure that coronary effluent could drain freely. The heart was then fully perfused by the warmed, gassed modified Krebs-Henseleit Buffer at a constant pressure manually maintained at 95-105 cmH_2O. The perfused heart temperature was measured using a thermometer (Testo 925) with a fine wire probe (Testo 0602 0493). The equipment used for this procedure is described (Figure 3-6).

It was important to minimize the time from heart removal to establishment of *ex-vivo* perfusion, because during this time hearts suffers ischemia. Following considerable training and practice, I was able to achieve this within 120 seconds of neck dislocation and frequently within a shorter time period.

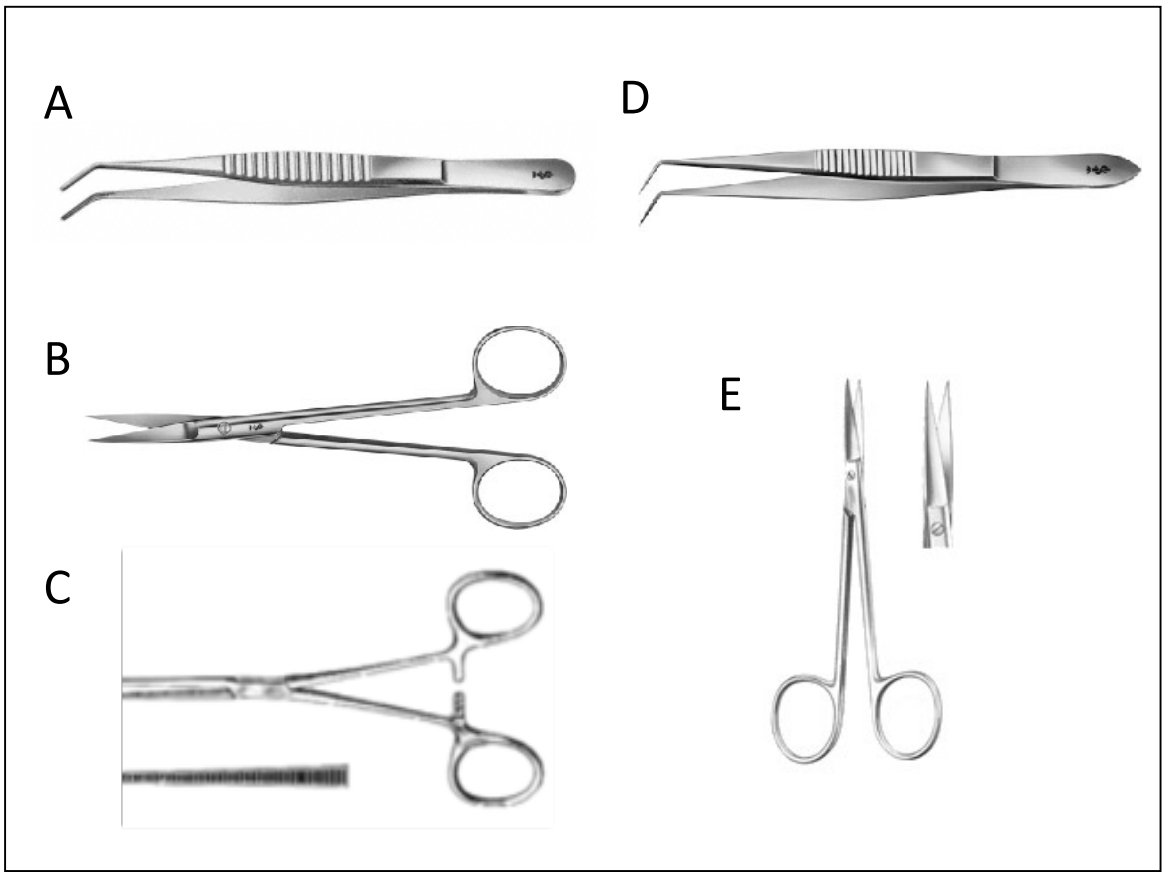

Figure 3-6: Surgical equipment used during the project for Langendorff heart cannulation. *(*(A) DeBakey Dissecting Forceps, FB401R, Aesculap (USA), 2mm wide, 150mm. (B) Joseph Straight Scissors, BC156R, Aesculap (USA), 150mm (C) Kocher 14cm Forceps, 914-0370, Gowllands Medical Devices Ltd (UK), (D) 100mm Microscopy Angled Forceps (n=2) BD321R, Aesculap (USA), (E) 12 cm straight Eye Scissors, 03-320-115, Allgaier instrumente (Germany). Instruments A-C were used for removal of the heart from the mediastinum. Instruments (D, n=2) and (E) were used to hang the heart on the Langendorff apparatus. (A) and (B) were used to perform the median sternomy. (C) was used to clip and reflect the sternum superiorly to expose the heart. (A) and (B) were then used to careful remove the heart from the mediastinum at the level of the aorta. The heart was then placed in ice-cold Krebs-Henseleit buffer. Extraneous heart tissue was used using (E) with manipulation by (D) and then the heart was hung on the Langendorff apparatus using two examples of (D).

3.6.4. Confirmation of appropriate heart perfusion

Stable heart perfusion was confirmed by the consistent and appropriate volume of coronary effluent, pH of coronary effluent, stable appropriate heart rate measured by continuous ECG monitoring, and appropriate heart beating and contractility. Unlike some Langendorff perfusion protocols[216,240], we opted not to utilize cardiac pacing to maintain heart rates; cardiac pacing might potentially mask imperfect perfusion and the absence of pacing would enable physiological heart rates with sinus rhythm and other haemodynamic parameters to be monitored.

ECG recording was made (BIOPAC System MP35) with electrodes (BIOPAC systems, SN410A201) to record the heart surface ECG. Analysis was undertaken using BSL Pro 3.7 software (BIOPAC systems). The positive electrode was clipped to the aortic cannula and both the negative and neutral electrodes were held gently against opposite walls of the LV. Heart rate was determined by measuring the mean R-R interval of 10 consecutive beats (see Figure 3-7).

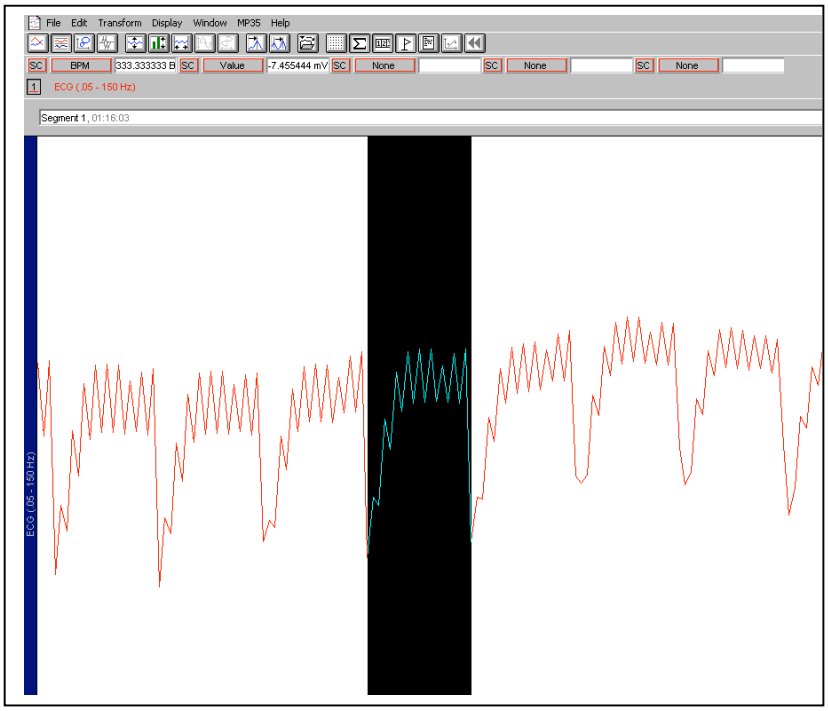

Figure 3-7: Surface ECG analysis of Langendorff rat heart. BSL Pro 3.7 software (BIOPAC Systems) was used with the aid of a positive electrode clipped to the aortic cannula and two negative electrode positioned either side of the LV. The R-R interval - highlighted in black – has been computed to represent 333 beats per minute (shown top left). 10 consecutive R-R intervals were measured and the mean of these measurements was used to represent heart rate at any particular time.

3.6.5. Coronary effluent collection and counting contaminating cells

Coronary effluent was collected by holding a 50 ml Falcon tube directly under the perfused heart for 60 seconds. Serial collections of coronary effluent were made at specific time points. The number of cells passing into the coronary effluent per minute was assessed by determining the mean cell concentration (cells/ml) of two measurements, using either a haemocytometer (Hawksky, UK) or a Countess Automated Cell Counter (Invitrogen, UK). This concentration was then multiplied by the coronary effluent volume.

3.6.6. RBC leakage into coronary effluent

Unexpectedly, a countable number of cells were observed in the coronary effluent without donor cell injection. These cells were assessed further. Five minutes after hanging the heart, the coronary effluent was collected, smeared on a Polylysine slide glass (Thermo Scientific) and air dried for 30 minutes (as described in 3.3.4). They were then fixed by briefly placing the slides in a Coplin Jar containing 100% methanol (Fisher Chemical, catalogue M/3950/PC17) and further air dried. The cells were then incubated with Haematoxylin (Sigma-Aldrich, catalogue: MHS16) for 5 minutes at room temperature. After washing with water, the slides were dried and observed by light microscopy (BZ7000, Keyence). The cells were found to have the typical morphology of RBC (refer to 3.3.4). Confirmatory evidence that the cells were not nucleated was obtained using DAPI staining. As detailed in 3.3.4, coronary effluent cells were smeared on a Polylysine slide glass and air dried for 30 minutes. The cells were then fixed with PFA 4% for 15 minutes at room temperature. After 3 washing steps with PBS, the cells were stained with DAPI (1:1000 in PBS) for 5 minutes followed by a further 3 washing steps. The slides were then mounted and viewed using a fluorescent microscope (BZ7000, Keyence). Control images were obtained for isolated BMMNC (without injection into the heart) which were fixed and stained using the same protocol. We serially counted the number of the RBC contained in the coronary effluent and found that the number of RBC decreased with time after perfusion. This number was less than 5×10^4 cells/min, a figure much lower than the donor cell number in the coronary effluent by the time of IC cell injection (refer to 4.3.3).

3.6.7. IC cell injection into Langendorff-perfused hearts

After 20 minutes stabilization of Langendorff perfusion, donor cells were administered into the isolated beating heart. At this time, the hearts were usually stably perfused with showing stable perfusion parameters such as coronary flow, heart rate, and regular sinus rhythm without arrhythmias. In addition, the number of RBC counted in the coronary effluent after 20 minutes was low enough for the project's purposes (refer to 4.3.3). That is to say, after cell injection, the donor cells would make up the great majority of cells in the coronary effluent; RBC would therefore only make a trivial contribution to the total coronary effluent cell number.

A designated number of donor cells (either BMMNC or MSC) were suspended in 3 ml PBS and injected into the heart from a side port (3-way tap) of the aortic cannula using a 5 ml luer-lock syringe (BD Syringe, Catalogue: 301027). Cell injection was performed over 20 seconds. It was opted to use this timing because the mean coronary flow rates immediately prior to injection were approximately 9 ml/min (refer to 4.3.1) and injecting 3 ml PBS cell solution over 20 seconds would therefore not substantially modify the coronary effluent flow rate. During injection, the aortic valve remains physiologically closed and all cells pass through the coronary circulation. The donor cells therefore enter the right and left coronary arteries.

Donor cell number injected: It was important for the project to utilize a range of cell doses which mimic those used in clinical trials; weight adjusted for rat hearts. For clinical studies of IC injection of BMMNC, the cell number IC injected typically ranged from $\leq 1\times10^{8}$ (for example, the ASTAMI study[154]), $\leq 1\times10^{9}$ (REPAIR-AMI,[46] Janssens et al,[45] Huang et al[252]) and to $\leq 1\times10^{10}$ (Kang et el,[156] the BOOST study[43,253]). In contrast to our model where cells were injected into all the major coronary arteries (right, left anterior descending and left circumflex), clinical trials usually injected the cells into a single coronary artery. The assumption was made that the median cell number used in clinical trials was 1×10^{9}

BMMNC for a 75kg human and that a rat's weight is 200g. Therefore the equivalent dose for a single rat artery would be 2.7×10^6 BMMNC, or 8×10^6 BMMNC injected into all three arteries. Based on this calculation, we decided to investigate the 3 BMMNC numbers; 1×10^6, 8×10^6 and 40×10^6.

Negligible donor cells retained in the Langendorff apparatus itself*:* This system was designed so that the dead space for cell injection was minimized (<20 μl). To confirm whether donor cells were retained in the Langendorff apparatus itself or the injection syringe/needle, 8×10^6 BMMNC suspended in 3 ml PBS were injected into the side port of the apparatus as described, without heart cannulation/perfusion (n=3). Subsequently warmed, oxygenated Krebs-Henseleit buffer was flushed through. All the flushed effluent was collected in a 50 ml Falcon tube and the cell concentration in the effluent was determined using a Countess Automated Cell Counter (Invitrogen, UK) to count the donor cell number flushed out. As a result, it was confirmed that no donor cells were retained in the Langendorff apparatus, injecting syringe or aspiration needle and that no cells ruptured during the injection process. (refer to 4.3.4).

3.6.8. Coronary effluent cell counting and calculation of retention efficiency

Coronary effluent cell concentrations (cells/ml) were assessed using a haemocytometer (Hawksky, UK) or a Countess Automated Cell Counter (Invitrogen, UK). The coronary effluent flow rate (ml/min) was noted and utilized to calculate the Coronary Effluent Cell Count at each minute (cells/min). At the same time, size of cells was measured by using a Countess Automated Cell Counter. All measurements were made in duplication.

Because it was noted that there was a low level of RBC contamination in the coronary effluent at the time of donor cell injection, a formula was developed to remove this contaminating factor, for the precise quantification of donor cell loss in the coronary

effluent, as below. Given that the RBC counts in the coronary effluent slowly decreased over time, it was decided to take a Baseline RBC Count which was the mean of the RBC count in the 1 minute immediately preceding cell injection and the count at 5 minutes following cell administration. It was confirmed that almost 100% of BMMNC leakage from normal hearts occurred within 5 minutes (refer to 4.4.2). Therefore, the **Coronary Effluent Donor Cell Number** in each minute was calculated at each minute after injection by the following formula:

(**Coronary Effluent Cell Count**) - (**Baseline RBC Count**)

Total Donor Cell Number in the Coronary Effluent within 5 minutes was thus calculated as the sum of all included Coronary Effluent Donor Cell Number, for each of the first five minutes. If the Coronary Effluent Donor Cell Count value was negative, it was deemed that all the donor cells had exited the heart. The value for that minute and subsequent minutes were not included in subsequent analyses. Finally, **Donor Cell Retention Efficiency** (%) was calculated as follows:

$$\frac{\textbf{(Injected Donor Cell Number) – (Total Donor Cell Number in the Coronary Effluent)}}{\textbf{(Injected Donor Cell Number)}} \textbf{ x 100}$$

A simplified version of the model for assessing donor cell retention is shown in Figure 3-8.

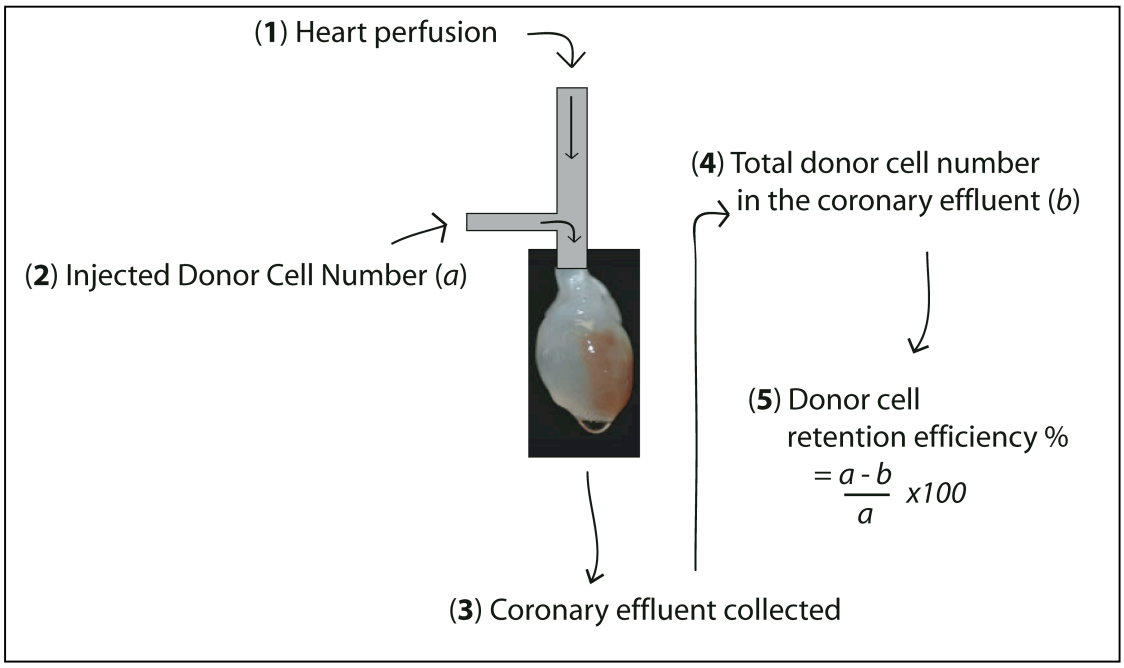

Figure 3-8: Simplified version of modified ex-vivo Langendorff model for quantification of cell retention.

3.7. Ischaemia-Reperfusion (I-R) heart model

It was hypothesised that I-R injury would change the expression of adhesion-related molecules on the coronary endothelium, or change the status of the microvasculature, and that therefore donor cell retention after IC injection would be affected. After stable heart perfusion with a Langendorff apparatus was achieved as described (refer to 3.6.3), global ischaemia was induced by the total cessation of coronary flow by closing the 3-way tap. Normothermia was maintained by submerging the hearts in non-oxygenated Krebs-Henseleit buffer in glassware within the Langendorff circuit, which satisfactorily maintained the heart temperatures between 36-37^{o}C[254,255].

After 30 minutes, the warmed Krebs-Henseleit buffer was drained and coronary flow was re-established by opening the 3 way tap. Hearts were carefully monitored for

ventricular fibrillation which was terminated by manual heart compression between forceps. Heart rate and coronary effluent data were collected at 10, 20 and 30 minutes of reperfusion. The chosen numbers of donor cells were injected into the heart at 30 minutes of reperfusion.

3.8. Immunohistochemical assessments

3.8.1. Immunohistochemistry of donor cell retention

The hearts injected with 8×10^6 PKH67-labelled BMMNC were collected at a set time points (5 or 60 minutes) following IC cell injection, and immediately placed in ice-cold modified Krebs-Henseleit buffer. Promptly, three transverse segments of equal thickness were cut from apex to base and the specimens were incubated in 4% ice-cold PFA for 1 hour, followed by overnight incubation in 30% sucrose at 4^{o}C. These segments were then rapidly frozen in Optimum Cutting Temperature (OCT) compound (VWR International, 361603E) using liquid nitrogen, from which 7.5 μm transverse cryosections were cut using a cryostat (OTF5000, Bright). Cryosections were allowed to air dry for 60 minutes at room temperature and then stored at -80^{o}C or in liquid nitrogen until analysis.

For immunohistochemistry, samples were brought up to room temperature and incubated in PBS at room temperature for 5 minutes, which was repeated 3 times to remove the OCT compound. A DAKO pen (DAKO) was used to mark the boundary of the section. Following incubation with blocking solution (10% goat serum [Gibco 16210-064]) in PBS for 60 minutes. The sections were incubated with 1/100 Biotinylated *Griffonia* (*Bandeiraea*) *Simplicifolia* Lectin I Isolectin B4 antibody (Vector laboratories, 0.5mg/ml, catalogue number B1205) in 5% goat serum for 60 minutes. Isolectin-B4 is useful as a marker for endothelial cells[256] from non-primates such as mouse, rat, rabbit, and goat and has been used

to characterize the localization/distribution of retained donor cells. After washing 3 times in PBS, this was followed by incubation with 1/400 dilution of Streptavidin - Alexa 594 (Invitrogen, UK, 2 mg/ml, Catalogue number s32356), together with 1/1000 dilution of 4'6-Diamidine-2'phenylindole dihydrochloride (DAPI, Roche, Catalogue: 10236276001) for nuclear counterstaining, for a further 60 minutes. Washing steps and antibody dilution were performed with PBS. All the staining reactions were performed at room temperature. The sections were mounted using DAKO fluorescence mounting medium (Catalogue: SC3023) and observed using fluorescent microscopy (BZ7000, Keyence) with DAPI-B (blue), GFP (green) and TxRed (red) filters (Keyence).

Each segment (apex, mid section, base) was analysed separately per heart. One section of each segment was viewed in detail and each PKH67 positive cell was counted. The location within the ventricular wall was noted: endocardium, myocardium or epicardium (divided by eye into 3 equal proportions (Figure 3-9).

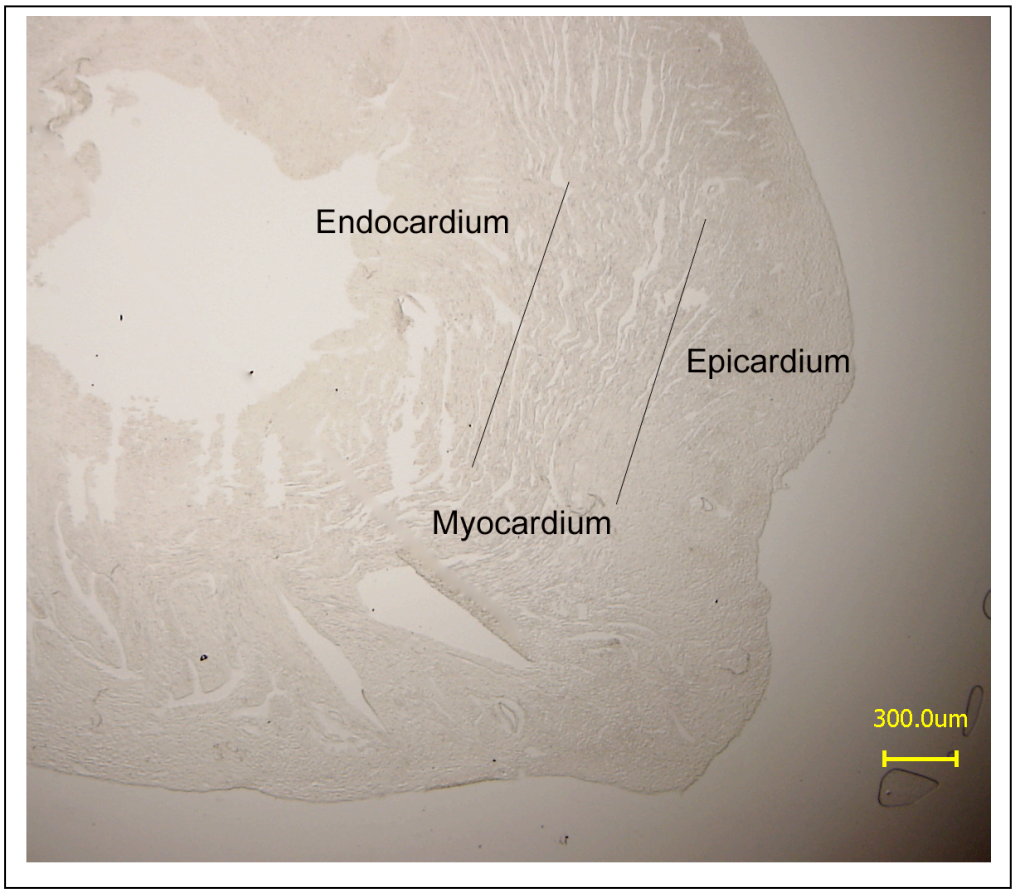

Figure 3-9: Determination of location of fluorescently-labelled donor cells in the ventricular wall. The location of PKH67-labelled donor cells in the ventricular wall was determined by dividing the wall into three layers by eye: endocardium, myocardium and epicardium.

A number of bright field images of each section on low magnification were taken and the images were combined using the Photomerge software function in Photoshop CS2 (Adobe). The magic wand software feature was then used to remove the background. These compound images were then imported into Image J software so that the merged images could be analysed (the Keyence Microscope analysis software does not have a capability to analyse merged images in this fashion).

Analysis in ImageJ was undertaken as follows: an image with a known distance scale was loaded, a line was drawing to mimic the scale and "Analyse -> set scale" was selected; the known distance and units were then entered. The image was converted to an 8-bit image (Image->Type->select "8-bit") and the threshold was adjusted (Image->Adjust->Threshold)

until the whole image was red. “Set” and then “OK” were then selected and the threshold box was closed. “Analyse->Analyse particles” was selected, the minimum pixel size was changed to 50 and OK was clicked. The cross sectional area result was recorded.

3.8.2. Immunohistochemistry of endothelial cell surface molecules in the heart

Expression of intercellular adhesion-related molecules expressed in the coronary endothelium may be a determining factor of donor cell retention, and this would be affected by I-R injury prior to cell injection. Based on the previous literature (please refer to 1.8.3), we thought that P-selectin and ICAM-1 might have a role in initial retention of donor BMMNC after IC injection. Therefore, the expression pattern of these molecules was investigated in normal as well as I-R hearts.

The rat hearts were perfused on the Langendorff apparatus for at least 20 minutes for stabilisation and collected with or with additional I-R. No donor cells were injected. These perfused hearts were removed, transported in PBS on ice, cut into three segments (apex, mid section and base), then fixed with 4% PFA at room temperature, incubated in 30% sucrose at 4^{o}C overnight, placed in OCT compound and stored at -80^{o}C (as described – refer to 3.8.1). 7.5 μm thick sections were cut using a Cryostat (OTF5000, Bright), allowed to air dry at room temperature for 1 hour and then stored at -80^{o}C prior to analysis.

For immunohistochemistry, samples were brought up to room temperature and incubated in PBS at room temperature for 5 minutes, which was repeated 3 times to remove the OCT compound. A DAKO pen (DAKO) was used to mark the boundary of the section. For antigen retrieval, the sections were placed in 10 mM sodium citrate buffer (pH: 6.0) within Coplin Jars and autoclaved at 121^{o}C for 7 minutes (Boxer Laboratory Equipment, Ware, UK). Once cooled, the sections were washed 3 times with PBS for 5 minutes. Following incubation with blocking solution (10% goat serum in PBS / 0.025% triton X 100,

refer to 3.2) for 60 minutes. The sections were incubated with goat anti-rat P-selectin polyclonal antibody (Santa Cruz, sc-6941, 0.2 µg/ µl; 1/10 dilution), mouse anti-rat ICAM-1 monoclonal antibody (Abcam, Ab33894, 0.1 µg/µl; 1/10 dilution), overnight at 4^{o}C. The following day, the sections were washed 3 times with PBS (5 minutes) and incubated with PBS containing 5% goat serum for 1 hour at room temperature. After 3 time washing in PBS, this was followed by incubation with Alexa Fluor 488-conjugated donkey anti-goat IgG (Invitrogen, A11055; for P-selectin detection) or Alexa Fluor 488-conjugated goat anti-mouse IgG (Invitrogen, A11001; for ICAM-1 detection), respectively, at a concentration of 1/100 diluted in PBS for 1 hour at room temperature, shielded from the light. The sections were washed again and then counterstained for endothelium (Isolectin B4) and nuclei (DAPI) as previous described (see 3.8.1.). The concentration of each antibody was optimized by pilot experiments (data not shown). The sections were mounted using DAKO fluorescence mounting medium and observed using fluorescent microscopy (BZ7000, Keyence).

From previous reports, it was expected that both these molecules would not be detected by immunohistochemistry in normal hearts, and that the expression of P-selectin, but not ICAM-1, would be detectable after 30 minutes ischaemia and 30 minutes reperfusion[213,229]. It has previously been reported that in a cat LCD ligation model, ICAM-1 was detected by immunohistochemistry after 270 minutes reperfusion[230]. Therefore appropriate positive control heart samples for ICAM-1 were generated as follows (with the kind assistance of Dr Masahiro Kaneko, William Harvey Research Institute) to convincingly carry out immunohistochemical studies of ICAM-1.

Positive control samples for ICAM-1 were generated using male Sprague-Dawley rats (220g) purchased from Charles-River. Anaesthesia was induced with 5% isofluorane inhalation and subcutaneous injection of 0.1mg/kg Buprenorphine and maintained with 1.5-2% isofluorane (Abbot, catalogue: B506). The trachea was intubated with an 18G cannula

(Bio-Flon, Catalogue: MMK424) to deliver mechanical ventilation (Vet Tech Solutions, Ltd with Fluorovac, Harvard Apparatus) with 2% isofluorane. The chest wall was shaved, sterilized with ethanol and draped. A small incision was made from the xiphoid sternum towards the left axilla and dissection was performed in layers. The muscles within the 3rd or 4th intercostal space were retracted to gain access to the heart. Using a 6-0 Nylon suture (Bear Medic, Japan, Catalogue: VT08V06H-45), a single bite was taken posterior to the mid left anterior descending coronary artery. Both ends of the suture were passed through a 22G cannula (BioFlon) and the cannula was then slid down the two suture ends, with tension applied to occlude coronary flow. Myocardial ischaemia was confirmed by change in myocardial colour (became pale). After 30 minutes ischaemia, tension on the cannula was released to enable reperfusion. The suture was removed, the intercostal space and skin were both closed with a 4-0 Nylon suture (Bear Medic, Japan, Catalogue: S13G04N-75) and anaesthesia was ceased. The rat was extubated and returned to its cage. Then two hearts each were collected at 270 minutes of reperfusion after cervical dislocation (under isofluorane anaesthesia). The heart was explanted from the chest using the same method of removing the heart for Langendorff perfusion (refer to 3.6.3) and the heart was transported in ice-cold PBS. Then these heart samples were investigated in the same manner as above (refer to 3.8.1).

3.9. Statistical analysis and software utilized

Normally distributed data was expressed as mean ± standard error of the mean (SEM). Where the data was not normally distributed, a median value was quoted. Throughout the thesis, a p value <0.05 was deemed to represent statistical significance.

Data was collated in Microsoft Excel 2007. GraphPad Prism 5.01 and SPSS12.0 were used for the purposes of statistical analysis. When comparing two sets of quantitative data, a paired or unpaired T-test (where appropriate) was utilized. When comparing more than two sets of quantitative data, a one-way ANOVA test was utilized with a Bonferroni post-hoc test. A comparison of two populations was made using non-linear regression a comparison between the two best fitting curves, generated by second-order (quadratic) or third order (cubic) polynomial functions where appropriate; an F-test was then used to compare the curves.

The graphs were generated in GraphPad Prism 5.01, Datagraph 3.0 and Microsoft Excel 2007. Other images were generated using Adobe Illustrator CS2, Adobe Photoshop CS2, Datagraph 3.0, Summit 4.3 and Omnigraffle Professional 5.4. The manuscript was written with Microsoft Word 2011 and Scrivener (Beta version). Endnote X2.01 was used to import references into the document.

Chapter 4 - RESULTS

4.1. Bone Marrow Mononuclear Cell (BMMNC) collection and characterization

4.1.1. Purity, quantity and viability of isolated BMMNC

Rat BMMNC were isolated as previously described (refer to 3.3.1). Efficiency of cell collection, determined by counting the number of isolated BMMNC per animal (n=5) was $3.57 \pm 0.74 \times 10^8$. The viability of isolated BMMNC, determined with Trypan Blue staining (separate isolated samples n=5, total cells measured n=3,254), was 99.4 ± 0.2%.

The nucleation of isolated BMMNC was determined by performing a smear of isolated cells, fixing the cells with 4% PFA and then staining the cells with DAPI. The proportion of mono-nucleated cells in the isolated BMMNC population was calculated as 99.5 ± 0.2% (n=3 different animals). There were a small number of DAPI-negative cells, which were thought to be red blood cells (RBC) (Figure 4-1).

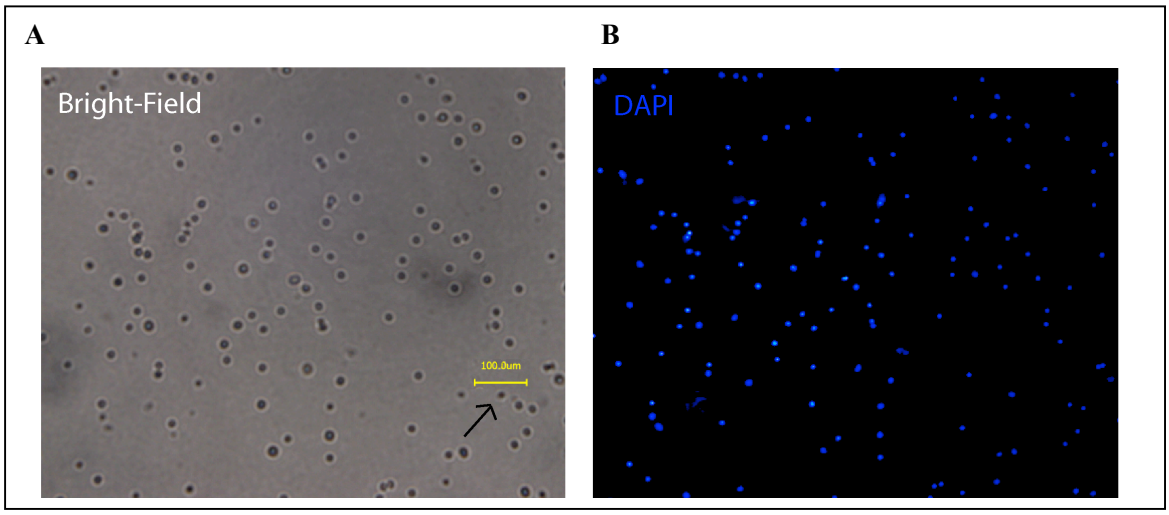

Figure 4-1: DAPI staining of isolated rat BMMNC. Smeared cells were fixed with 4% PFA and stained with DAPI. Bright field (A) and DAPI positive cells (B) are shown. 99.5% of cells had one round nucleus. Rarely, non-nucleated cells (DAPI negative cells) were seen (marked with a black arrow) and thought to be RBC. (Scale bar = 100 μm).

4.1.2. Morphology

Cell morphology of collected rat BMMNC was analysed (Figure 4-2). Cells in suspension were pipetted into a haemocytometer with phase contrast imaging (Biozero microscope, Keyence). To further investigate morphology, cytospin was used to adhere the isolated BMMNC to a slide glass. The cells were then stained with haematoxylin. The majority of the cells were round although there was some heterogeneity. To the eye, the cells were < 10μm in diameter.

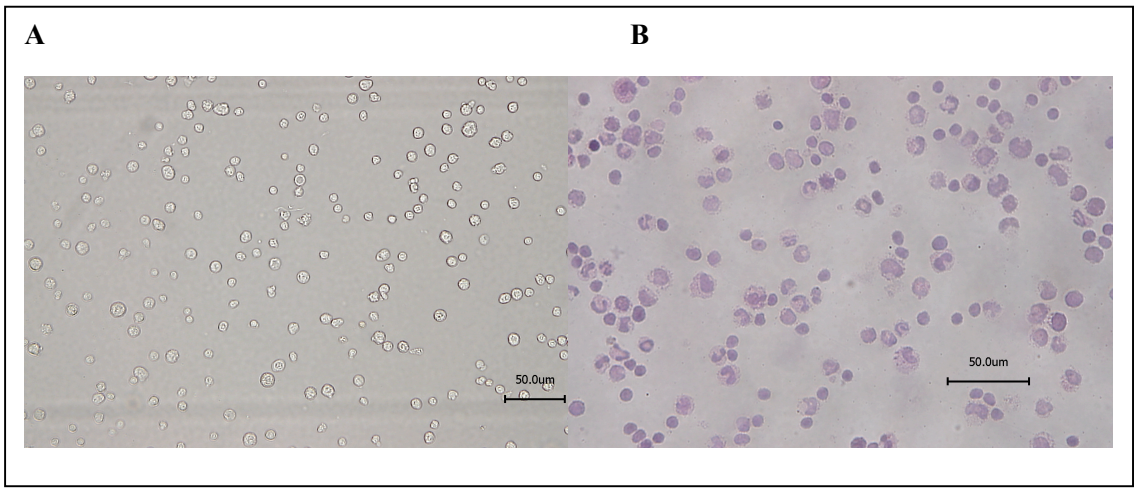

Figure 4-2: BMMNC morphology. BMMNC suspended in PBS were viewed using phase contrast imaging (A). Haematoxylin was used to stain isolated cells subjected to cytospin (B). The majority of the cells were round although there was some heterogeneity in shape. The cells were < 10 μm in size. Scale bar = 50 μm

The size distribution of BMMNC was measured using a Countess Automated Cell Counter (Invitrogen) and calculated from n=11 individual bone marrow samples acquired on different days. Particles < 5 μm were not included in the analysis because they were deemed to be debris. The distribution of cells is shown in Figure 4-3. The mean cell size was 7.0 μm, the median cell size was 7.0 μm and the population had a parabolic distribution with a leftwards skew. Cells ≥14 μm accounted for only 0.8% of the total population. The distribution of cell sizes were grouped into the ranges 5-6 μm, 7 μm and ≥8 μm. Using this categorization, the 3 categories were each approximately of equal size, which suggests that this subdivision broadly classifies cell sizes into tertiles, or cells below the median size, the median size and above the median size.

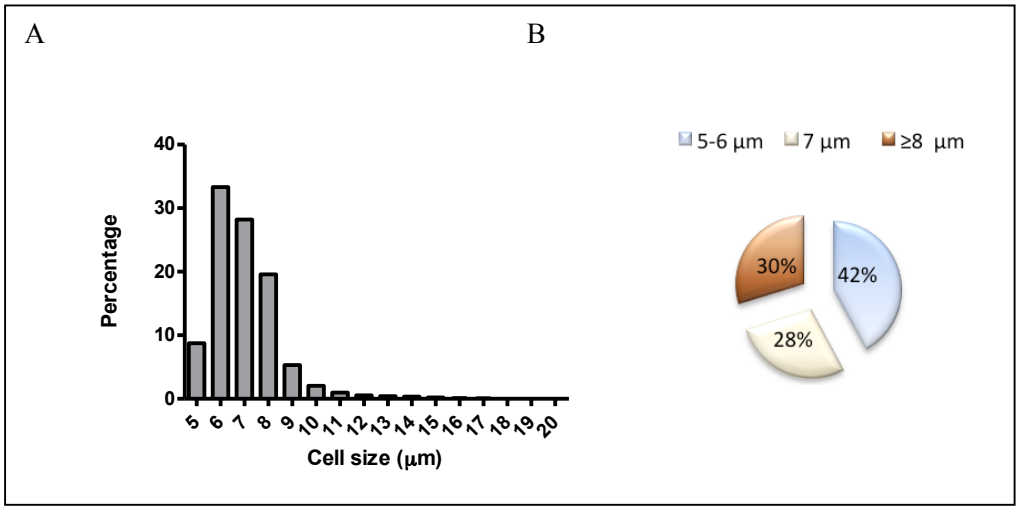

Figure 4-3. Cell size distribution of isolated BMMNC. The distribution of isolated BMMNC was plotted according to individual cell size, expressed as a percentage of all the cells (A). When the cells were grouped into the categories 5-6 μm (below the median), 7 μm (the median) and ≥8 μm (above the median), the three categories were broadly of equal size (B).

4.1.3. Surface marker expression of BMMNC

Surface markers of interest of collected BMMNC were determined by flow cytometric analysis, in at least 3 separate experiments for each marker. Representative images are shown in Figure 4-4. The proportion of viable cells measured by Propidium Iodide in all staining protocols was >92%. The mean expression in collected BMMNC (Figure 4-4) was CD11b: 17.8 ± 0.6% (n=5), CD18: 29.5 ± 1.2% (n=5), CD29: 96.7 ± 0.7% (n=7), CD31: 42.1 ± 4.4% (n=4), CD34: -0.57 ± 0.6% (n=3), CD44: 41.4 ± 2.3% (n=6), CD45: 83.7 ± 0.9% (n=5) and CD90: 56.6 ± 2.1% (n=5). The expression of CD34 was taken to be 0%.

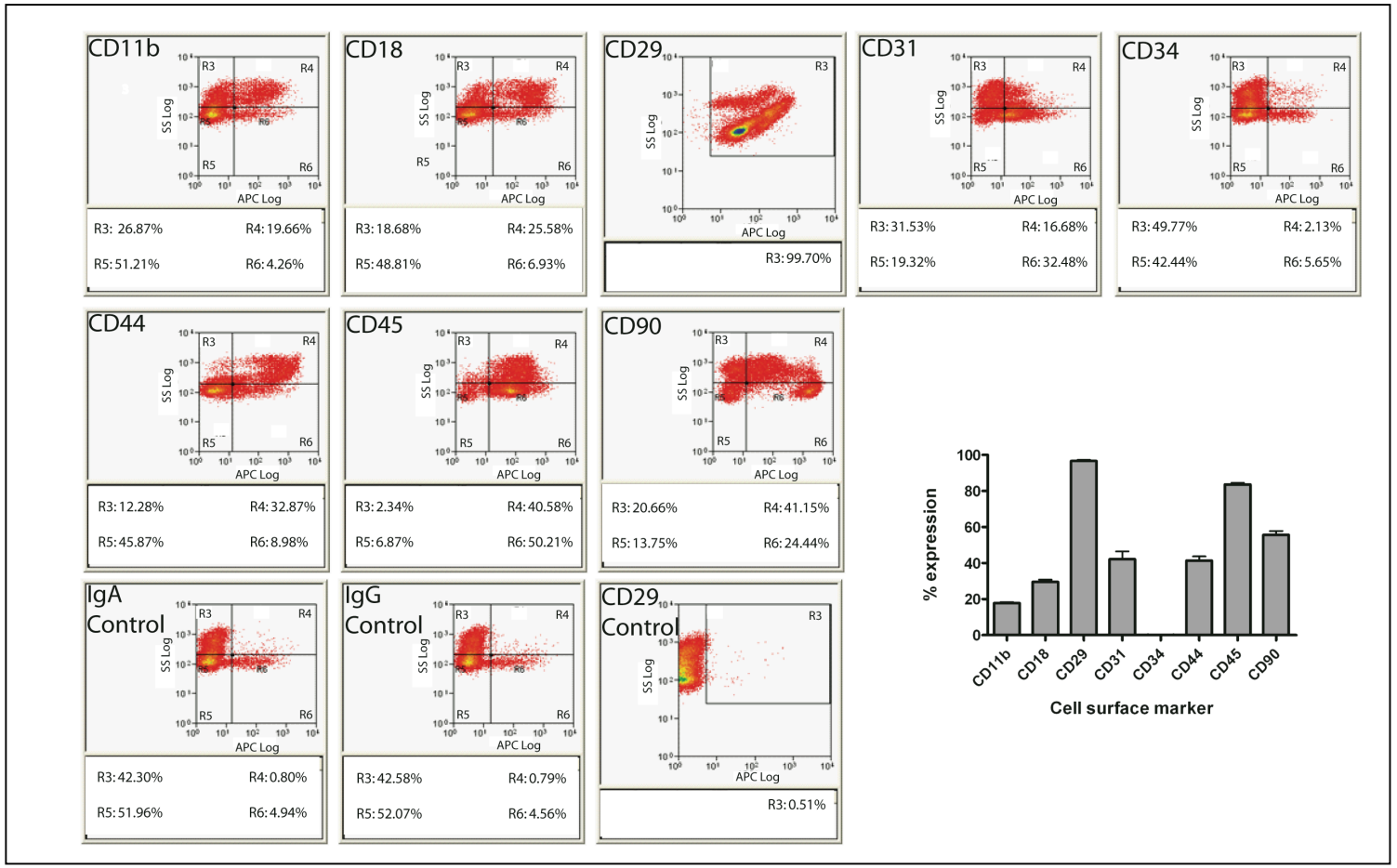

Figure 4-4. Representative images for flow cytometry analysis of BMMNC, after gating for viable cells and cell size/granularity. IgA control is for CD11b. IgG control was for all the other markers, with the exception of CD29. Mean expression of each marker is shown in the bar graph; n=3-7 from different animals. Error bars represent SEM.

4.1.4. Labelling of BMMNC with PKH67

Collected rat BMMNC were labelled with PKH67 to determine their intracardiac location by histological assessments after IC injection. The manufacturer's recommended staining concentration of PKH67 is 2 μM for 5 minutes, but the optimal staining condition is likely to depend on cell type. To optimize staining conditions, the staining efficiency and effect on cell viability was determined using different staining concentrations (0, 0.4, 2.0 and 10.0 μM) for 5 minutes. Following PKH67 staining of $1x10^7$ BMMNC with each condition, the cells were stained with trypan blue and viewed under both bright field imaging (Figure 4-5, A-D) and fluorescent imaging (Figure 4-5, E-H).

As a result, it was found that increasing concentration of PKH67 resulted in an increased number of trypan blue-stained (non-viable) cells (Figure 4-6). However, this increase also resulted in a greater proportion of fluorescent labelled cells that could be observed with shorter exposure times (Figure 4-7) The proportions of both measures were plotted to determine the optimum staining concentration (Figure 4-6). It was found that the optimum staining concentration for BMMNC was 2 μM, which is supportive of the manufacturer's recommendation. This concentration was used for subsequent experiments in the project.

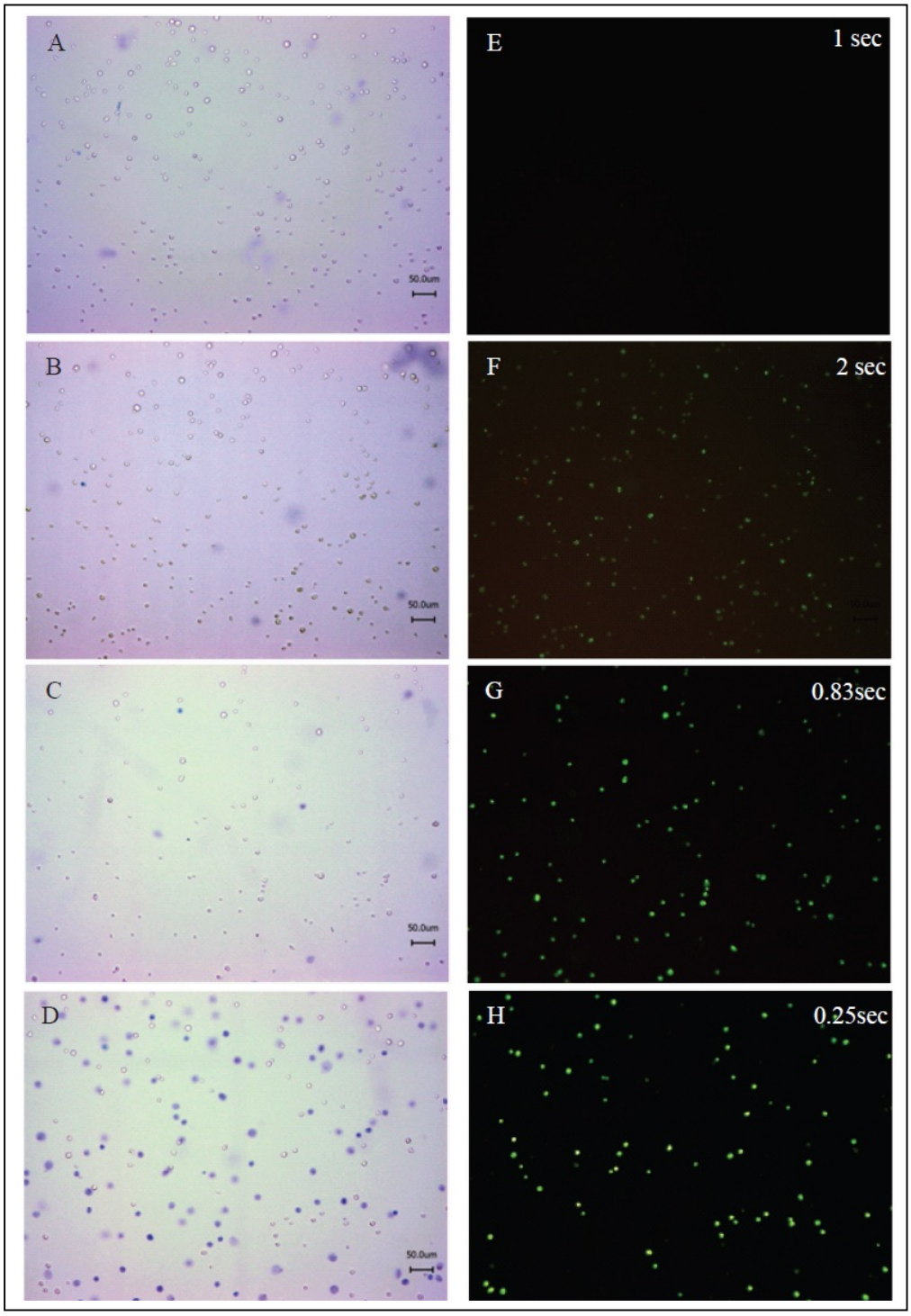

Figure 4-5: Optimization of PKH67 staining of isolated BMMNC. BMMNC were stained with for 5 minutes with PKH67 concentrations of 0 μM (A,E), 0.4 μM (B,F), 2 μM (C,G) and 10 μM (D,H). Trypan blue and bright field imaging was used to determine viability (A-D). Green fluorescent imaging for the same concentrations (E-H) was used to assess staining efficiency with an exposure time of 1, 2, 0.83 and 0.25 seconds exposure time respectively. An increasing concentration of PKH67 resulted in brighter fluorescent intensity. Scale bars = 50 μm.

Concentration	Dead cells (% of total cells)	PKH+ cells **(% of viable cells)**	Total Cells
0 μM	**13 (4.7)**	**0 (0)**	**276**
0.4 μM	**10 (3.9)**	**202 (82.4)**	**255**
2 μM	**8 (6.5)**	**113 (98.2)**	**123**
10 μM	**90 (51.4)**	**85 (100)**	**175**

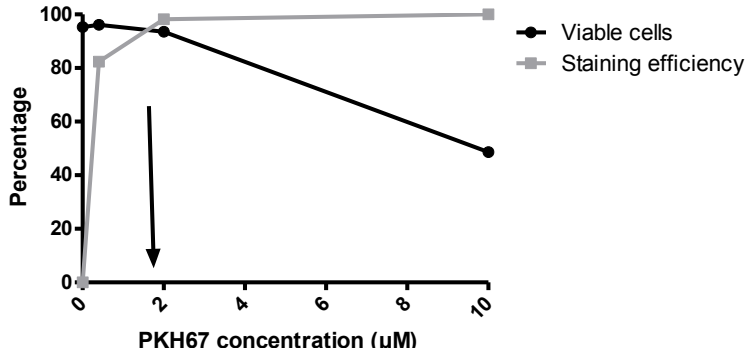

Figure 4-6: Viability and staining efficiency of PKH67 staining of BMMNC with different dye concentrations. Staining efficiency was calculated as a proportion of viable cells. The optimum dye concentration was determined to be approximately 2 μM.

In a further pilot optimization experiment, it was assessed whether staining conditions for BMMNC could be further improved by increasing the PKH67 staining time from 5 minutes to 10 minutes, or whether this would adversely affect viability. Staining with 0 μM PKH67 was utilized as a control. Data was obtained from 2 separate experiments performed on different days. The staining efficiency (positive cell ratio) was not significantly improved by staining for 10 minutes (mean 92.0% *vs.* 97.8%, 5 minutes *vs.* 10 minutes, n=2). However, it was observed that the signal intensity subjectively appeared stronger with a more uniform pattern of staining (Figure 4-7). The viability of PKH67 stained BMMNC was assessed using trypan blue, in duplicate. Mean viability was not different between the two incubation times (97.2% *vs.* 98.3% for 5 and 10 minutes samples respectively). Collectively, it was

decided that the optimum staining condition for injected BMMNC was 2 μM PKH for 10 minutes and this was used for subsequent experiments.

Efficiency of PKH67 staining with the optimized condition (2 μM for 10 minutes) of BMMNC was also assessed by flow cytometry. PKH67 negative and positive cells were gated for green fluorescence (Figure 4-8). The calculated PKH67 positivity was 99.35 ± 0.05% (n=35 separate samples measured on 3 separate days).

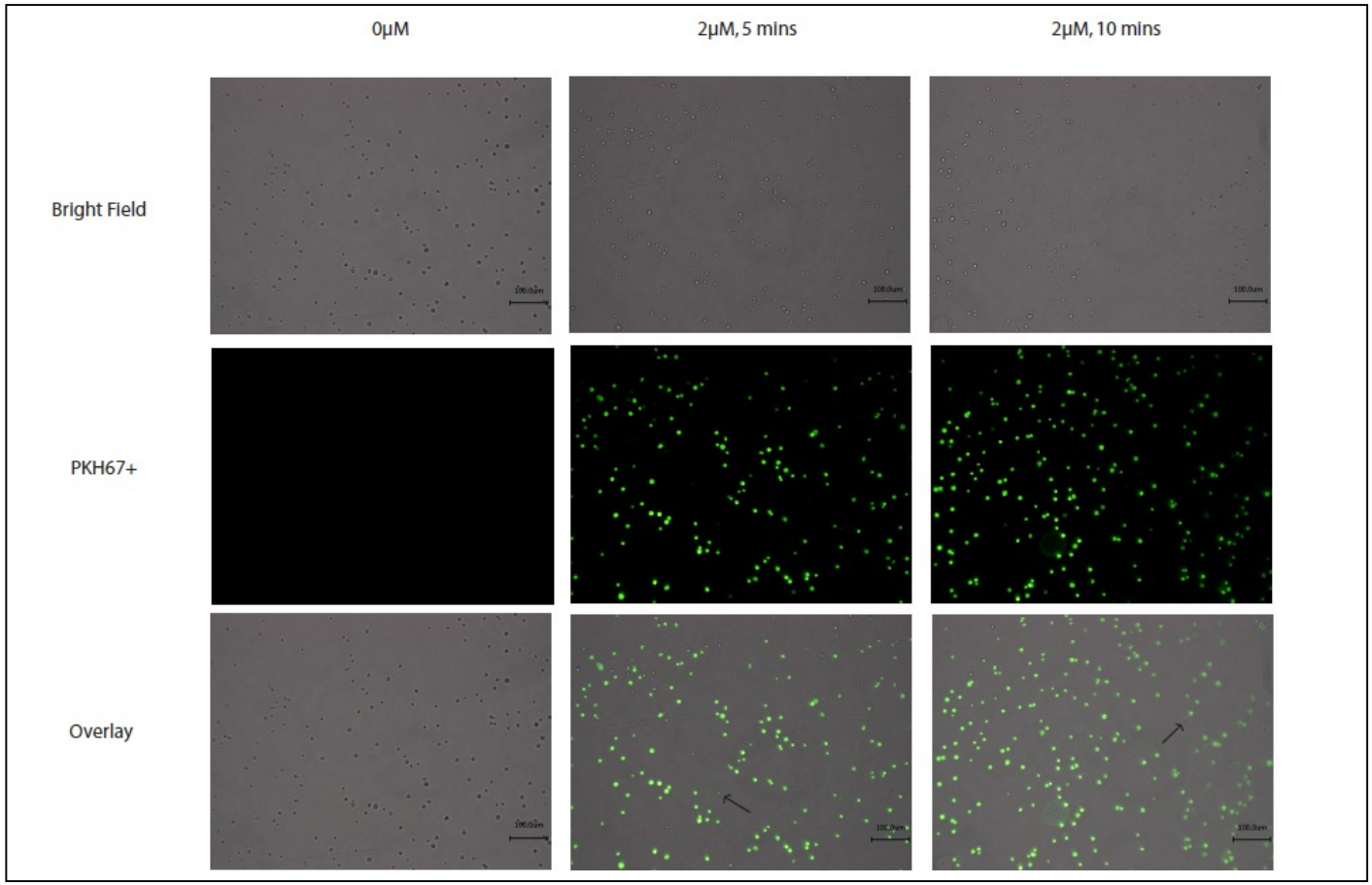

Figure 4-7: Representative images of PKH67 staining (2 µM) of BMMNC for different staining times. Black arrows represent unstained cells. The exposure time for green fluorescence was 0.1 seconds. Incubation with PKH67 for 10 minutes resulted in a more reliable, stronger signal intensity. 0 µM PKH was used as a control. Scale bars represent 100 µm.

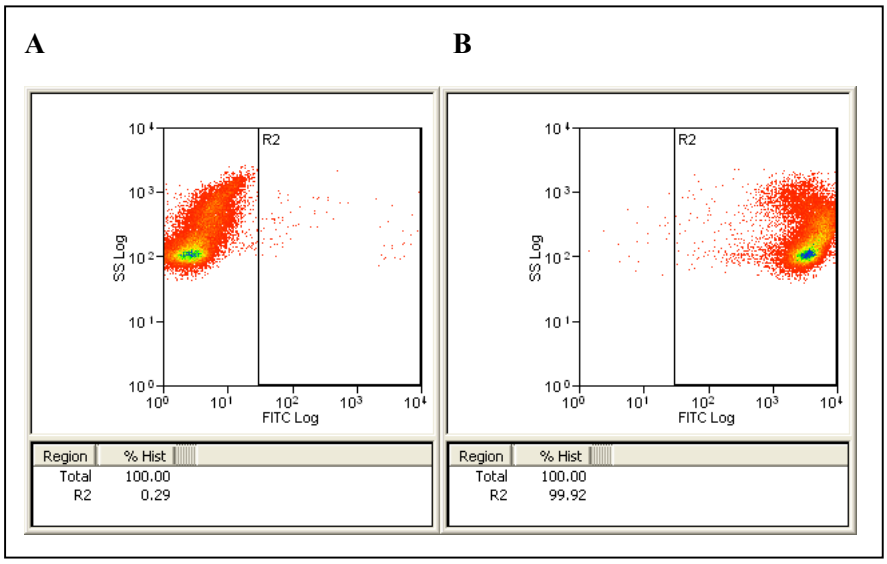

Figure 4-8: PKH67 staining efficiency assessed by flow cytometry. Representative images of (A) negative control stained with 0 μM PKH67 and (B) PKH67 staining with the optimized condition; 2 μM for 10 minutes. The proportion of PKH positive cells was >99.5% (R2).

4.1.5. Possible adverse effects of PKH67 staining on BMMNC

PKH67 staining might affect important cell properties of BMMNC, which could influence donor cell retention after IC injection into the heart. Considering previous literature and information provided by the manufacturer, this risk was thought to be negligible. However, to clarify that this risk did not apply, it was investigated whether PKH67 labelling of BMMNC affected their cell size and/or surface protein expression, which are thought important in donor cell retention.

On three separate days, BMMNC were stained with PKH67 (2 μM for 10 minutes), and cell size and surface protein expression were determined with an automated cell counter and flow cytometry, respectively, and compared with non-stained cells. There was no significant difference between the stained and unstained cells in terms of any surface proteins examined (Figure 4-9) or cell size (Figure 4-10). This data strongly suggested that PKH67 labelling would not affect cellular properties of BMMNC, which are relevant to

BMMNC retention after IC injection. Therefore, PKH67 was used for the reminder of the study below.

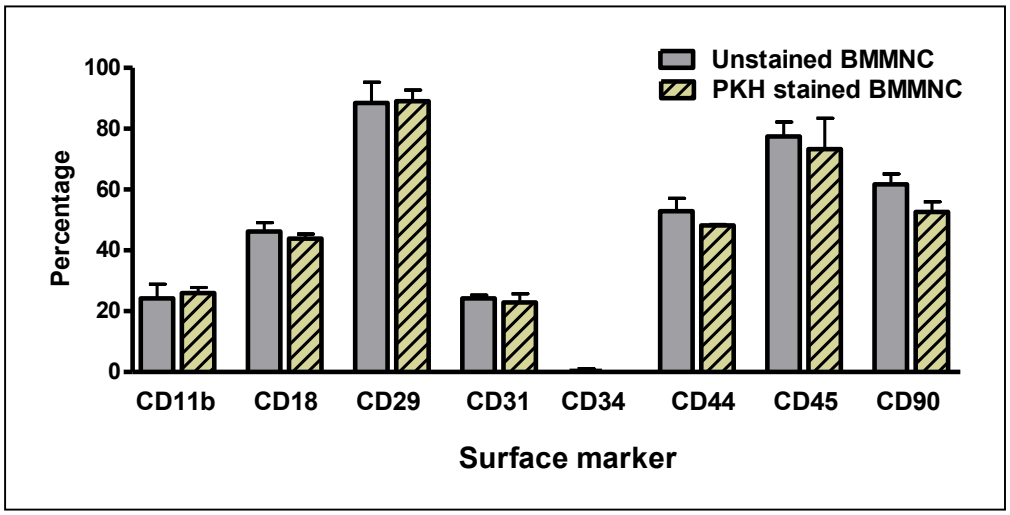

Figure 4-9: Changes in surface proteins of BMMNC by PKH67 labelling. Flow cytometry analysis demonstrated that there was no difference in CD proteins studied between PKH67-stained and non-stained cells. Data are presented as mean ± SEM. Paired T-test: NS.

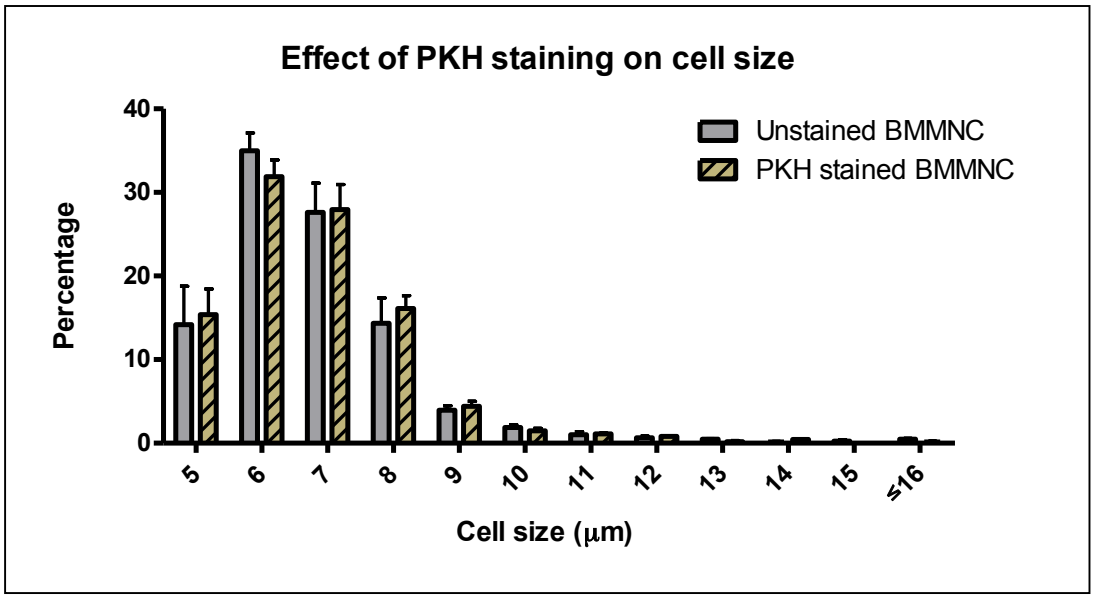

Figure 4-10: Changes in size of BMMNC by PKH67 labelling. There was no difference in cell size between PKH67-stained and non-stained cells. Mean percentage distribution of cell sizes from PKH67 unstained (total n=3,511) and stained (total n=2,214) cells measured on 3 separate days. Data are presented as means ± SEM. Paired T-test: NS.

4.2. Mesenchymal Stem Cell (MSC) collection and characterization

4.2.1. Efficiency of MSC isolation and expansion

Whole bone marrow cells were collected for MSC collection from 4 adult Sprague-Dawley rats. The mean number of whole bone marrow cells obtained from each animal was 6.5 ± 0.6 $x10^8$ (n=4). The cells from each rat were plated in a separate 25cm^2 flasks, at a passage 0 initial mean plating concentration of 2.6 ± 0.3 $x10^7$ cells/cm^2 (this included a large number of non-adherent, non-MSC). MSC adhered to the culture dish within two days and started proliferating. After a mean of 7.4 days, attached cells were found to be approximately 90% confluent. At passage 1, the mean number of MSC obtained from each initial animal was 6.6 ± 1.0 $x10^6$ and these cells were then passaged into 75cm^2 flasks, which equated to a plating concentration of $2x10^4$ ± 0.2 cells/cm^2.

After a further mean 3.9 days, 90% confluence was obtained and at passage 2, $2.1x10^7$ cells were obtained from each initial animal. The doubling time from passages 1 to 2 was therefore 2.4 days. Cells from each 75cm flask were placed in a 175cm^2 flask which equated to a plating concentration of $2.9x10^4$ cells/cm^2.

After a further mean 5.8 days, 90% confluence was achieved and at passage 3, mean $4.9x10^7$ cells per initial animal were obtained. The doubling time from passages 2 to 3 as therefore 4.8 days. The cells from each flask were subdivided and placed in two 175cm^2 flasks, which equates to a plating concentration of $6.0x10^4$ cells/cm^2.

After an additional mean 4.0 days, 90% confluence was obtained. $9.8x10^7$ cells were obtained from each initial animal, equating to a doubling time from passages 3-4 of 4.0 days. Therefore, using this protocol it was demonstrated that approximately $1x10^8$ MSC could be collected from each initial donor animal within 17-21 days of commencing culture.

4.2.2. MSC morphology and size

The morphology of MSC was analysed using phase contrast light microscopy over progressive passages. Initially after plating, the presence of rounded cells was observed, most likely representing RBC and leukocytes. The presence of these cells was abolished after passaging and multiple medium changes. A heterogeneous population of cells was then seen with some oblong / elongating cells beginning to appear (Figure 4-11, A). By day 10 of initial plating, spindle-shaped cells grew rapidly and formed discrete colonies. When passaged in a new flask at a lower cell / surface area concentration (Figure 4-11, B) spindle-shaped cells could be clearly visualized with few examples of the rounder cells. The spindle-shaped cells grew in a uniform monolayer (Figure 4-11, C). Over time the spindle-shaped morphology remained but the cells became wider and began to resemble the morphology of fibroblasts (Figure 4-11, D).

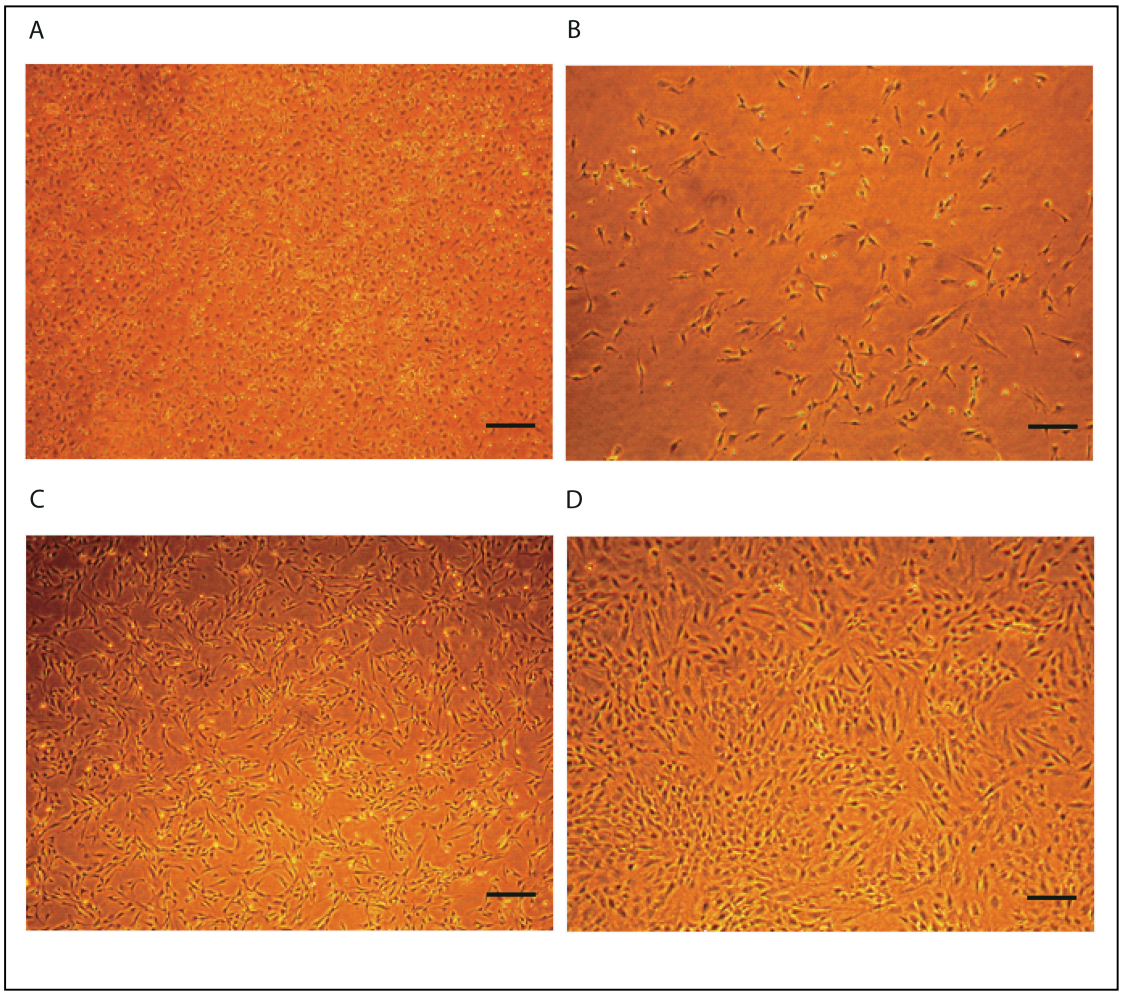

Figure 4-11: MSC morphology. Cultured MSC were viewed by light microscopy and phase-contrast images were acquired with Nikon Coolpix 4500, x4 magnification. (A) Day 5 passage 0, (B) Day 10 passage 1, (C) Day 15 passage 2 (D) Day 21 passage 3. Scale bar=200 µm.

Passage 2-4 MSC were analysed using an automated cell counter to determine cell size (Figure 4-12). For passage 2 MSC, a total of n=17 separate 175cm^2 flasks (9,091 total cells) were analysed. The median and mean cell sizes were 10.5 μm and 12.1 μm, respectively. For passage 3 cells, 7 different 175cm^2 flasks were analysed with a total of 5,166 cells assessed. The median cell diameter was 11.5 μm and the mean cell diameter was also 11.5 μm. For passage 4 MSC, a total of 9 separate 175cm^2 flasks were analysed with a total of 5,976 cells assessed. The median and mean cell sizes were 11.5 μm and 12.2 μm respectively.

The cell size of MSC appears to shift to the right with progressive passaging. Passage 3 resembles a composite of the populations of passage 2 and passage 4 cells (Figure 4-12). However, the populations of cell diameters were compared by non-linear regression by generating second order polynomial (quadratic) best fit lines; there was no significant difference between the distribution of cell diameters between the groups ($p=0.99$ for all comparisons, Sum of Squares F-test).

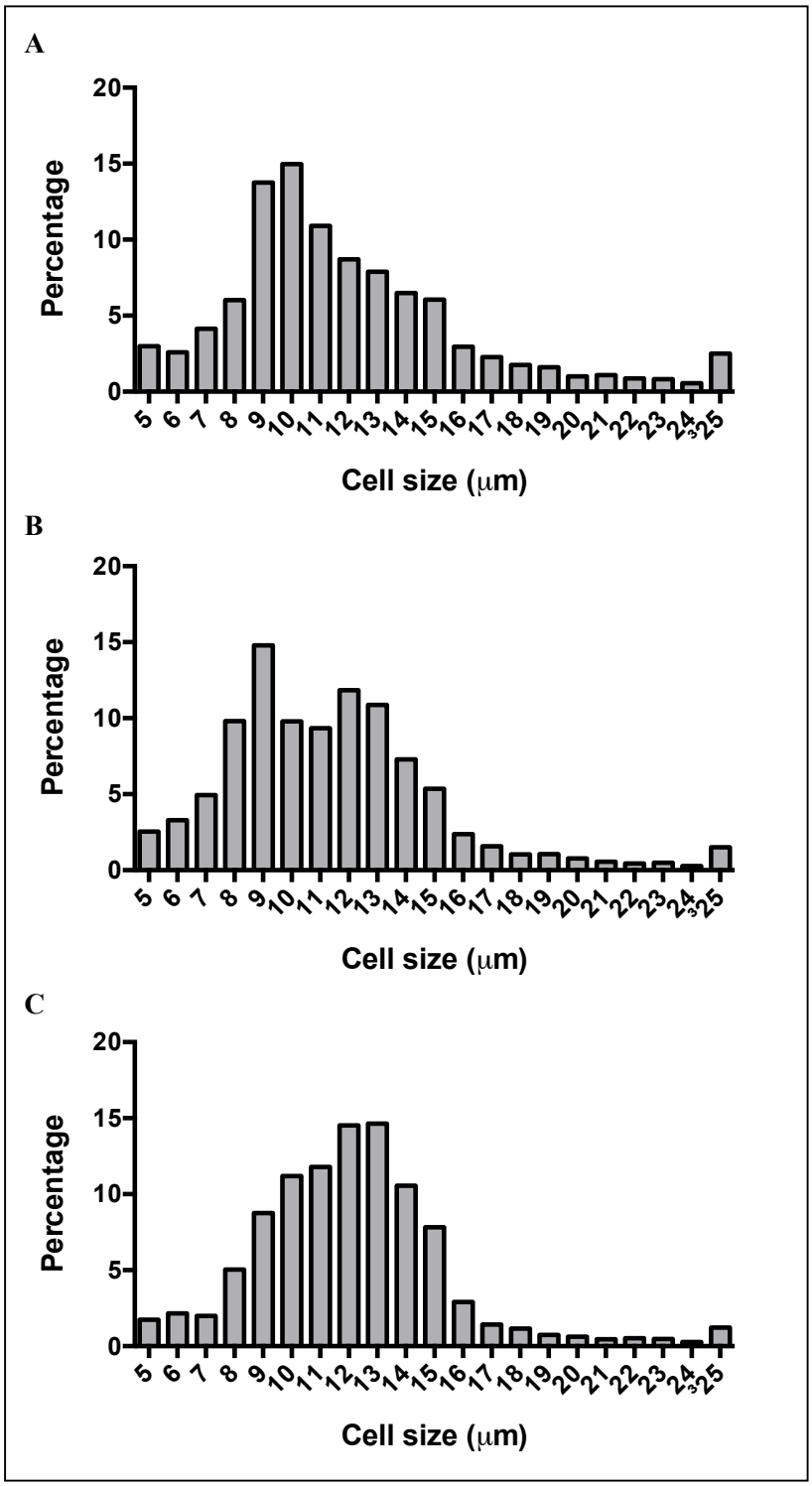

Figure 4-12: Cell size of MSC during culture. The cell size distribution of cultured rat bone marrow derived MSC was assessed using an automated cell counter. The numbers of MSC for each cell size were calculated and expressed as a fraction of the total number of MSC for each passage.
(A) Passage 2 MSC, n=9,091 cells (B) passage 3 MSC, n=8,266 cells (C) passage 4 MSC, n=5,976 cells.

4.2.3. MSC surface markers

Expression of MSC identification markers (CD29, CD34, CD45 and CD90) on the cultured MSC (passage 4) was assessed by flow cytometry. The cultured cells were highly positive for CD29 (99.4%) and CD90 (99.4%) and almost exclusively negative for CD34 (0.1%) and CD45 (-0.17%, taken to be 0%), as expected (Figure 4-13).

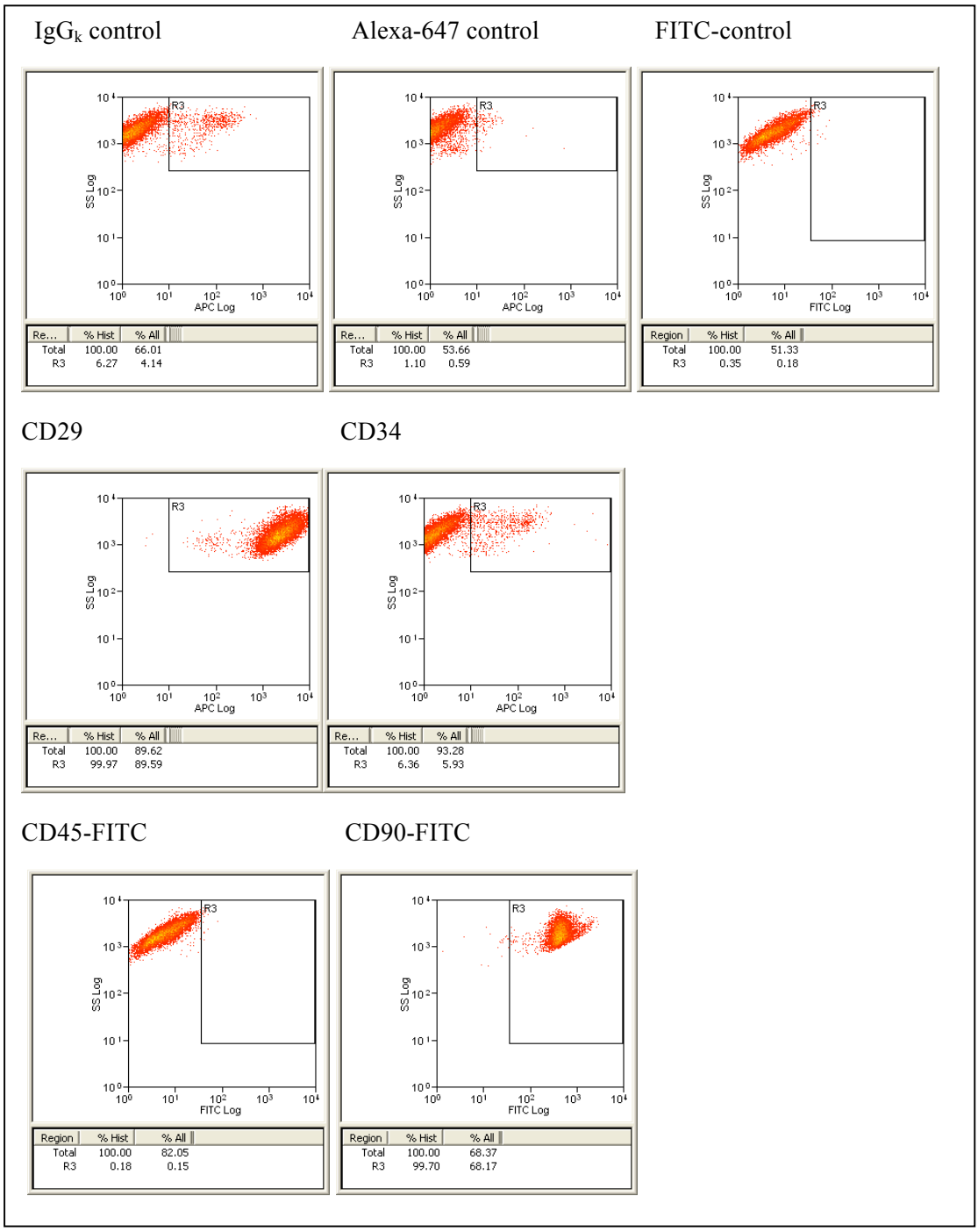

Figure 4-13: Surface markers of passage 4 MSC (representative images). The cultured MSC were highly positive for CD29 and CD90 and negative for CD34 and CD45. The IgG_k control was for CD34. The Alexa-649 control was for CD29. The FITC-control was for CD45 and CD90.

4.2.4. Differentiation capacity of cultured MSC

Passage 3 MSC were examined for their differentiation capacity to mesenchymal lineages as described (refer to 3.4.4). After 21 days of culture with adipogenic differentiation medium, Oil-O-Red staining demonstrated multiple lipid vesicles within individual cells which stained the cells red, confirming the typical appearances of adipocytes. Similarly, cultured cells incubated with osteogenic differentiation medium were stained for alkaline phosphatase and alizarin red. Colonies were observed with co-staining of alkaline phosphatase and calcium, demonstrating the typical appearances of osteocytes (Figure 4-14).

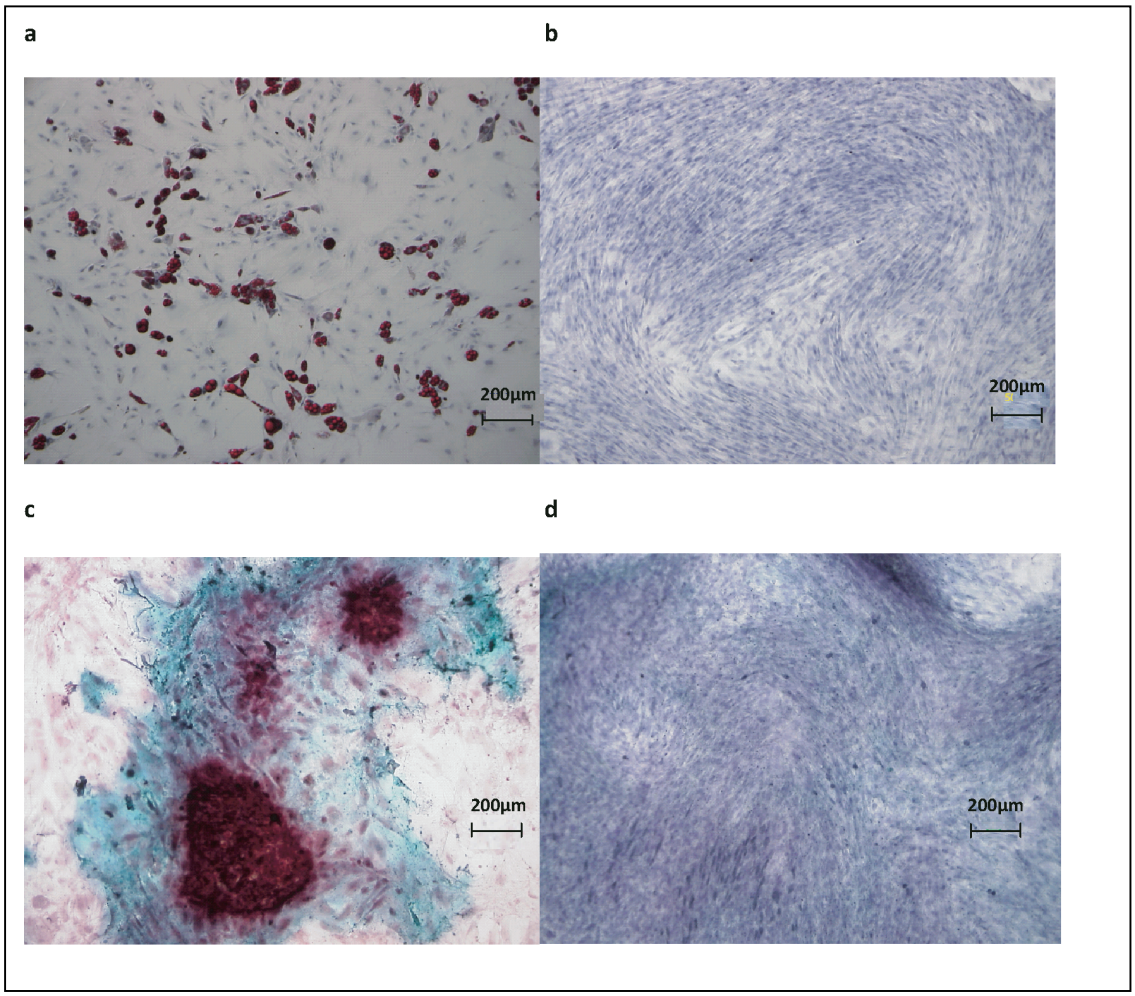

Figure 4-14: Differentiation capacity of passage 3 MSC (representative images). Adipocytes differentiated from MSC (a) and Control cells (b) were stained with Oil-O-Red. Osteocytes differentiated from MSC (c) and control cells (d) were stained with alkaline phosphatase (ALP) and alizarin red for calcium deposition. All assays were counterstained with haematoxylin. Lipid particles (red) within the adipocytes were a frequent finding (a). Co-localization of ALP (light blue) and calcium (dark red) was detected in the osteogenic assays. These findings were not observed in the control assays. Scale bar = 200 µm.

4.2.5. Labelling with PKH67

For optimization of labelling of MSC with PKH67,,2x10^6 passage 3 MSC were stained with 2 μM PKH67 for either 5 minutes or 10 minutes. Control cells were suspended in Diluent C without PKH67. Staining efficiency was assessed using fluorescent microscopy. For both time points, PKH67 staining was highly efficient and almost all cells on imaging were stained; mean 5 minute staining efficiency was 99.6% (n=3 samples, n=801 cells) and mean 10 minute staining efficiency was 99.7% (n=3 samples, n=1,320 cells). A representative image is shown in Figure 4-15.

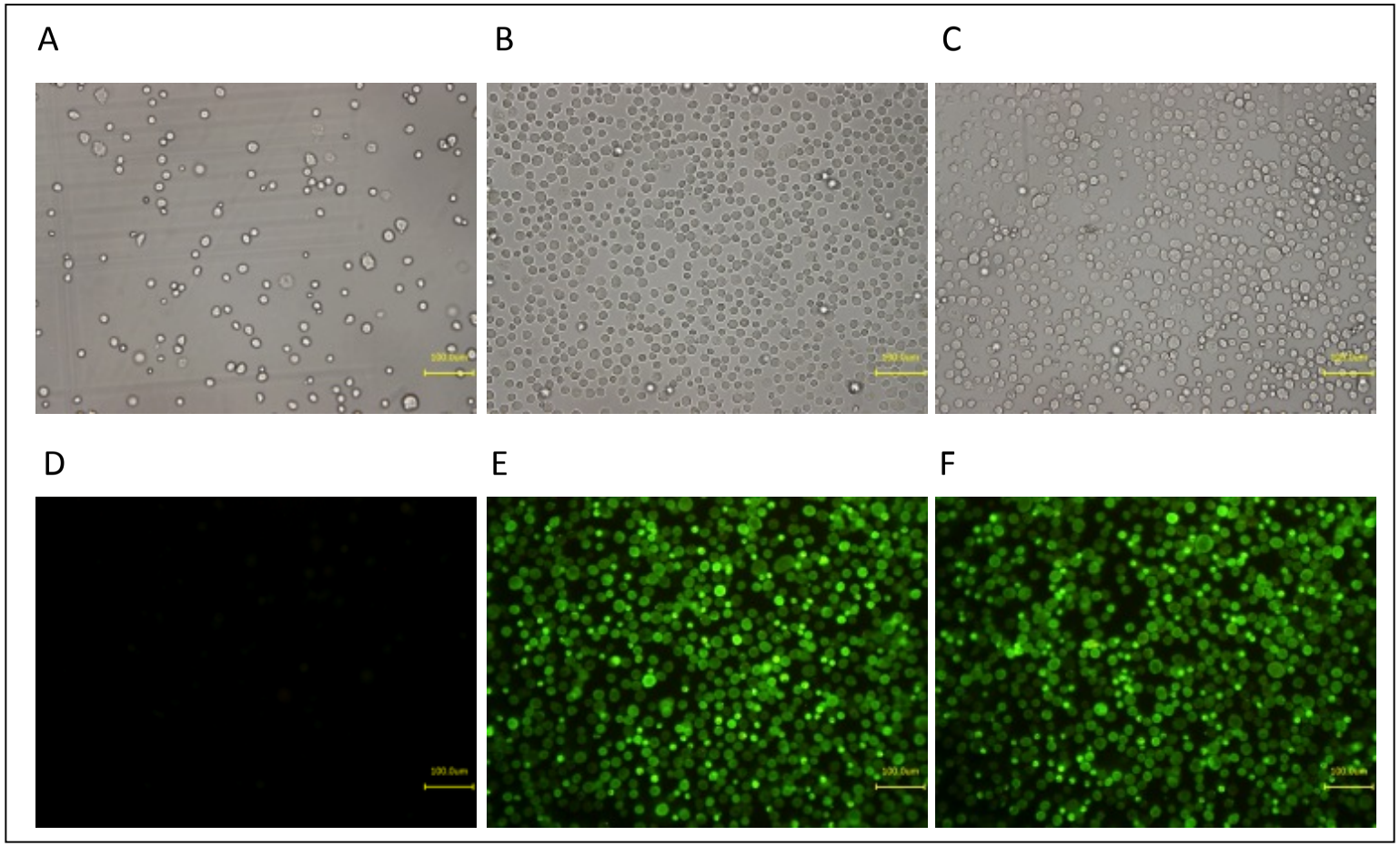

Figure 4-15: Efficiency of staining with PKH67 of passage 3 MSC. Cells were stained at a final concentration of 2 µl PKH67 for 5 minutes (B and E) or 10 minutes (C and F) and compared with cells not stained with PKH67 (A and D). The top images are bright field images and the lower images are green fluorescent images. After PKH67 staining, most cells were brightly stained at 5 minutes; staining efficiency was not enhanced by staining for 10 minutes. Scale bar = 100 µm.

In addition, the viability of n=380-740 cells were determined for each PKH67 labelling condition using trypan blue staining. The experiment was performed in duplicate on separate days. The mean viability was 97.5% and 94.0% for 2 μM for 5 minutes *vs.* 2 μM for 10 minutes respectively. Viability in the control sample (0 μM) was 97.5%.

Given the similar labelling efficiency with a higher viability, it was decided to utilize 5 minutes incubation of 2μl PKH67 for the main staining experiments. The effect of this PKH67 staining condition on cell size was also analysed. The distribution of cell size from pre-stained cells and from post-stained cells were compared (Figure 4-16). There was no significant difference in cell size following PKH67 staining (paired T-test: NS).

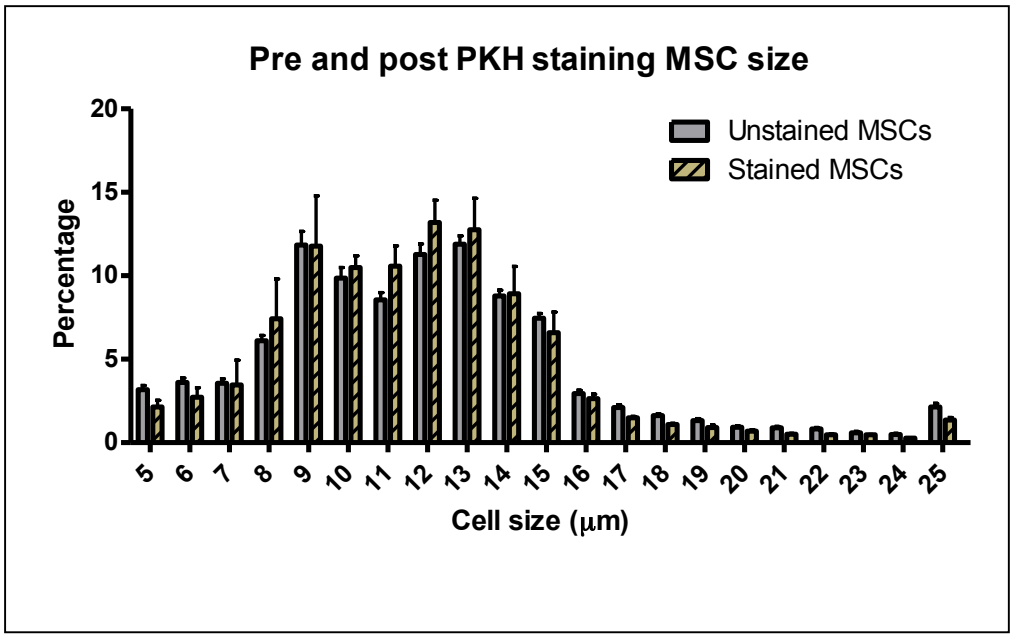

Figure 4-16: Size distribution of MSC before and after staining with PKH67. Cell size was measured with automated cell counter. There was no significant impact on cell size after cell staining. Error Bars represent SEM.

4.3. Establishment of a rat model to investigate initial retention of stem/progenitor cells after intracoronary injection

4.3.1. Langendorff rat heart perfusion - reproducibility without cell injection

It was first determined whether stable and reproducible perfusion was obtained for normal rat hearts during Langendorff *ex-vivo* perfusion. After multiple practice attempts using >20 rat hearts, n=6 hearts were perfused and measurements for heart rate, coronary effluent flow rate, and temperature and pH of the coronary effluent, were serially recorded at 10, 20, 30 and 40 minutes after hanging (Figure 4-17)

Variations between samples were small enough at each measurement time point, judging from the small SEM. This suggested that the perfusion model is reproducible. There was no significant difference in any measurements over time (One-way ANOVA). From the bar chart appearances, it was concluded that stabilization had occurred 20 minutes after heart hanging. Therefore, in the normal heart model, cells were injected at this time point (Methods 3.6.7). Similarly, this was the stabilization period used before subjecting the perfused hearts to the ischaemia-reperfusion protocol (refer to 3.7).

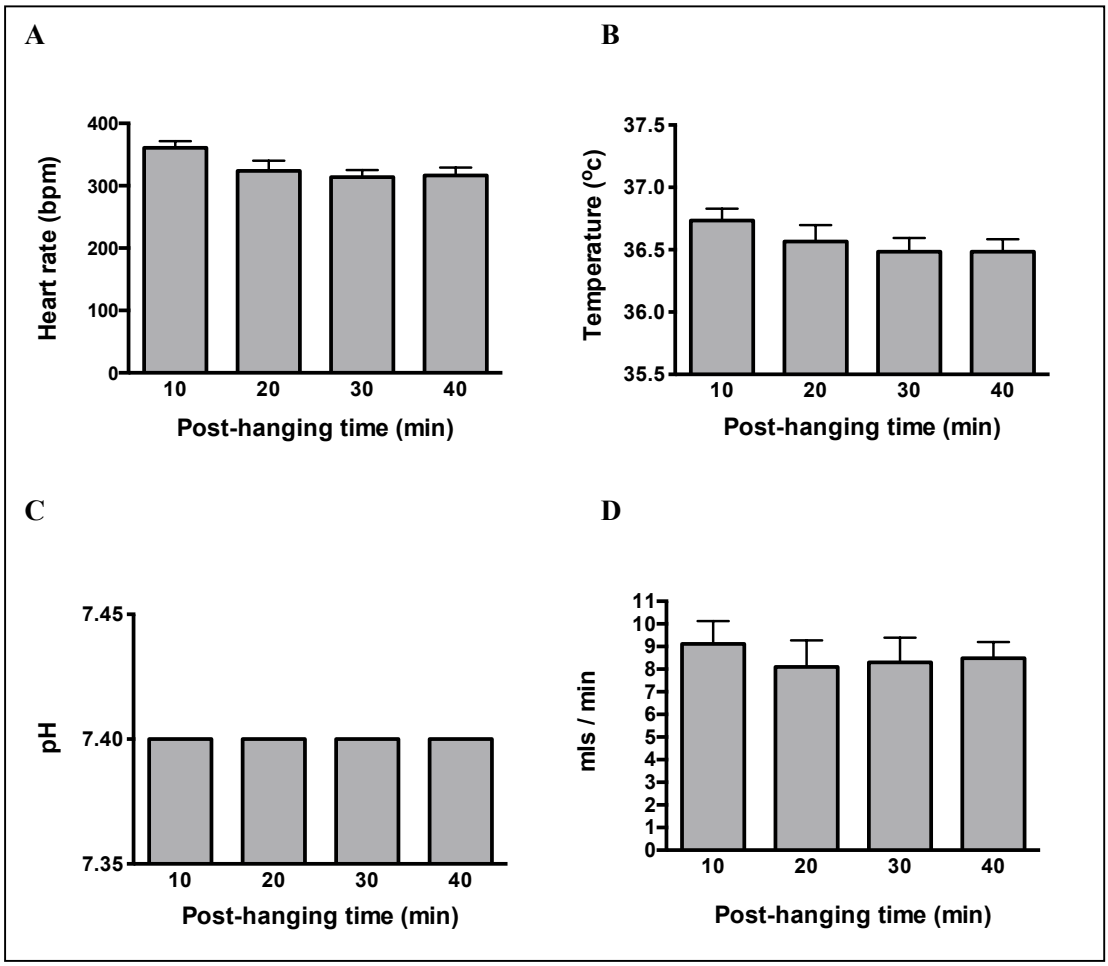

Figure 4-17: Stable perfusion obtained for normal rat hearts using Langendorff apparatus. Heart rate (A), temperature of coronary effluent (B), pH of coronary effluent (C) and coronary effluent volume (D) were obtained for n=6 hearts following hanging on Langendorff apparatus with normal perfusion. Error bars indicate SEM.

4.3.2. Langendorff model optimization and RBC contamination in coronary effluent

Early in the process of optimizing the Langendorff model for normal heart perfusion, it was observed that cells were present in the coronary effluent after hanging the heart, without donor cell injection. This was an unexpected finding and had the potential to affect the ability of the model to quantify donor cells in the coronary effluent. These cells were quantified further.

Five minutes after hanging the heart, the coronary effluent was smeared on a slide glass and stained with haematoxylin. It was demonstrated that the cells had the appearances of biconcave discs (Figure 4-18). It was concluded that these cells were red blood cells (RBC). At later time points, there was a lower visual concentration of RBC under microscopic examination (not shown).

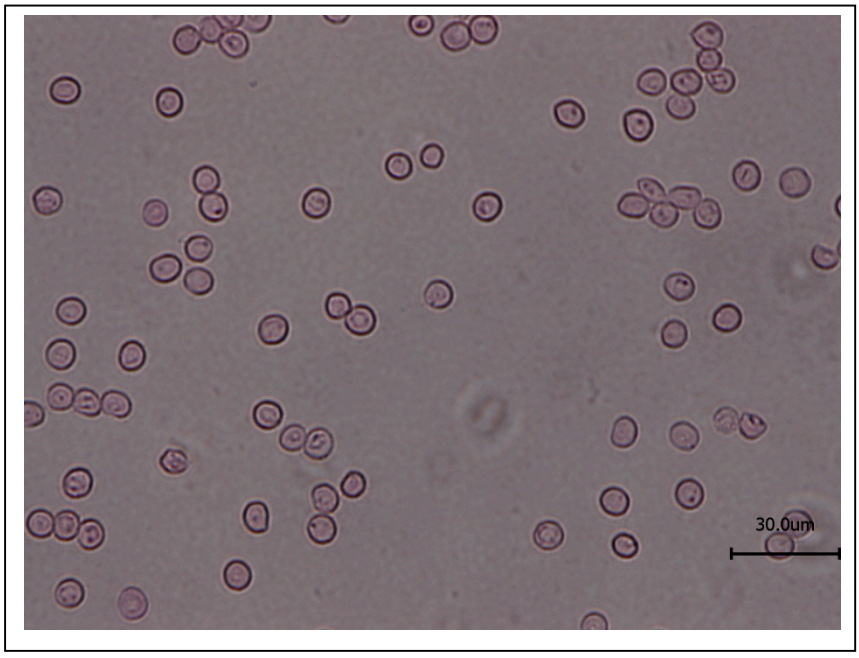

Figure 4-18: RBC in the coronary effluent. Coronary effluent leaving the heart 5 minutes after hanging was smeared on a slide glass. The cells were fixed and stained with haematoxylin. Microscopy demonstrated biconcave discs; the typical appearances consistent with red blood cells.

Confirmatory evidence that the cells were not nucleated was obtained using DAPI staining. Control images were obtained for isolated BMMNC (Figure 4-19). It was found that cells in the coronary effluent were not nucleated, suggesting that they were RBC. The BMMNC positive control almost exclusively exhibited DAPI nuclear staining.

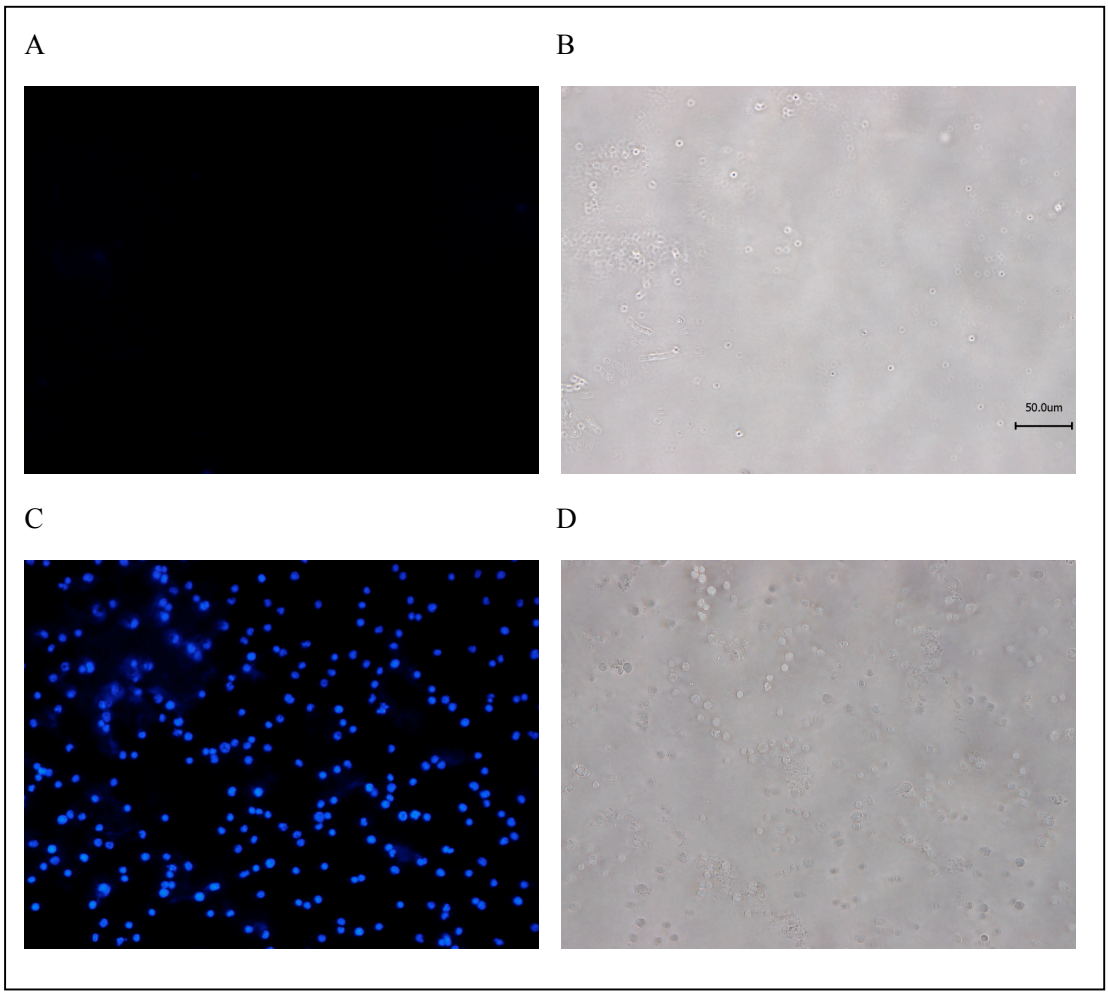

Figure 4-19: Staining of coronary effluent cells with DAPI. It was demonstrated that the coronary effluent cells were not nucleated. DAPI stain (A) viewed at 0.125 seconds exposure, Bright field image (B) shown. Control images were obtained for isolated BMMNC which were fixed, stained and viewed using the same protocol and exposure times (C and D). Scale bar represents 50 μm.

It was observed that the frequency of RBC leakage was highest immediately after hanging and progressively decreased. At each time point, cell number was counted using a haemocytometer (Figure 4-20). It was found that the number of RBC at 20 minutes of heart hanging was $4.1 \pm 1.9 \times 10^4$ cells/min. This was considered to be sufficiently small compared to the number of donor cells in coronary effluent. The number continued to gradually decrease and at 60 minutes, the mean count was approximately 1×10^3 cells/min.

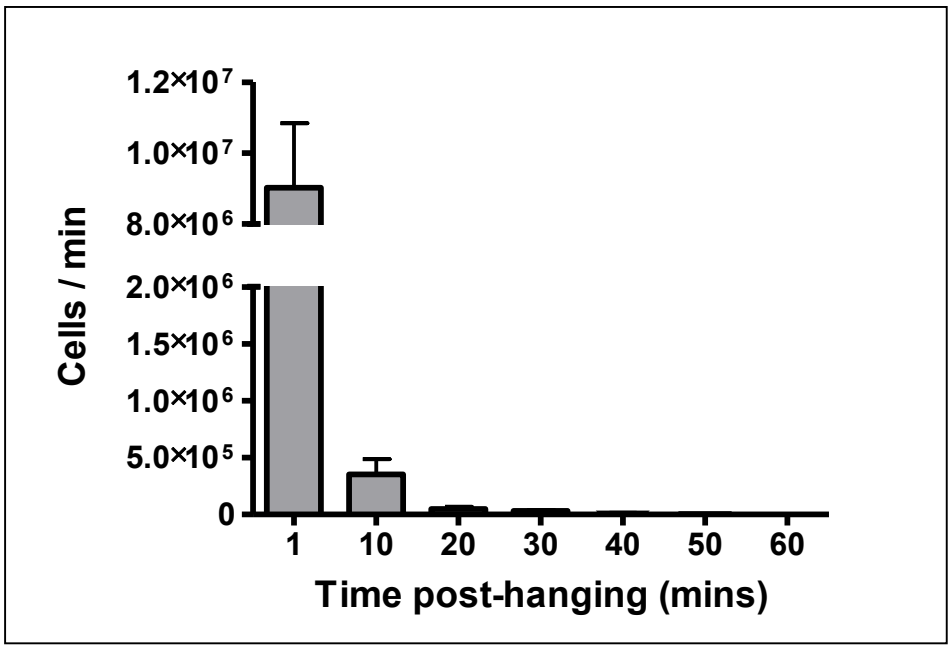

Figure 4-20: RBC exiting the heart in the coronary effluent after heart hanging. Rat hearts were perfused on the Langendorff apparatus (n=7). Immediately after heart hanging, a large amount of RBC exited the heart (approximately 9×10^6 cells / min) that decreased over time. At 20 minutes after hanging, the number of cells exiting the heart was approximately 1×10^5 cells / min. This level decreased to approximately 1×10^3 cells / min by 60 minutes post-hanging. The cell number is expressed on a logarithmic scale. Data expressed as mean ± SEM

4.3.3. RBC contamination in coronary effluent after cell injection

To ensure that RBC contamination was at a low enough level compared to the donor cell count in coronary effluent, the ratio of RBC in coronary effluent cells was analysed. $8x10^6$ PKH67-labelled BMMNC were injected into perfused normal Langendorff after 20 minutes of stabilization on 3 separate days. The cell counts prior to injection (RBC) were low on each occasion ($<5.0x10^4$). The coronary effluent was observed minute-by-minute to determine the proportion of PKH67-positive cells in all coronary effluent cells (Figure 4-21). In all experiments, almost 100% of the cells in the coronary effluent within the first 1 minute of injection were PKH67 positive. The total number of cells observed per field progressively decreased each minute after injection. After 5 minutes when the cell counts in the coronary effluent had returned to baseline, very few cells, either PKH67 positive or negative, were observed.

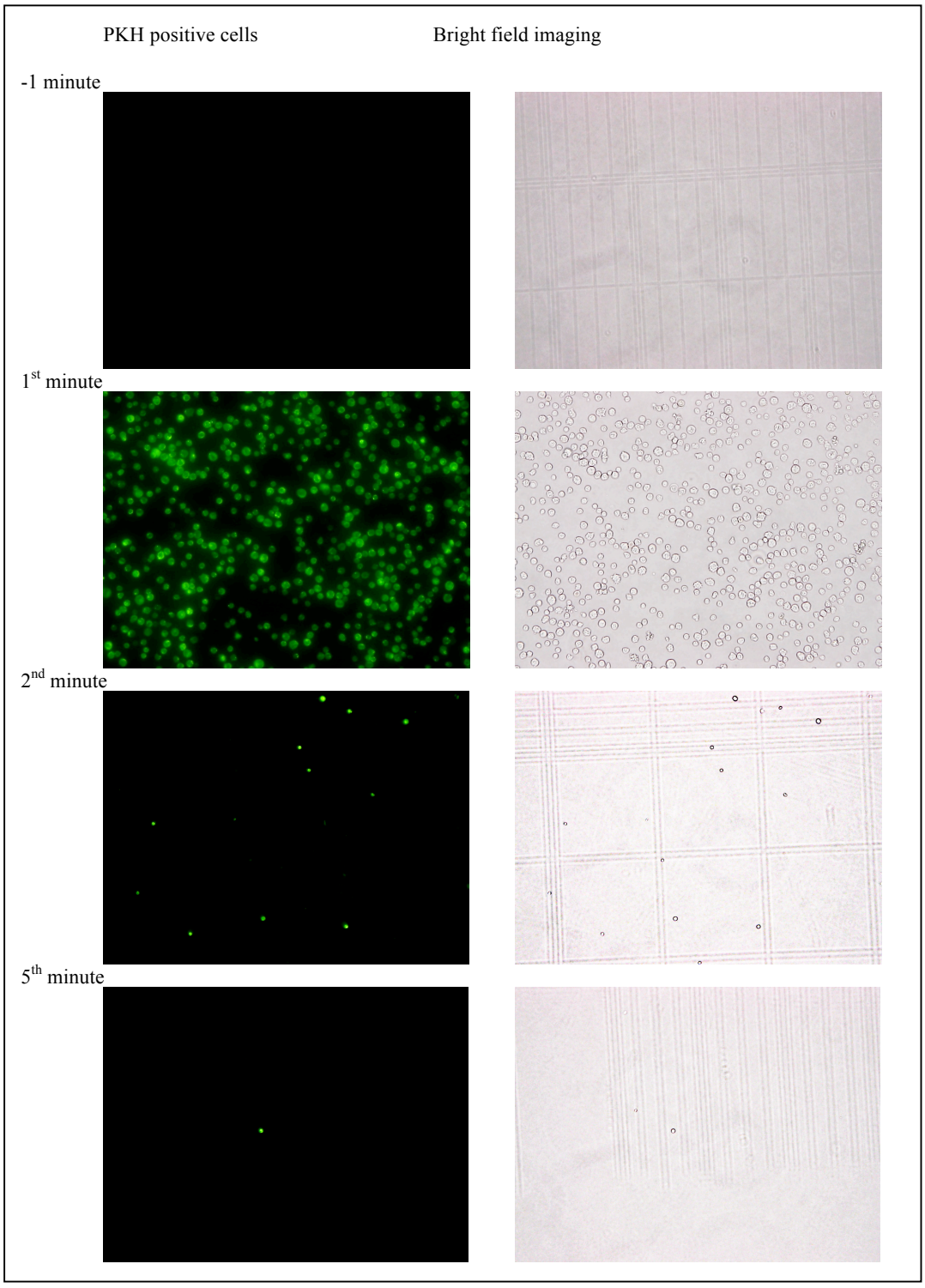

Figure 4-21: Negligible RBC contamination in coronary effluent after cell injection. After injection of $8x10^6$ PKH67-labelled BMMNC into normal Langendorff-perfused hearts, almost all the cells in the coronary effluent were PKH67 positive. Representative fluorescent and bright field images are shown for the 1 minute prior to injection (-1), the first 2 minutes after injection and the 5th minute post injection. Cells - either PKH67 positive or negative - were only very rarely seen in the coronary effluent beyond 5 minutes donor cell injection.

4.3.4. Negligible numbers of donor cells retained in the Langendorff apparatus

For assessing the possible retention/attachment of injected cells in the Langendorff apparatus and injection syringe/needle, $8x10^6$ BMMNC suspended in 3 ml PBS (n=3) were injected into the side port of the Langendorff apparatus, collected in a 50 ml Falcon tube and flushed through with warmed, oxygenated Krebs-Henseleit buffer (without heart hanging/perfusion).

The mean cell counts in the three samples were $7.99x10^6$, $8.03x10^6$ and $8.06x10^6$. This demonstrated that no cells injected into the side port were retained in the Langendorff apparatus itself (paired T-test *versus* counts of $8x10^6$, NS) and that there was only a very small margin of error (<1% of the total) after counting the same population of cells.

4.3.5. Ischaemia-reperfusion heart – reproducibility without cell injection

To determine whether subjecting hearts to 30 minutes ischaemia followed by 30 minutes reperfusion during Langendorff perfusion led to a reproducible experimental state, n=5 rat hearts were perfused in this fashion and data was collected for coronary effluent flow rate, coronary effluent temperature, heart rate and number of RBC exiting the heart without donor cell injection (Figure 4-22)

It was observed that within a couple of minutes of ischaemia, the heart ceased contraction although it was not possible to record to record the ECG because the heart was submerged in warmed Krebs-Henseleit buffer. During this non-flow, global ischaemia, the temperature was maintained at 37^{o}C. Within 2 minutes of reperfusion, the heart was observed to contract sporadically, progressively increasing in regularity. The first recording of heart rate was made 10 minutes after reperfusion which had a lower heart rate than that recorded prior to ischaemia. Heart rate progressively increased during reperfusion. The 30 minutes reperfusion heart rates were lower than those recorded prior to ischaemia at 20 minutes stabilization (270 ± 22 bpm *vs.* 310 ± 16 bpm) although this reduction was not statistically significant (p=0.09). Immediately following reperfusion, atrial fibrillation with a rapid ventricular rate and ventricular fibrillation were also noted occasionally in the early stages. Mechanical cardioversion by flicking the heart with one finger typically cardioverted the rhythm but this was not always successful. Hearts with intractable tachyarrhythmias following reperfusion were excluded from the analysis as a stable heart condition did not occur, though this occurred infrequently.

In the reperfusion period, temperatures were also observed to be variable, although these had stabilized by 30 minutes of reperfusion. There was no significant difference between the pre-ischaemia and reperfusion temperatures (p=0.79, One-way ANOVA). I-R did not have any effect on the rate of coronary effluent flow rate at the recorded time

points. (p=0.99, One-way ANOVA). Immediately following reperfusion within the first 1-3 minutes, it was noted that coronary effluent flow rates appeared to be increased. However these volumes had stabilized by the time the first formal measurement was made at 10 minutes.

The number of RBC leaving the heart was measured with an automated cell counter (Figure 4-22). The number of RBC within the stabilization period was similar to those reported previously (refer to 4.3.2), but this number was consistently even lower after 30 minutes of reperfusion ($\leq 1x10^4$ cells).

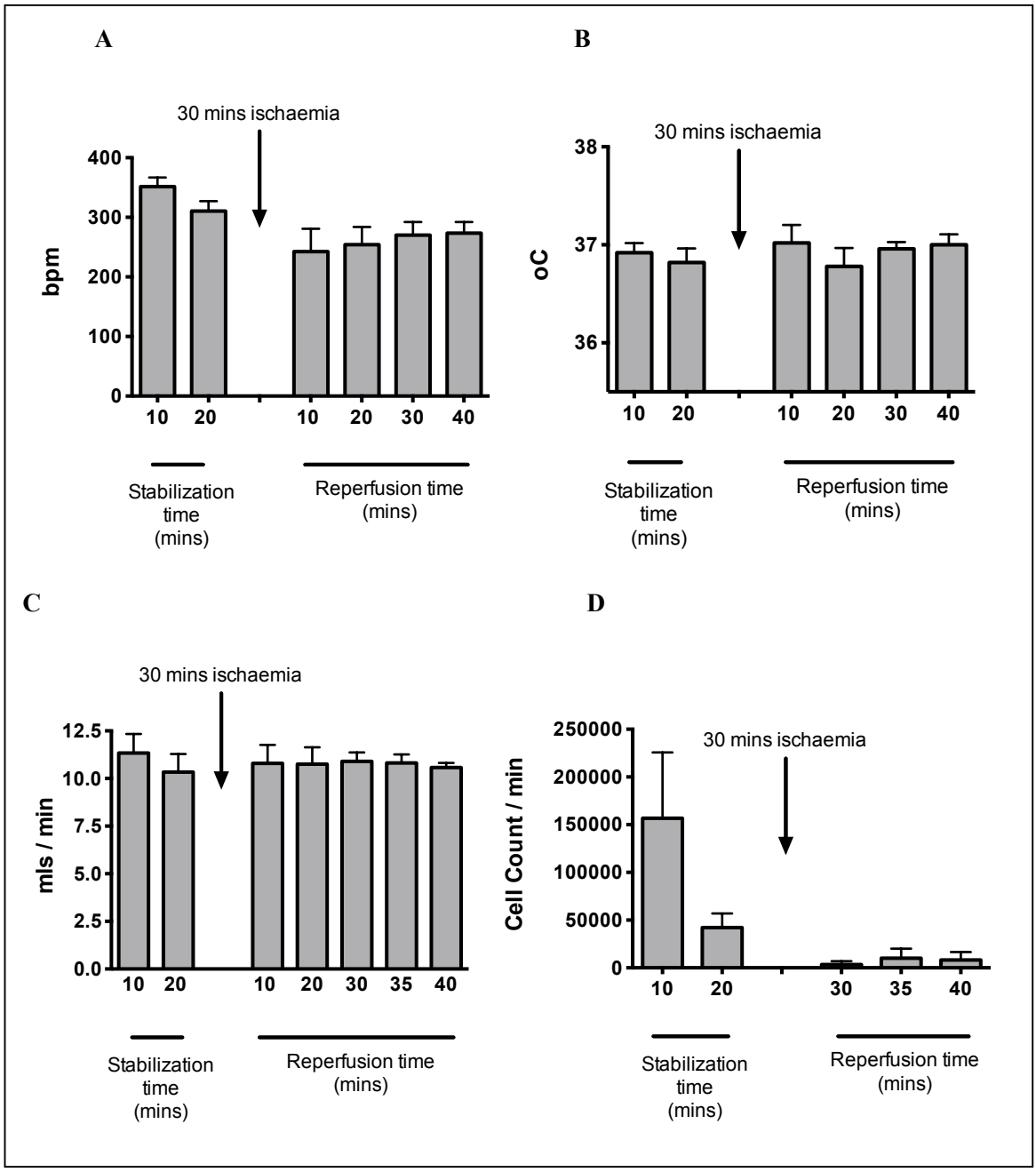

Figure 4-22: Langendorff parameters and RBC leakage before and after ischaemia-reperfusion, without cell injection. Heart rate (A), temperature of coronary effluent exiting the heart (B) and coronary effluent flow rate (C) and RBC loss in the coronary effluent (D) are shown (n-5). Data expressed as mean ± SEM.

4.3.6. Expression of adhesion molecules in coronary endothelium

Based on previous reports, it was suggested that P-selectin and ICAM-1 would not be expressed in normal intact hearts (refer to 1.8.3). Furthermore, after 30 minutes ischaemia and 30 minutes reperfusion in ex-vivo Langendorff hearts, P-selectin would be upregulated but that ICAM-1 would not be upregulated. In this project, these molecules were assessed by immunohistochemistry in I-R hearts and normal hearts subjected to 30 minutes normal perfusion only (n=2 hearts, I-R and controls each).

As expected, it was found that P-selectin was expressed in hearts subjected to 30 minutes ischaemia and 30 minutes reperfusion. I-R. It was noted that P-selectin was most strongly expressed in larger vessels (representative image Figure 4-23). Using the same staining conditions with the same antibody concentrations, P-selectin was not detectable in sections from the normal hearts.

It was expected that ICAM-1 would not be expressed in normal hearts or hearts with 30 minutes ischaemia and 30 minutes reperfusion. Therefore, positive control hearts were generated (n=2 each); hearts with 30 minute ischaemia and 4.5 hour reperfusion hearts for ICAM-1 (see Methods 3.8.2.). Using the staining protocol, it was observed that the positive controls expressed ICAM-1 staining, particularly in the larger vessels. In contrast, in both the normal hearts and hearts with 30 minutes ischaemia and 30 minutes reperfusion, no ICAM-1 expression was identified in any of the small or large coronary vasculature (representative image Figure 4-24).

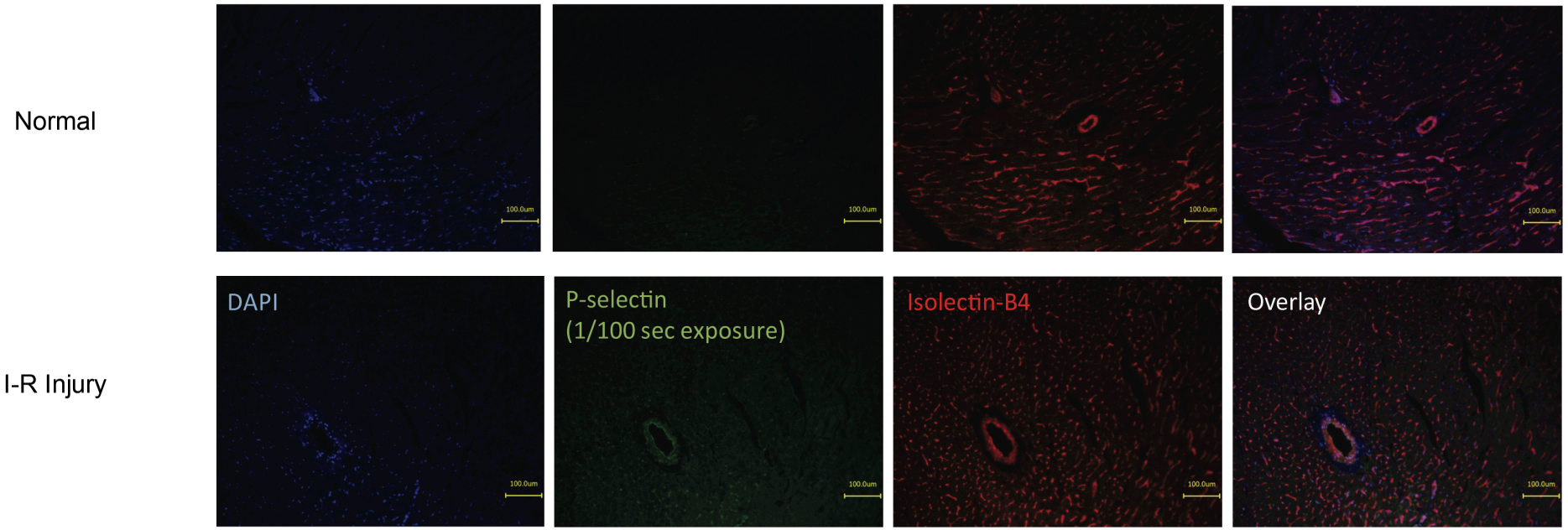

Figure 4-23: P-selectin staining of normal and I-R hearts. Representative images are shown. Heart sections were stained with a nuclear stain (DAPI: blue), an endothelial marker (Isolectin-B4: red) and incubated with anti-P-selectin antibody under optimized conditions. Vascular P-selectin expression (green) was observed in I-R hearts but not in normal hearts. Scale bar: 100 μm.

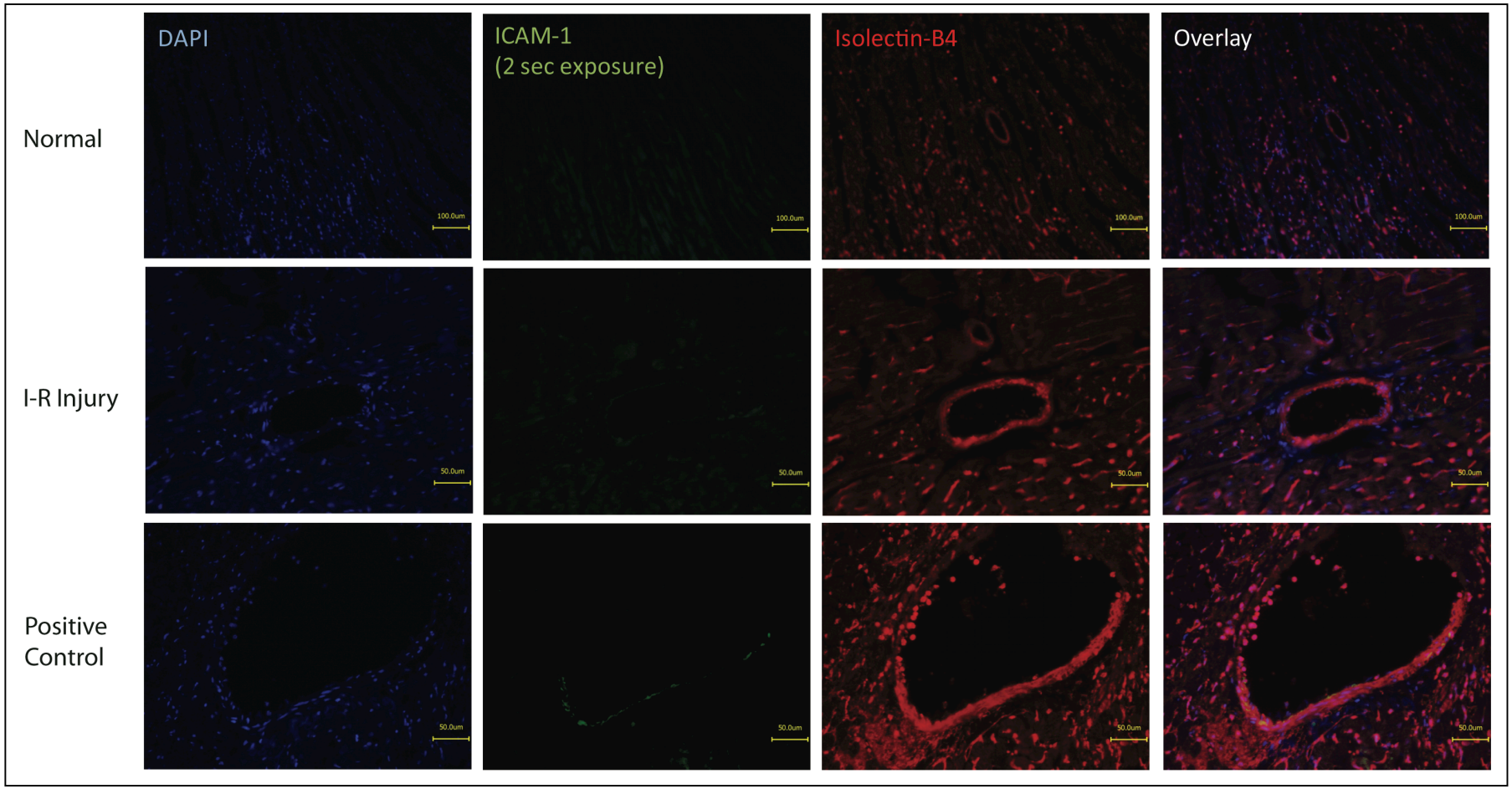

Figure 4-24: ICAM-1 staining of normal and I-R hearts, with positive control hearts. Representative images are shown. Heart sections were stained with a nuclear stain (DAPI: blue), an endothelial marker (Isolectin-B4: red) and incubated with anti-ICAM-1 antibody under optimized conditions. Vascular ICAM-1 expression (green) was observed in the positive control hearts, I-R hearts but not in normal or I-R injury hearts. Scale bar: 100 μm.

4.4. Retention of BMMNC after IC injection into normal hearts

4.4.1. Langendorff parameters after BMMNC injection

IC cell injection carries a risk of coronary embolism, deteriorating cardiac perfusion and function. This risk could be dependent on donor cell numbers to be injected. It was therefore determined whether cell injection significantly affected coronary perfusion flow rates after injection of 1×10^6, 8×10^6 and 40×10^6 BMMNC into normal hearts (Figure 4-25).

In the first minute during cell injection, there was a slight increase in coronary effluent flow rates (but this volume included the 3mls of cell suspension). Post injection in the subsequent minutes, there was no change in coronary effluent volume after any injected cell dose. Correspondingly, there was no significant change found in the temperature or heart rate (Figure 4-26) of the perfused hearts before and after cell injection in any groups. This suggests that this range of BMMNC doses do not result in acute damage to the heart or coronary embolism.

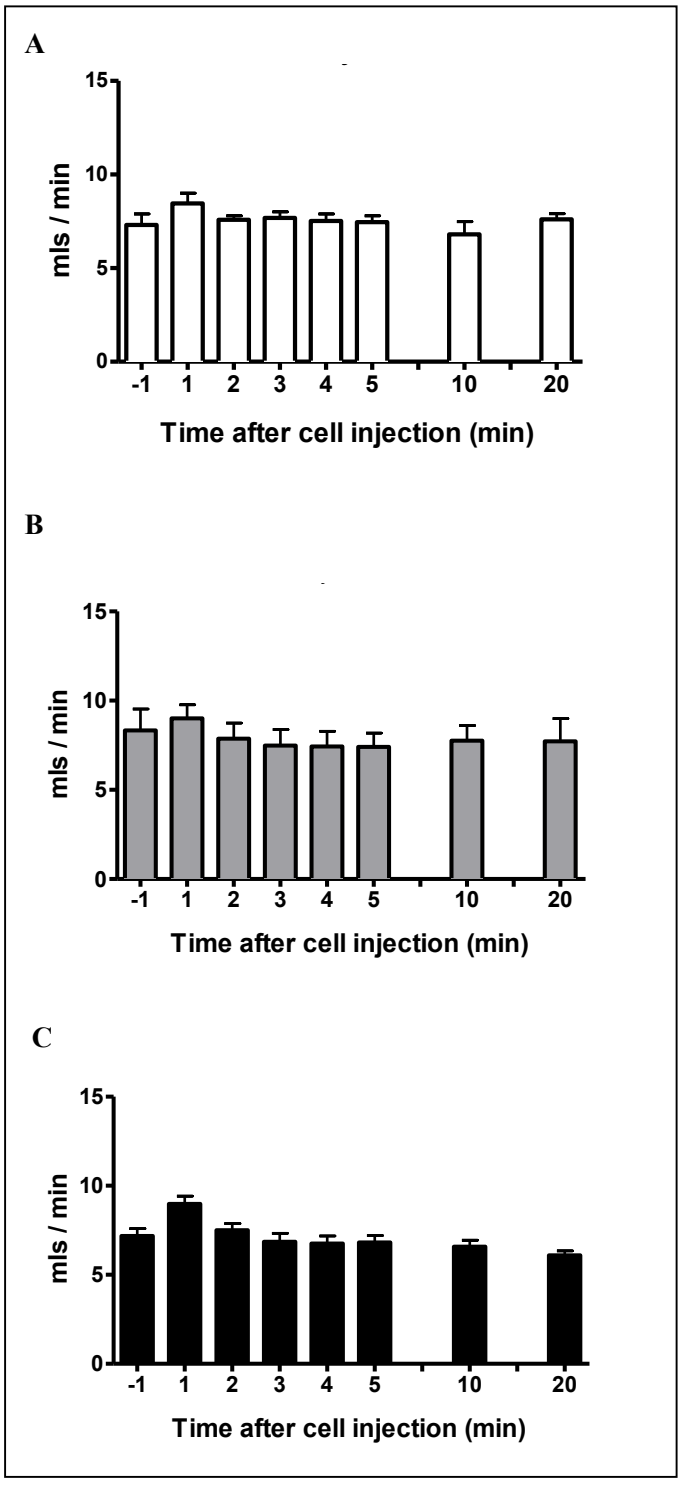

Figure 4-25: Coronary flow before and after BMMNC injection into normal hearts. Data shown for different donor cell numbers injected: (A) 1×10^6, n=5, (B) 8×10^6, n=10 (C) and 40×10^6 n=7. The coronary effluent volume collected immediately prior to the cell injection is labelled -1. The coronary effluent within the 1st minute of cell injection is labelled 1 and includes the 3 ml of Krebs-Henseleit buffer in which the cells were suspended. Data expressed as mean ± SEM.

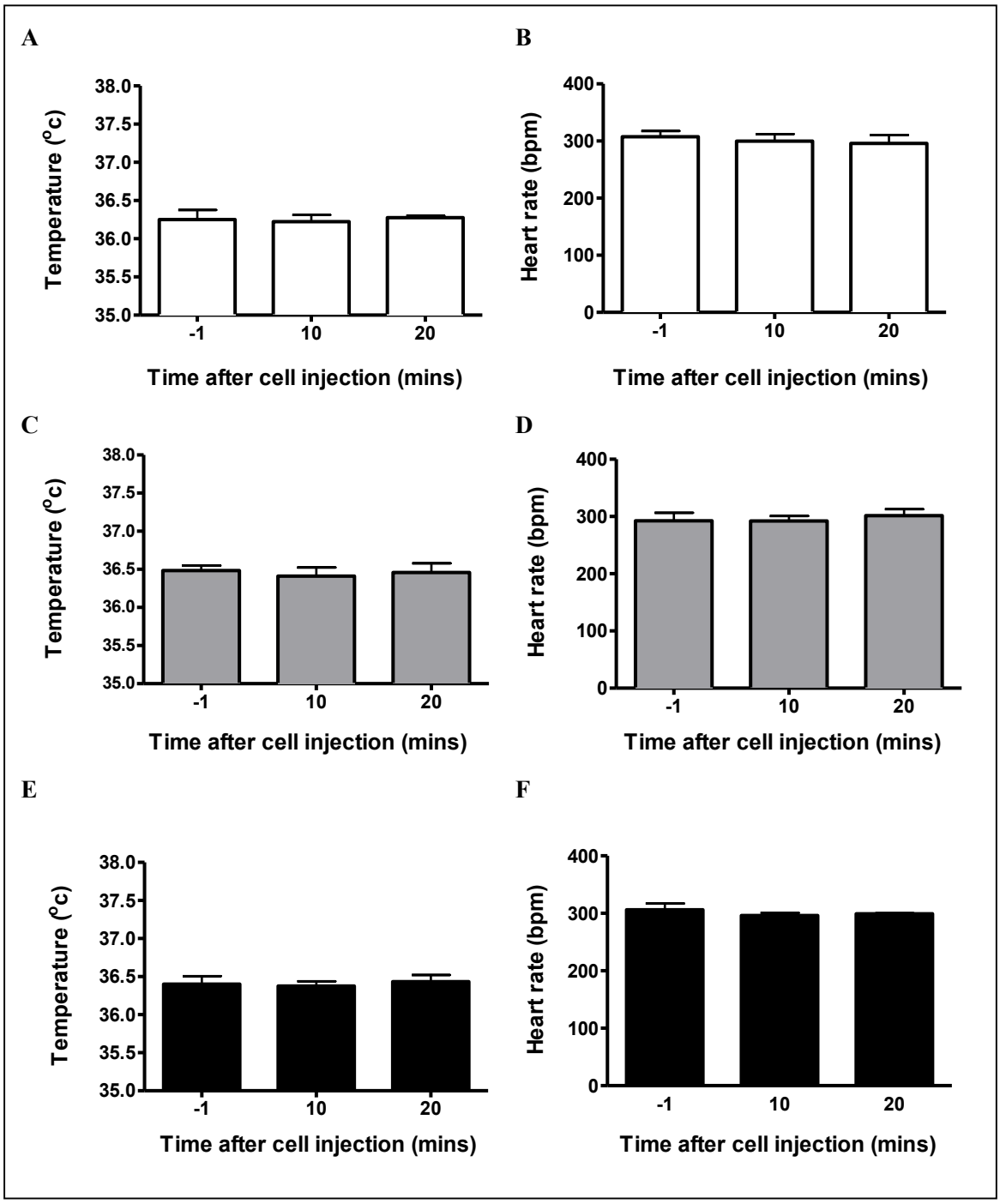

Figure 4-26: Temperature and heart rate of Langendorff perfused normal hearts. The temperature and heart rate of coronary perfusate exiting the heart was recorded before and after injection of different cell numbers (A and B) $1x10^6$, n=5, (C and D) $8x10^6$, n=10 (E and F) and $40x10^6$ n=7. The time in the minute prior to injection is labelled "-1". Data expressed as mean ± SEM.

4.4.2. Pattern of BMMNC loss into coronary effluent

Cell counts in the coronary effluent after injection of 1×10^6, 8×10^6 and 40×10^6 BMMNC into normal hearts were serially quantified (Figure 4-27). As described in 3.6.6, there was a small (but measurable), number of RBC that continued to leak into the coronary effluent prior to cell injection, Within the 1st minute of cell injection, there was a rapid increase in donor cells in the coronary effluent which progressively decreased over the subsequent minutes. Within 5 minutes, the cell count per minute had returned to the baseline level. This pattern of cell loss in the coronary effluent appeared to be the same between the groups. The baseline level was deemed to be the background RBC loss.

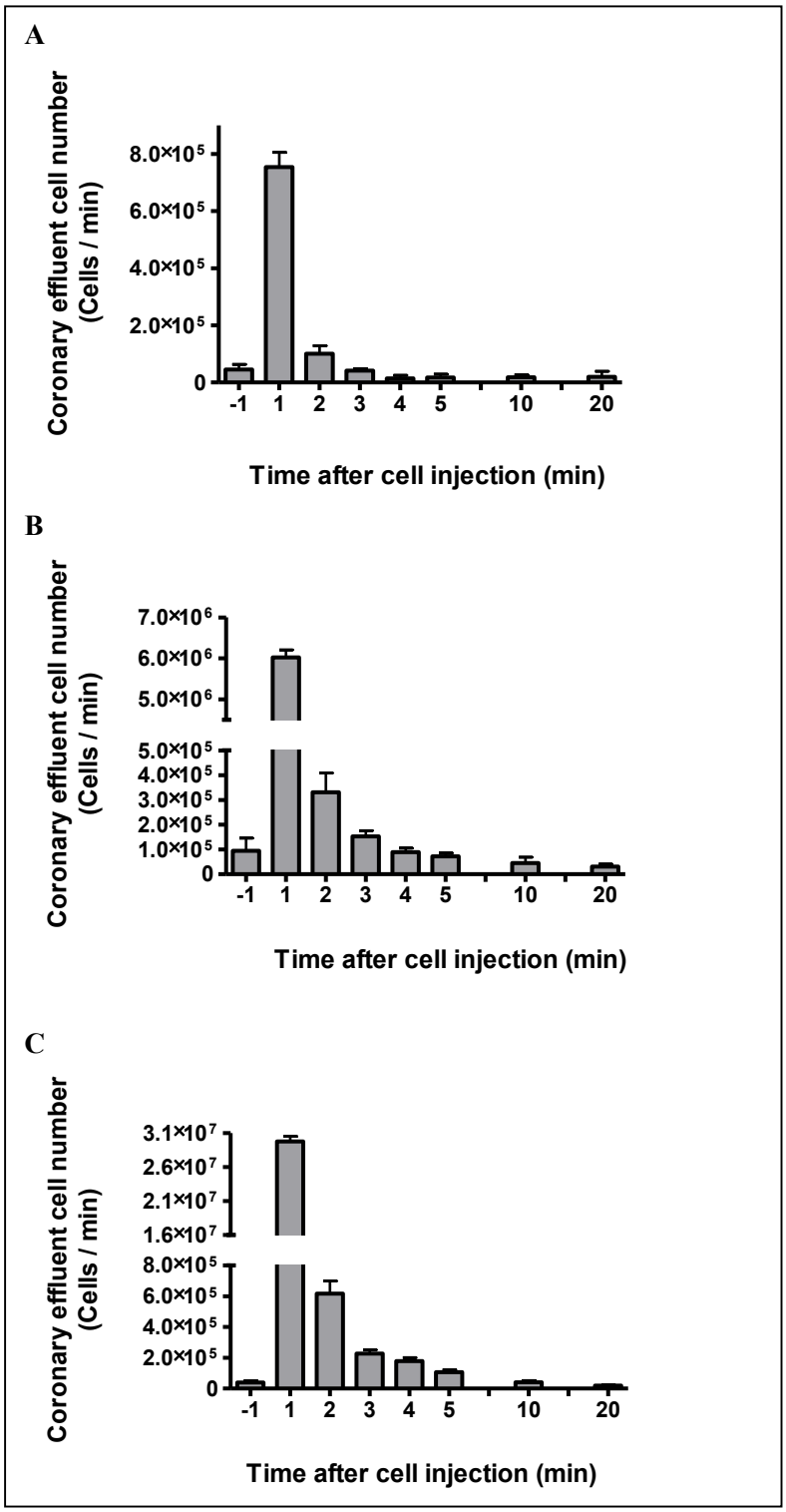

Figure 4-27: Cell numbers in the coronary effluent before and after injection of BMMNC into normal hearts. Data is shown for injection of (A) 1×10^6 BMMNC, n=5, (B) 8×10^6 BMMNC, n=13 and (C) 40×10^6 BMMNC, n=8. -1 represents the minute prior to injection. Error bars represent SEM.

To precisely quantify the donor cell retention rate, these cell numbers in the coronary effluent were adjusted by subtracting the RBC number in the coronary effluent. As discussed in 3.6.8, the mean cell count for the minute prior to injection and the fifth minute post injection were used to calculate the baseline RBC level in the coronary effluent. This was subtracted from the cell counts obtained during the first 5 minutes of cell injection. The justification for this was as follows: the cell count in the coronary effluent at 5 minutes was not statistically different from the cell count for the minute immediately preceding BMMNC injection. This suggested that all detectable donor cells had been flushed out of the heart within the first 5 minutes and that the cell count at 5 minutes had returned to the baseline RBC count.

Using this concept, the pattern of calculated donor cell loss is shown after injection of 1×10^6, 8×10^6 and 40×10^6 BMMNC (Figure 4-28). The time course of the pattern of donor cell leakage was broadly the same between the groups. Within the first minute, the cell loss was at its highest, but this number progressively decreases in a logarithmically decreasing pattern. By 5 minutes, the number of donor cells leaving the heart was very small and did not make a large contribution to overall cell loss. At the fifth minute, the mean cell count in the coronary effluent was undetectable after injection of 1×10^6 BMMNC, $<1.5\times10^4$ cells per minute after injection of 8×10^6 BMMNC and $<5.0\times10^4$ cells per minute after injection of 40×10^6 BMMNC.

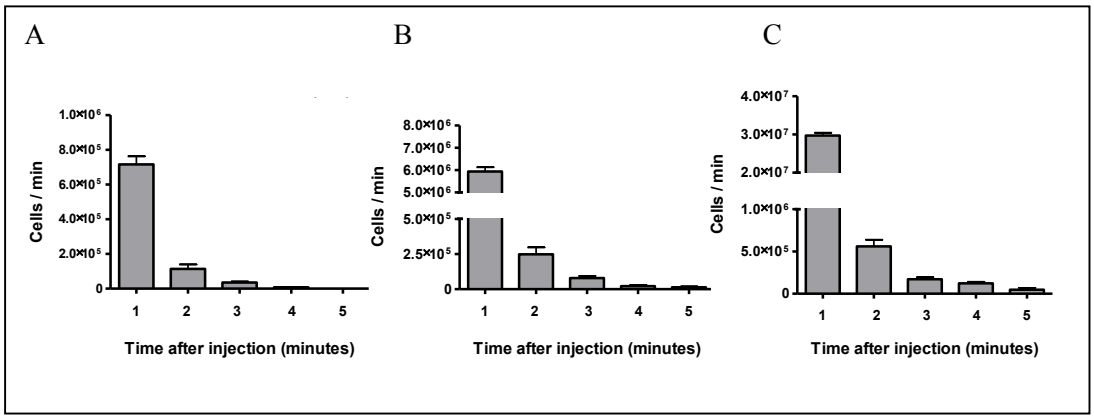

Figure 4-28: Calculated donor cell numbers in the coronary effluent after injection of BMMNC into normal hearts. Data is shown for injection of (A) 1×10^6 BMMNC, n=5, (B) 8×10^6 BMMNC, n=13 and (C) 40×10^6 BMMNC, n=8. Error bars represent SEM.

To further clarify whether the rate and pattern of cell loss was similar between the injected cell numbers, the cell counts for each minute were expressed as a fraction of the total coronary effluent BMMNC loss (Figure 4-29). It was determined that within the first minute of cell injection, 90.1 ± 5.0% ($1x10^6$ group), 94.9 ± 0.8% ($8x10^6$ group), and 97.0 ± 0.3% ($40x10^6$ group) of all the donor cells lost had leaked into the coronary effluent.

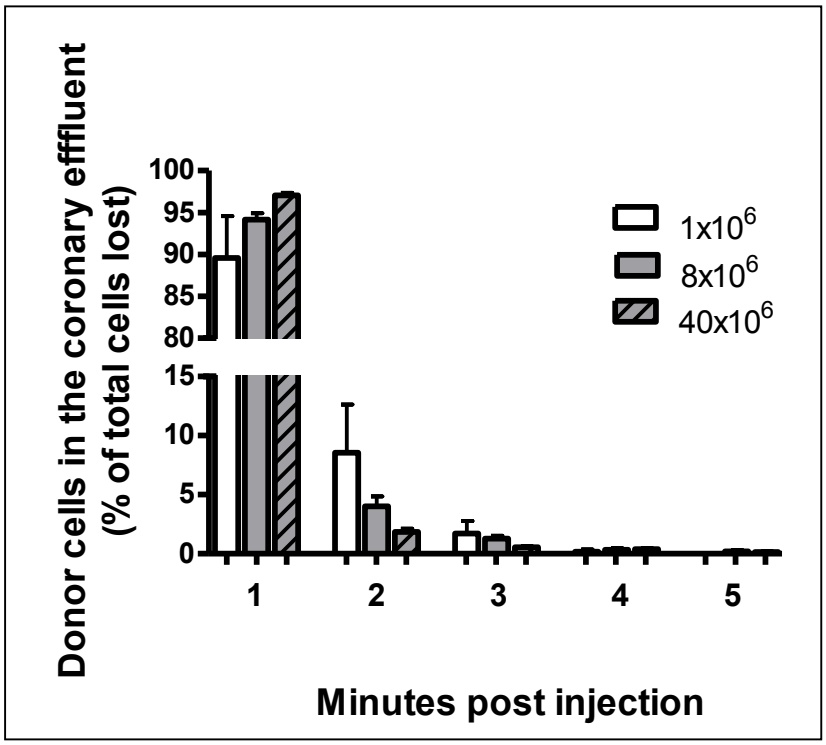

Figure 4-29: BMMNC loss into coronary effluent after injection into normal hearts. The patterns of cell loss between the three BMMNC number groups injected into normal hearts were compared. The cell count for each minute was expressed as a fraction of the total cell loss in the coronary effluent up until 5 minutes. (n=5, 13, and 8 for injection of 1, 8, and $40x10^6$ BMMNC). Error bars = SEM.

4.4.3. BMMNC retention efficiency in normal hearts

The absolute number of donor BMMNC retained in the heart after IC injection was calculated with knowledge of the donor cell number in the coronary effluent (refer to 4.4.2) and the total injected cell number and compared between the 3 BMMNC cell doses (1×10^6, 8×10^6 and 40×10^6). The absolute number of retained donor BMMNC was significantly increased following a higher injected cell dose ($p<0.0001$, One-way ANOVA). The mean absolute retention cell numbers for 1×10^6, 8×10^6 and 40×10^6 groups were $0.20 \pm 0.04 \times10^6$ (n=5), $1.70 \pm 0.18 \times10^6$ (n=13) and $9.40 \pm 0.74 \times10^6$ (n=8) respectively (Figure 4-30, A). The proportion of the retained cells at 5 minutes as a fraction of the total injected cell dose was then calculated (Figure 4-30, B). It was found that there was no difference between the retained proportions of cells between the 3 groups. The retained proportions of injected 1×10^6, 8×10^6 and 40×10^6 BMMNC were the same (20.0 ± 3.5%, 21.2 ± 2.2 and 23.5 ± 2.2% respectively).

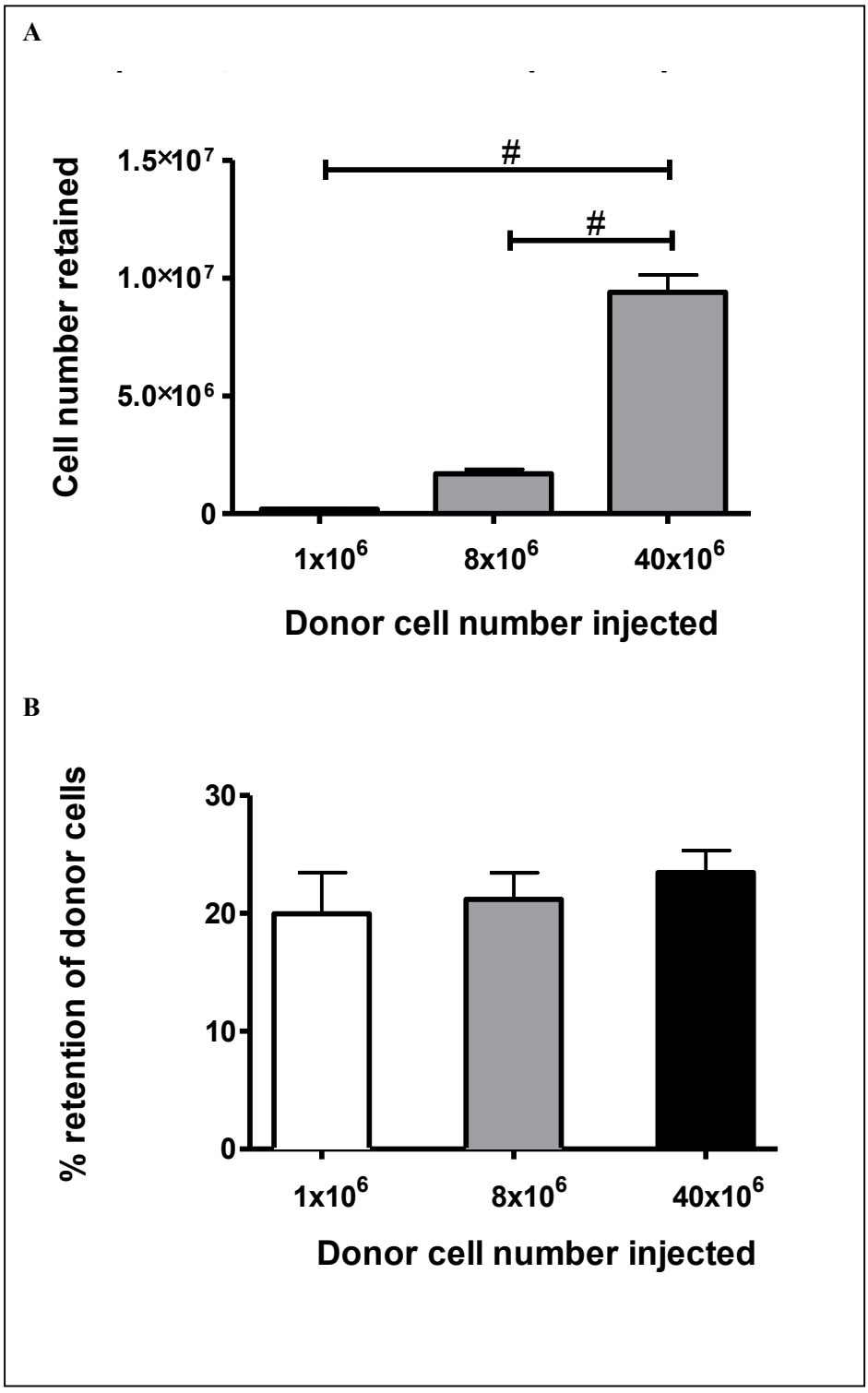

Figure 4-30: BMMNC retention in normal hearts. Donor cell retention in the heart after IC injection of different BMMNC doses is shown for (A) absolute number of cells retained and (B) retained cells as a proportion of the injected number. Error bars indicate SEM. (n=5, 13, and 8 for injection of 1, 8, and $40x10^6$ BMMNC). #=$p<0.05$, Bonferroni's multiple comparison test

I further analysed the initial BMMNC retention after IC injection into normal hearts with a focus on minute-by-minute changes in the retention efficiency for the first five minutes post injection (Figure 4-31). There was a slight decrease in the proportion of injected cells in the heart over time, but this pattern did not differ between the injected cell numbers (Two-way ANOVA for each time point). Additionally, there was no difference between the cell retention over 5 minutes for each cell group. This suggests that BMMNC retained at 1 minute after IC injection were mostly retained after 5 minutes, regardless of cell numbers injected.

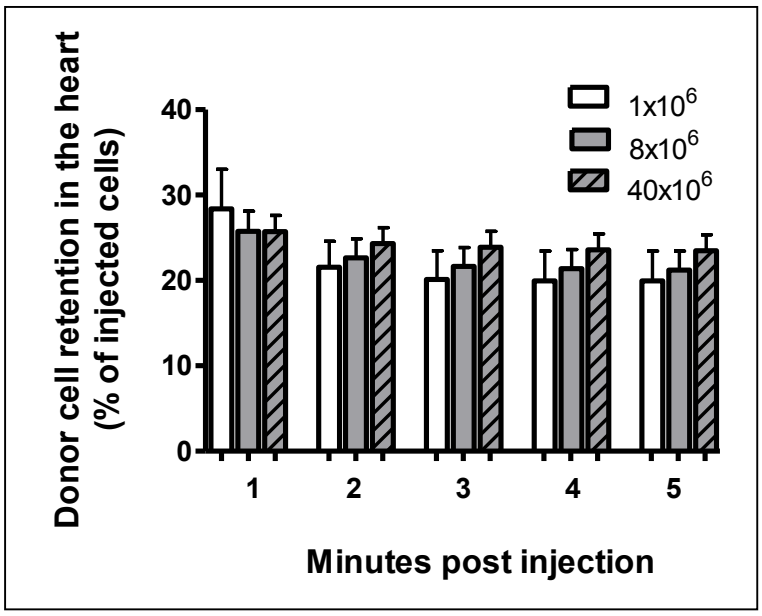

Figure 4-31: Minute-by-minute BMMNC retention efficiency in the normal heart after IC injection. The proportion of injected donor cells retained in the heart was calculated for each of the first 5 minutes post injection. For each cell number injected, there was a subtle decrease in retained cells. Error bars indicate SEM. n=5, 13, and 8 for 1×10^6, 8×10^6 and 40×10^6 BMMNC injection groups.

4.4.4. Cell surface markers of BMMNC in coronary effluent

The surface marker expression of BMMNC in the coronary effluent was assessed by flow cytometry and compared with BMMNC prior to injection, with a view to determining whether cells with a particular surface protein were preferentially retained in the heart after IC injection. Three separate experiments were performed using cells obtained from the coronary effluent after 40×10^6 BMMNC injection into normal hearts. It was observed that the expression of each surface marker investigated was not altered between pre-injection BMMNC and BMMNC in the coronary effluent (Figure 4-32; unpaired T-test: NS for each marker). This suggests cell retention using these experimental conditions is not dependent on these cell surface markers.

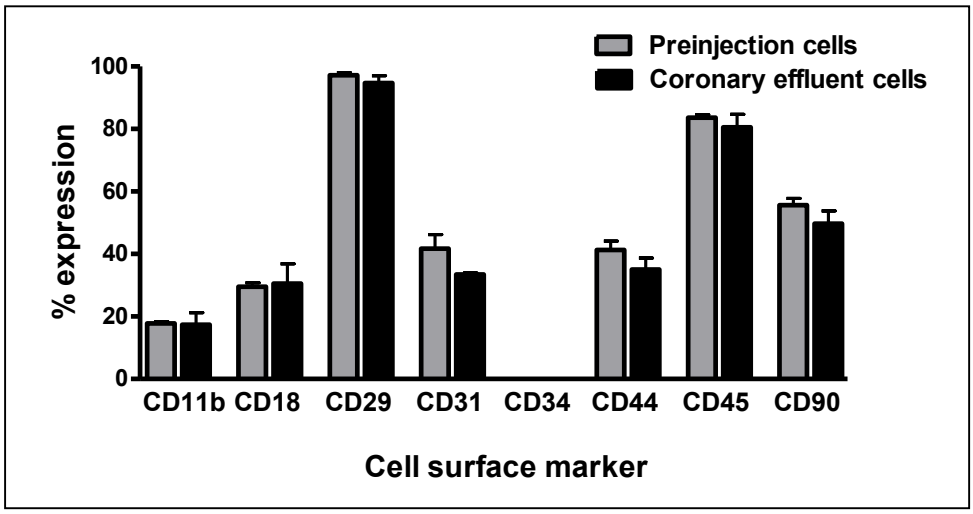

Figure 4-32: Surface marker expression in BMMNC in coronary effluent. CD marker expression of donor cells pre-injection (n=5) and donor cells in the coronary effluent (n=3) was not different. Error bars indicate SEM.

4.4.5. Size of BMMNC in coronary effluent

To study the hypothesis that cell size is a factor which determines donor cell retention after IC injection, the cell size distribution of BMMNC in the coronary effluent was determined using an automated cell counter and compared with BMMNC before injection.

The mean cell size of BMMNC in the coronary effluent was 6.85 μm and the median cell size was 7 μm. This compared to the mean and median cell size of 7.0 μm in the pre-injection sample (refer to 4.1.1). The coronary effluent cells had a trend towards a leftwards shift in cell size, with an increase in the proportion of smaller BMMNC and a reduction in the proportion of larger BMMNC (Figure 4-33).

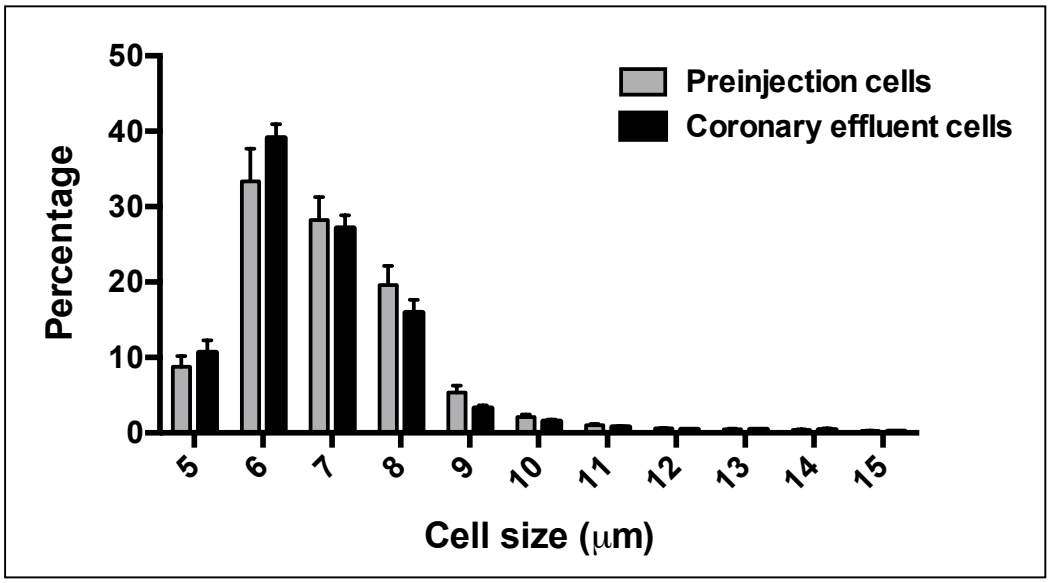

Figure 4-33: Cell size distribution of BMMNC in coronary effluent after injection into normal vs. pre-injection hearts. The distribution of BMMNC size of donor cell prior to injection and in the coronary effluent were compared with an automated cell counter for n=6 normally perfused hearts. The number of BMMNC for each cell size was calculated and expressed as a fraction of all the BMMNC in each group. There appeared to be a leftwards shift in the size of coronary effluent cells compared to the pre-injection cells. n=23,942 pre-injection cells. Error bars indicate SEM.

Because the total cell number within the coronary effluent and the distribution of pre-injection donor cell sizes were known, the proportion of retained cells according to cell size could be calculated. For further analysis, the cells were subdivided into three groups; cells with size of 5-6 μm (below the median size), 7 μm (the median size) and ≥ 8 μm (above the median size). Figure 4-34 demonstrates the relative proportions of cell sizes for pre-injection donor cells and donor cells retained in the heart. The proportion of retained BMMNC with a below-median pre-injection diameter (5-6 μm) was lower than that of pre-injection BMMNC. In contrast, the proportion of retained BMMNC with an above-median pre-injection diameter (≥ 8 μm) was greater than that of pre-injection BMMNC. The proportion of retained BMMNC with a median cell diameter (7 μm) was unchanged compared with the pre-injection samples of all the retained cells in the heart.

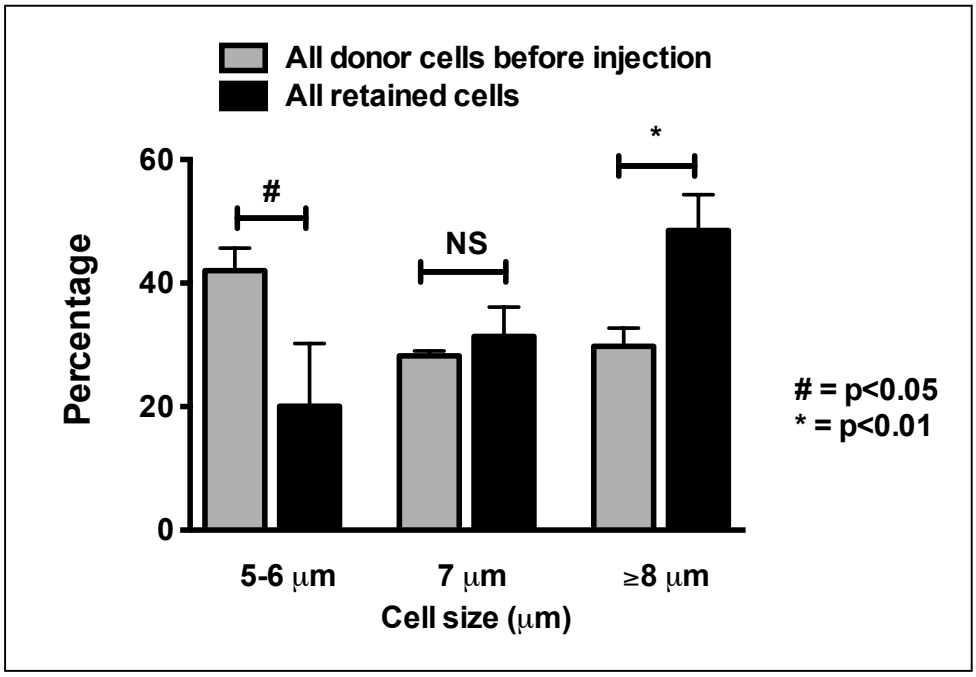

Figure 4-34: Cell size distribution of donor BMMNC prior to injection and of retained BMMNC after IC injection into the normal heart. The proportions of cells below the median (5-6 μm), the median (7 μm) and above the median ≥8 μm were calculated. The proportion of smaller BMMNC retained in the heart below the median size was lower than that of pre-injection BMMNC. Conversely, larger cells were retained with increased efficiency. Error bars indicate SEM, n=11, # = $p<0.05$ (2-tailed unpaired T-test).

The relationship between donor BMMNC size and retention efficiency after IC injection into the normal heart was further analysed. This result clearly showed that there was an increase in cell retention efficiency with greater donor cell size ($p<0.05$, One-way ANOVA). The proportion of injected BMMNC ≥ 8 μm that were retained was 2.41-fold larger (48.8% *vs*. 20.2%, $p<0.05$) than that for BMMNC with a 5-6 μm cell size (Figure 4-35).

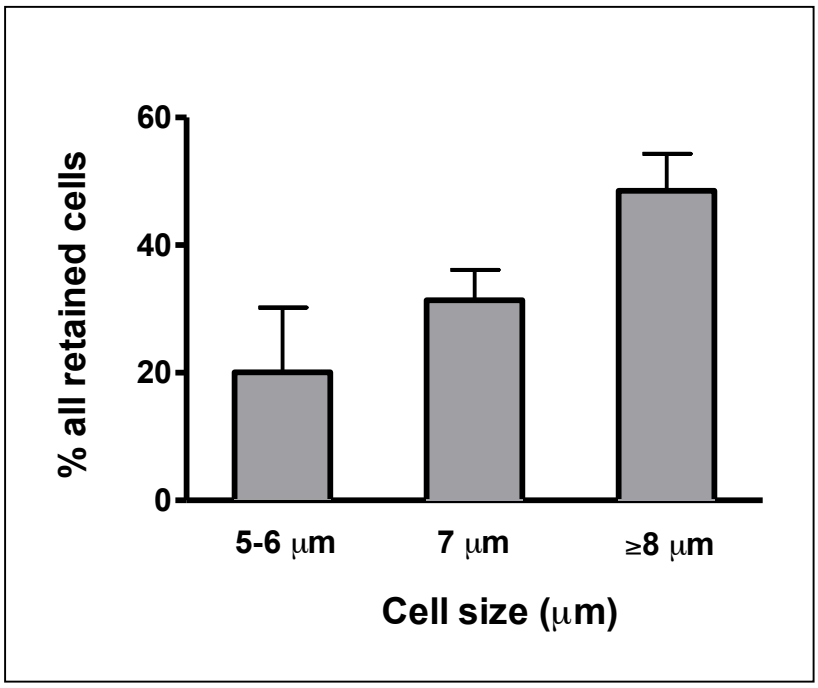

Figure 4-35: Retention efficiency of BMMNC according to their cell size. The proportions of the sizes of donor cells retained in the heart were calculated (n=5). Larger cells were preferentially retained ($p<0.05$, One-way ANOVA). Error bars indicate SEM.

4.4.6. Histological distribution of retained BMMNC in the heart

The anatomical location of PKH67-positive donor BMMNC within the recipient normal hearts after IC injection was histologically determined (refer to 3.8.1). In brief, each segment (apex, mid section, base) was analysed separately per heart and the anatomical location of every PKH67-labelled cell was recorded. The cross-sectional area of each myocardial section was calculated using ImageJ software analysis. The results showed that there was a trend towards a higher concentration of cells localized in the mid section, but this was not statistically significant (Figure 4-36; Mid: 1.4 ± 0.3, n=8 hearts, Apex: 0.9 ± 0.1, n =5 hearts, Base: 0.7 ± 0.1 cells/mm^2, n=5 hearts, p=0.06, One-way ANOVA).

Next, the location of donor cells within the ventricular wall was noted - endocardium, myocardium or epicardium (divided by eye into 3 equal proportions). There was a progressive increase in concentration of donor cells towards the endocardium. There was a three times higher concentration of donor cells in the endocardium compared to the epicardium ($p<0.0001$, One-way ANOVA)

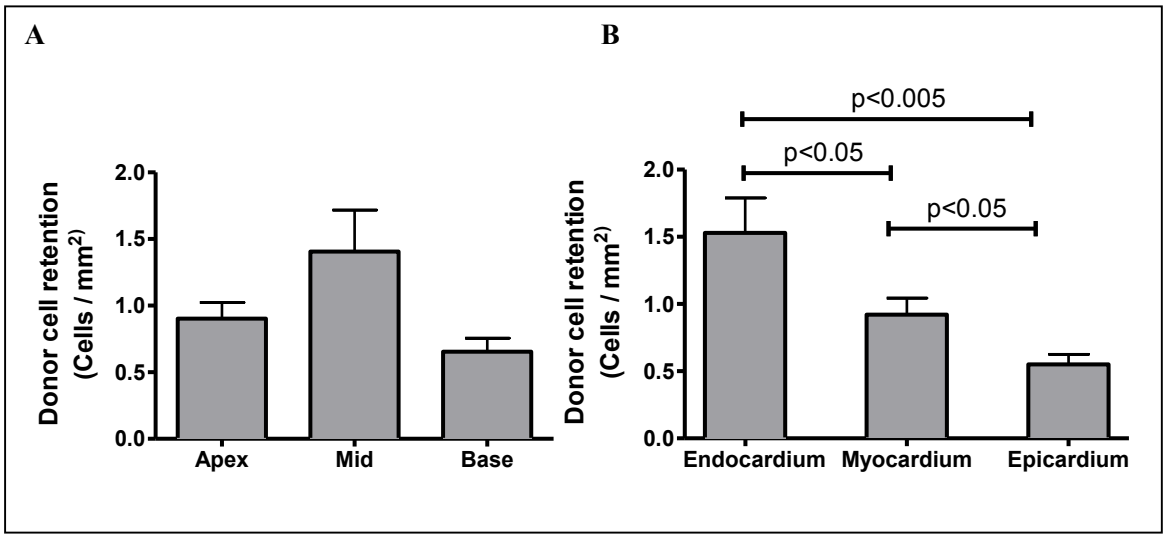

Figure 4-36: Location of retained donor cells within the normal heart. The number of fluorescently-labelled cells in the apex (n=8), mid-section (n=6) and base (n=5) were compared after injection of 8×10^6 cells into normally perfused Langendorff hearts, corrected for the cross-sectional area (A). There was no significant difference between the three sections (p=0.06, One-Way ANOVA). Additionally, the depth of cells within the ventricular wall was noted on all the heart sections (B). The concentration of cells progressively increased from the epicardium (n=13) to the myocardium (n=19) to the endocardium (n=19); p<0.0001, One-way ANOVA.

4.4.7. Anatomical relationship between retained cells and the coronary vasculature

The location of cells related to the coronary vasculature (inside or outside of the vascular cavity; endothelial adhesion or extravasation) was determined by injection of PKH67-labelled BMMNC injected hearts with isolectin-B4 and DAPI staining. At 5 minutes after cell injection, all the observed PKH67-labelled cells were inside the vasculature (representative images: Figures 4-37 and 4-38). In further analyses of the hearts obtained for sectioning 60 minutes after cell injection, no observed PKH67-labelled cell was observed to have extravasated out of the coronary vasculature (representative images: Figures 4-39 and 40). There were no findings to suggest coronary embolism histologically.

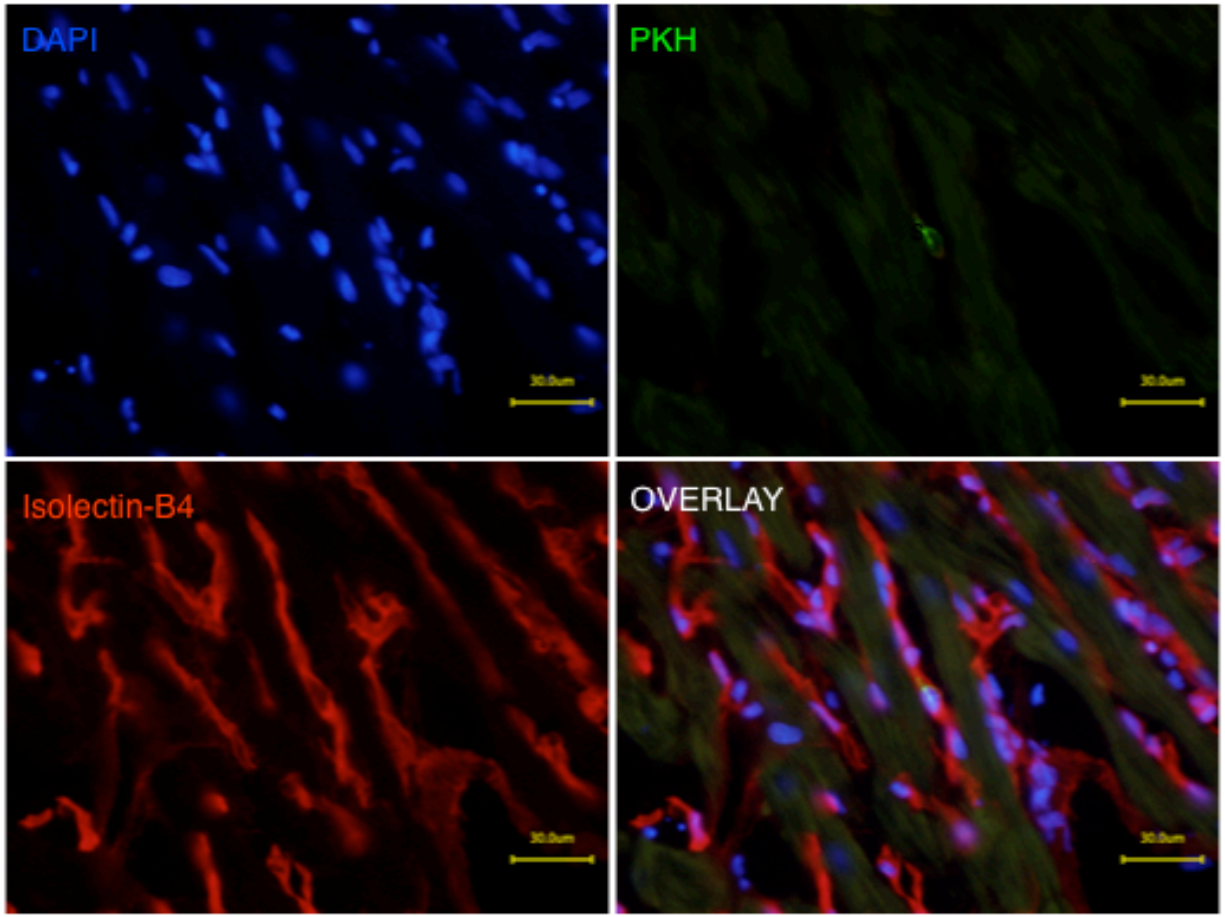

Figure 4-37: Typical image of retained donor BMMNC at 5 minutes of IC injection in normal hearts (low magnification). 5 minutes after injection of PKH67 (green)-labelled BMMNC into normal hearts, the hearts were acquired and analysed. Sections were stained with a nuclear marker (DAPI; blue) and an endothelial marker (Isolectin-B4; red). All cells were seen inside the vascular lumen. Usually PKH67-positive cells were observed in isolation and always inside the vessels. Scale bar = 30 μm.

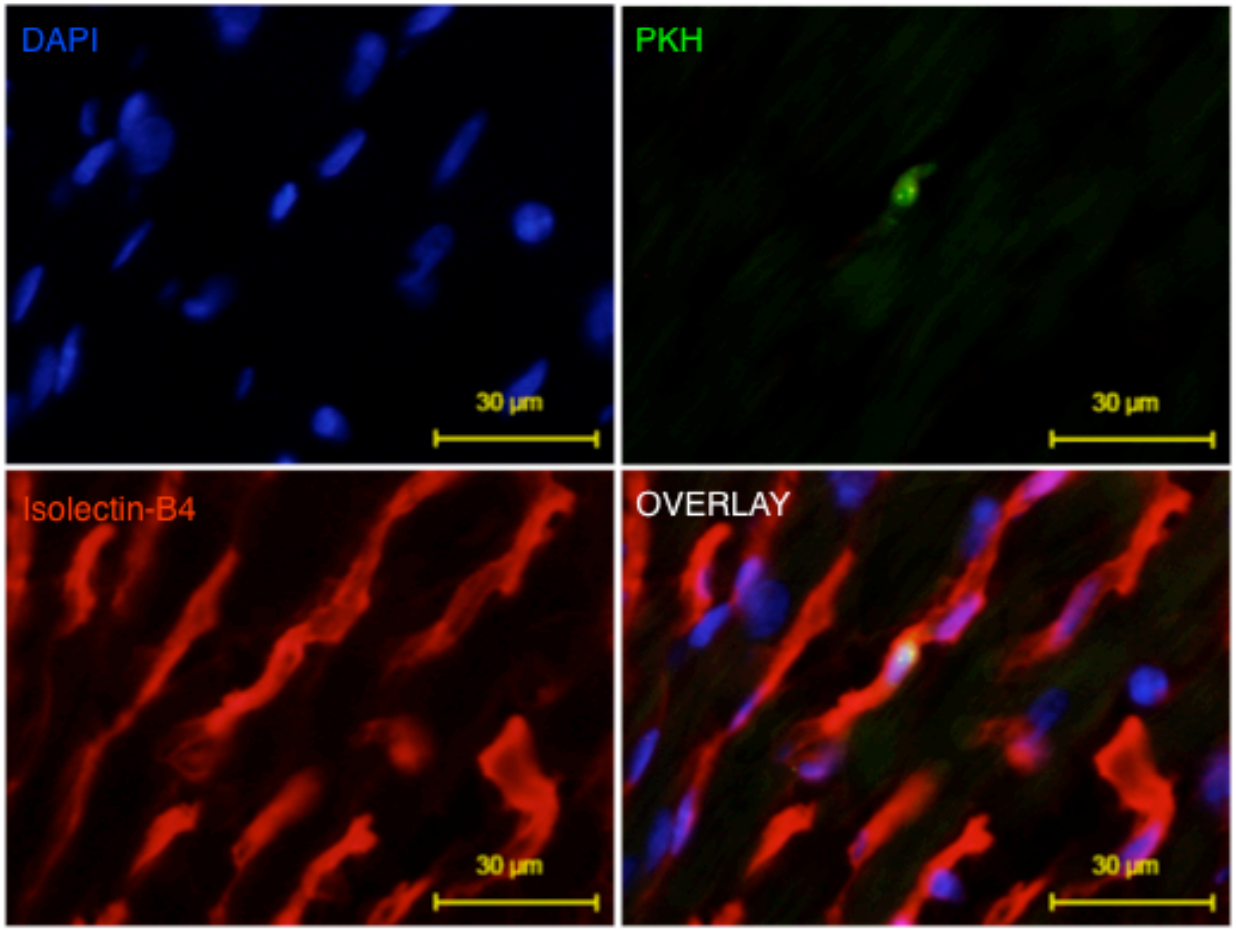

Figure 4-38: Typical image of retained donor BMMNC at 5 minutes of IC injection in normal hearts (high magnification). 5 minutes after injection of PKH67 (green)-labelled BMMNC into normal hearts, the hearts were acquired and analysed. Sections were stained with a nuclear marker (DAPI; blue) and an endothelial marker (Isolectin-B4; red). All cells were seen inside the vascular lumen. Usually PKH67-positive cells were observed in isolation and always inside the vessels. Scale bar = 30 µm.

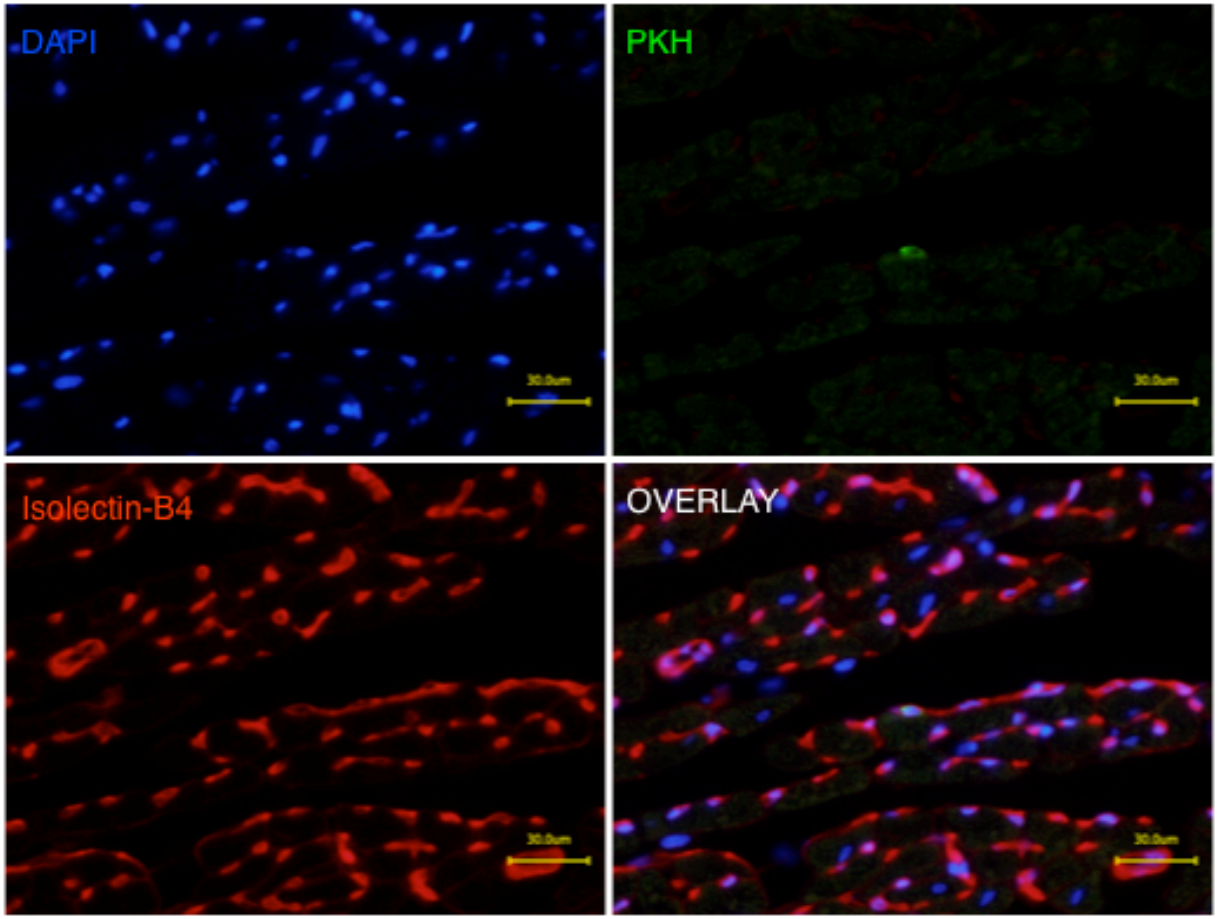

Figure 4-39: Typical image of retained donor BMMNC at 60 minutes of IC injection in normal hearts (low magnification). 60 minutes after injection of PKH67 (green)-labelled BMMNC into normal hearts, the hearts were acquired and analysed. Sections were stained with a nuclear marker (DAPI; blue) and an endothelial marker (Isolectin-B4; red). All cells were seen inside the vascular lumen. Usually PKH67-positive cells were observed in isolation and always inside the vessels. Scale bar = 30 μm.

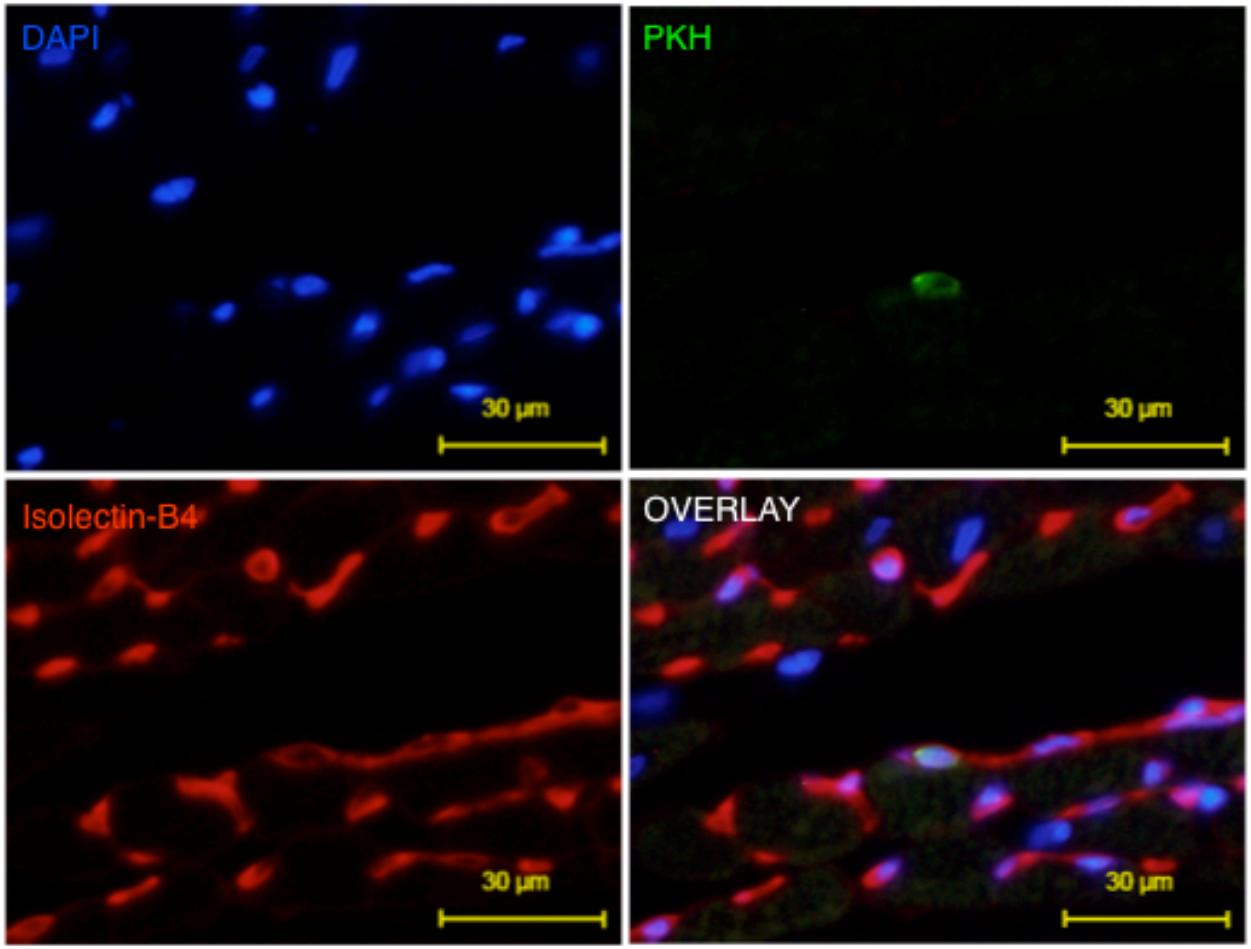

Figure 4-40: Typical image of retained donor BMMNC at 60 minutes of IC injection in normal hearts (high magnification). 60 minutes after injection of PKH67 (green)-labelled BMMNC into normal hearts, the hearts were acquired and analysed. Sections were stained with a nuclear marker (DAPI; blue) and an endothelial marker (Isolectin-B4; red). All cells were seen inside the vascular lumen. Usually PKH67-positive cells were observed in isolation and always inside the vessels. Scale bar = 30 µm.

4.5. Retention of BMMNC after IC injection into I-R hearts

4.5.1. Langendorff parameters of I-R hearts after BMMNC injection

IC injection after I-R may be more likely to result in coronary embolism, which would lead to decreased coronary effluent volumes and derangement of cardiac function compared to the normal heart. This could also be dependent on donor cell numbers. It was determined whether cell injection affected coronary perfusion after injection of $1x10^6$, $8x10^6$ and $40x10^6$ BMMNC into I-R hearts.

There was no decrease in the coronary effluent flow rate after injection after any injected cell dose (Figure 4-41). Similarly, there was no significant change found in temperature or heart rate (Figure 4-42) of the perfused hearts before and after cell injection in any groups. This suggests that this range of BMMNC doses did not result in acute damage to the heart or coronary embolism after IC injection in I-R hearts.

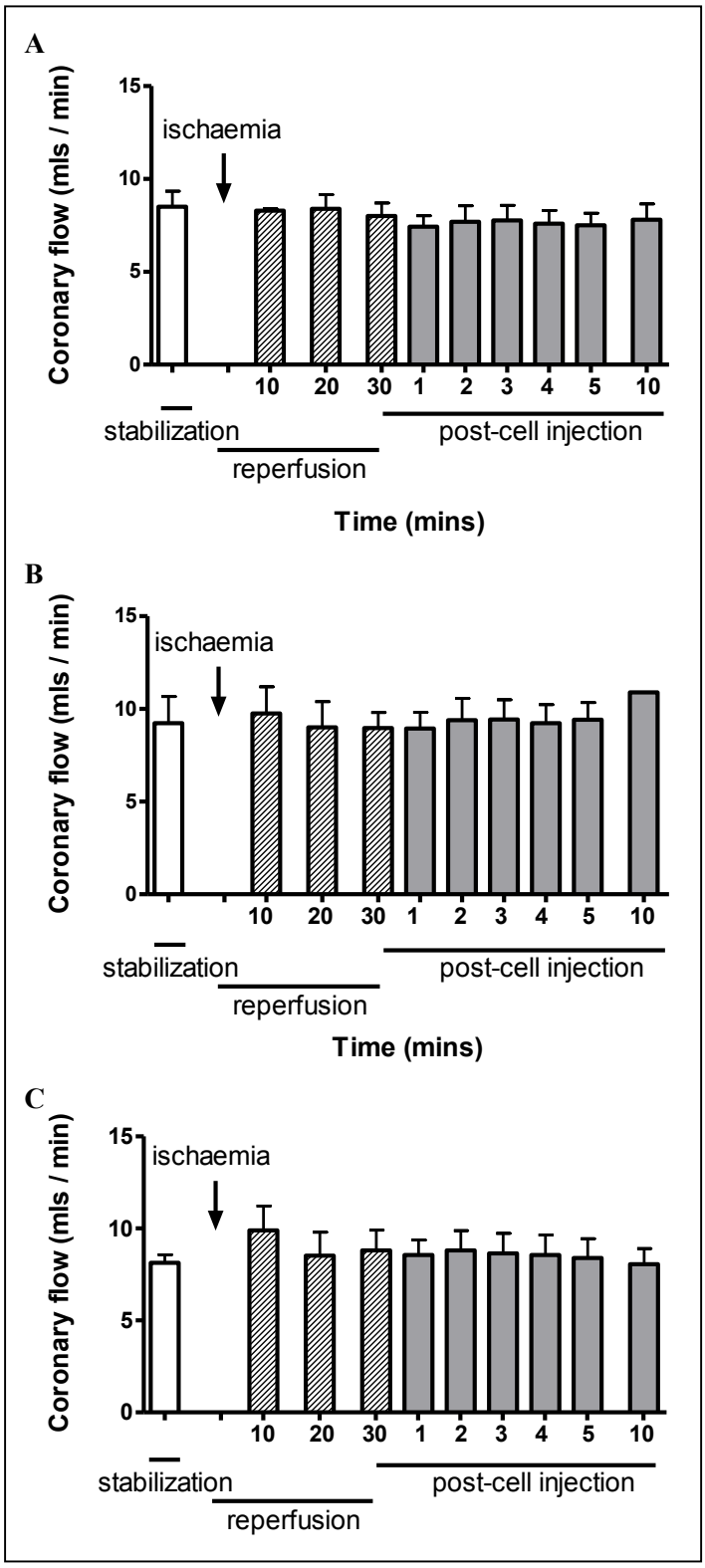

Figure 4-41: Coronary flow before and after IC BMMNC injection into I-R hearts. Data are shown for different cell numbers injected: (A) $1^{x}10^{6}$ BMMNC (n=4), (B) $8^{x}10^{6}$ BMMNC (n=4) and (C) $40^{x}10^{6}$ BMMNC (n=6). Stabilization = 1 minute prior to ischaemia. Error bars indicate SEM.

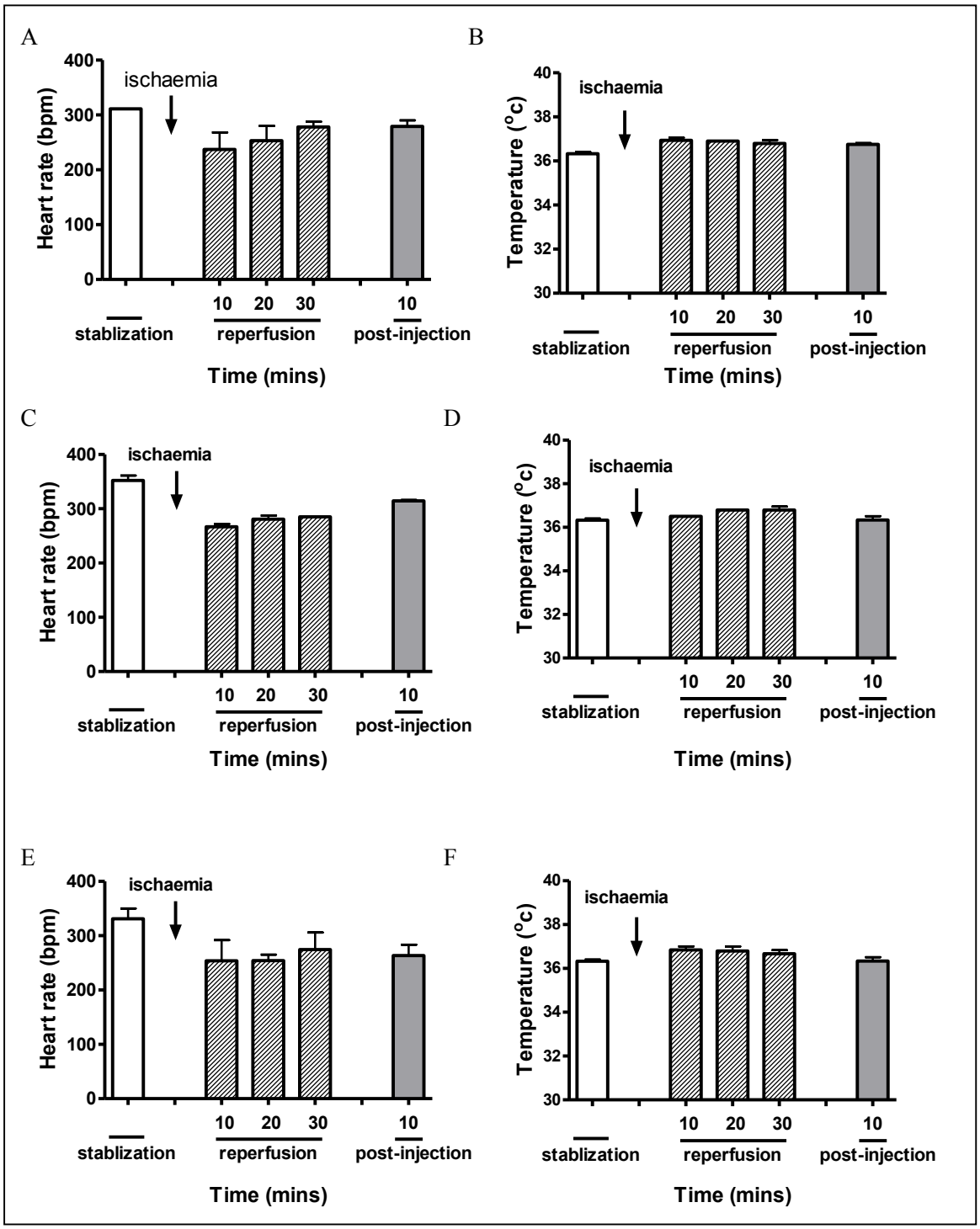

Figure 4-42: Heart rate and temperature during stabilization, reperfusion and after injection of BMMNC into I-R hearts. Data is shown for (A and B) $1x10^6$ BMMNC, (C and D) $8x10^6$ BMMNC and (E and F) $40x10^6$ BMMNC. Stabilization = 1 minute prior to ischaemia. Data is expressed as mean ± SEM.

4.5.2. Pattern of BMMNC loss into coronary effluent

Cell counts in the coronary effluent after IC BMMNC injection into I-R hearts were quantified. As discussed in 3.6.8, the baseline RBC level in the coronary effluent was calculated for each heart sample. This was subtracted from the cell counts obtained during the first 5 minutes of cell injection.

Using this concept, the pattern of donor cell loss into coronary effluent is shown after injection of $1x10^6$, $8x10^6$ and $40x10^6$ BMMNC (Figure 4-43). The time course of the pattern of donor cell leakage was similar between the groups. Within the first minute, donor cell loss rates in the coronary effluent were at their highest, but this loss progressively decreased in a logarithmically decreasing pattern. By 5 minutes the number of donor cells leaving the heart was very small and did not make a sizable contribution to overall donor cell loss. At the fifth minute, the mean cell count in the coronary effluent was $2.1x10^4$ cells per minute after injection of $1x10^6$ BMMNC, $3.6x10^4$ cells per minute after injection of $8x10^6$ BMMNC, and $6.1x10^4$ cells per minute after injection of $40x10^6$ BMMNC.

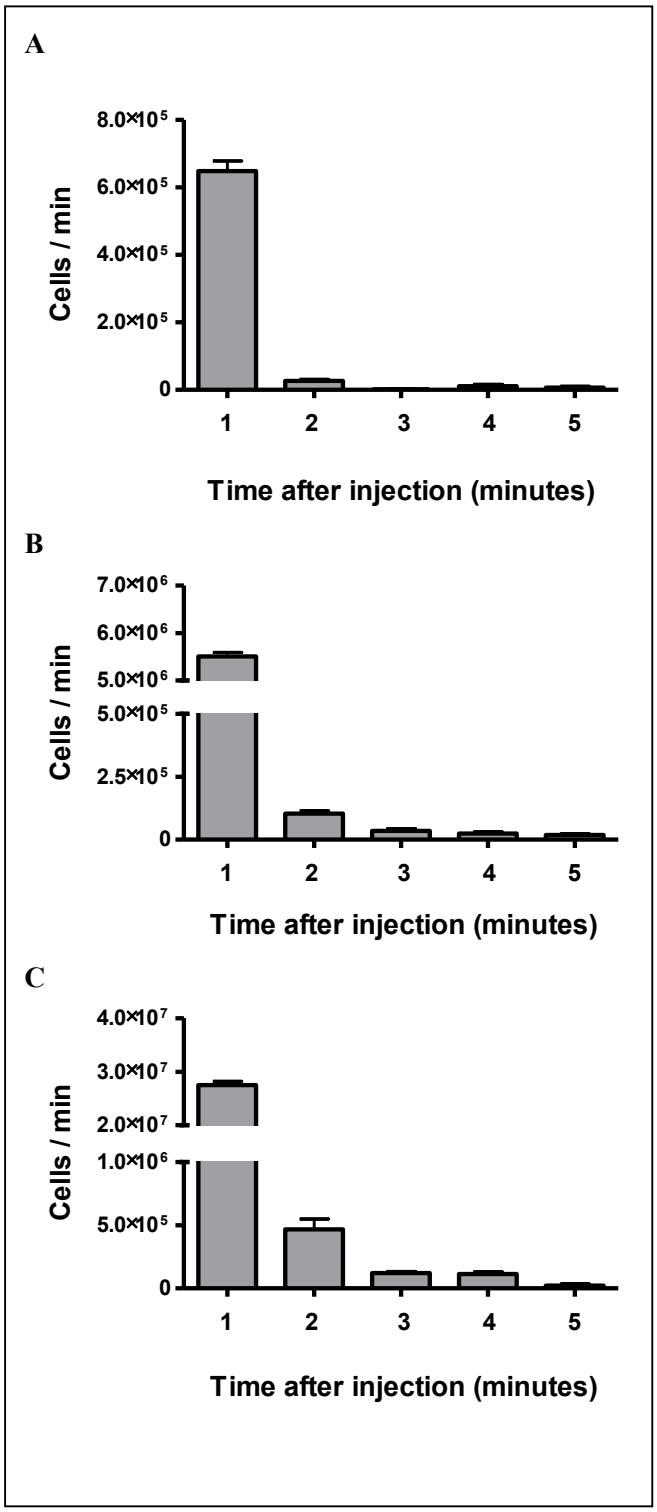

Figure 4-43: Calculated donor cell numbers in the coronary effluent after injection of BMMNC into I-R hearts. Data is shown for injection of (A) $1x10^6$ BMMNC (n=4), (B) $8x10^6$ BMMNC (n=11) and (C) $40x10^6$ BMMNC (n=6) into IR Langendorff hearts after stabilisation. Error bars represent SEM.

To further assess if the rate of cell loss was different between the injected cell numbers ($1x10^6$, $8x10^6$ and $40x10^6$), the cell counts for each minute were expressed as a fraction of the total coronary effluent cell loss (Figure 4-44). It was determined that within the first minute of cell injection, 95.0 ± 2.1% ($1x10^6$ group), 97.2 ± 0.3% ($8x10^6$ group), and 97.5 ± 0.4% ($40x10^6$ group) of the original donor cell number were lost into the coronary effluent (p=0.12, One-way ANOVA).

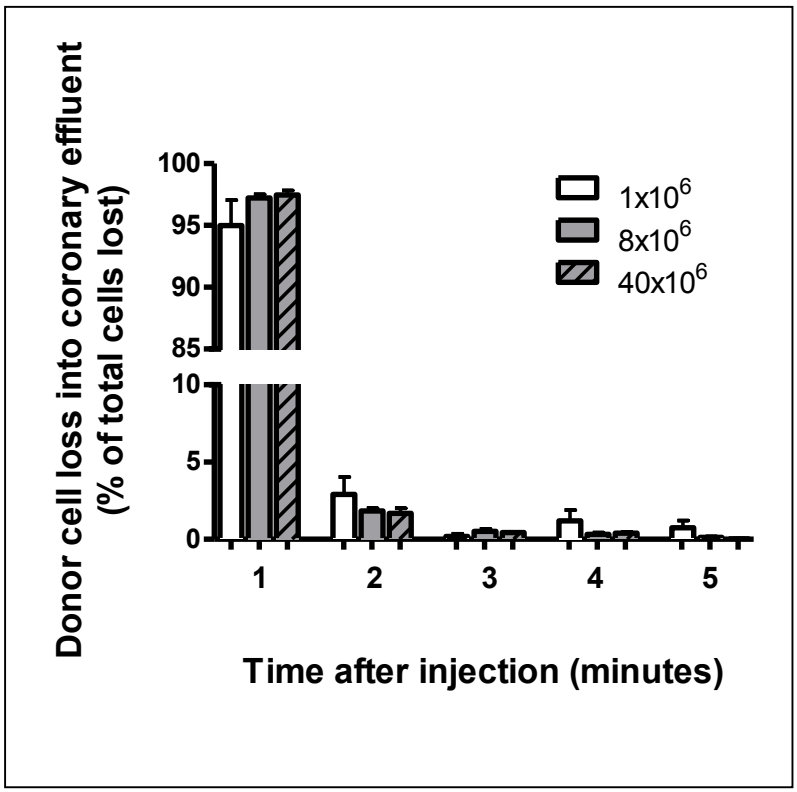

Figure 4-44: BMMNC loss into coronary effluent after injection into I-R hearts. The patterns of cell loss between the three BMMNC number groups injected into I-R hearts were compared. The cell count for each minute was expressed as a fraction of the total cell loss in the coronary effluent up until 5 minutes. Error bars = SEM.

4.5.3. BMMNC retention efficiency in I-R hearts

The absolute number of donor cells retained in the heart after IC injection was compared between the 3 BMMNC cell doses. The absolute number of retained donor BMMNC was significantly increased following a higher injected cell dose (Figure 4-45). The mean absolute cell number retention for $1x10^6$, $8x10^6$ and $40x10^6$ were $0.32 \pm 0.03 \times 10^6$ (n=4), $2.33 \pm 0.08 \times 10^6$ (n=11) and $11.8 \pm 0.70 \times 10^6$ (n=6), respectively ($p<0.0001$, One-Way ANOVA). The proportion of the retained cells at 5 minutes as a fraction of the total injected cell dose was then calculated (Figure 4-45). It was found that there was no difference between the retained cell proportions between the 3 groups. The retained proportion of injected $1x10^6$, $8x10^6$ and $40x10^6$ BMMNC were the same ($31.7 \pm 2.8\%$, $29.2 \pm 1.0\%$ and $29.5 \pm 1.7\%$ respectively, $p=0.37$, One-way ANOVA).

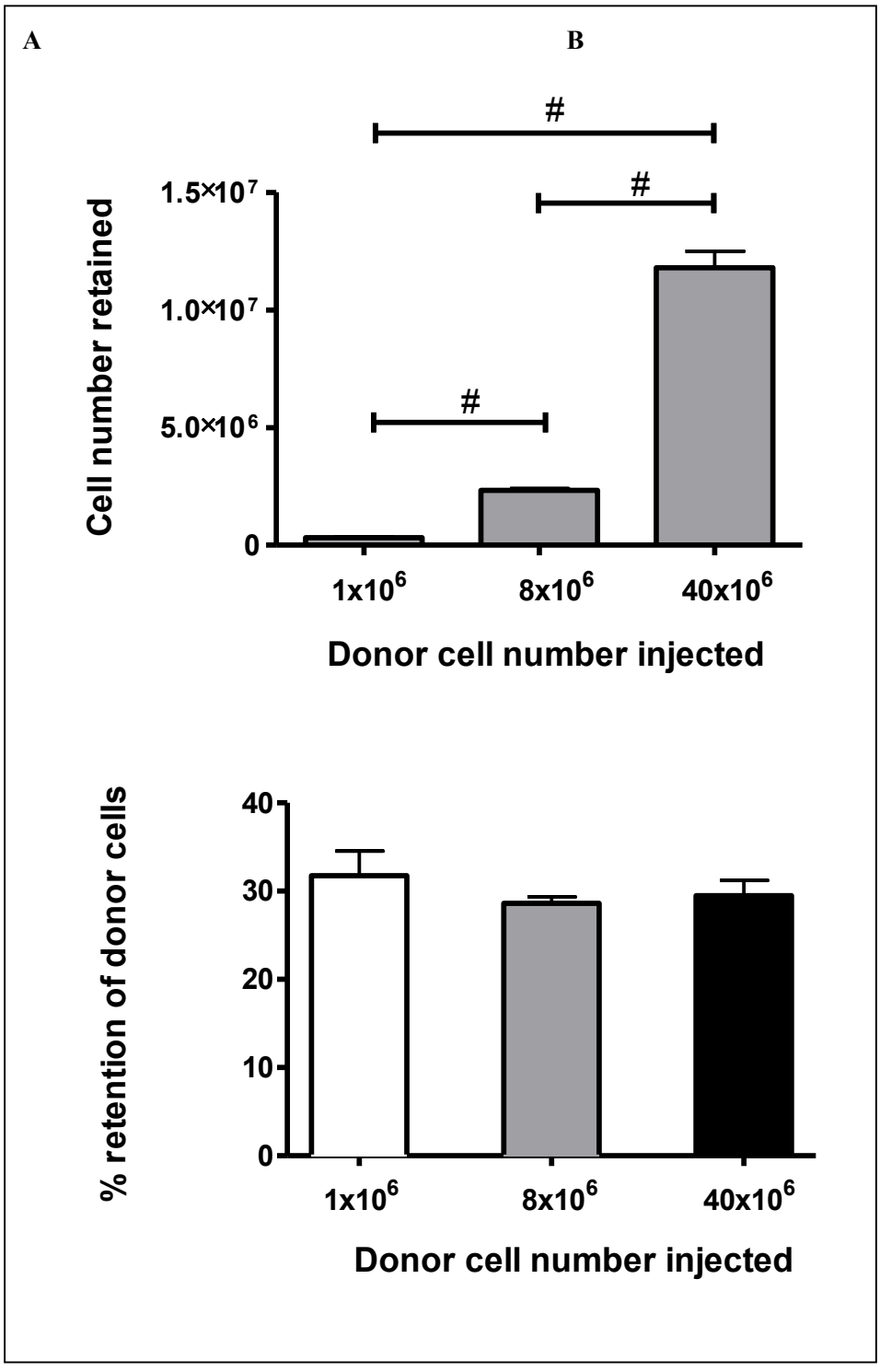

Figure 4-45: BMMNC retention after IC injection into I-R hearts. Donor cell retention in the heart after IC injection of BMMNC doses is shown for (A) absolute number of cells retained and (B) retained cells as a proportion of the injected number. Error bars indicate SEM. #=$p<0.05$, Bonferroni's Multiple Comparison Test.

A further analysis of the initial BMMNC retention after IC injection into I-R hearts was undertaken, with a focus on minute-by-minute changes in the retention efficiency for the first five minutes post injection (Figure 4-46). The pattern of retention did not differ between the injected cell numbers (Two-way ANOVA). Additionally, there was no difference between the cell retention after 1 minute and after 5 minutes (Two-way ANOVA). This suggests that BMMNC retained at 1 minute after IC injection were mostly retained after 5 minutes, regardless of cell number injected.

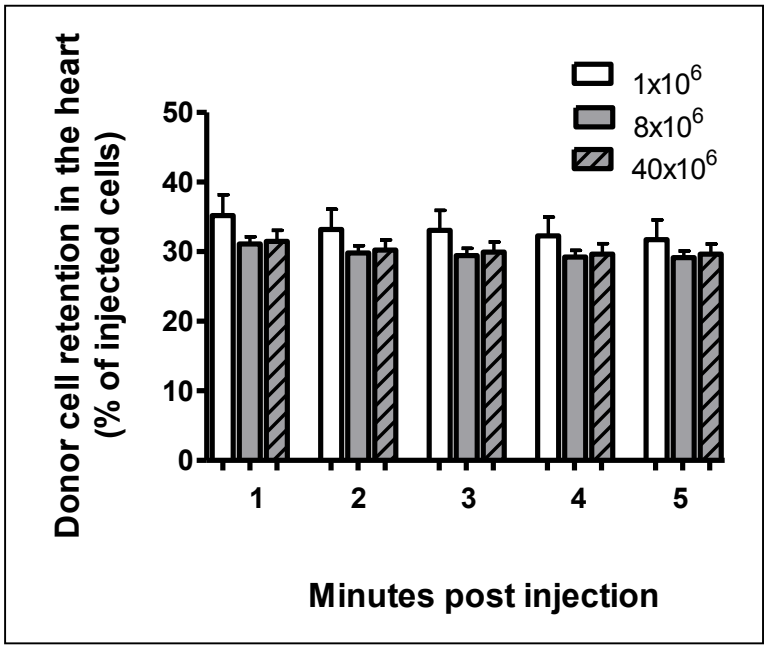

Figure 4-46: Donor cell retention efficiency in I-R hearts immediately after IC injection of BMMNC. The proportion of injected donor cells retained in the heart was calculated for each of the first 5 minutes post injection. For each cell number injected, there was a slow decrease in retained cells. Error bars indicate SEM. $1x10^6$ (n=5), $8x10^6$ (n=13), $40x10^6$ (n=8).

4.5.4. Surface markers of retained BMMNC in I-R hearts

The surface marker expression of BMMNC in the coronary effluent after IC injection into I-R hearts was assessed by flow cytometry and compared with BMMNC prior to injection, with a view to determining whether cells with a particular surface protein were preferentially retained in I-R hearts after IC injection. The mean surface marker expression for pre-injection cells was collated from pre-injection cells from both normal and I-R hearts (n=5) experiments. Two separate experiments were performed using the cells from the coronary effluent after $40x10^6$ BMMNC injection into I-R hearts. It was observed that the expression of each surface marker investigated was not altered between pre-injection BMMNC and BMMNC in the coronary effluent (Figure 4-47, unpaired T-test). This suggests cell retention in these I-R heart protocols is not dependent on these cell surface markers.

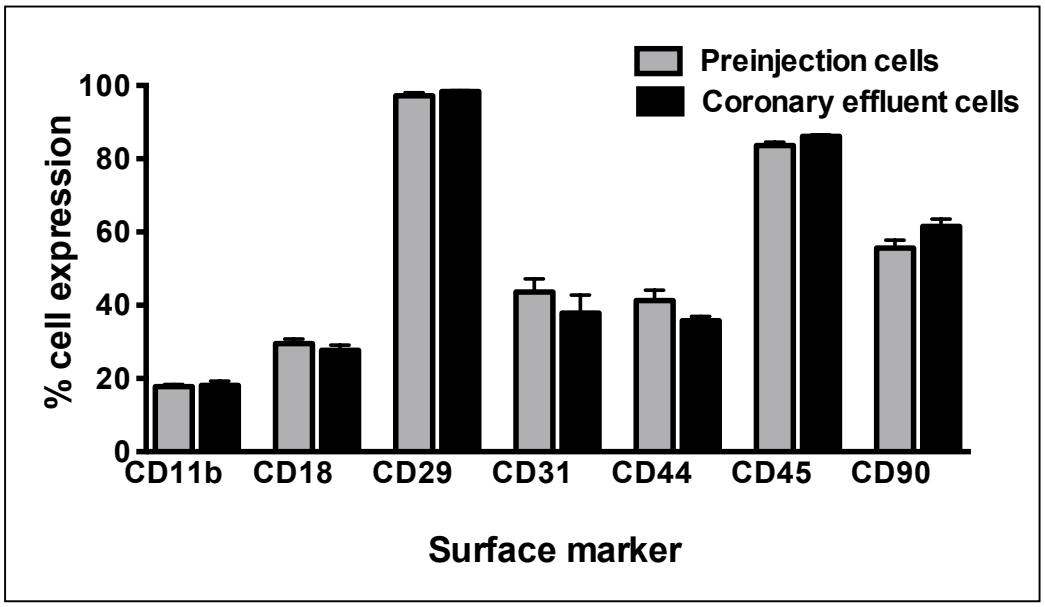

Figure 4-47: Surface marker expression in BMMNC in coronary effluent after IC injection into I-R hearts. CD marker expression of donor cells pre-injection (n=5) and donor cells in the coronary effluent after IC injection to I-R hearts (n=2) was not different. Error bars indicate SEM.

4.5.5. Size of retained BMMNC in I-R hearts

To determine whether cell size is a factor that affects donor cell retention after IC injection into I-R hearts (n=6), the cell size distribution of BMMNC in the coronary effluent was determined using an automated cell counter and compared with BMMNC before injection (Figure 4-48).

The mean cell size in donor cells in coronary effluent was 6.44 μm and the median cell size was 6 μm. This compared to the mean and median cell size of 7.0 μm in the pre-injection sample (refer to 4.1.1). The coronary effluent cells appeared to have a leftwards shift in cell size, with an increase in the proportion of smaller BMMNC and a reduction in the proportion of larger BMMNC, but this observation was not statistically significant (p=0.94, F-test, Sum of Squares).

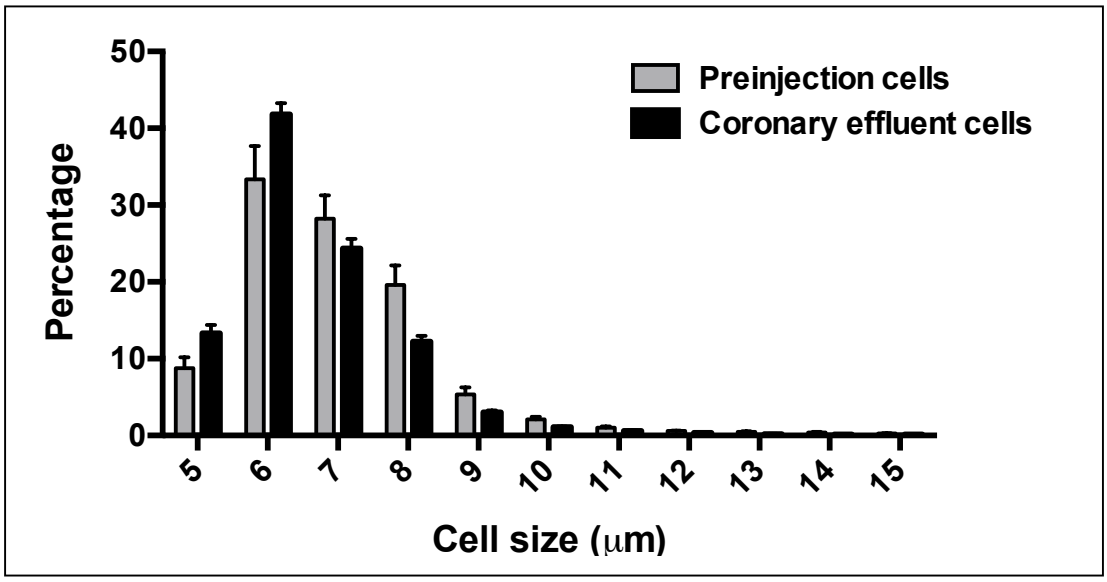

Figure 4-48: Cell size distribution of BMMNC in coronary effluent after injection into I-R heart vs. pre-injection cells. The distribution of cell sizes were compared with an automated cell counter for I-R perfused hearts (n=6). The number of BMMNC for each cell size was calculated and expressed as a fraction of all the BMMNC in each group. There appeared to be a leftwards shift in the coronary effluent cells compared to the pre-injection cells. n=23,942 pre-injection cells. Error bars indicate SEM

Because the total cell number within the coronary effluent and the distribution of pre-injection donor cell sizes were known, the proportion of retained cells according to cell size could be calculated. For further analysis, the cells were subdivided into three groups; cells with size of 5-6 μm (below the median size), 7 μm (the median size) and ≥ 8 μm (above the median size). Figure 4-49 demonstrates the relative proportions of cell sizes for pre-injection donor cells and donor cells retained in the heart. Although cells sized 5-6 μm in diameter accounted for 41% of the pre-injection BMMNC, only 12% of the retained cells were this size. There was an increase in the proportion the retention of cells with a median diameter and an even greater increase in the retention of cells with a diameter above the median; the largest BMMNC accounted for 53% of retained cells, whereas this size only constituted 30% of the pre-injection cells.

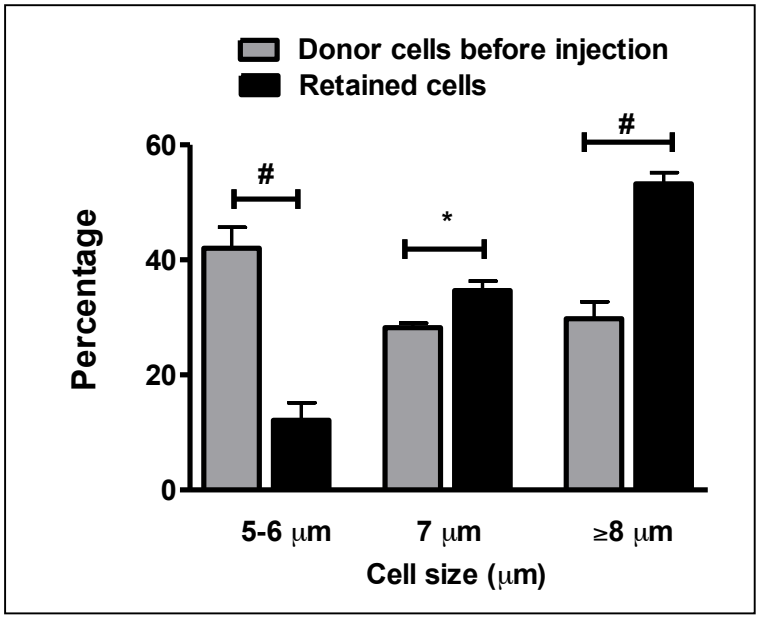

Figure 4-49: Cell size distribution of donor BMMNC prior to injection and of retained BMMNC after IC injection into the I-R heart. The proportions of cells below the median (5-6 μm), the median (7 μm) and above the median ≥8 μm were calculated. The proportion of smaller cells retained in the heart below the median size was lower than expected. Conversely, larger cells were retained with increased efficiency. Error bars indicate SEM, n=11 samples for pre-injection samples hearts, n=6 for coronary effluent samples, # = $p<0.0001$, * = $p<0.01$

The relationship between donor BMMNC size and retention efficiency after IC injection into the I-R heart was further analysed (Figure 4-50). There was a clear increase in cell retention efficiency with greater cell size (One-way ANOVA, $p<0.0001$). Bonferroni's multiple comparison post-hoc test demonstrated that there was a significantly (6-fold) greater proportion of injected ≥ 8 μm cells retained than injected 5-6 μm cells (58.5% *vs.* 9.5%, $p<0.0001$).

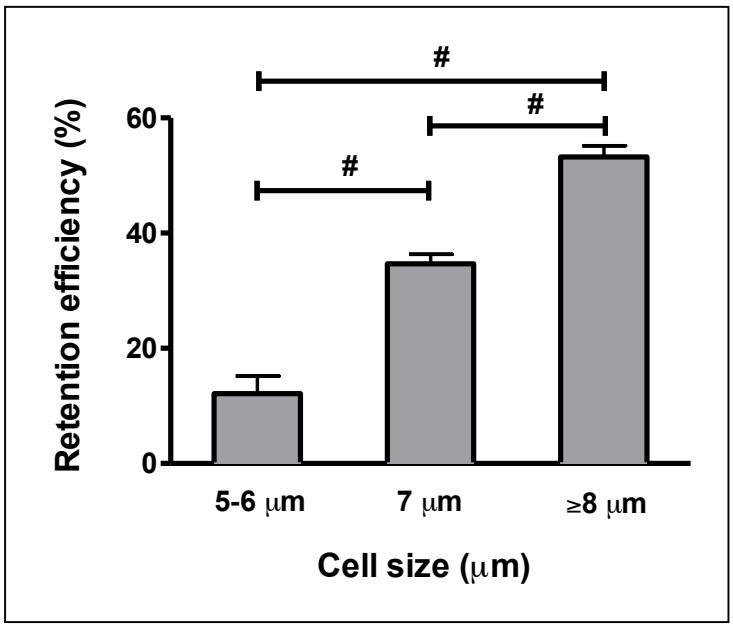

Figure 4-50: Retention efficiency of BMMNC after IC injection into I-R hearts and their cell size. The proportions of each sized donor cells retained in the heart were calculated (n=6). Larger cells were more efficiently retained. Error bars indicate SEM. # = $p<0.05$, Bonferroni's multiple comparison test.

4.5.6. Histological distribution of retained BMMNC in the heart

The anatomical location of PKH67-positive donor BMMNC within the recipient I-R hearts after IC injection was determined using immunohistochemistry (refer to 3.8.1). In brief, the apex, mid-section and base were analysed separately per heart and the anatomical location of each PKH67 labelled cell was recorded. The apex, mid-section and base were not compared because no difference was found in the normal heart samples.The cross-sectional area of each myocardial section (epicardium, mid myocardium and endocardium) was calculated using ImageJ software analysis. The results showed that there appeared to be a progressive increase in the concentration of donor cells towards the epicardium (Figure 4-51). There were double the number of cells in the epicardium compared to the endocardium. However, this result was not statistically significant (n=6 hearts, p=0.059, One-way ANOVA).

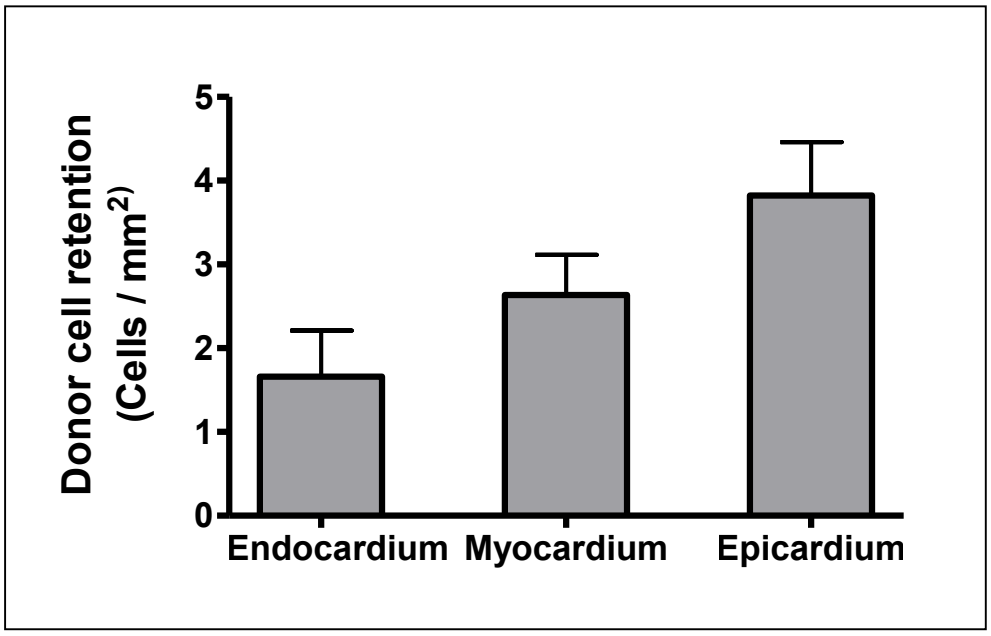

Figure 4-51: Intramyocardial location of retained donor cells within the I-R heart. The number of fluorescent-labelled cells in the apex, mid-section and base were compared after injection of $8x10^6$ cells into normally perfused Langendorff hearts, corrected for cross-sectional area. There was a trend toward a significant increase in the proportion of cells found in the epicardium (n=6 hearts, One-Way ANOVA). Error bars indicate SEM.

4.5.7. Anatomical relationship between retained cells and the coronary vasculature

The location of cells related to the coronary vasculature was determined by injecting PKH67-labelled BMMNC into I-R hearts with isolectin-B4 and DAPI staining. At 5 minutes after cell injection, all the observed PKH67-labelled cells were located inside the vasculature (representative images: Figure 4-52 and Figure 4-53). In further analyses of hearts obtained for sectioning 60 minutes after cell injection, no observed PKH-labelled cell was observed to have extravasated outside of the coronary lumen (representative images: Figure 4-54 and Figure 4-55). There were no histological findings suggesting that coronary embolism had occurred in any sample.

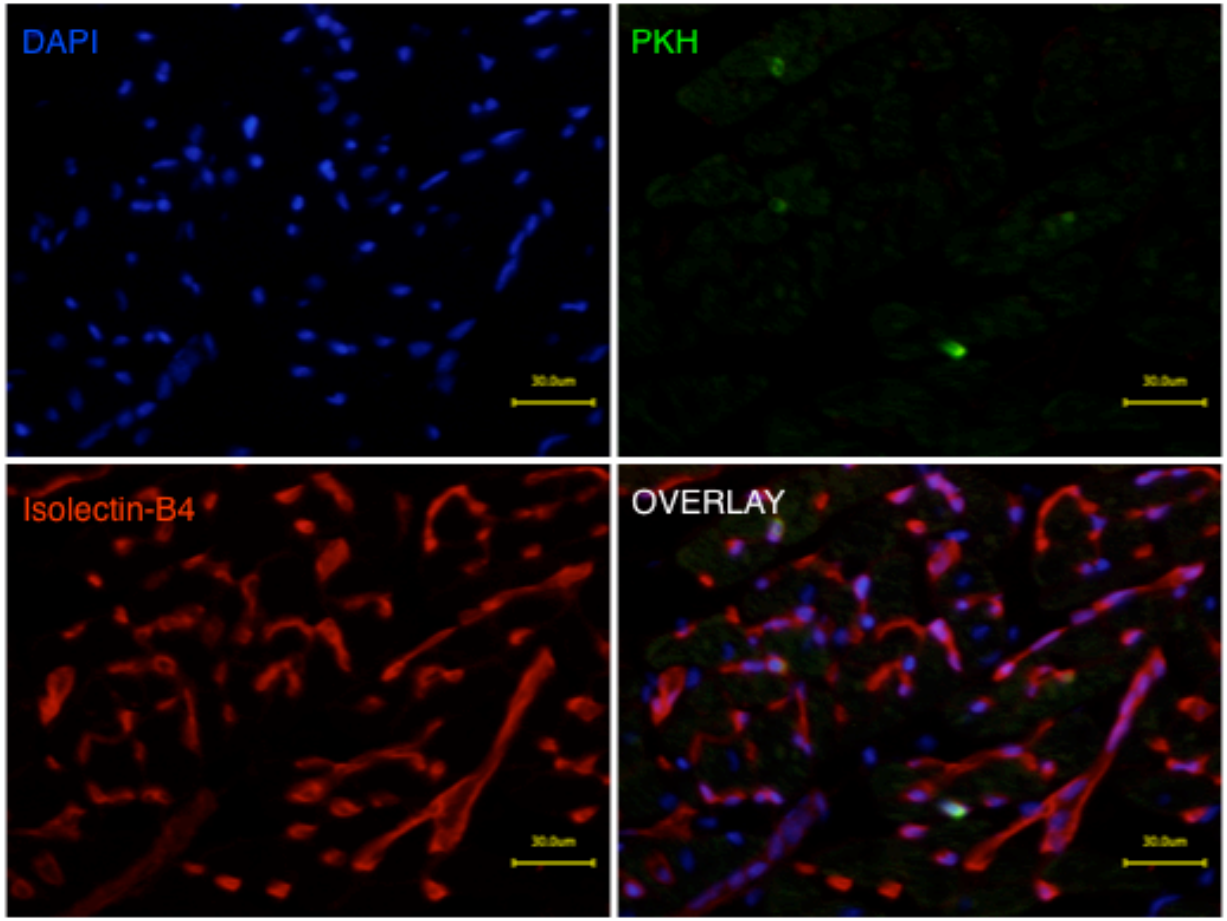

Figure 4-52: Typical image of retained donor BMMNC 5 minutes after IC injection in I-R hearts (low magnification). 5 minutes after injection of PKH67-labelled BMMNC (green) into I-R hearts, the hearts were acquired and analysed. Sections were stained with a nuclear marker (DAPI; blue) and an endothelial marker (Isolectin-B4; red). All cells were seen inside the vascular lumen. Scale bar = 30 μm.

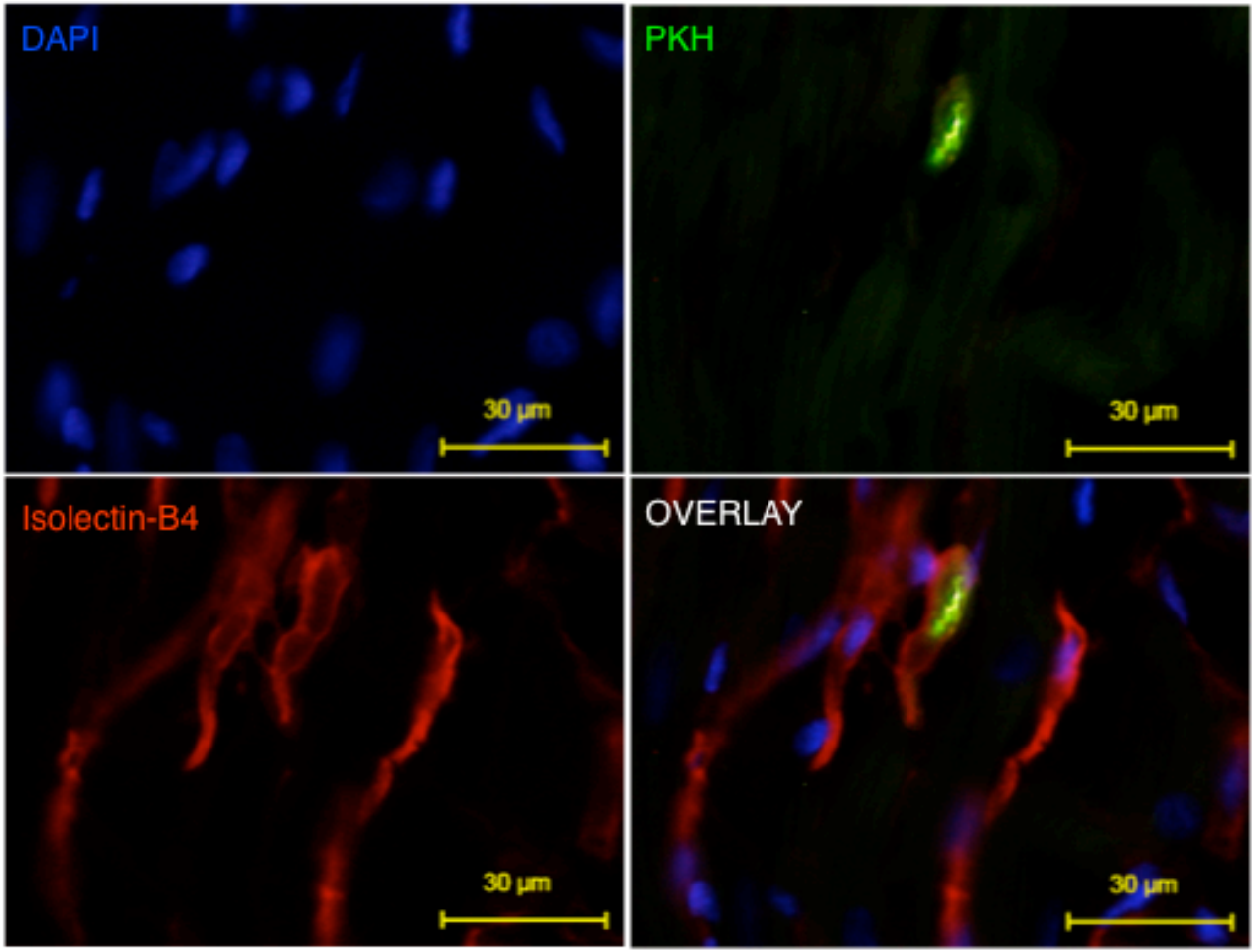

Figure 4-53: Typical image of retained donor BMMNC 5 minutes after IC injection in I-R hearts (high magnification). 5 minutes after injection of PKH67-labelled BMMNC (green) into I-R hearts, the hearts were acquired and analysed. Sections were stained with a nuclear marker (DAPI; blue) and an endothelial marker (Isolectin-B4; red). All cells were seen inside the vascular lumen. Scale bar = 30 µm.

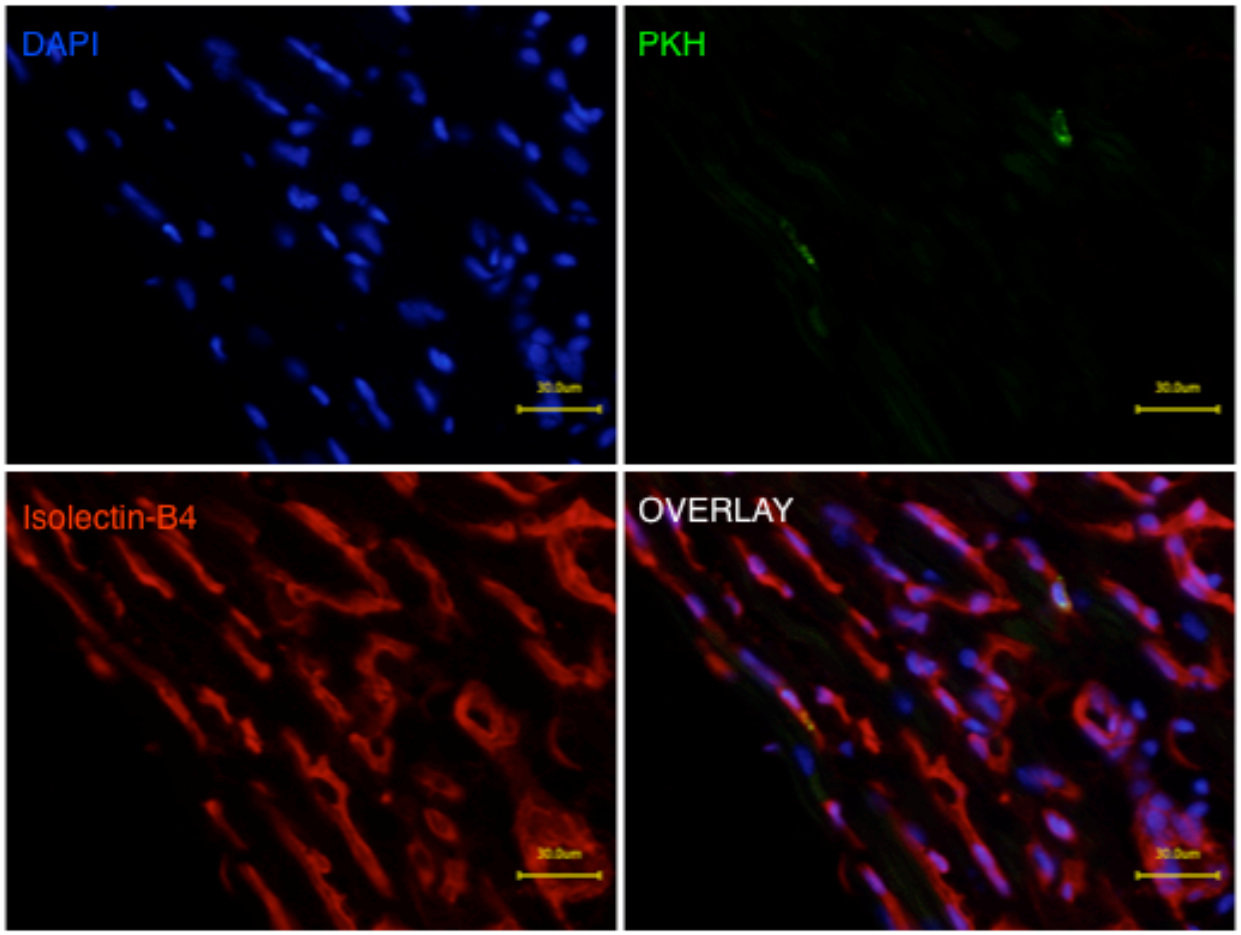

Figure 4-54: Typical image of retained donor BMMNC 60 minutes after IC injection in I-R hearts (low magnification). 60 minutes after injection of PKH67-labelled BMMNC (green) into I-R hearts, the hearts were acquired and analysed. Sections were stained with a nuclear marker (DAPI; blue) and an endothelial marker (Isolectin-B4; red). All cells were seen inside the vascular lumen. Scale bar = 30 μm.

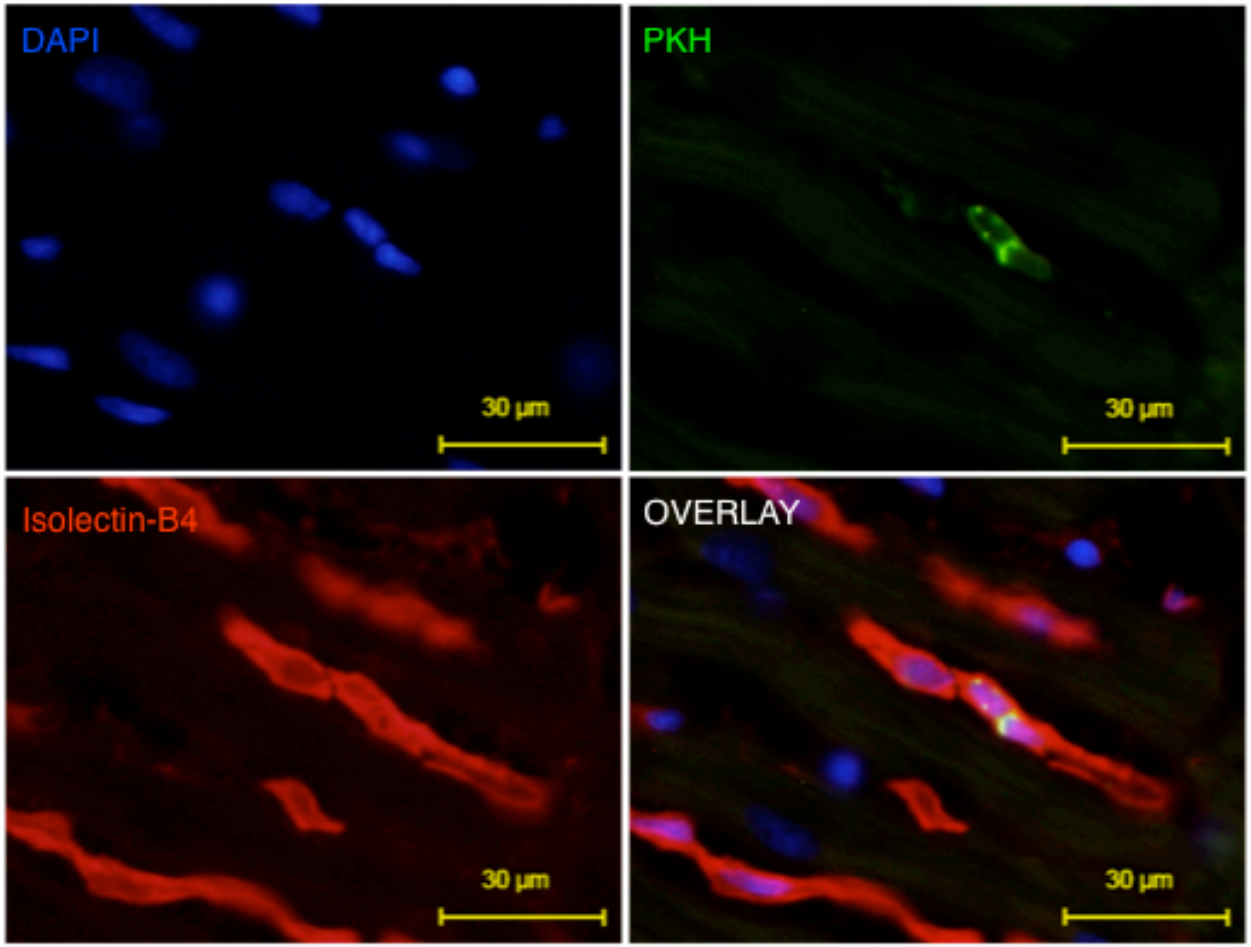

Figure 4-55: Typical image of retained donor BMMNC 60 minutes after IC injection in I-R hearts (high magnification). 60 minutes after injection of PKH67-labelled BMMNC (green) into I-R hearts, the hearts were acquired and analysed. Sections were stained with a nuclear marker (DAPI; blue) and an endothelial marker (Isolectin-B4; red). All cells were seen inside the vascular lumen. Scale bar = 30 µm.

4.6. Comparison of BMMNC retention in normal and I-R hearts

In order to elucidate further the possible effect of I-R on donor cell retention after IC injection, more detailed direct comparisons between normal heart experiments (4.4) and I-R heart experiments (4.5) were made. Although there are some duplicated data with previous sections, I believe that direct comparisons in this section are useful to highlight similarities and differences between the two experimental conditions.

4.6.1. Pattern of BMMNC loss into coronary effluent

The pattern of calculated cell loss into coronary effluent for the initial 5 minutes was compared between BMMNC injected into normal hearts and into hearts subjected to 30 minutes ishaemia-30 minutes reperfusion. This comparison was made after injection of $1x10^6$, 8×10^6 and 40×10^6 (Figure 4-56). It was found that the number of donor BMMNC in the coronary effluent tended to be higher (though not statistically significant) after injection into normal hearts than I-R hearts at most time points studied.

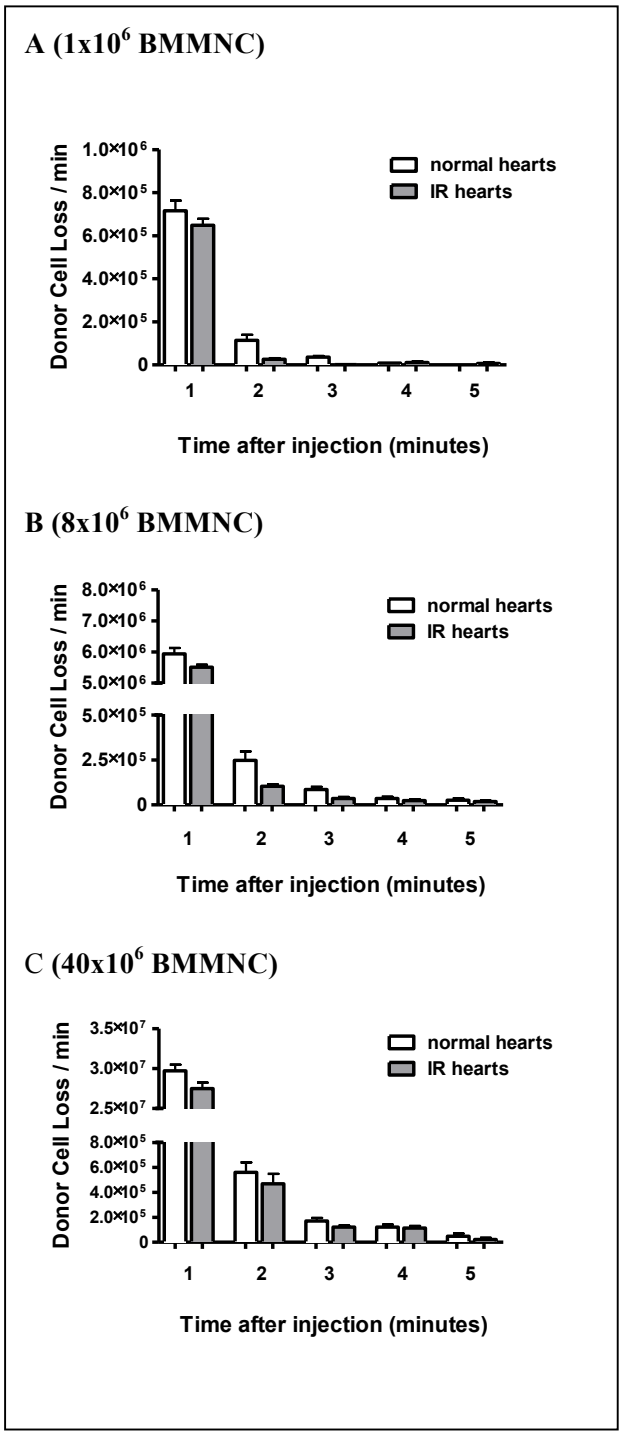

Figure 4-56: Donor cell loss into the coronary effluent from normal and I-R hearts. The pattern of donor cell loss was compared after injection of (A) $1x10^6$ BMMNC, (B) $8x10^6$ BMMNC and (C) $40x10^6$ BMMNC into normal and I-R hearts. The number of donor BMMNC loss in the coronary effluent tended to be higher (though not statistically significant) after injection into normal hearts than I-R hearts at most time points studied. n=4-13 each group. Error bars = SEM.

The time course of donor cell loss into the coronary effluent was analysed in a different way. The pattern of cell loss was compared by analysing the cells lost in each minute into the coronary effluent as a percentage of the total cells lost (Figure 4-57). There were no significant differences between the distributions between the normal and I-R groups for each cell number (paired T-test). However, in the normal groups, the proportion of cells lost within the first minute tended to be lower and higher in the second minute, regardless of donor cell number injected, compared to the I-R groups. This suggests that cell loss may be more rapid in the I-R groups.

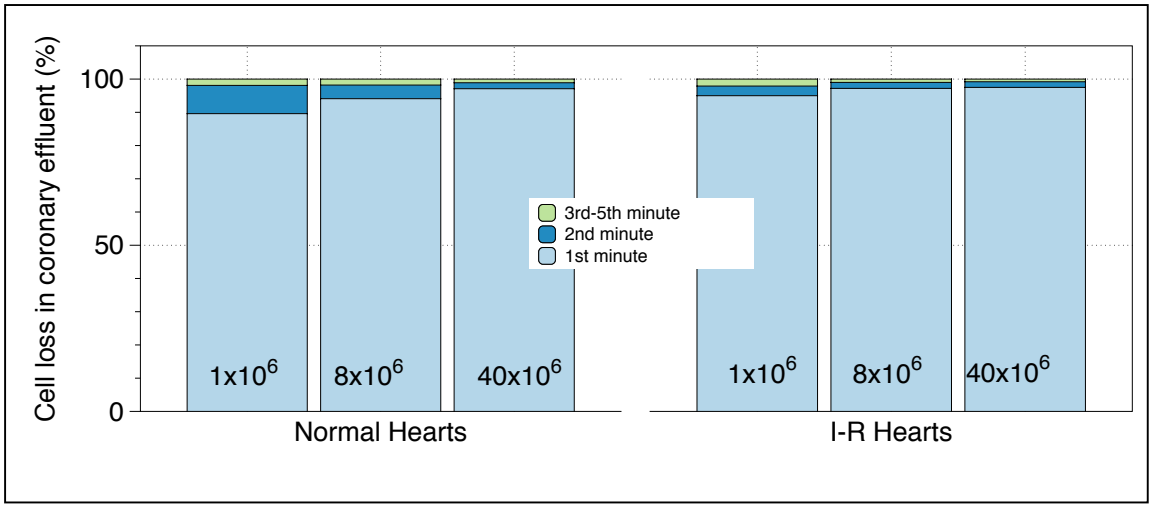

Figure 4-57: Cells lost each minute in the coronary effluent, expressed as a percentage of the total cells lost. The numbers of cells lost within the 1st minute, the 2nd minute and the 3rd-5th minute were expressed as a fraction of the total cells lost within the first 5 minutes. It was observed that the majority of the cells were lost within the first minute. However, the data suggests that cell loss into the coronary effluent from the I-R hearts may have been more rapid than from the normal hearts. n=4-13 each group.

4.6.2. Absolute and relative BMMNC retention efficiency

Absolute cell number retained at 5 minutes after IC injection of $1x10^6$, $8x10^6$ and $40x10^6$ BMMNC were compared between normal and I-R hearts (Figure 4-58, A). For each cell number, the absolute number of cells retained in the heart was significantly increased in the I-R hearts compared to the normal hearts ($p<0.0001$, 2-way ANOVA).

The cell numbers retained were then expressed as a proportion of the original donor cell number injection and compared between the normal and I-R hearts for each cell number (Figure 4-58, B). The retention efficiency of BMMNC injected into I-R hearts was higher (approximately 30%), compared with a retention efficiency of approximately 20% after injection into normal hearts ($p<0.0001$, 2-way ANOVA).

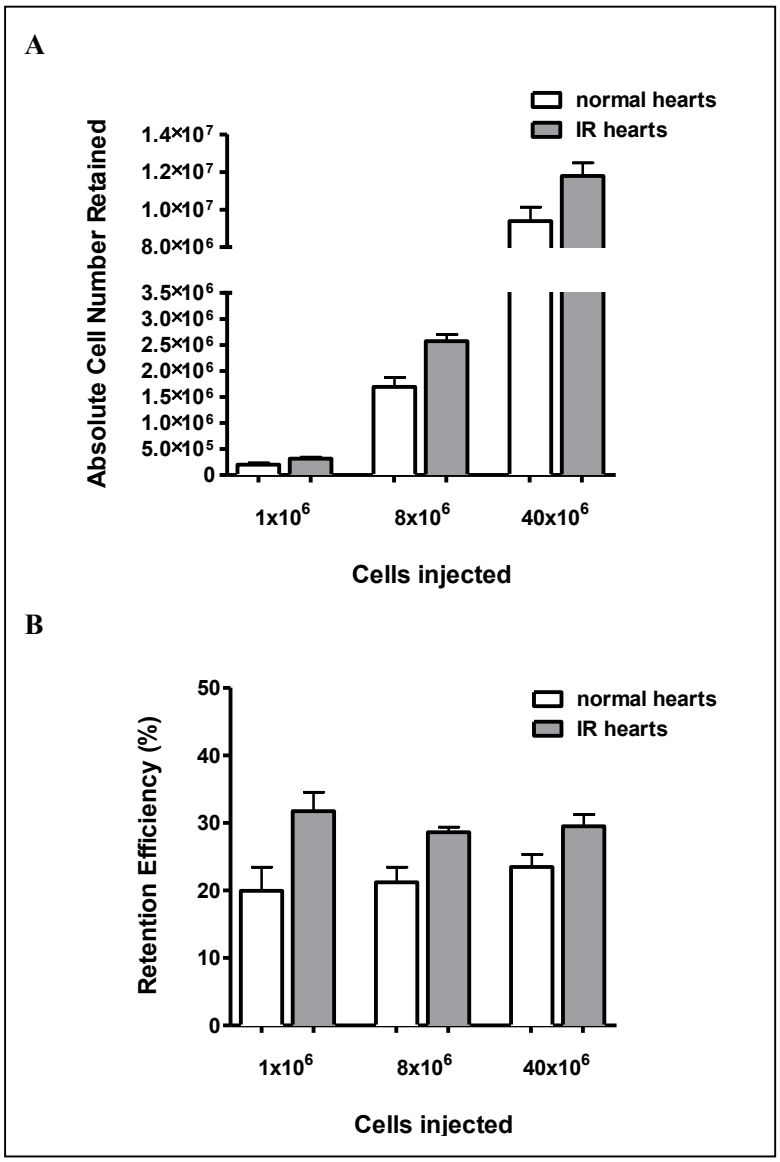

Figure 4-58: Comparison of retention of BMMNC after IC injection in normal and I-R hearts. The absolute numbers of retained cells at 5 minutes after IC BMMNC injection into normal and I-R hearts (three different cell numbers) were compared (A). There was a significant increase in absolute retention in I-R hearts for each cell number injection ($p=0.01$: Two-Way ANOVA). The retention efficiency of cells were also compared, expressed as a fraction of the initial donor cell dose (B). There was an increase in efficiency of cell retention after BMMNC were injected into I-R hearts compared with normal hearts, at each cell number ($p<0.0001$, Two-way ANOVA). n=4-13 each group. Data expressed as mean ± SEM.

4.6.3. Size of retained cells

The size of donor BMMNC in the coronary effluent was compared after injection into normal (n=5) and I-R (n=6) hearts. In the normal group, the mean cell size was 6.85 μm and the median cell size was 7 μm. In the I-R group, the mean cell size was 6.44 μm and the median cell size was 6 μm. Furthermore, the populations of cell diameters were compared by non-linear regression by generating second order polynomial (quadratic) best fit lines (Figure 4-59). There was no difference between the distributions of cell diameters between the groups (p=0.94: Sum of Squares F-test).

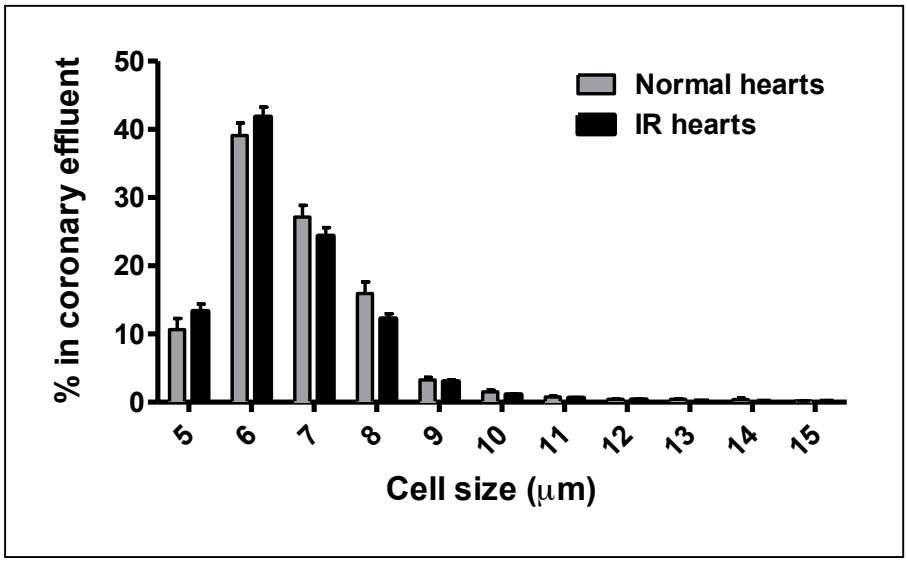

Figure 4-59: Cell diameter distributions of BMMNC in coronary effluent after injection into normal and I-R hearts. The cell size distribution of donor BMMNC lost in the coronary effluent after IC injection into normal and I-R hearts were compared. The number of BMMNC for each cell size was calculated and expressed as a fraction of all the BMMNC in each group. After IC injection into I-R hearts, the cell size distribution appears to shift leftwards but there was no statistical difference between the groups. n=5 normal hearts coronary effluent samples, n= I-R injury heart coronary effluent sample samples. Data expressed as mean ± SEM.

For clarifying these observations, the proportions of retained BMMNC were subdivided by cell size into three groups; a smaller diameter than the median size (5-6 µm), the median size (7 µm) and cells with a greater diameter than the median (≥8 µm), and expressed as a fraction of the total retained cells (Figure 4-60). Larger BMMNC accounted for a greater proportion of the retained cells in both groups, but the proportions of BMMNC of different sizes within the heart were not substantially different after I-R compared with injection into normal hearts.

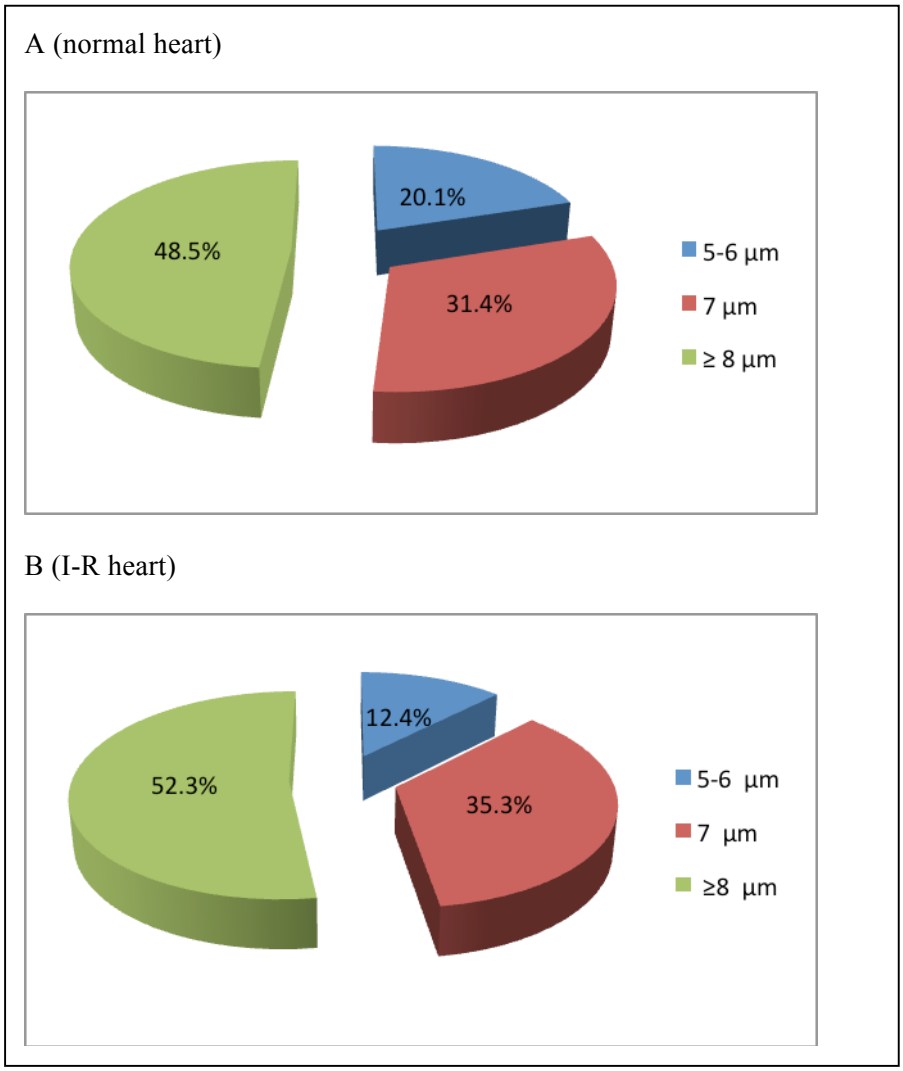

Figure 4-60: Cell size distribution of donor BMMNC retained within the heart, after injection into normal and I-R hearts. The cell sizes of donor BMMNC retained in the heart was analysed and expressed as a fraction of all the retained cells, after (A) normal and (B) I-R heart injection. The proportion of cells sized 5-6 µm was lower in the I-R hearts and the proportion of cells sized ≥ 8 µm was increased, but these findings did not reach statistical significance (p=0.068, Two-way ANOVA).

Next, the retention efficiency of each cell-size subpopulation of donor BMMNC was assessed and compared in both normal and I-R hearts. Cells were subdivided into groups of the same 3 cell sizes, as described. The results are expressed as a fraction of the number of injected donor cells of each size (shown in Figure 4-61). In both groups, larger cells were more efficiency retained. In I-R hearts, cells sized ≥8 μm were retained 1.4 times more efficiently than similar sized cells in normal hearts (58.5 ± 2.4 *vs.* 42.8 ± 4.7%, p=0.01). There was a trend towards increased retention efficiency after I-R of cells sized 7 μm (40.5 ± 2.8 *vs.* 29.3 ± 4.7%) although this did not reach statistical significance (p=0.061). I-R did not affect the retention of cells with a diameter of 5-6 μm.

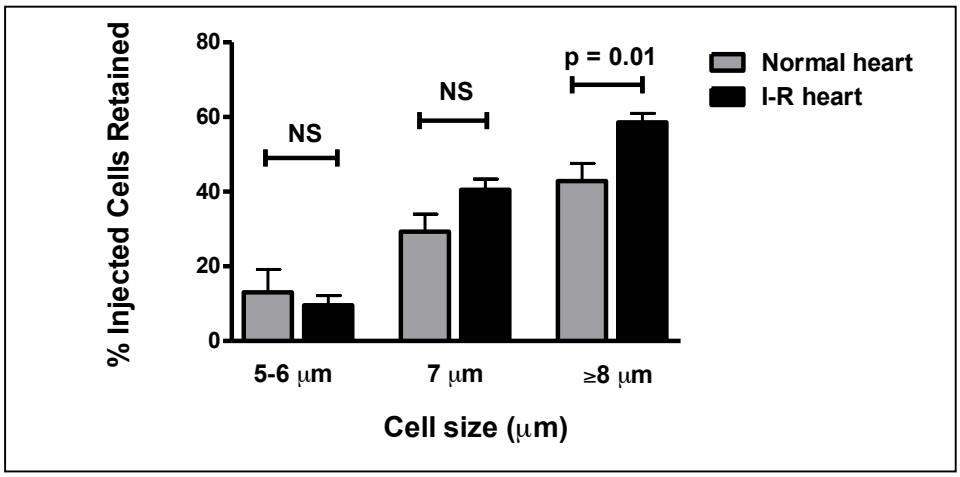

Figure 4-61: Proportion of cells of different diameters retained in the heart after IC injection of BMMNC into normal and I-R hearts. The diameters of cells retained in the heart were subdivided into diameters below the median (5-6 μm), the median (7 μm) and above the median (≥8 μm) for injection into normal (n=5) and I-R (n=6) hearts. The proportions of the original injected donor cell fractions for each cell size that were retained in the heart were calculated. There was a non-significant increase in cells sized below 7 μm retained after I-R. The proportion of cells >8 μm retained in the heart increased after I-R (unpaired T-tests).

4.6.4. Histological distribution of retained BMMNC

Using immunohistochemical analysis, all donor BMMNC were observed inside the coronary vasculature up to 60 minutes post-injection in both normal and I-R hearts. This suggests that extravasation of donor BMMNC does not occur within this timeframe and that I-R does not result in a different pattern of cell retention at a microscopic level. No histological observation consistent with coronary embolization was seen in either normal or I-R hearts.

The semi-quantitative counts of retained cells were compared between normal and I-R hearts. In normal hearts and I-R hearts 5 minutes after injection, there were respectively 1.32 ± 0.13 and 2.93 ± 0.28 cells / mm^2. After 60 minutes, there were 0.71 ± 0.04 and 2.25 ± 0.08 cells/mm^2 respectively in normal and I-R hearts. Though semi-quantitative, the frequency of BMMNC retention was higher in I-R hearts at each time point, supporting the quantitative results of BMMNC retention above (refer to 4.6.2).

The ventricular wall was divided into three equally-wide areas (endocardium, mid myocardium and epicardium) and the number of cells in each area was expressed as a percentage of the total retained cells for normal and I-R hearts (Figure 4-62). Interestingly, the intramyocardial distribution of retained BMMNC was markedly different between normal (n=19) and I-R (n=6) hearts ($p<0.0001$, Two-way ANOVA). There was no difference between the number of cells in the mid myocardium (31.8 ± 2.7% *vs.* 31.6 ± 4.4%, normal *vs.* I-R, mean ± SEM, $p=0.97$). However, the distributions of cells in the endocardium and epicardium were totally reversed; the proportion of cells in the endocardium was 48.7 ± 2.9% *vs.* 19.6 ± 2.1% (normal *vs.* I-R, $p<0.001$) whereas the proportion of cells in the epicardium was 19.6 ± 2.1% *vs.* 46.0 ± 5.6% (normal *vs.* I-R, $p<0.001$, Bonferroni's Multiple Comparison Test).

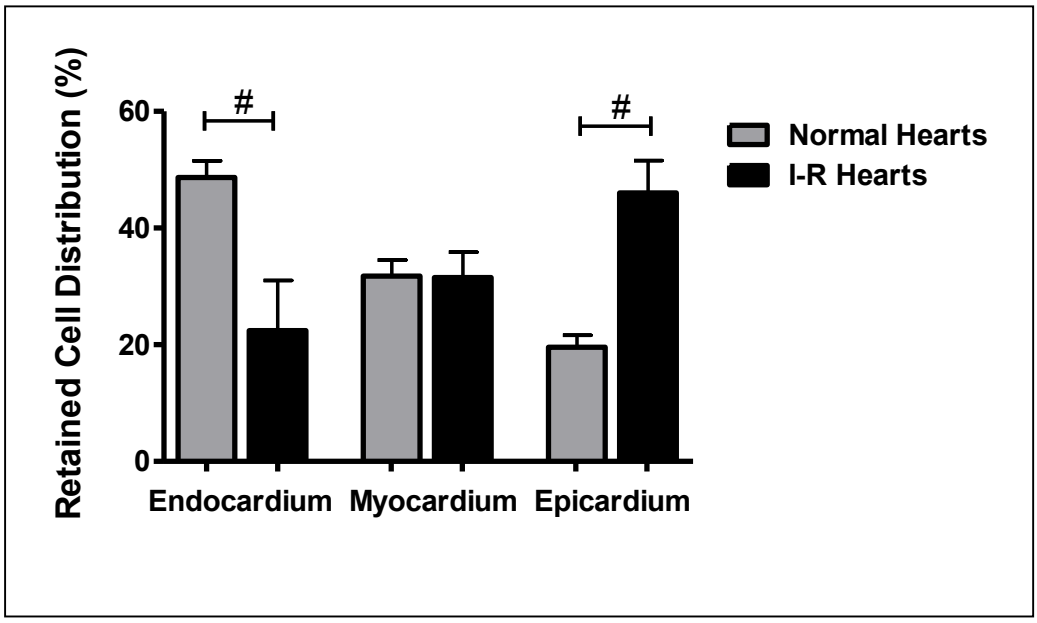

Figure 4-62: Distribution of retained BMMNC within the ventricular wall in normal and I-R hearts. The ventricular wall was subdivided into three equal areas; endocardium, myocardium and epicardium, and the numbers of cells in each area were expressed as percentages. The distributions of cells across the ventricular wall in the two groups were reversed. n=19 normal heart samples, n=6 I-R injury heart samples. #=$p<0.001$, Bonferroni's Multiple Comparison Test. Error bars = mean ± SEM.

4.7. Retention of MSC after IC injection into normal hearts

4.7.1. Perfusion parameters after MSC injection

$8x10^6$ passage 4 rat bone marrow-derived MSC suspended in 3 ml PBS were injected into the aortic root of Langendorff-perfused rat hearts (n=14) over 20 seconds in the same manner as BMMNC injection. It was noted that within the 20 seconds of cell injection, all the hearts temporally developed asystole and dilated. Over the next few minutes, the hearts were seen to recommence beating. The heart rates were lower at 5 minutes post injection and partially recovered towards the pre-injection levels over the following 40 minutes (Figure 4-63) One of the hearts was noted to cease beating after 20 minutes and no ECG recording was detectable, indicating asystole. This heart was excluded from analysis.

Coronary effluent volume (coronary flow) was measured for the minute preceding cell injection, the first five minutes following the initiation of cell injection and at 10 minutes, 20 minutes, 40 minutes and 60 minutes post cell injection (Figure 4-63). The mean coronary flow rate prior to injection was comparable to that obtained in other previous experiments (refer to Figure 4-25). However, in the minute immediately following cell injection, the coronary flow was seen to decrease to about one third of the pre-injection levels. By 5 minutes, this had partially recovered and it returned to the pre-injection levels by 10 minutes post injection.

The temperature decreased by 10 minutes after cell injection, indicating reduced myocardial perfusion and a less stable physiological state. The mean temperature partially recovered approaching 40 minutes following cell injection, although greater temperature variability and wider confidence intervals were observed.

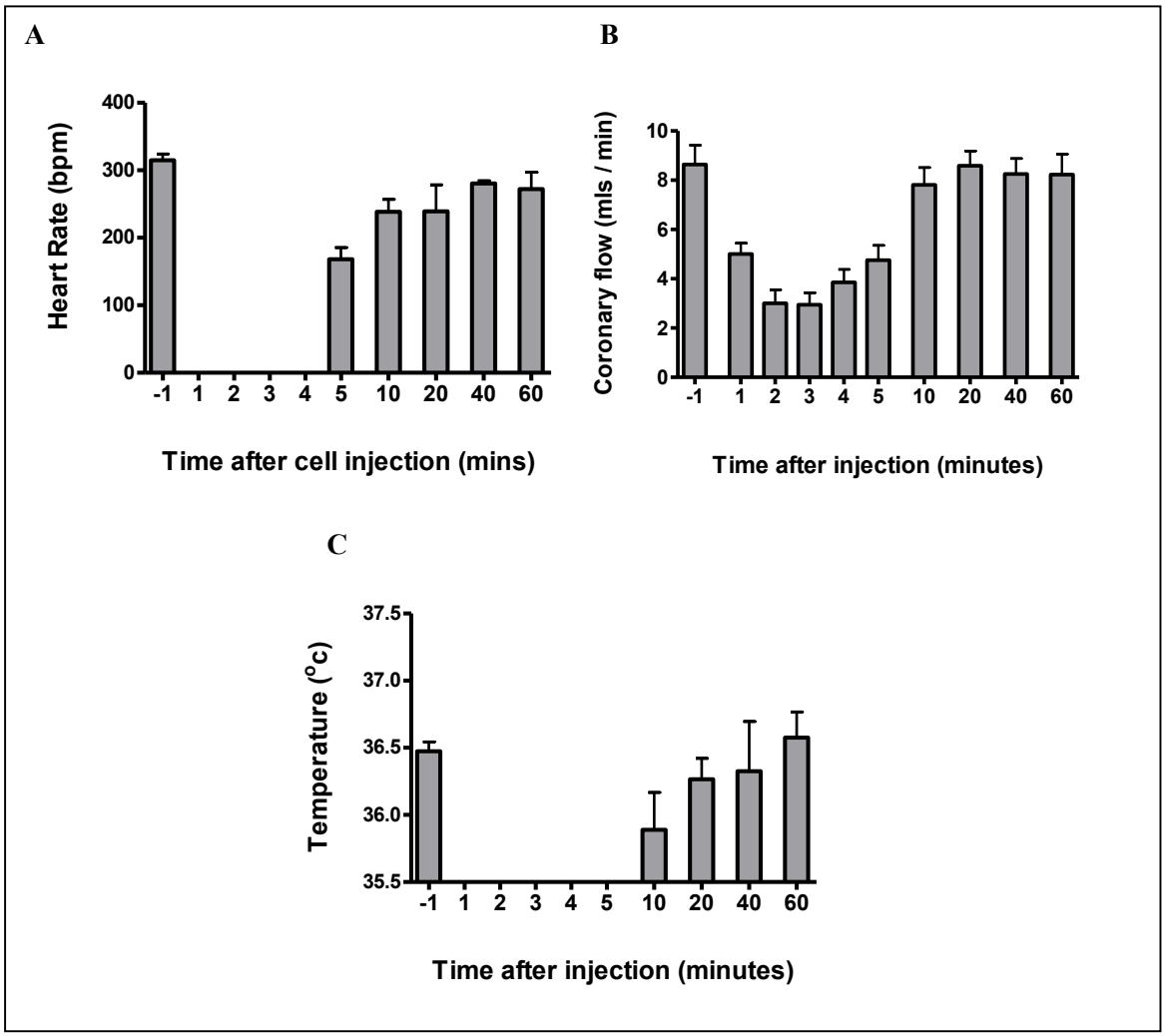

Figure 4-63: Changes in perfusion parameters before and after MSC injection into normal hearts. $8x10^6$ MSC were injected into normal hearts (n=13). Heart rate (A), coronary effluent flow rate (B) and temperature of coronary effluent exiting the heart (C) were recorded before injection and up to 60 minutes post injection. No heart rate or temperature measurement was recorded during the first 5 minutes after cell injection, because coronary effluent was collected each minute. "-1" indicates the minute immediately prior to cell injection. Error bars = SEM.

4.7.2. Time course of MSC loss into coronary effluent after IC injection

The minute-by-minute pattern of donor MSC loss into the coronary effluent was quantified after injection of $8x10^6$ MSC. The baseline RBC count ($2.3x10^4$ cells / min) in the coronary effluent was subtracted from the observed total cell count in coronary effluent as described above for the BMMNC experiments (refer to 3.6.8). The mean combined cell counts for n=8 hearts with measurements up to 20 minutes and n=5 hearts with measurements up to 5 minutes are shown (Figure 4-64).

It was observed that 89.8% and 7.1% of lost donor MSC passed into the coronary effluent within the 1st and 2nd minutes respectively. At 5 minutes after IC injection, the number of donor cells in the coronary effluent was calculated to be negligible.

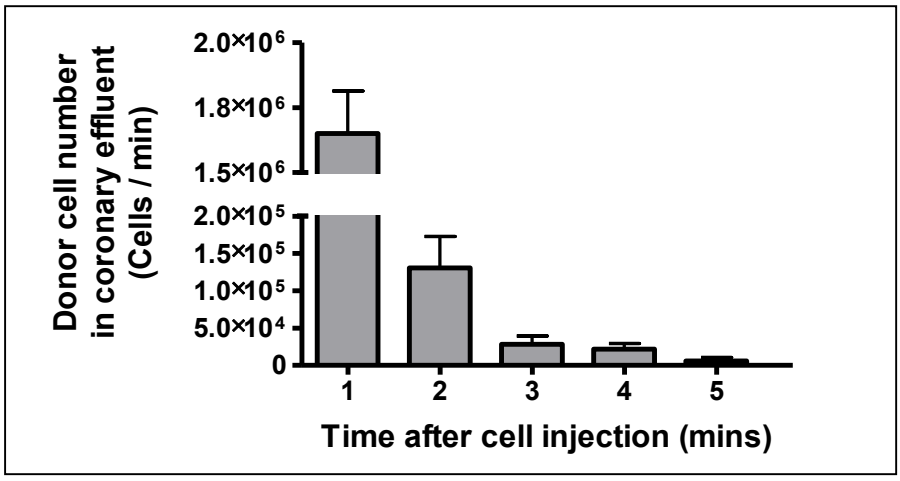

Figure 4-64: Donor cell numbers in the coronary effluent after IC injection of $8x10^6$ MSC. The numbers of MSC exiting the heart after IC injection were calculated for each minute. The largest number of MSC exited the heart in the first minute. In the second minute, the number of cells was approximately 10 times fewer. MSC loss for the subsequent minutes was negligible. n=13, Error bars = SEM.

4.7.3. Absolute and relative cell retention efficiency

The number of MSC in the coronary effluent over 5 minutes after IC injection of $8x10^6$ MSC into the normal heart was calculated to be 1.80 ± 0.14 cells (n=13). Therefore, the retained cell efficiency was 77.5 ± 1.8%.

4.7.4. Size of MSC in coronary effluent

The diameters of MSC before injection and in the coronary effluent were compared after analysis with an automated cell counter. The median and mean diameter of the pre-injection sample were 11.5 μm and 12.2 μm, which compares to the coronary effluent sample median 11.3 μm and mean 10.6 μm. The cell size distributions are shown in Figure 4-65. The distribution of cell diameters in the pre-injection and coronary effluent samples were compared by non-linear regression by generating second order polynomial (quadratic) best-fit lines and were found to be significantly different ($p<0.05$, Sum of Squares F-test). Although the proportion of cells with the smallest diameter (5-7 μm) only accounted for a small proportion of the pre-injection population (5.9%), they represented a much larger population (33.6%) of the cells in the coronary effluent.

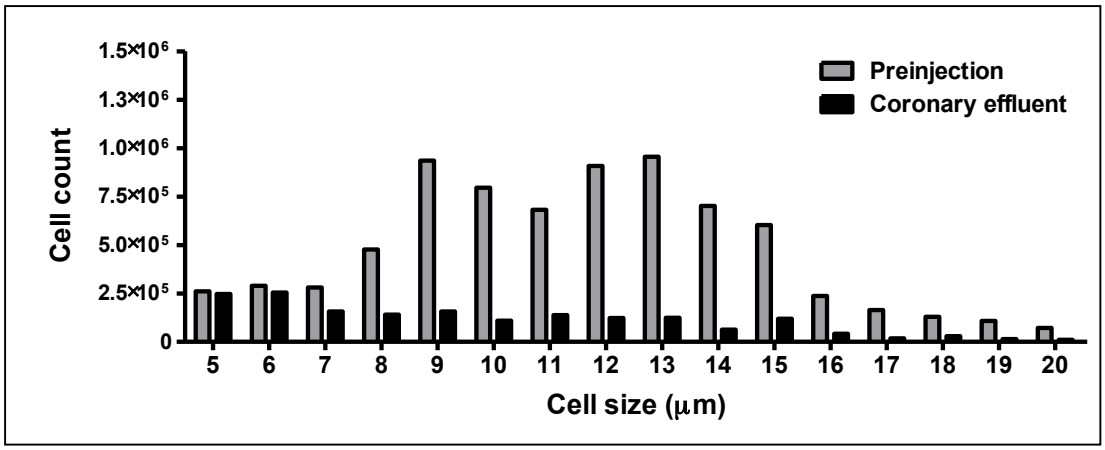

Figure 4-65: Distribution of cell diameters of MSC prior to injection into normal hearts and of donor MSC within the coronary effluent cells. The cell size of pre-injection and coronary effluent MSC were compared after analysis with an automated cell counter. The cell size distributions were different between the groups ($p<0.05$, Sum of Squares F-test).

With the use of the absolute cell retention number and the distribution of pre-injection coronary effluent cell diameters, the retention efficiency of MSC according to their diameter was calculated (Figure 4-66). Among the smaller MSC (5-9 μm), there was a positive relationship between cell size and retention efficiency; the retention rate for 5 μm was 5.2 ± 17.2%, for 6 μm was 12.3 ± 12.4%, for 7 μm was 44.1 ± 12.5%, and for 8 μm was 70.6 ± 5.3%. At cell diameter ≥ 9 μm (larger MSC), cell retention efficiency reached a plateau, ranging between 80-100%.

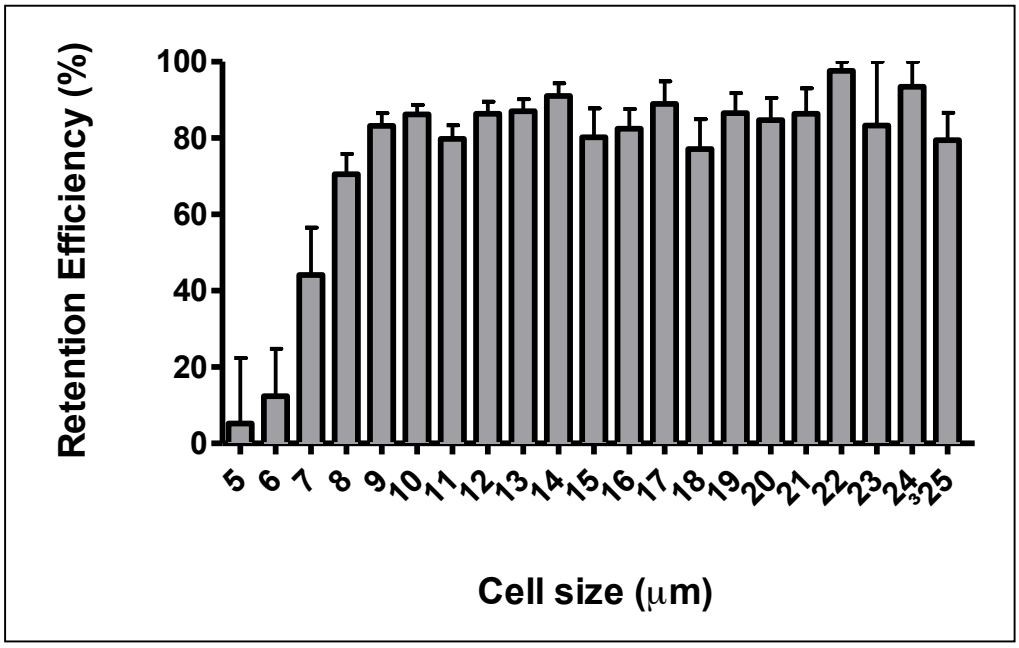

Figure 4-66: Cell retention efficiency calculated according to the size of MSC after IC injection into normal hearts. The coronary effluent was collected from n=8 separate Langendorff heart injections of $8x10^6$ MSC. The numbers of cells retained in the heart for each cell size were calculated and expressed as a fraction of the number of the pre-injection MSC of each size. The smallest MSC had a lower retention rate but that increased with larger cell diameter. The retention efficiency for cells ≥ 9 μm reached a plateau. Error bars represent SEM.

4.7.5 Distribution and location of retained MSC in relationship to the vasculature

At either 5 or 60 minutes after injection of $8x10^6$ PKH67-labelled MSC into Langendorff perfused normal hearts, the hearts were collected, fixed, sectioned and subjected to immunohistochemical analysis for assessing the distribution and localisation of retained MSC.

At low magnification, a countable number of retained PKH67 labelled MSC were found in isolation (Figure 4-67) at 5 minutes after cell injection. The frequency and pattern of MSC distribution at 5 minutes was found to be similar to 60 minutes after cell injection (Figure 4-68). Higher magnification observation clearly revealed that all retained MSC were within the coronary lumen at both 5 and 60 minutes after cell injection (Figures 4-69 and 4-70). No cells were observed to have extravasated by 60 minutes post injection.

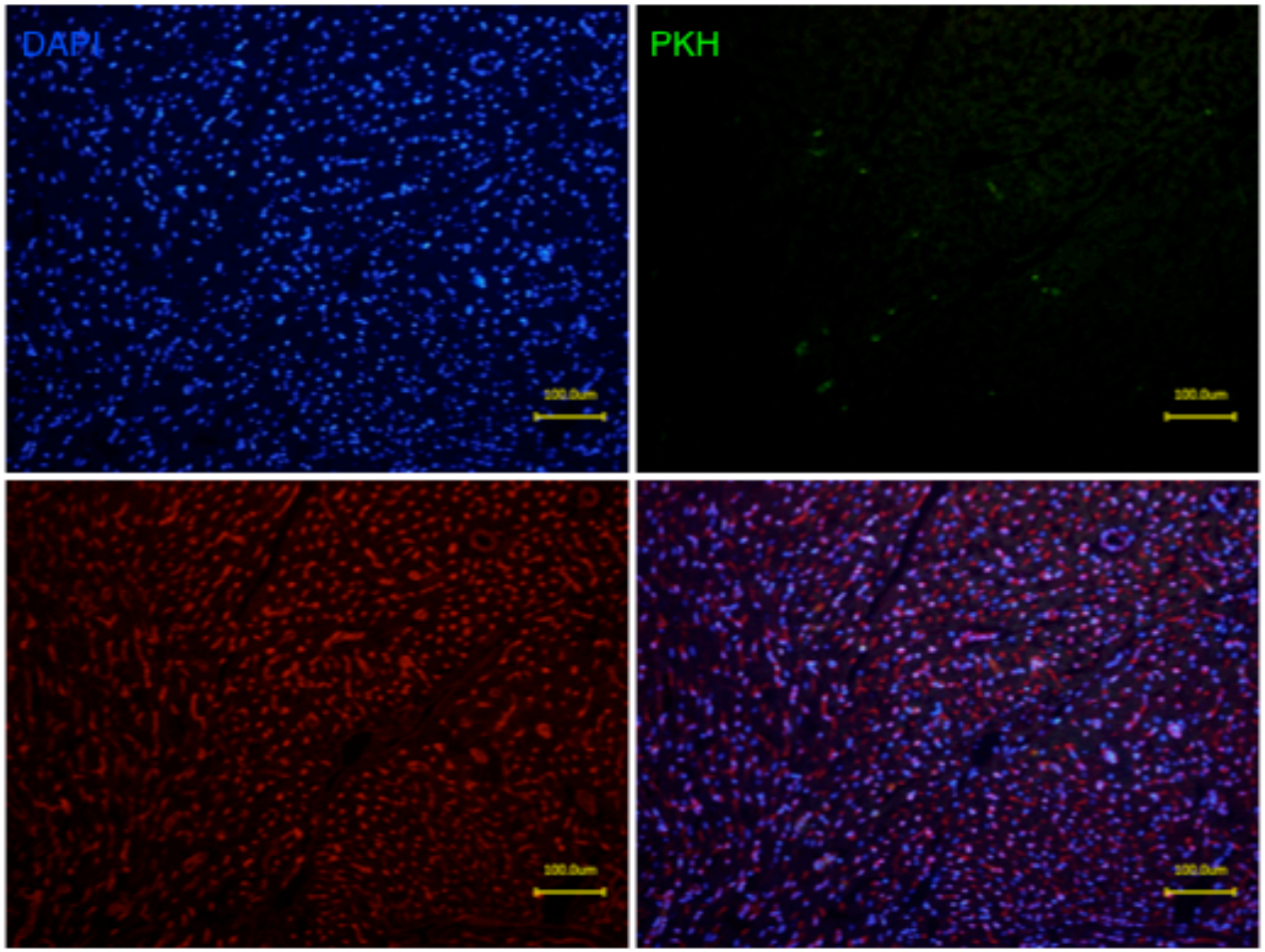

Figure 4-67: Retained MSC location in the heart 5 minutes after injection (low magnification). $8x10^6$ PKH67-labelled MSC were injected into normal hearts and the hearts were collected at 5 minutes. The sections were stained with a nuclear marker (DAPI; blue) and an endothelial marker (Isolectin-B4; red). A number of bright fluorescent MSC (green) could be seen at low (x10) magnification. The relationship of the cells to the lumen could not be clearly determined at this magnification. Scale bar: 100 μm.

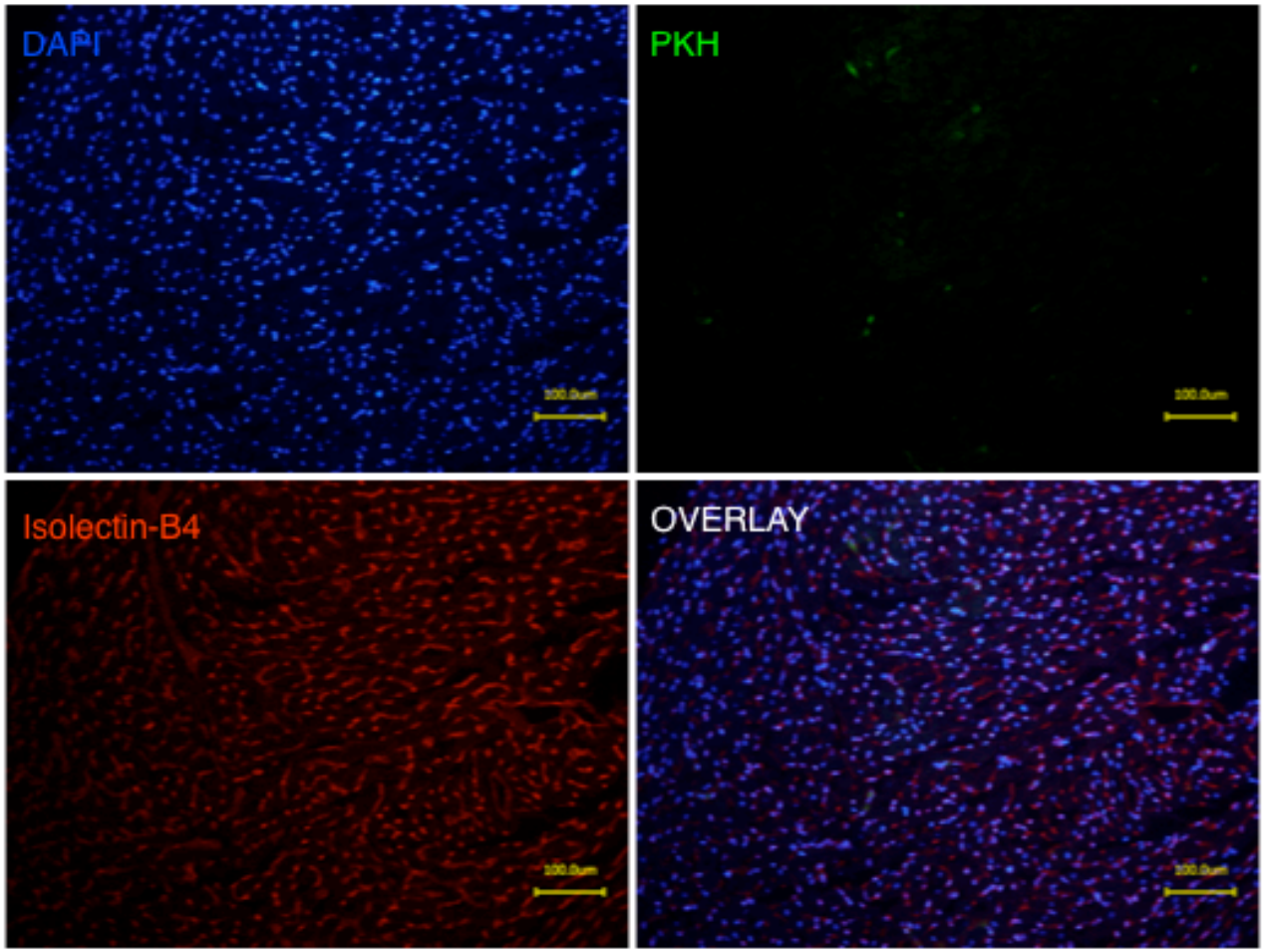

Figure 4-68: Retained MSC location in the heart 60 minutes after injection (low magnification). $8x10^6$ PKH67-labelled MSC were injected into normal hearts. The hearts were collected at 60 minutes and the sections were stained with a nuclear marker (DAPI; blue) and an endothelial marker (Isolectin-B4; red). A number of bright fluorescent MSC (green) could be seen at low (x10) magnification. The relationship of the cells to the lumen could not be clearly determined at this magnification. Scale bar: 100 μm.

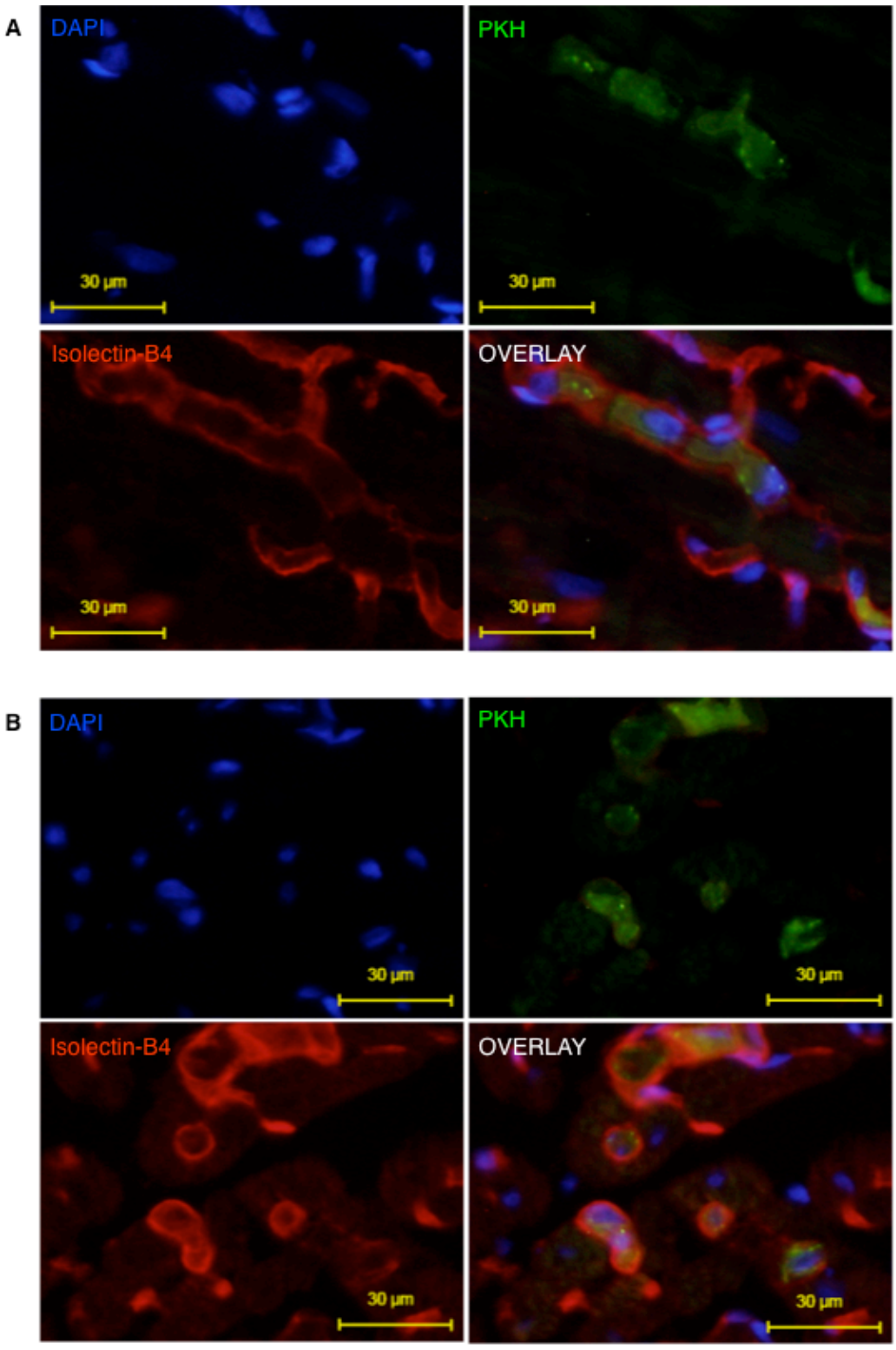

Figure 4-69: Retained MSC location in the heart 5 minutes after injection (high magnification).
$8x10^6$ PKH67-labelled MSC were injected into normal hearts. All PKH67-labelled MSC (green) were found inside the vascular lumen. Two representative images (A and B) are presented.
Scale bar = 30 µm.

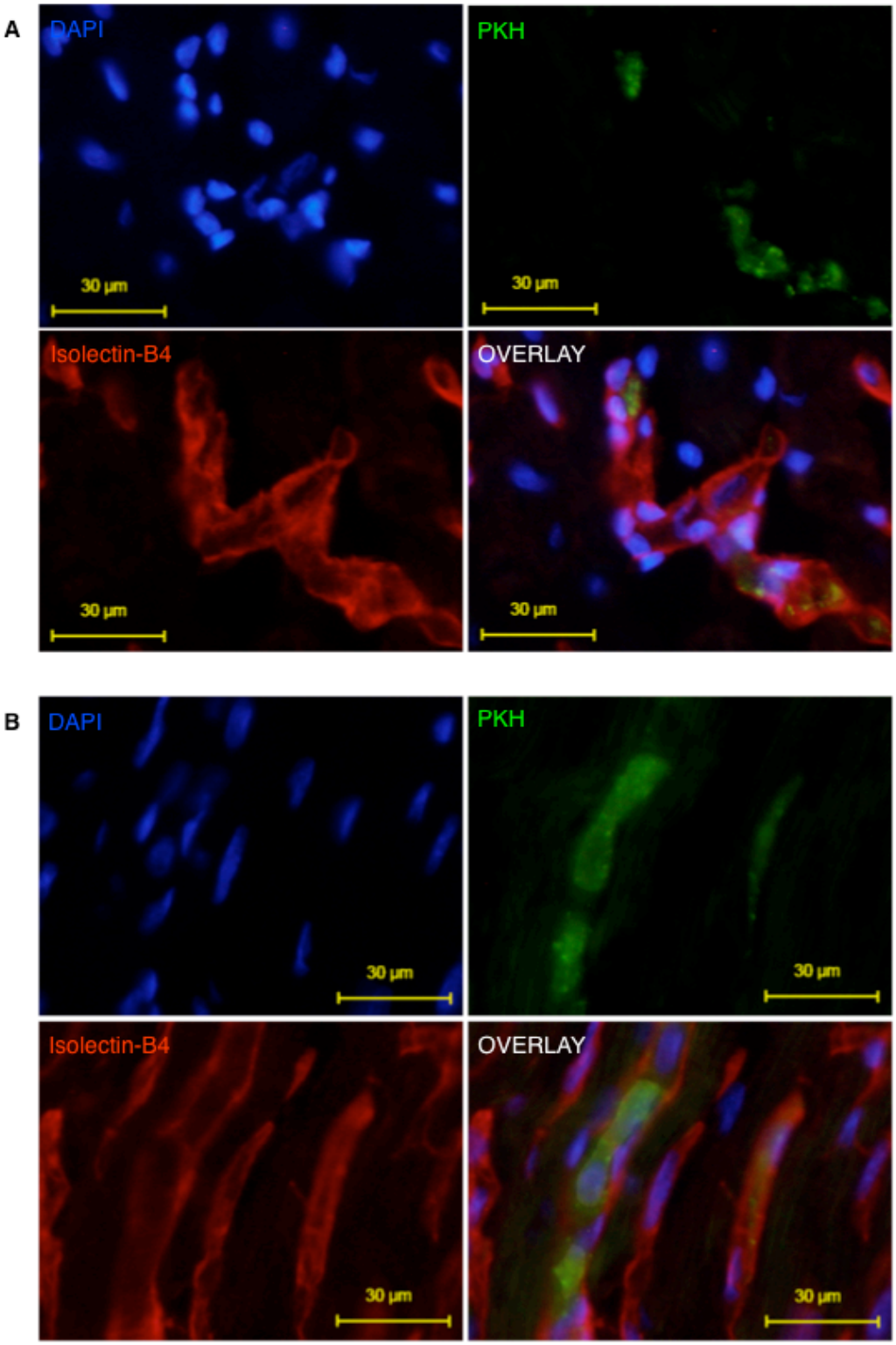

Figure 4-70*: *Retained MSC location in the heart 60 minutes after injection (high magnification).
$8x10^6$ PKH67-labelled MSC were injected into normal hearts. All PKH67-labelled MSC (green) were still found inside the vascular lumen. Two representative images (A and B) are presented.
Scale bar: 30 µm.

4.8. Comparison of retention of BMMNC and MSC in normal hearts

In order to elucidate further the possible effect of cell-type differences on donor cell retention after IC injection, more detailed direct comparisons between BMMNC injection (4.4) and bone marrow-derived MSC injection (4.7) into normal hearts were made. Although there are some duplicated data, I believe that in this section direct comparisons are useful to highlight similarities and differences between the two cell types.

4.8.1. Pre-injection donor cells

MSC and BMMNC had different morphology, particularly regarding their cell size. Flow cytometric studies showed that the population of MSC was larger (determined by Forward Scatter) and had a greater granularity compared to BMMNC (Figure 4-71).

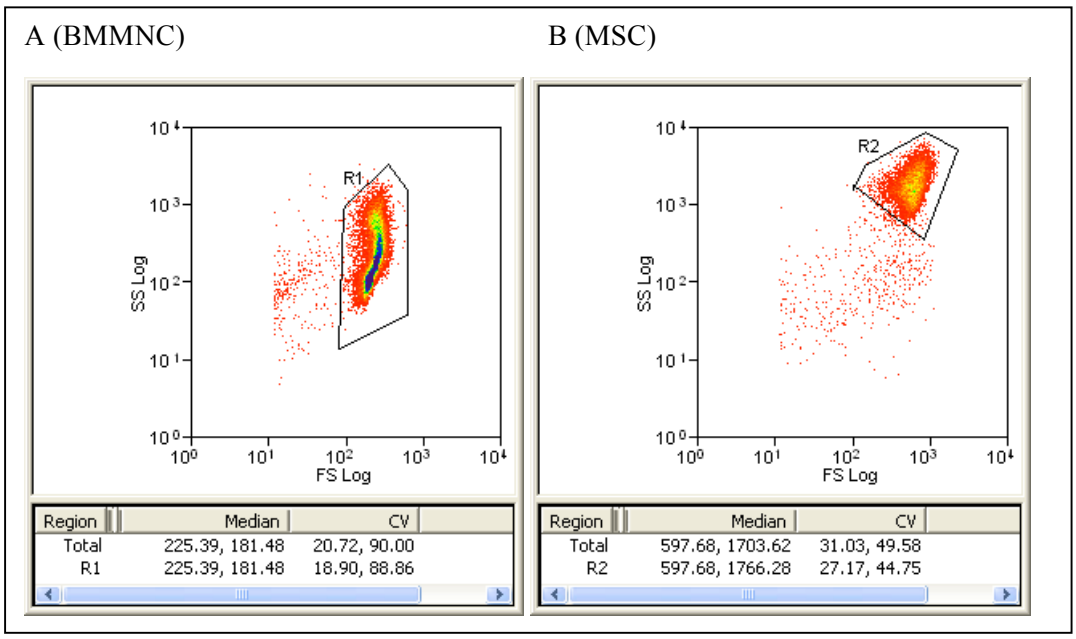

Figure 4-71: Flow cytometric analysis of BMMNC (A) and MSC (B). The same voltage settings for forward scatter (FS) and side scatter (SS) were used. Median ± coefficient of variance for FS and SS are shown (arbitrary units). The MSC were larger and had a greater granularity as assessed by flow cytometry (R2 *vs.* R1).

The size of pre-injection BMMNC and MSC were also compared using an Automated Cell Counter (Figure 4-72). The distribution of cell sizes of MSC was larger with a mean cell diameter of 12.1 μm, compared to a mean BMMNC diameter of 7.0 μm. The populations of cell diameters were compared by non-linear regression by generating second order polynomial (quadratic) best-fit lines and were found to be significantly different ($p<0.001$: Sum of Squares F-test).

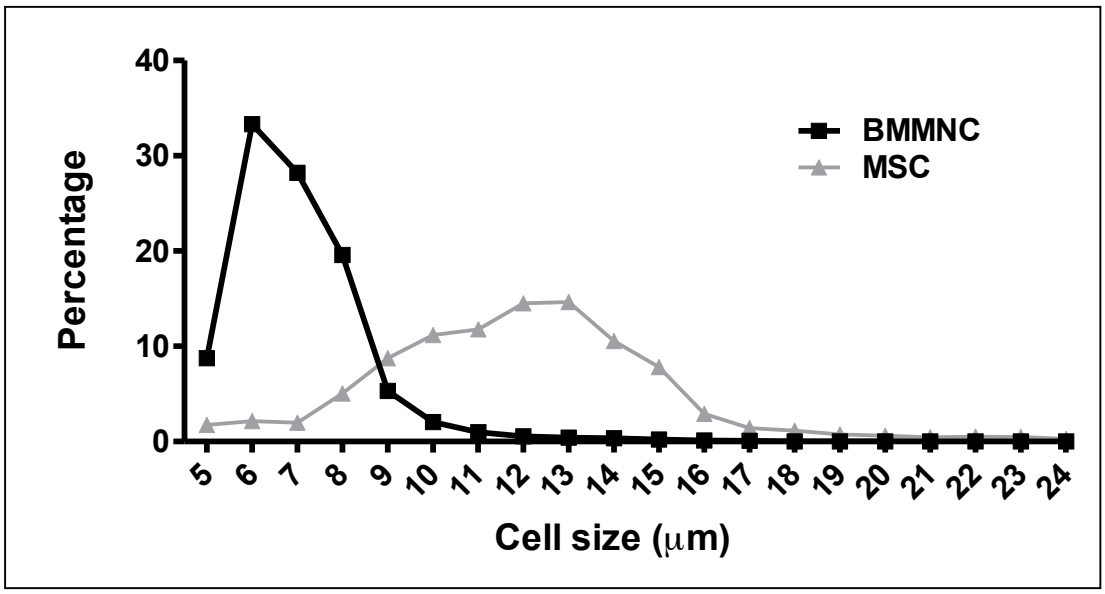

Figure 4-72: Distribution of diameters of BMMNC and MSC prior to injection. The diameters of isolated BMMNC and cultured passage 4 MSC, prior to injection were measured. The number of cells with each diameter were calculated and expressed as a fraction of all the total number of cells in each group. The size of MSC was larger than BMMNC.

4.8.2. Pattern of cell loss into coronary effluent

Donor cell loss into the coronary effluent, minute by minute, after cell $8x10^6$ injection of BMMNC or MSC into normal hearts for the first 5 minutes was compared (Figure 4-73, A). The majority of cell loss into the coronary effluent occurred in the first minute after cell injection of either cell type. There was a marked difference in the number of cells lost in the coronary effluent within the first minute between BMMNC and MSC (5.9 ± 1.9 *vs.* $1.7 \pm 1.6 \times 10^6$ respectively, n=13 each group, $p<0.0001$; Two-way ANOVA and Bonferroni's Multiple Comparison Test). There was no absolute difference in cell loss between the 2 groups for the subsequent 4 minutes.

Next, donor cell loss in the effluent for each minute was expressed as a fraction of all of the cells lost in the coronary effluent, and compared between BMMNC and MSC (Figure 4-73, B). The pattern of donor MSC cell loss was similar to that after BMMNC injection into normal hearts ($p=0.09$, Two-way ANOVA).

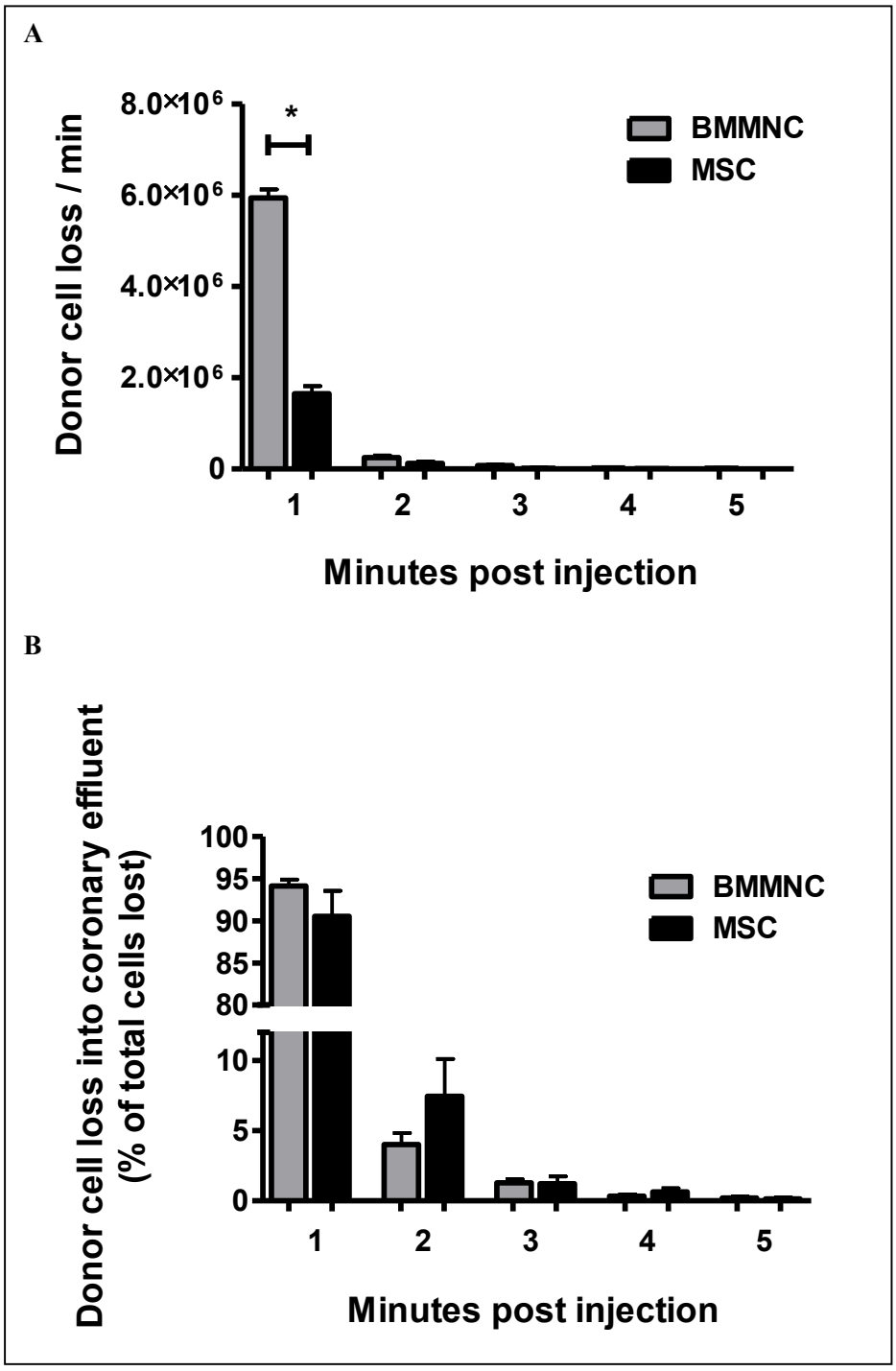

Figure 4-73: Donor cell loss into the coronary effluent after IC injection of BMMNC and MSC into normal hearts. $8x10^6$ freshly collected BMMNC and passage 4 MSC were IC injected into normal hearts (n=13 in each group) and the absolute donor cells in the coronary effluent were counted for the first 5 minutes (A). There was 3 times the number of BMMNC in the coronary effluent in the first minute compared with MSC. Error bars = SEM. *=$p<0.001$ (Bonferroni's Multiple Comparison Test). The pattern of cell loss was also calculated minute by minute as a fraction of the total cell loss and expressed as a percentage (B). There was no difference in the pattern of cell loss between the two cell types overall (Two-way ANOVA). Error bars = SEM.

4.8.3. Cell retention in the normal heart

The absolute numbers of retained cells following IC injection of BMMNC and MSC were compared at each minute following injection (Figure 4-74). The absolute number of donor cells in the heart was approximately three times higher after MSC injection at each time point. After 5 minutes there were a mean of $6.2x10^6$ MSC *vs.* $1.7x10^6$ BMMNC retained in the heart ($p<0.0001$, Two-way ANOVA and Bonferroni's Multiple Comparison Test).

In both the BMMNC and MSC injected hearts, there was a slight decrease in the number of cells retained in the heart over time, but this was not statistically significant ($p=0.50$, Two-way ANOVA). Therefore in both groups, the number of cells retained in the heart at 5 minutes was dependent on the number of cells retained within the first minute.

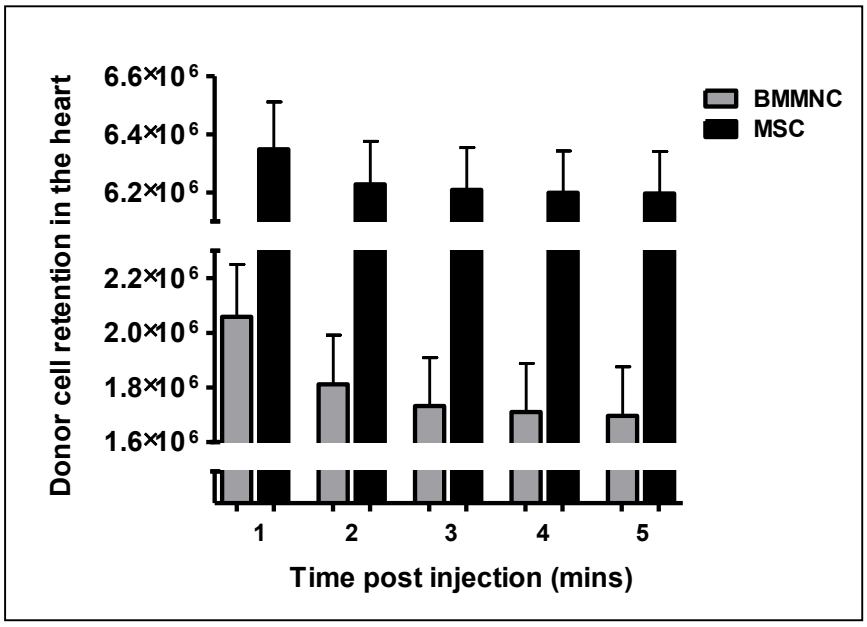

Figure 4-74: Absolute cell retention numbers within the first 5 minutes after IC injection of BMMNC and MSC. There was a significant difference in donor cell retention (absolute number) between the BMMNC and MSC groups at each time point ($p<0.0001$, Two-way ANOVA). The number of cells in the heart in each group over time did not change ($p=0.5$, Two-way ANOVA). Error bars = SEM.

Next, the 5-minute retention of cells after injection of $8x10^6$ BMMNC (into normal and I-R hearts) and $8x10^6$ MSC (into normal hearts) were compared directly (Figure 4-75). The proportion of MSC retention in the normal hearts was markedly higher than BMMNC retention into either normal or I-R hearts ($p<0.0001$, One-way ANOVA with Bonferroni's Multiple Comparison Test).

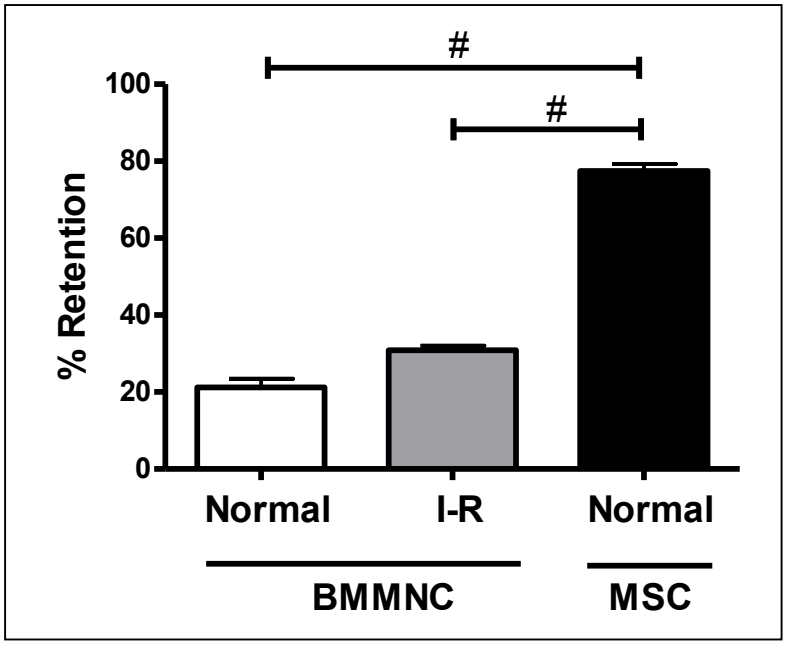

Figure 4-75: Retention efficiency after first 5 minutes after IC injection of $8x10^6$ BMMNC and MSC. The retention efficiency of donor cells in the heart was compared after 5 minutes following IC injection of $8x10^6$ BMMNC into normal and I-R hearts and $8x10^6$ MSC into normal hearts. The retention of MSC was greater than BMMNC retention in both normal and I-R hearts. Percentages are expressed as a proportion of the total injected cell number. n=11-13 each group, #= $p<0.05$, Bonferroni's Multiple Comparison Test. Error bars = SEM.

To provide additional confirmatory evidence that there was a greater number of MSC retained in the heart compared to BMMNC, a semi-quantitative immunohistochemical analysis was performed. Representative low magnification fields were obtained from hearts 60 minutes after injection of $8x10^6$ BMMNC (Figure 4-76) or MSC (Figure 4-77). A greater number of cells was observed in the MSC hearts (19.6 ± 2.4, $n=7$) compared to the BMMNC hearts (2.6 ± 0.5, $n=11$; $p<0.0001$, unpaired T-test, Figure 4-78). This semi-quantitative donor cell retention result was consistent to that of the quantitative measurement (please see 3.6.8).

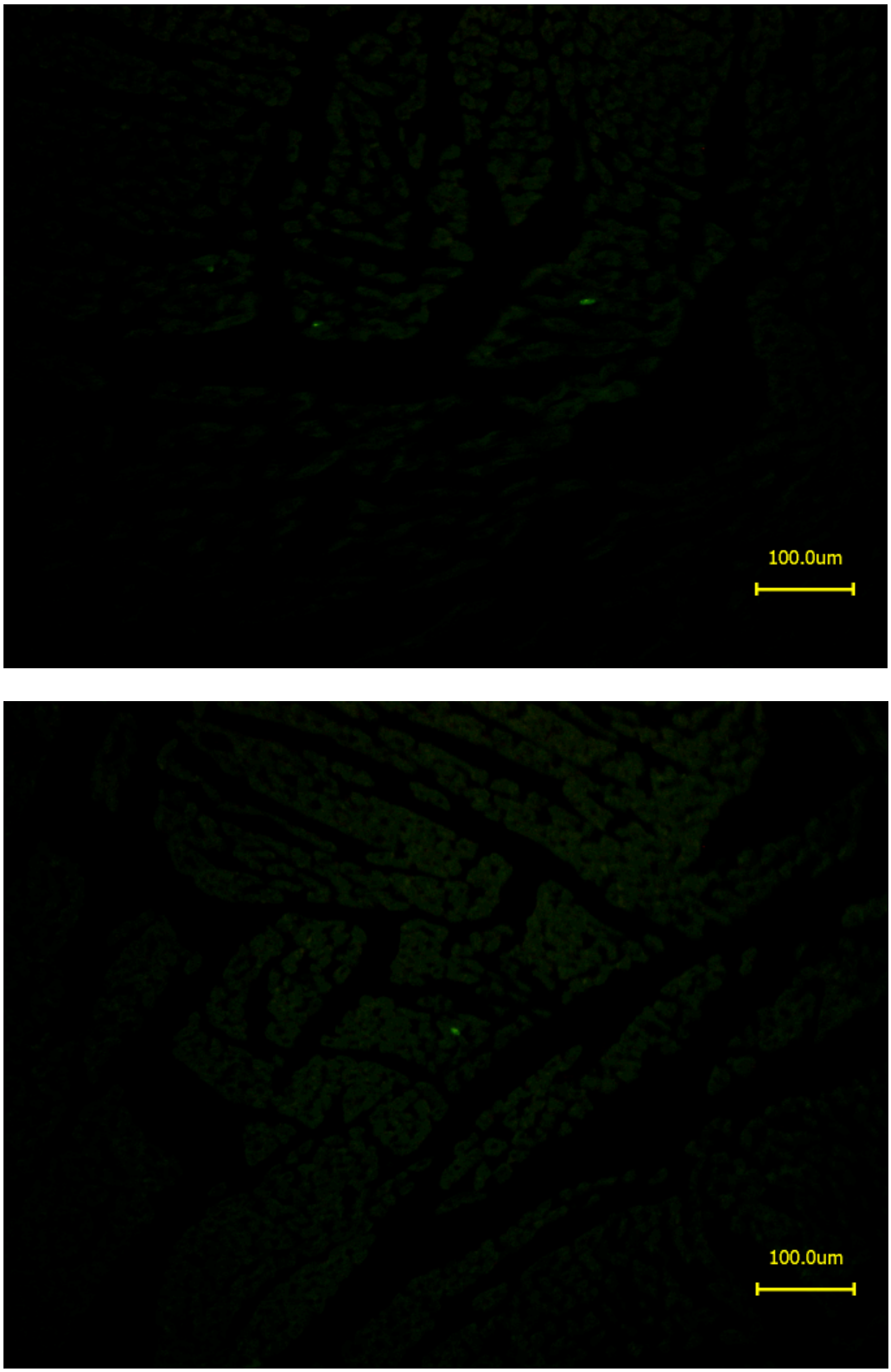

Figure 4-76: Representative images of hearts after injection of BMMNC (low magnification). Low magnification images (x10) were acquired of normal hearts 60 minutes after injection of $8x10^6$ BMMNC. A small number of cells could be observed in each field. Green fluorescent images only are shown. Scale bar 100μm.

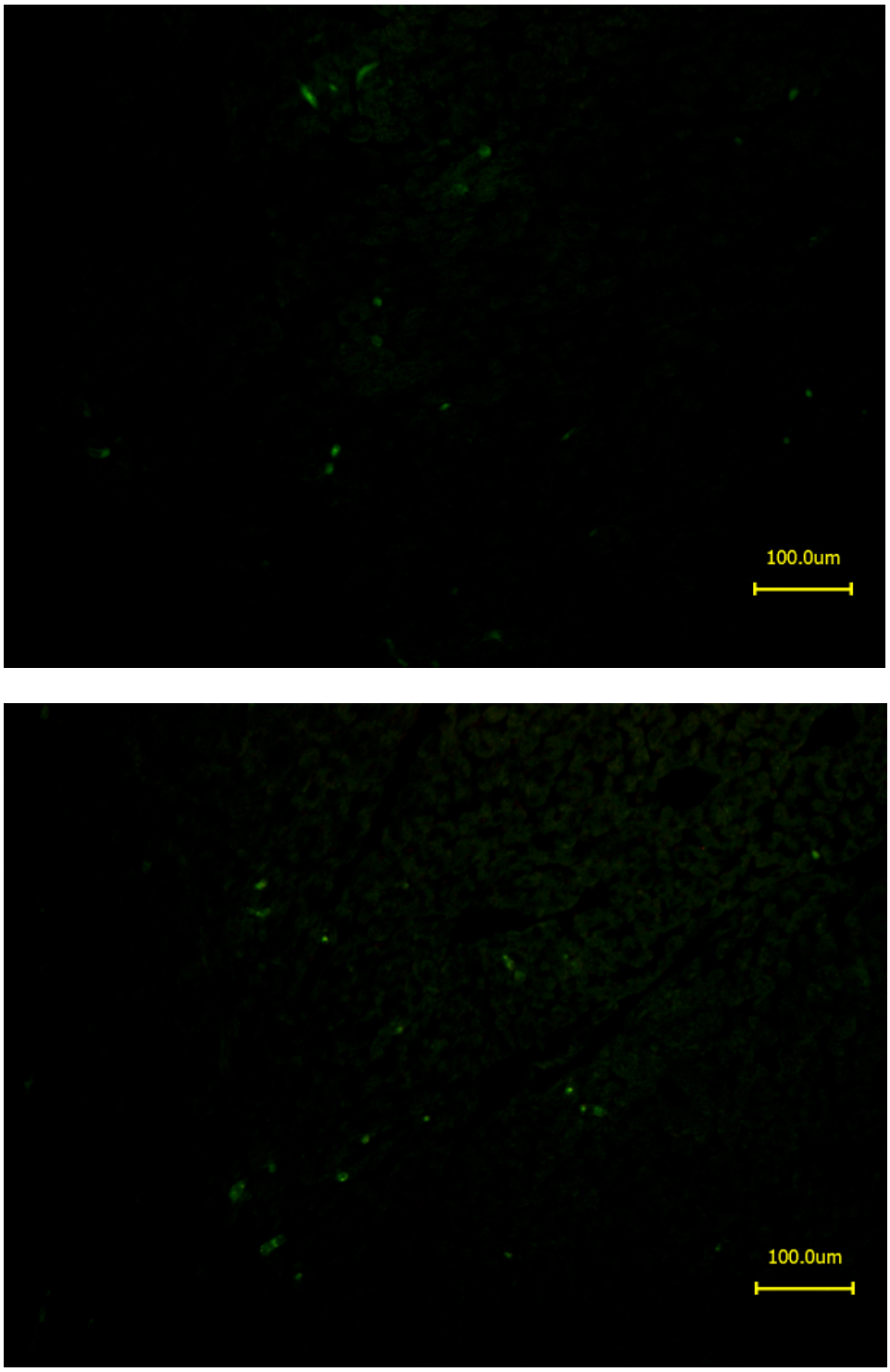

Figure 4-77: Representative images of hearts after injection of MSC (low magnification). Low magnification images (x10) were acquired of normal hearts 60 minutes after injection of $8x10^6$ MSC. Many donor cells could be observed in each field. Green fluorescent images only are shown. Scale bar 100μm.

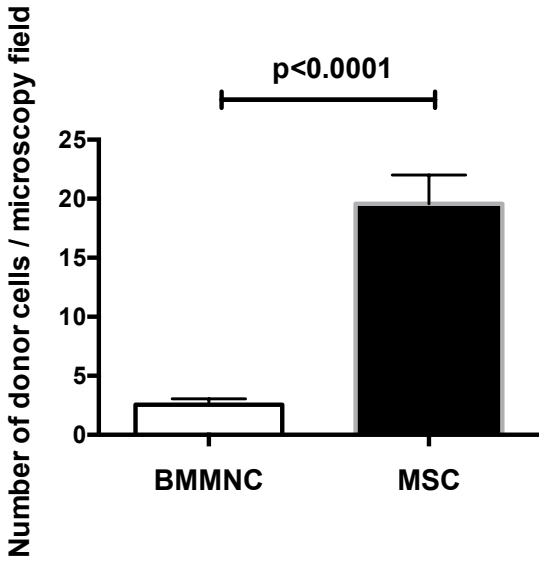

Figure 4-78: Semi-quantitative analysis of $8x10^6$ BMMNC and MSC retained in the heart.
Representative images at x10 magnification were obtained from immunohistochemical images taken of hearts 60 minutes after cell injection of 8x106 BMMNC or MSC. There were a greater number of donor cells in the representative images from the MSC hearts compared to the BMMNC hearts ($p<0.0001$).

The higher retention rate of MSC was thought to be as a consequence of their larger cell size, compared to BMMNC. To further investigate this aspect, the size of BMMNC and MSC retained in the heart were directly compared. Donor cells were subdivided into the following cell size categories to enable a meaningful comparison: 5-6 μm, 7 μm and ≥ 8 μm. This determined that MSC with a larger diameter were retained with increased efficiency compared to BMMNC ($p<0.05$, Two-way ANOVA; Figure 4-79). Post-hoc analysis (Bonferroni's Multiple Comparison Test) demonstrated that the retention efficiency for the smallest cells (5-6 μm) was similarly low in the BMMNC and MSC groups (13.0 ± 6.2 *vs.* 9.0 ± 12.6% respectively, $p=0.80$). There appeared to be an increase in retention of MSC sized 7 μm compared to similarly sized BMMNC but this finding was not statistically significant ($p=0.39$). MSC sized ≥ 8 μm were retained with double the efficiency of BMMNC ($p<0.0001$).

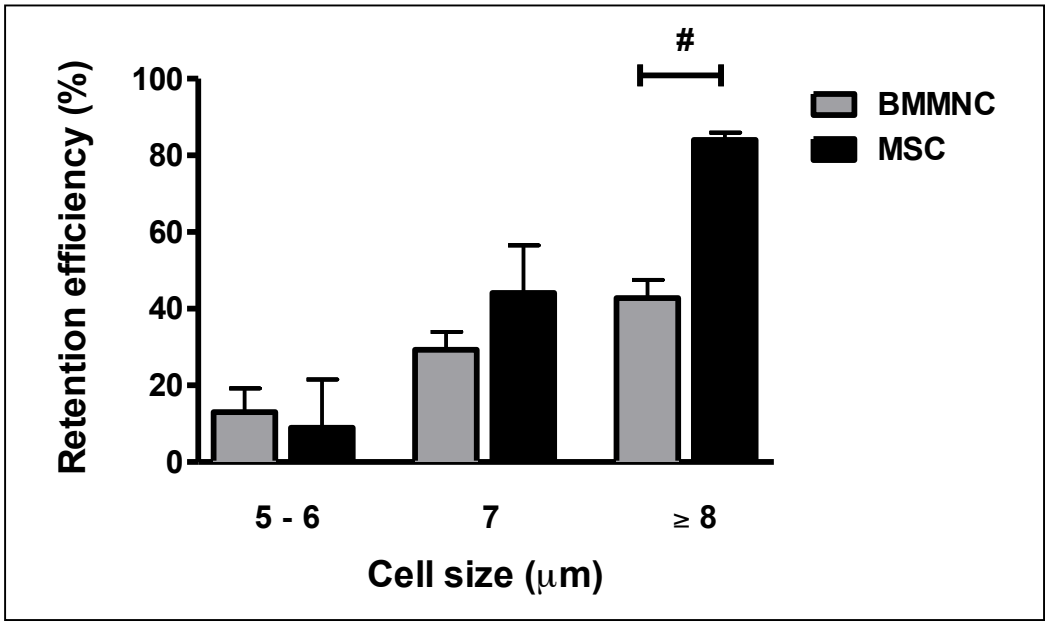

Figure 4-79: Donor cell retention efficiency in the normal heart, according to cell size of donor BMMNC and MSC. Cell sizes of pre-injection donor cells and of the donor cells in the coronary effluent were assessed by an automated cell counter. The retention efficiency of different cell sizes of donor BMMNC and MSC were compared. Larger MSC were retained with increased efficiency compared to BMMNC ($p<0.05$, Two-way ANOVA). n=5 BMMNC heart samples, n=8 MSC heart samples, #=$p<0.05$, Bonferroni's Multiple Comparison Test. Error bars = SEM.

4.8.4. Coronary embolism after IC injection

Larger cells may result in higher retention rate, but in turn could have an increased risk of coronary embolism. This issue was investigated by direct comparison between two cell types with different cell sizes. The pattern of coronary effluent flow rates before and after injection of $8x10^6$ BMMNC or MSC into normal hearts was compared by non-linear regression by generating second order polynomial (quadratic) best-fit lines and were found to be significantly different ($p<0.0001$: Sum of Squares F-test) (Figure 4-80). The coronary effluent flow rates decreased in the MSC-injected hearts but returned to that of the BMMNC-injected hearts by 10 minutes. This reduction of myocardial perfusion was associated with reduction of heart rate and myocardial temperature (refer to 4.7.1). In contrast these changes were not observed after injection of the same, or an even larger (up to $40x10^6$) number of BMMNC into normal hearts (refer to 4.4.1).

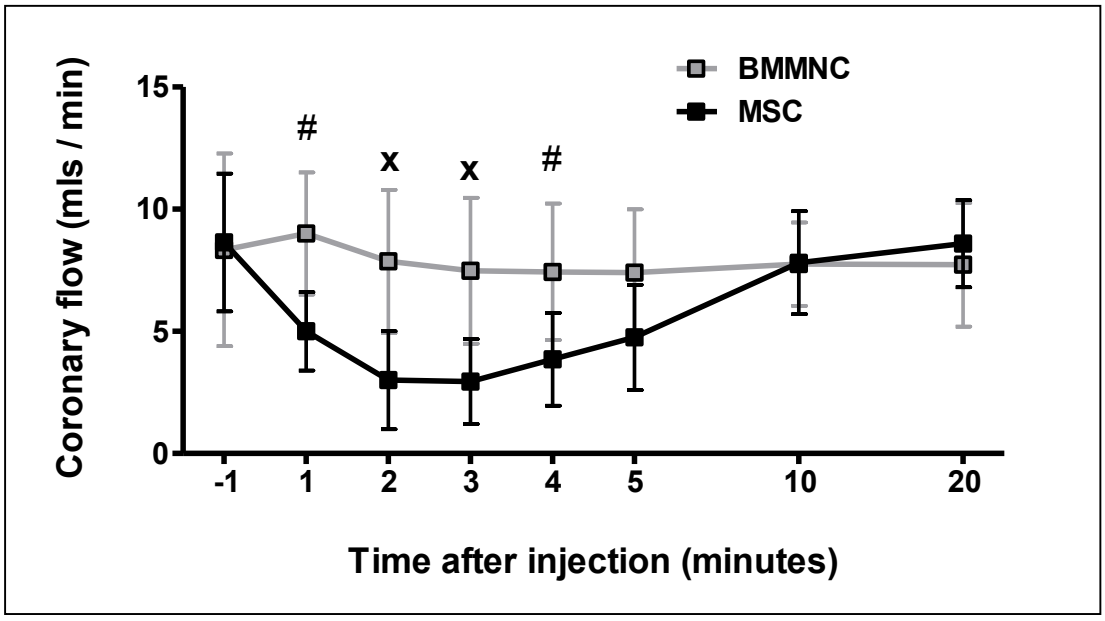

Figure 4-80: Pattern of coronary effluent flow rate before and after IC injection of BMMNC or MSC into normal hearts. The coronary effluent flow rates were compared before and after IC injection of $8x10^6$ BMMNC and MSC in normal hearts. Whereas coronary effluent flow rate remained unchanged after BMMNC injection, it decreased after MSC injection and slowly recovered over the subsequent 10 minutes. #=$p<0.01$, ×=$p<0.001$, n=13 each group, Bonferroni's Multiple Comparison Test. Error bars indicate SEM.

Using immunohistochemical analysis, retained BMMNC were always seen in isolation (refer to 4.4.7) within the heart. However after MSC injection, although retained cells were also seen in isolation, they were frequently seen in clusters or in very close proximity, suggesting that clumping or coronary embolization had occurred (refer to Figures 4-67, 4-68, 4-69 and 4-70). This provides further supporting evidence that reduction of coronary flow after MSC retention was caused by cellular coronary embolization.

Chapter 5 – DISCUSSION

5.1. Overview of the project

Cell transplantation is a promising approach for the treatment of AMI and chronic heart failure. Meta-analyses have shown that IC injection of BMMNC has therapeutic benefits, but one major problem with this approach is that the number of cells that engraft in the heart is low. A more detailed understanding of the underlying mechanisms and fate of cells is required if this treatment is to enter widespread clinical practice. Initial donor cell retention within minutes of IC cell injection is considered to be a key factor limiting donor cell engraftment. This project set out to investigate the patterns and mechanisms of the initial cell retention in the heart after IC injection.

In the initial work for the project, a substantial amount of time was spent developing the ex-vivo Langendorff model for use with mice, but reproducible data could not be consistently obtained with this species. However, an original rat *ex-vivo* Langendorff heart preparation was successfully generated and utilized for quantitative measurements of initial donor cell retention after IC cell injection. In this model, a known number of donor cells were injected into the coronary arteries *via* the aortic root, and the coronary effluent was collected minute-by-minute, from which the numbers of donor cells were counted. With knowledge of the injected donor cell number and the number of cells in the coronary effluent, the number of cells retained in the heart could be quantified in a reproducible manner. Comparison of the pre-injection and coronary effluent cell populations enabled the study of whether there were cell-related factors that affected retention, such as donor cell size and expression of adhesion-related molecules. Fluorescent labelling of donor cells enabled the early fate of donor cells in the heart to be assessed using immunohistochemistry.

BMMNC injection into the normal intact heart resulted in initial donor cell retention efficiency of approximately 20% within the first 5 minutes. Addition of 30 minutes ischaemia followed by 30 minutes reperfusion resulted in an increase in the initial retention efficiency to approximately 30%. Increasing the BMMNC dose from 1×10^6 to 40×10^6 cells proportionally increased the number of retained cells without inducing coronary embolism, while the efficiency of donor cell retention was not affected by the donor cell number injected. Injection of bone marrow derived MSC, a larger cell type, increased retention efficiency to approximately 80%, but led to coronary embolism. Furthermore, larger subpopulations of BMMNC and MSC were preferentially retained in the heart. Conversely, surface protein expression of BMMNC did not influence cell retention. Immunohistochemistry demonstrated that all retained donor cells - both BMMNC and MSC - were observed inside the coronary lumen. However, BMMNC were found in isolation whereas MSC were frequently found in clumps. This data therefore suggests that extravasation of donor cells, or incorporation into the vessel wall did not occur up to 60 minutes after IC injection of BMMNC or MSC.

In summary, these findings collectively demonstrate that our original experimental model was reproducible and can be used to assess initial donor cell retention after IC cell injection in a quantitative manner in small rodents. Because cell size had a large impact on donor cell retention but cell surface marker expression did not, the data highly suggests that mechanical passive entrapment, rather than active processes *via* intercellular interactions between donor cells and coronary endothelium, is predominantly responsible for initial donor cell retention after IC injection of BMMNC or MSC, at least in the settings of this research (hearts with normal coronary arteries and after I-R injury of this duration). The obtained results and the translational/clinical implications of this data for future work are discussed below.

5.2. Establishment of the model to quantitatively assess initial retention of donor BMMNC and MSC after IC injection in rat

5.2.1. Ex-vivo Langendorff heart perfusion model

The *ex-vivo* Langendorff heart perfusion model is an established and frequently used technique in cardiovascular research. I utilized a modified version of this model whereby a known number of cells were injected IC into the heart and the cells collected from the coronary effluent. From comparison of these two cell populations, we quantified initial donor cell retention and characterized subpopulations that are preferentially retained within the heart. To my knowledge, this is the only model to enable quantitative assessment of donor cell retention after IC injection in small rodents.

First, it was confirmed that this rat *ex-vivo* Langendorff heart perfusion model could be used to achieve appropriate stable myocardial perfusion before cell injection. Perfusion parameters (coronary effluent, heart rate and temperature of coronary effluent exiting the heart) were all stable and reproducible (refer to 4.3.1). In addition, these parameters were comparable to those reported previously using Langendorff heart preparations in rats[255,257]. After injection of a standardized numbers of BMMNC (1×106, 8×10^6 and 40×10^6), Langendorff parameters were also reproducible (refer to 4.4.1 and 4.7.1). Similarly, there were reproducible perfusion parameters after injection of MSC. More importantly, the pattern of donor cell loss in the coronary effluent after injection, with both BMMNC and MSC, was consistent using every experimental condition studied in this project (refer to 4.8.2).

An unexpected finding in this model was that there was a low, but countable, level of endogenous cell leakage from the perfused *ex-vivo* hearts in the coronary effluent, even 20-30 minutes after perfusion (refer to 4.3.3). These cells were identified to be RBC (refer to

4.3.3). Therefore, I adjusted the cell number in the coronary effluent by subtracting the baseline RBC number in my calculation of initial donor cell retention. Although this cell number was relatively small compared to that of donor cell loss into the coronary effluent, this modification enabled the highest accuracy of the measurement of donor cell retention in the model to be obtained (refer to 4.4.2).

Using this model and calculation formula, it was estimated that IC BMMNC injection into normal hearts resulted in an initial donor cell retention efficiency of approximately 20% within the first 5 minutes. The clinical studies that have previously investigated cell retention after IC injection have found that at 1 hour, 1-10% of donor cells persist in the heart with further attrition at 24 hours (refer to Table 1-2). *In vivo* animal studies investigating cell retention have found similar cell retention proportions at these later time points after injection[117,118]. Doyle and colleagues examined IC-injected radiolabelled donor cells into a pig AMI model using cycles of balloon occlusion / reperfusion[182]. Using dynamic studies, they found that myocardial tracer activity dropped to 20% of its peak during the restoration of coronary flow.

Our data obtained in rat is compatible with these previous data, validating my original method to measure initial donor cell retention. It was considered that the normal heart model would be analogous to IC injection of cells into patients with dilated cardiomyopathy who do not have coronary artery disease. This model would also mimic some aspects of post-MI chronic heart failure (ischaemic cardiomyopathy), where the expression of adhesion molecule-related proteins on the coronary vasculature would not be expected to be substantially different from that of normal hearts.

5.2.2. Ischaemia-reperfusion (I-R) injury model

I-R injury may influence intercellular adhesion-related molecules in the host coronary endothelium, which could then affect initial donor cell retention after IC injection. To investigate this, 30 minutes global ischaemia followed by 30 minutes reperfusion was chosen as a model of I-R injury (refer to 4.3.5), which has been frequently used in previous studies to study myocardial I-R injury[218,258,259].

There are several different techniques which have been previously reported to induce I-R injury in the heart[260]. Neely *et al.* utilised low flow global ischaemia induced during *ex-vivo* Langendorff perfusion by placing a one-way valve in the aortic outflow tract, which prevented retrograde perfusion of the coronary arteries during diastole and reduced coronary blood flow by about 60%[261,262]. However, I believe that our model is more relevant to clinical settings of AMI. In addition, careful consideration was given to utilizing the technique of left coronary artery ligation to induce localised I-R injury and MI. This has previously been reported and validated in many previous small animal studies[107,208,263]. The potential advantage of this method would be that cell injection could occur *ex-vivo* at various time points post-MI. It would then be able to assess donor cell retention serially at various time points post MI, which is an important and controversial question in the field of stem cell therapy to the heart[173].

However if this model was used, it would be likely that after global cell injection the injected donor cells would preferentially flow down a non-infarct coronary artery. This is because the non-infarct artery would have a lower flow resistance for injected cells than the infarct artery. The non-infarct artery would also be less likely to exhibit the no-reflow phenomenon which frequently occurs in an infarct artery[264]. Given these probable outcomes, our model would not have been able to assess changes in overall donor cell retention quantitatively. This could have been overcome by independent dual perfusion of left and right coronary arteries in the isolated rat hearts[265] or selective injection of cells into an

individual coronary artery, but these models would have been extremely challenging to establish.

5.2.3. Isolation, culture and characterization of donor cells

BMMNC and bone marrow derived MSC were chosen as donor cells to be investigated in this project. Both of these cell types have been frequently examined in animal and clinical studies, and are among the cell types with the most potential in future clinical application of cell therapy to the heart. For the collection of these cells, previously reported isolation/culture methods were used with modifications.

3.6×10^8 unselected BMMNC per adult rat with a high purity (>99.5%) and high viability (99.3%) were obtained (refer to 4.1). Although RBC contamination has been shown to affect the efficacy of BMMNC therapy in the clinical setting[266], the rate in my study was sufficiently low (<0.05%). The expression of cell surface markers was also comparable to other reports in general[46,100,146,150,152,174,175,267], although the majority of previous studies have not comprehensively reported surface markers expression on BMMNC as shown in Table 5-1. When propagating MSC using established culture protocols, it was demonstrated that approximately 1×10^8 MSC (passage 4) could be collected from the bone marrow of each initial donor animal, within 17-21 days of culture. The collected MSC showed all the cellular properties used for identification of this cell type[76] as follows. The cells were plastic-adherent and showed a typical morphology (fibroblast-like spindle shape). They were shown by flow cytometry analysis to express typical cell surface marker expression; positive for CD29 and CD90 and negative for CD34 and CD45. In addition, the cultured cells demonstrated multipotency to mesenchymal lineages, *via* their ability to differentiate to adipocytes and osteocytes.

Overall, these data indicate successful collection of rat BMMNC and MSC and that they could be used in this experimental model of cell transplantation.

Table 5-1: Previously reported surface markers of isolated BMMNC – comparison with this study's results.

	Strauer [149] (2002)	Assmuss [268] (2002)	BOOST [43] (2004)	Janssens [12] (2006)	Lunde [154] (2006)	Meluzin [241] (2006)	Fukushima [128] (2007)	Penicka [157] (2007)	FINCELL [20] (2008)	Kim [53] (2010)	Fukushima [213] (2011)	This Study
Species	Human	Human	Human	Human	Human	Human	Rat	Human	Human	Mouse	Mouse	Rat
CD3	-	-	-	-	-	44.9%	-	-	-	-	-	-
CD11b	-	-	-	-	-	-	-	-	-	-	-	17.8%
CD16	-	-	-	-	-	3.5%	-	-	-	-	-	-
CD18	-	-	-	-	-	-	-	-	-	-	57.5%	29.5%
CD19	-	-	-	-	-	12.0%	-	-	-	-	-	-
CD29	-	-	-	-	-	-	-	-	-	-	-	96.6%
CD31	-	-	-	-	-	-	-	-	-	34%	-	42.1%
CD33	-	-	-	-	-	0.4%	-	-	-	-	-	-
CD34	2.1%	<4%	0.3%	0.9%	1.0	1.0%	4.5%	0.05%	0.7%	-	0.9%	0%
CD44	-	-	-	-	-	-	-	-	-	-	-	41.4%
CD45	-	-	-	-	-	-	75.5%	-	-	-	95.4%	83.7%
CD73	-	-	-	10.5%	-	-	-	-	-	-	-	-
CD90	-	-	-	0.02%	-	-	-	-	-	-	-	56.6%
CD105	-	-	-	0.8%	-	-	-	-	-	-	-	-
CD117 / c-kit	-	-	-	2.3%	-	-	-	-	-	-	-	-
CD133	0.65%	-	-	0.7%	-	-	-	-	-	-	-	-
PSGL-1	-	-	-	0.9%	-	-	-	-	-	-	49.3%	-

5.2.4. Limitations of the model

Overall, the *ex-vivo* Langendorff model we utilized was shown to be suitable for the purposes of this project, and able to provide reproducible and quantitative information regarding the initial retention of donor cells after IC injection. However, there are some limitations to this model.

The model was able to assess donor cell retention in the heart in a quantitative manner, but only within the first hour of cell injection. This was because Langendorff – based crystalloid perfusion offers only several hours stable perfusion in rat hearts[269]. Although immunohistochemical analysis enabled the location of donor cells within the coronary vasculature to be determined up to 60 minutes, the longer-term fate of donor cells could not be investigated. In addition, because the experimental model's duration after cell injection was too short, it could not be determined whether different initial donor cell retention has any influence on improvements in post-transplant cardiac performance. Similarly, due to limitations in total perfusion time, donor cells needed to be injected shortly (30 minutes in my study) after reperfusion in the I-R model. Differences in donor cell retention between normal and I-R hearts might be more striking if the cells were injected into I-R hearts at later time points after reperfusion. The reasons for not generating MI *in vivo* and then assessing cell retention using the *ex-vivo* model have been described (refer to 5.2.2).

This Langendorff model provided continuous coronary flow using a crystalloid solution. In the heart *in vivo*, the coronary arteries are perfused with blood in a pulsatile fashion. It must be considered that other blood constituents could impact on donor cell retention after IC injection (please refer to 1.7.3). Furthermore, all small animal models of MI potentially suffer from the same limiting question: is an acute cardiac ischaemic episode in a previously healthy small animal without atherosclerosis comparable to an acute cardiac ischaemic event in a chronically-diseased human patient?

5.3. Mechanisms underlying initial donor cell retention after IC injection - physical entrapment and/or active adhesion

It was hypothesized that initial donor cell retention occurs as a result of passive, physical entrapment within the vasculature and/or active adhesion to the vascular endothelium *via* adhesion molecules/ligands. Therefore, the frequency, pattern and underlying mechanisms of retention of stem/progenitor cells would vary between donor cell-types, which have different cell sizes and different expression profiles of endothelial adhesion-related molecules.

To determine whether donor cells are retained *via* active retention mechanisms, the proportions of cells expressing each adhesion-related cell surface molecule were investigated in pre-injection donor BMMNC and BMMNC in the coronary effluent. If there had been a reduction in the proportion of cells expressing a particular adhesion molecule or other protein, this would have implied that cells expressing this surface marker were preferentially retained within the first few minutes of injection. In this project, the surface proteins investigated were CD11b, CD18, CD29, CD31, CD34, CD44, CD45 and CD90. Because there was no agreement between the clinical studies for which markers should be assessed, with the exception of CD34, a number of surface proteins that could hypothetically be involved in donor cell–endothelial cell interactions were examined (please refer to 1.3.2).

However, unexpectedly, there was no difference in the proportions of these donor cell surface markers between the pre-injection and coronary effluent BMMNC samples. This phenomenon was observed after injection into both normal and I-R hearts (refer to 4.4.4 and 4.5.4). This strongly suggests that donor cell surface proteins are not critical for BMMNC retention. However, it is not possible to deny the possibility that other cell surface proteins - which were not investigated here - are actively involved in BMMNC – coronary

endothelium interactions. These proteins could include PSGL-1 (which could not be examined due to the lack of available antibodies) or other unknown molecules.

Instead, an important observation was made regarding donor cell retention and donor cell size. Donor cell size had been previously been thought to be relevant for donor cell retention after IC injection but this had not been appropriately examined to date. For the quantification of retained donor cell sizes, a novel method was developed (refer to 4.4.5, 4.5.5 and 4.7.4). The confidence intervals of the findings were narrow and were replicated after injection of BMMNC into normal and I-R hearts (refer to 4.4.5 and 4.5.5 respectively) and also after MSC injection into normal hearts (refer to 4.7.4). This demonstrates that this novel technique for quantifying cell retention was reproducible.

Using this technique, for the first time, evidence has been provided that donor cell retention after IC injection is highly dependent on donor cell size. It was quantitatively demonstrated that larger BMMNC were preferentially retained after BMMNC injection into not only normal hearts but also I-R hearts (refer to 4.4.5 and 4.5.5). In addition, MSC (median passage 4 diameter 11.5 μm), much larger cells than BMMNC (median diameter 7.0 μm), showed markedly increased donor cell retention rate when IC injected into the normal hearts (80% for MSC versus 20% for BMMNC; refer to 5.7). Increased donor cell retention of MSC was associated with the observation of coronary embolism. Furthermore, within MSC, the larger MSC subpopulations were also preferentially retained with an increased frequency, although this enhanced retention appeared to plateau with cell diameters ≥ 9 μm (Figure 4-66). Only 9% of injected MSC sized 5-6 μm were retained, whereas 85% of MSC ≥ 9 μm were retained. Furthermore, the smallest MSC (5-7 μm) were retained with the same frequency as similar-sized BMMNC (Figure 4-79). These data are highly supportive of the concept that cell size is the critical factor that influences initial donor cell retention, independently of the cell type.

The diameter of coronary capillaries have been reported to be 5.6 ± 1.3 μm in dogs[270] and 5-7 μm in humans[271]. Intravital microscopy work has calculated the diameter of rat cremasteric capillaries to be 7.2 ± 0.3 μm[204]. The diameter of terminal coronary arterioles in rat perfused Langendorff hearts has been shown to be 10.4–11.4 μm[272]. These data agree with our data of donor cell retention of BMMNC and MSC. It could be speculated that most of BMMNC are mechanically entrapped in coronary capillaries whereas many MSC are retained at the level of the coronary arteriole system. This also supports the concept that it is unlikely that donor cell–coronary endothelial molecular interactions are critical for donor cell retention, as this interaction between leukocytes and coronary endothelial cells usually takes place in the post-capillary venules, rather than at the level of capillaries or arterioles.

5.4. Impact of the condition of recipient hearts on donor cell retention following IC injection

It was hypothesized that the pattern and frequency of initial donor cell retention following IC injection would be affected by the condition of recipient hearts, including the impact of prior I-R injury that will alter the expression profile of adhesion molecules on endothelial cells. The results obtained showed that after 30 minutes of ischaemia followed by 30 minutes of reperfusion, the retention efficiency of BMMNC was significantly enhanced. The retention efficiency of BMMNC in normal hearts was approximately 20% but this was improved to approximately 30% after I-R injury. These proportions were consistently observed after injection of all 3 injected cell numbers: 1×10^6, 8×10^6 and 40×10^6 (please refer to Figure 4-58). The increase in cell retention after I-R was also observed by an increase in the proportion of donor cells per cross-sectional area in hearts analysed by immunohistochemistry (see 4.3.3). Our group have previously reported donor cell retention in mouse hearts using the modified ex-vivo Langendorff model[213]. Retention efficiency after injection of a single dose of BMMNC into normal hearts was only 13.3%, but this increased to 36.5% after induction of 30 minutes ischaemia and 30 minutes of reperfusion; data generally comparable to that obtained in this study using rat hearts.

The pattern of cell loss into the coronary effluent was also different between injection into normal and I-R hearts (refer to Figures 4-56 and 4-57). Cumulative cell loss in the coronary effluent was lower from I-R hearts 2 minutes after injection (1.8% *vs.* 4.0% after injection of 8×10^6 BMMNC). This indicates that retained donor cells within the first minute after injection, could be flushed out into the coronary effluent in the subsequent few minutes and that this occurred to a greater degree in normal hearts, compared to I-R hearts. It is therefore suggested that there might be a mechanism by which I-R injury increases the

persistency of cells retained in the initial minute. This observation could be due to increased passive entrapment and/or enhanced active adhesion.

In addition, I-R injury had an effect on the retention efficiency of BMMNC populations of different diameters (Figure 4-59). When a comparison was made between the size of pre-injection cells and cells in the coronary effluent, there was a decrease in mean cell size between pre-injection (7.0 μm) and coronary effluent cells (6.85 μm) in normal hearts. This decrease was more pronounced in the donor coronary effluent cells from I-R hearts (mean cell size: 6.44 μm). BMMNC ≤7 μm were retained with the same efficiency after injection into I-R and normal hearts. However, cells ≥8 μm were retained with a greater efficiency after I-R injury (Figure 4-61). This suggests that I-R injury may induce a mechanism which prevents larger cells' release into the coronary effluent after IC injection. Following I-R injury, this mechanism could be due to changes in the physical properties of the microvasculature such as changes in vessel diameter (due to the injury itself or perivascular oedema) or alternatively due to changes of unknown molecular expression in the vasculature.

We confirmed that P-selectin was upregulated after 30 minutes ischaemia and 30 minutes reperfusion in Langendorff-perfused rat hearts, but that the expression of ICAM-1 was not detected. Expression of any of these molecules was not detected in normal hearts. Therefore, it would have been very useful in this project to investigate the role of PSGL-1 (P-selectin glycoprotein ligand) on increased BMMNC retention following I-R injury. However, unfortunately, due to unavailability of the appropriate antibody, this assessment could not be undertaken. Future work should address this, either using a different model such as a mouse model of I-R (in which a relevant antibody is available) or a rat model of I-R when an appropriate antibody becomes available.

We also tried to examine the expression of VCAM-1 in this project in normal and I-R hearts (data not shown). Previous studies would suggest that VCAM-1 would not have

been expressed after 30 minutes ischaemia, 30 minutes reperfusion (see Introduction). In an open-chest LAD ligation rat model, VCAM-1 was not detected by immunohistochemistry following ischaemia and 3 hours reperfusion, but was observed after 24 hours of reperfusion[235]. A positive control sample was generated (with the kind assistance of Dr Masahiro Kaneko) in the same way as described for the ICAM-1 positive control (refer to 3.8.2), although 24 hour reperfusion was allowed following 30 minutes ischaemia in 2 rat hearts. A very low, variable level of VCAM-1 expression was found in the positive control hearts with no expression found in the normal or I-R injury hearts (data not shown).

The effect of I-R injury to increase donor cell retention, observed in this project, may be only active shortly following reperfusion. Forest and colleagues[118] reported that retention of BMMNC in pigs was unaltered between post-MI day 7 pigs and normal pigs. This supports the concept that day 7 is too late post MI for enhanced cell retention to be observed.

These findings have important implications for clinical practice. Donor cell retention is affected by the types/conditions of not only donor cells but also by conditions of the host heart. Donor cell retention into hearts with normal coronary arteries (such as in dilated cardiomyopathy) should be considered differently from retention after injection into AMI hearts. The optimization of timing post-MI for BMMNC injection is essential to achieve the maximum benefits from BMMNC therapy.

5.5. Optimal donor cell number for IC injection

It was hypothesized that the cell number delivered would affect the frequency and pattern of the initial retention of donor cells after IC injection. It was thought that injection of a higher cell number would result in a greater retention, but administration of too many cells ran the risk of coronary embolism. It was anticipated that the result obtained would suggest the optimal donor cell number for IC injection that achieves the greatest retention without coronary embolization.

The effects of BMMNC dose on relative and absolute retention were assessed in both the normal heart and I-R heart models using injection of 1, 8 and 40×10^6 cells. These doses in rats were weight adjusted to equate to the range of doses used in clinical studies (refer to 3.6.7). The results obtained here support the original hypotheses. It was found that increasing the initial cell dose increased the absolute numbers of cells retained in the heart with a linear relationship (refer to Figure 4-30). However donor cell number injected did not affect the relative number of these retained donor cells, as a fraction of the donor cell dose injected (donor cell retention efficiency). In the normal hearts after injection of the 3 different doses, the retention efficiency of BMMNC after 5 minutes was approximately 20% and in I-R hearts, the retention efficiency was 30%. This observation that cell dose did not influence retention efficiency raised the speculation that distinct sub-populations of donor cells are critical for cell retention in normal and I-R hearts. Such sub-populations were investigated further in the project (see 5.7 below).

As regards the risk of coronary embolism, the clinically relevant range of BMMNC doses that were tested in this study were not deleterious to post-injection Langendorff parameters, suggesting that coronary embolism did not occur in this range of donor cell dose. In addition, immunohistochemical analysis using BMMNC labelled with PKH67

showed that individual cells were retained in the heart in a diffuse distribution and that no cell clumping was observed. This result is consistent to findings in previous studies. The benefits in LVEF improvement in IC BMMNC injection in clinical trials – even observed after injection of higher cell doses[25] – suggests that significant short-term myocardial damage does not occur using this approach. Bhakta and colleagues have examined this question in greater detail using a porcine model of chronic myocardial ischaemia, induced by ameroid cuff placement[273] around the circumflex artery.[274] They administered 15×10^6 BMMNC *via* IC injection and found no evidence of MI on gross inspection, histopathology or *via* Troponin-I levels. An upper 'safe' limit of BMMNC dose for IC injection was not found in our study following injection either into normal or I-R hearts, but further investigation is warranted.

The dose of stem cells used in clinical trials has varied widely but there is some evidence that increased cell dose improves outcome. Meluzin *et al.* randomized 60 patients to receive IC injection of high dose BMMNC (1×10^8 cells), lower dose BMMNC (1×10^7 cells) or placebo, 5-10 days after anterior STEMI[162]. There was an improvement in global measures of LV function assessed by SPECT at 3 months in the high dose group compared to placebo, which were maintained up to 1 year. These benefits were not seen in the lower dose group. Recently, a Cochrane meta-analysis of IC injection of BMMNC performed a heterogeneity analysis assessing the effects of cell dose[27] on LVEF assessed by MRI. In patients who received $\leq 1\times10^8$ cells, there was no improvement in LVEF. However, those who received $\leq 1\times10^9$ cells had a mean LVEF improvement of 2.6% from baseline to the end of the study (<12 months). Furthermore, a dose of $\leq 1\times10^{10}$ cells administered in 2 studies resulted in an increase in LVEF (5.7%) from baseline.

Our work provides the first evidence that increased BMMNC dose has a linear relationship with donor cell retention in the normal as well as injured hearts. Future protocols of clinical studies investigating IC injection of BMMNC should ensure that the

largest cell dose possible is used and associations should be reported between cell dose and clinical outcome.

In contrast to BMMNC, IC injection of 8×10^6 MSC had a deleterious effect on Langendorff perfusion parameters in rat. Heart rate, temperature of coronary effluent exiting the heart and coronary effluent flow rate all decreased after injection (refer to Figures 4-25, 4-26 and 4-63). Coronary effluent flow rates returned to pre-injection levels by 10 minutes post injection. Heart rate and temperature took longer to recover, but returned to pre-injection levels after approximately 40 minutes. This indicates that injection of 8×10^6 MSC resulted in transient disruption to cardiac perfusion and overall suggests injection of this number of MSC induced coronary embolism.

Assuming the weight of rats used in this project were 250g, the globally injected MSC dose was $32x10^6$ cells / kg or $10.1x10^6$ cells / body weight (kg) / artery. Vulliet and colleagues injected 5×10^5 MSC / per body weight (kg) into the left circumflex artery of 6 healthy dogs[91], (less than $1/10^{th}$ of the dose in our study). During cell administration, ECG changes consistent with MI were noted with increasing ST segment elevation with progressive cell delivery in all dogs. Gross examination with histological and immunohistochemical analysis confirmed focal areas of microinfarction. The levels of Troponin I increased in the 2 dogs in which it was measured, confirming post-injection myocardial necrosis. IC injection of $3x10^5$ MSC / body weight (kg) / artery has also been reported to result in improved LVEF and decreased infarct size (assessed by cardiac MRI) up to 8 weeks in a porcine model of AMI[275]. Again, this was a lower weight-adjusted MSC dose than was utilized in my project. However, the the largest reported clinical study to date investigating IC injection of MSC was performed by Chen and colleagues and utilized much higher doses of MSC than were used in this project[78]. Following PCI for AMI, 69 patients underwent a bone marrow biopsy and in-vitro culture of autologous MSC. Ten days later, approximately 50×10^9 MSC (or a dose of over $650x10^6$ MSC / body weight (kg) /artery in an

average human subject) were administered into the infarct artery in half the patients and the other patients received an IC injection of saline. This MSC dose is over 50 times the weight-adjusted, number-of-arteries adjusted MSC dose that I used. It was commented by the authors that there was a small rise in CK-MB in the MSC group compared to the PCI group alone, suggesting some myocardial damage post procedure. Cardiac function improved in both groups from baseline after 6 months, but this improvement in LVEF was enhanced in the MSC group. It will be important to optimise the MSC number that induces the maximum therapeutic effect with minimum risk of coronary embolism for future success of IC injection of MSC for the treatment of heart failure.

5.6. Different anatomical distributions of retained donor cells after IC injection in normal and I-R hearts.

One of the novel and interesting findings obtained in my research was that the anatomical pattern of donor cell retention (endocardium, mid myocardium and epicardium) was different between IC BMMNC injection into normal and I-R hearts (refer to Figure 4-62). Approximately 50% of retained donor BMMNC were found in the endocardium and 20% in the epicardium after IC injection into the normal heart. In contrast, in I-R hearts, these proportions were reversed and approximately 50% of cells were found in the epicardium with 20% in the endocardium. The proportion of cells in the mid myocardium was not affected. This phenomenon has not been reported in any previous animal or clinical studies.

This finding may be explained by previous studies that have shown that coronary flow is not uniform between the different layers of the ventricular wall and these areas are differentially affected by I-R injury / infarction. In normal subjects, in many species, endocardial coronary flow has been shown to exceed epicardial flow[276 277,278]. It is also known that the endocardium is the most vulnerable area of the LV to effects of

hypoperfusion and ischaemia[279] although the reasons for these transmural differences are not understood[280]. Therefore, it is likely that the endocardium was predominantly affected following 30 minutes of ischaemia and 30 minutes of reperfusion, and early damage may include impairment to microvascular flow. Therefore, coronary flow post I-R injury may be relatively enhanced *via* the epicardial vessels, resulting in increased donor cell retention in the epicardium.

5.7. Subpopulations of BMMNC are preferentially retained in the heart after IC injection

It is known that BMMNC are a heterogeneous cell population containing several distinct stem/progenitor cell populations, including EPC, MSC and haematopoietic stem cells, and non-stem cell populations. Within this mixed population, it was thought that certain subpopulations would show a greater ability to be retained in the heart. Identification of such subpopulations will be important in understanding and refining BMMNC transplantation.

Firstly as discussed above, cell size of BMMNC subpopulations was found to be a critical factor for initial donor cell retention after IC injection. The cell size distribution graphs show that there was a tendency towards a leftward shift in the donor BMMNC in coronary effluent compared to the pre-injection cells in normal hearts (Figure 4-33). That is to say that the smaller BMMNC subpopulations were more likely to be lost in the coronary effluent compared to the larger subpopulations. This effect was magnified when examining the donor coronary effluent cells from I-R hearts (Figure 4-48). After injection of BMMNC into normal hearts, cells with a diameter above the median (≥8 μm) accounted for 48.5% of all the retained cells, despite only accounting for 29.8% of the pre-injection samples. In contrast, cells with a diameter below the median (5-6 μm) accounted for 42.0% of the

pre-injection sample but only 20.1% of the cells retained in the heart (Figure 4-34). Furthermore, in I-R hearts, cells ≥8 μm accounted for 58.5% of retained cells whereas cells with a diameter 5-6 μm accounted for 9.5% of retained cells (Figure 4-49).

As described previously, it was thought that certain subpopulations of donor BMMNC expressing a specific surface protein would be preferentially retained *via* active donor cell-coronary endothelial cell interactions (refer to 5.3). However, we could not identify specific BMMNC subpopulations that were preferentially retained in the heart after IC injection according to cell surface proteins and therefore active retention involving these surface markers was not observed in normal heart or in I-R hearts. This all said, however, there were several limitations to this experiment. To fully conclude whether surface markers identify cells that are preferentially retained, an additional experiment would need to be performed whereby only cells expressing a single marker would be selected and then separately injected to quantify their retention. In addition, there may be other (unknown) molecules that distinguish the BMMNC subpopulations that are preferentially retained in the heart. PSGL-1 expression could not be examined due to the lack of suitable antibodies. Additionally, cells were only stained for single surface markers. Some reports have suggested that multiple surface markers are required to identify distinct functional populations of bone marrow stem / progenitor cells[48].

This study design does not provide any information as to whether cells with a larger diameter that are retained are otherwise functionally similar to small donor cells that are flushed out into the coronary effluent. However, it does provide an intriguing possibility for techniques to increase retention. In future work, larger selected BMMNC should be injected to quantify whether long-term engraftment is affected and whether this leads to functional benefits.

5.8. Fate of retained donor cells after IC injection

It was hypothesized that following active or passive attachment of donor cells to the coronary endothelium in the early phase of cell retention, they would subsequently undergo transendothelial migration into the myocardial interstitium or integration into the vascular walls. It was planned that the time scale and frequency of these events would be clarified.

To investigate this, this project firstly assessed BMMNC retention after IC injection using immunohistochemistry. Donor cells were typically found within the heart in isolation (refer to 4.4.7) and only very rarely were the cells found in the same vessel. Furthermore, 5 minutes after injection in normal hearts, all of the retained BMMNC observed in the heart were found within the lumen of the vessel. This finding was also observed 60 minutes after injection. This demonstrates that retained donor BMMNC remain within the coronary vasculature lumen but do not undergo transendothelial migration or extravasation out of the coronary lumen up to 60 minutes following transplantation. Ziegelhoffer et al[281] have previously demonstrated that BMMNC do not incorporate into the vessel wall.

MSC retention was assessed in the same way and it was found that retained MSC were also always localised within the lumen of the coronary vasculature, at 5 minutes and also at 60 minutes post injection. Retained MSC were typically found with a number of cells within the same field and frequently a number of MSC were seen within the same vessel as a cluster. The consequences of MSC retention observed here were similar to that reported by Toma and colleagues who utilized an intravital microscopy model to semi-quantitatively investigate patterns of MSC retention in the rat cremaster muscle microvasculature[204]. They utilized passage 10 rat MSC with a calculated mean diameter of 22 μm, which was much larger than the diameters of MSC used in this project (passage 4 cells). The authors reported that 92% of injected cells stopped and interrupted flow at the pre-capillary level. This is a similar retention efficiency seen in our study for the largest MSC. 3 days later, semi-

quantitative assessment found that only 14% of the retained cells were still present in the heart. After 1 day, the cells were found spread out on the luminal side of the basement membrane, but by 3 days after injection, they had become incorporated into the vascular wall.

Overall, extravasation from the vasculature using BMMNC and MSC did not occur within the timescale investigated. In contrast to 8×10^6 BMMNC injection into normal hearts, injection of the same number of MSC *via* the IC approach results in coronary embolism and disruption to coronary flow, although this was transient. Given that MSC remain within the intravascular space, it is not necessarily straightforward to explain why coronary flow rates (and the other Langendorff parameters) returned to normal. It is possible that coronary flow rates normalized because of shunting around the occluded coronary vasculature. Prinzmetal and colleagues injected glass spheres into the coronary arteries of post mortem human hearts and described shunts of 70 – 220 μm in diameter between the coronary arteries and both ventricular cavities, in addition to AV shunts into the coronary sinus of 70-170 μm.[282]

5.9. Future directions

There are a range of important implications of this work for future laboratory and clinical studies investigating IC stem cell administration to the heart.

This project found that a larger number of donor cells are lost from the heart within minutes of IC injection of BMMNC. The finding that approximately 80% of donor cells are lost within that time frame after injection into normal hearts and 70% of cells are lost after injection into I-R hearts means that only a small fraction of injected donor cells are able to exert their effects within the heart. There is an urgent need to develop techniques to enhance cell retention in the heart after IC injection if this approach is to enter widespread clinical use. No clinical study has measured retention or survival of stem cells in the heart as an outcome[25] but retention efficiency should be routinely quantified at least in animal studies of IC injection.

The major finding from this work - that larger cells are preferentially retained in the heart after IC injection - requires future study. The first important avenue to pursue is the comprehensive characterization of larger cell types within the unfractionated BMMNC population. These cells could be selected with mechanical filtering techniques[283].

Immunomagnetic beads may be an alternative approach to isolate larger cells from bone marrow in a closed system but specific markers to larger cells will need to be investigated. The cell surface markers of larger BMMNC should be widely investigated using a number of surface markers in addition to those chosen in this project. The surface markers utilized in this project were chosen because it was hypothesized that they might exert a ligand effect on active donor cell-endothelial cell interactions, but it remains possible that other surface marker proteins without a ligand effect could select larger cell types. In addition, this characterization would clarify to what extent these larger cells represent specific lineages

within the bone marrow (such as mesenchymal stem cells or ?granulocytes - check) and the fraction of progenitor cells (such as ?myelocytic precursors). Another feature of cells with a larger diameter that needs to be investigated is whether this population have a different cortical tension to smaller cells. This could be investigated using the bolus filtration method[204,284]. It could be hypothesized that if larger cells had a higher cortical tension, they would be less likely to deform whilst moving through the coronary circulation.

The distribution of diameters of unfractionated BMMNC was characterized in this project using a homogenous group of younger animals. It remains unknown whether this distribution is maintained in adult humans with a range of comorbidities. It could be hypothesized that the heterogeneity seen in response to cell therapy is partly to the proportion of larger autologous BMMNC administered, which itself is affected by patient related factors. The distribution of donor cell sizes therefore should be characterized in patients undergoing clinical studies; it could then be determined whether the proportion of larger cells correlates with subsequent clinical response.

Following the characterization of these cells, it should then be confirmed whether larger cells injected in isolation have a superior retention efficiency using an ex-vivo Langendorff model. Subsequent to this, larger cells should be injected in vivo and it should be determined whether this leads to enhanced clinical benefits of cell therapy. This would be best performed using larger animals, because smaller animal *in vivo* models of cell injection are mostly dependent on IM injection (which may be dependent on other retention processes). If large animal studies were shown to derive clinical benefit, then this work should be translated into human studies.

Furthermore, the longer term survival of these cells as well as potential clinical benefits of administration of only BMMNC with a larger diameter need to be clarified, in long-term cell tracking models *in vivo*.

Using the *ex-vivo* Langendorff-perfused heart model, it would be of additional interest to determine whether chemical treatments are able to influence donor cell retention after IC injection. These chemical treatments could potentially be applied either to the heart or the donor cells themselves prior to administration. One such potential molecule that could be investigated would be adenosine. It has been shown that stimulation of adenosine receptors increases EPC adhesion to endothelial cells, within minutes, with static and flow models[223]. Additionally, adenosine increased the retention of embryo-derived EPC (eEPC) after injection in a mouse Langendorff-perfused heart model. After a stabilization period, the hearts were perfused with fluorescein isothiocyanate (FITC) to stain the endothelial cells. Then cells labelled with DiI were administered, with or without adenosine perfusion. As a result, it was found that adenosine significantly increased the proportion of the vascular area occupied by eEPC. Adenosine increased the upregulation of P-selectin on endothelial cells and increased EPC-endothelium binding. This effect of adenosine *in vitro* could be partially blocked if EPC were pre-incubated with a PSGL-1 antibody.

The cell dose of MSC that was used in this project suggested that a high proportion of donor cells were retained, but with associated damage to the heart. However, only a single dose of MSC was used for investigation. It is important to investigate the effects of lower MSC doses on cell retention and perfusion parameters in the modified ex-vivo Langendorff model. It could be hypothesized that lower doses would be less likely to induce cardiac damage but with a high relative fraction of donor cell retention. This would also provide additional important mechanistic information about cell embolism. It remains unclear whether the coronary embolism of a single MSC affects the likelihood of retention of another MSC. Investigation of a number of MSC cell doses will enable important speculation about these interactions.

Another important question that requires investigation is the effect of repeated cell doses on cell retention. In the clinical setting, a number of bolus injections of lower cell

doses are frequently used rather than a single larger dose. It could be speculated that cumulative injections of lower cell doses have a beneficial effect on retention without inducing coronary embolism. The modified ex-vivo model is well suited to investigating this question and would provide further important information about the mechanisms of early cell retention.

It was demonstrated that MSC diameter increases with advancing cell passage. If MSC are going to enter widespread clinical practice, it is important to determine the optimum passage timing for cell injection. Earlier time passages may incorporate cell populations that are not purified MSC but later time passages may have a reduced differentiation potential. The modified ex-vivo model is again well suited to investigating the effects of different cell passages on early retention and would provide supporting evidence as to whether MSC retention is an entirely passive (mechanical) process, or whether it involves active donor cell-coronary endothelial cell interactions.

Stem cell therapy to the heart requires further understanding if it is to enter widespread clinical practice. This project has demonstrated that this novel ex-vivo model provides a robust and reproducible quantification and characterization of donor cells after intracoronary injection to the heart. This work has also provided important novel insights into the initial processes underpinning initial stem cell retention within the first few minutes of IC injection. It is to be hoped that this model will be utilized by other investigators who wish to embark on new IC delivery approaches to the heart, that it will lead onto further knowledge in this emerging field and enable the optimization of stem cell administration protocols in future clinical trials.

References

1. Lloyd-Jones DM, Larson MG, Leip EP, et al. Lifetime Risk for Developing Congestive Heart Failure. Circulation2002:3068-72.

2. McMurray J, McDonagh T, Morrison CE, Dargie HJ. Trends in hospitalization for heart failure in Scotland 1980-1990. European Heart Journal1993:1158-62.

3. McMurray JJV, Pfeffer MA. Heart failure. The Lancet 2005;365:1877-89.

4. Rosamond W, Flegal K, Friday G, et al. Heart Disease and Stroke Statistics--2007 Update: A Report From the American Heart Association Statistics Committee and Stroke Statistics Subcommittee. Circulation 2007;115:e69-171.

5. Frigerio M, Roubina E. Drugs for left ventricular remodeling in heart failure. Am J Cardiol 2005;96:10L-8L.

6. Flaherty JD, Davidson CJ, Faxon DP. Percutaneous coronary intervention for myocardial infarction with left ventricular dysfunction. Am J Cardiol 2008;102:38G-41G.

7. Elefteriades JA, Tolis G, Levi E, Mills LK, Zaret BL. Coronary artery bypass grafting in severe left-ventricular dysfunction - excellent survival with improved ejection fraction and function state. Journal of the American College of Cardiology 1993;22:1411-7.

8. Bristow MR, Saxon LA, Boehmer J, et al. Cardiac-Resynchronization Therapy with or without an Implantable Defibrillator in Advanced Chronic Heart Failure. N Engl J Med2004:2140-50.

9. Kadish A, Mehra M. Heart Failure Devices: Implantable Cardioverter-Defibrillators and Biventricular Pacing Therapy. Circulation 2005;111:3327-35.

10. Thiele H, Smalling RW, Schuler GC. Percutaneous left ventricular assist devices in acute myocardial infarction complicated by cardiogenic shock. European Heart Journal 2007;28:2057-63.

11. Whelan RS, Kaplinskiy V, Kitsis RN. Cell Death in the Pathogenesis of Heart Disease: Mechanisms and Significance. Annual Review of Physiology 2010;72:19-44.

12. Boilson BA, Raichlin E, Park SJ, Kushwaha SS. Device Therapy and Cardiac Transplantation for End-Stage Heart Failure. Current Problems in Cardiology 2010;35:8-64.

13. Verfaillie CM. Adult stem cells: assessing the case for pluripotency. Trends in Cell Biology 2002;12:502-8.

14. Orkin SH, Zon LI. Hematopoiesis and stem cells: plasticity versus developmental heterogeneity. Nat Immunol 2002;3:323-8.

15. Anderson DJ, Gage FH, Weissman IL. Can stem cells cross lineage boundaries? Nat Med 2001;7:393-5.

16. Mathur A, Martin JF. Stem cells and repair of the heart. The Lancet 2004;364:183-92.

17. Janssens S. Stem cells in the treatment of heart disease. Annu Rev Med 2010;61:287-300.

18. Beitnes JO, Hopp E, Lunde K, et al. Long term results after intracoronary injection of autologous mononuclear bone marrow cells in acute myocardial infarction. The ASTAMI randomized, controlled study. Heart 2009:hrt.2009.178913.

19. Schachinger V, Erbs S, Elsasser A, et al. Improved clinical outcome after intracoronary administration of bone-marrow-derived progenitor cells in acute myocardial infarction: final 1-year results of the REPAIR-AMI trial. Eur Heart J 2006;27:2775-83.

20. Huikuri HV, Kervinen K, Niemela M, et al. Effects of intracoronary injection of mononuclear bone marrow cells on left ventricular function, arrhythmia risk profile, and restenosis after thrombolytic therapy of acute myocardial infarction. Eur Heart J 2008;29:2273-737.

21. Tendera M, Wojakowski W, Ruzyllo W, et al. Intracoronary infusion of bone marrow-derived selected CD34+CXCR4+ cells and non-selected mononuclear cells in patients with acute STEMI and reduced left ventricular ejection fraction: results of

randomized, multicentre Myocardial Regeneration by Intracoronary Infusion of Selected Population of Stem Cells in Acute Myocardial Infarction (REGENT) Trial. Eur Heart J 2009;30:1313-21.

22. van der Laan A, Hirsch A, Nijveldt R, et al. Bone marrow cell therapy after acute myocardial infarction: the HEBE trial in perspective, first results. Neth Heart J 2008;16:436-9.

23. Gyongyosi M, Lang I, Dettke M, et al. Combined delivery approach of bone marrow mononuclear stem cells early and late after myocardial infarction: the MYSTAR prospective, randomized study. Nat Clin Pract Cardiovasc Med 2009;6:70-81.

24. Abdel-Latif A, Bolli R, Tleyjeh IM, et al. Adult bone marrow-derived cells for cardiac repair: a systematic review and meta-analysis. Arch Intern Med 2007;167:989-97.

25. Martin-Rendon E, Brunskill S, Doree C, et al. Stem cell treatment for acute myocardial infarction. Cochrane Database Syst Rev 2008:CD006536.

26. Lipinski MJ, Biondi-Zoccai GG, Abbate A, et al. Impact of intracoronary cell therapy on left ventricular function in the setting of acute myocardial infarction: a collaborative systematic review and meta-analysis of controlled clinical trials. J Am Coll Cardiol 2007;50:1761-7.

27. Clifford DM, Fisher SA, Brunskill SJ, et al. Stem cell treatment for acute myocardial infarction. Cochrane Database Syst Rev 2012;2:CD006536.

28. Scherschel JA, Soonpaa MH, Srour EF, Field LJ, Rubart M. Adult bone marrow-derived cells do not acquire functional attributes of cardiomyocytes when transplanted into peri-infarct myocardium. Mol Ther 2008;16:1129-37.

29. Balsam LB, Wagers AJ, Christensen JL, Kofidis T, Weissman IL, Robbins RC. Haematopoietic stem cells adopt mature haematopoietic fates in ischaemic myocardium. Nature 2004;428:668-73.

30. Murry C, Jennings R, Reimer K. Preconditioning with ischemia: a delay of lethal cell injury in ischemic myocardium. Circulation 1986;74:1124-36.

31. Gnecchi M, Zhang Z, Ni A, Dzau VJ. Paracrine Mechanisms in Adult Stem Cell Signaling and Therapy. Circ Res 2008;103:1204-19.

32. Shintani Y, Fukushima S, Varela-Carver A, et al. Donor cell-type specific paracrine effects of cell transplantation for post-infarction heart failure. Journal of Molecular and Cellular Cardiology 2009;47:288-95.

33. Tousoulis D, Briasoulis A, Antoniades C, Stefanadi E, Stefanadis C. Heart regeneration: what cells to use and how? Current Opinion in Pharmacology 2008;8:211-8.

34. Takahashi K, Yamanaka S. Induction of pluripotent stem cells from mouse embryonic and adult fibroblast cultures by defined factors. Cell 2006;126:663-76.

35. Menasché P. Skeletal Myoblasts as a Therapeutic Agent. Progress in Cardiovascular Diseases 2007;50:7-17.

36. Laflamme MA, Murry CE. Regenerating the heart. Nat Biotechnol 2005;23:845-56.

37. Gavira JJ, Abizanda G, PÃ©rez-Ilzarbe M, et al. Skeletal myoblasts for cardiac repair in animal models. European Heart Journal Supplements 2008;10:K11-K5.

38. Reinecke H, Poppa V, Murry CE. Skeletal Muscle Stem Cells Do Not Transdifferentiate Into Cardiomyocytes After Cardiac Grafting. Journal of Molecular and Cellular Cardiology 2002;34:241-9.

39. Menasché P, Hagège AA, Vilquin J-T, et al. Autologous skeletal myoblast transplantation for severe postinfarction left ventricular dysfunction. Journal of the American College of Cardiology 2003;41:1078-83.

40. Smits PC, van Geuns R-JM, Poldermans D, et al. Catheter-Based intramyocardial injection of autologous skeletal myoblasts as a primary treatment of ischemic heart failure: Clinical experience with Six-Month Follow-Up. Journal of the American College of Cardiology 2003;42:2063-9.

41. Menasche P. Stem Cell Therapy for Heart Failure: Are Arrhythmias a Real Safety Concern? Circulation 2009;119:2735-40.

42. Menasche P, Alfieri O, Janssens S, et al. The Myoblast Autologous Grafting in Ischemic Cardiomyopathy (MAGIC) trial: first randomized placebo-controlled study of myoblast transplantation. Circulation 2008;117:1189-200.

43. Wollert KC, Meyer GP, Lotz J, et al. Intracoronary autologous bone-marrow cell transfer after myocardial infarction: the BOOST randomised controlled clinical trial. Lancet 2004;364:141-8.

44. Meyer GP, Wollert KC, Lotz J, et al. Intracoronary bone marrow cell transfer after myocardial infarction: 5-year follow-up from the randomized-controlled BOOST trial. Eur Heart J 2009.

45. Janssens S, Dubois C, Bogaert J, et al. Autologous bone marrow-derived stem-cell transfer in patients with ST-segment elevation myocardial infarction: double-blind, randomised controlled trial. The Lancet 2006;367:113-21.

46. Schachinger V, Erbs S, Elsasser A, et al. Intracoronary bone marrow-derived progenitor cells in acute myocardial infarction. N Engl J Med 2006;355:1210-21.

47. van der Bogt KE, Sheikh AY, Schrepfer S, et al. Comparison of different adult stem cell types for treatment of myocardial ischemia. Circulation 2008;118:S121-9.

48. Barbosa da Fonseca LM, Gutfilen B, Rosado de Castro PH, et al. Migration and homing of bone-marrow mononuclear cells in chronic ischemic stroke after intra-arterial injection. Experimental Neurology 2010;221:122-8.

49. Solovjov DA, Pluskota E, Plow EF. Distinct Roles for the Î± and Î² Subunits in the Functions of Integrin Î±MÎ²2. Journal of Biological Chemistry 2005;280:1336-45.

50. Roebuck K, Finnegan A. Regulation of intercellular adhesion molecule-1 (CD54) gene expression. Journal of Leukocyte Biology 1999;66:876-88.

51. Mousa S. Cell Adhesion Molecules: Potential Therapeutic & Diagnostic Implications. Molecular Biotechnology 2008;38:33-40.

52. Scott LM, Priestley GV, Papayannopoulou T. Deletion of {alpha}4 Integrins from Adult Hematopoietic Cells Reveals Roles in Homeostasis, Regeneration, and Homing. Mol Cell Biol 2003;23:9349-60.

53. Kim H, Cho H-J, Kim S-W, et al. CD31+ Cells Represent Highly Angiogenic and Vasculogenic Cells in Bone Marrow. Novel Role of Nonendothelial CD31+ Cells in Neovascularization and Their Therapeutic Effects on Ischemic Vascular Disease. Circ Res 2010;107:602-14.

54. Woodfin A, Voisin MB, Nourshargh S. PECAM-1: a multi-functional molecule in inflammation and vascular biology. Arterioscler Thromb Vasc Biol 2007;27:2514-23.

55. Vasa M, Fichtlscherer S, Aicher A, et al. Number and Migratory Activity of Circulating Endothelial Progenitor Cells Inversely Correlate With Risk Factors for Coronary Artery Disease. Circ Res 2001;89:e1-7.

56. Dimitroff CJ, Lee JY, Rafii S, Fuhlbrigge RC, Sackstein R. Cd44 Is a Major E-Selectin Ligand on Human Hematopoietic Progenitor Cells. The Journal of Cell Biology 2001;153:1277-86.

57. Katayama Y, Hidalgo As, Chang J, Peired A, Frenette PS. CD44 is a physiological E-selectin ligand on neutrophils. The Journal of Experimental Medicine 2005;201:1183-9.

58. Hidalgo A, Peired AJ, Wild MK, Vestweber D, Frenette PS. Complete Identification of E-Selectin Ligands on Neutrophils Reveals Distinct Functions of PSGL-1, ESL-1, and CD44. Immunity 2007;26:477-89.

59. Yilmaz G, Vital S, Yilmaz CE, Stokes KY, Alexander JS, Granger DN. Selectin-mediated recruitment of bone marrow stromal cells in the postischemic cerebral microvasculature. Stroke 2011;42:806-11.

60. Jin S-Z, Meng X-W, Sun X, et al. Granulocyte Colony-Stimulating Factor Enhances Bone Marrow Mononuclear Cell Homing to the Liver in a Mouse Model of Acute Hepatic Injury. Digestive Diseases and Sciences 2010;55:2805-13.

61. Hermiston ML, Xu Z, Weiss A. CD45: A Critical Regulator of Signaling Thresholds in Immune Cells. Annual Review of Immunology 2003;21:107-37.

62. Sunderland CA, McMaster WR, Williams AF. Purification with monoclonal antibody of a predominant leukocyte-common antigen and glycoprotein from rat thymocytes. European Journal of Immunology 1979;9:155-9.

63. Thomas ML. The Leukocyte Common Anitgen Family. Annual Review of Immunology 1989;7:339-69.

64. Zamoyska R. Why Is There so Much CD45 on T Cells? Immunity 2007;27:421-3.

65. Holmes N. CD45: all is not yet crystal clear. Immunology 2006;117:145-55.

66. Thierfelder S. Haemopoietic stem cells of rats but not of mice express Th-1.1 alloantigen. Nature 1977;269:691-3.

67. Goldschneider I, Metcalf D, Battye F, Mandel T. Analysis of rat hemopoietic cells on the fluorescence-activated cell sorter. I. Isolation of pluripotent hemopoietic stem cells and granulocyte-macrophage progenitor cells. J Exp Med 1980;152:419-37.

68. Craig W, Kay R, Cutler RL, Lansdorp PM. Expression of Thy-1 on human hematopoietic progenitor cells. The Journal of Experimental Medicine 1993;177:1331-42.

69. Schubert K, Polte T, Bönisch U, et al. Thy-1 (CD90) regulates the extravasation of leukocytes during inflammation. European Journal of Immunology 2011;41:645-56.

70. An G, Wang H, Tang R, et al. P-Selectin Glycoprotein Ligand-1 Is Highly Expressed on Ly-6Chi Monocytes and a Major Determinant for Ly-6Chi Monocyte Recruitment to Sites of Atherosclerosis in Mice. Circulation 2008;117:3227-37.

71. Wang H, Zhang W, Tang R, et al. Core2 1-6-N-Glucosaminyltransferase-I Deficiency Protects Injured Arteries From Neointima Formation in ApoE-Deficient Mice. Arterioscler Thromb Vasc Biol 2009;29:1053-9.

72. Pittenger MF, Martin BJ. Mesenchymal Stem Cells and Their Potential as Cardiac Therapeutics. Circ Res 2004;95:9-20.

73. Rochefort GY, Delorme B, Lopez A, et al. Multipotential mesenchymal stem cells are mobilized into peripheral blood by hypoxia. Stem Cells 2006;24:2202-8.

74. Toma C, Pittenger MF, Cahill KS, Byrne BJ, Kessler PD. Human Mesenchymal Stem Cells Differentiate to a Cardiomyocyte Phenotype in the Adult Murine Heart. Circulation 2002;105:93-8.

75. Oswald J, Boxberger S, Jørgensen B, et al. Mesenchymal Stem Cells Can Be Differentiated Into Endothelial Cells In Vitro. Stem Cells 2004;22:377-84.

76. Dominici M, Le Blanc K, Mueller I, et al. Minimal criteria for defining multipotent mesenchymal stromal cells. The International Society for Cellular Therapy position statement. Cytotherapy 2006;8:315-7.

77. Nguyen BK, Maltais S, Perrault LP, et al. Improved Function and Myocardial Repair of Infarcted Heart by Intracoronary Injection of Mesenchymal Stem Cell-Derived Growth Factors. J Cardiovasc Transl Res 2010.

78. Chen S-l, Fang W-w, Ye F, et al. Effect on left ventricular function of intracoronary transplantation of autologous bone marrow mesenchymal stem cell in patients with acute myocardial infarction. The American Journal of Cardiology 2004;94:92-5.

79. Katritsis DG, Sotiropoulou PA, Karvouni E, et al. Transcoronary transplantation of autologous mesenchymal stem cells and endothelial progenitors into infarcted human myocardium. Catheterization and Cardiovascular Interventions 2005;65:321-9.

80. National Library of Medicine (NLM) at the National Institutes of Health. http://www.clinicaltrials.gov. [Accessed October 2012].

81. Tse WT, Pendleton JD, Beyer WM, Egalka MC, Guinan EC. Suppression of allogeneic T-cell proliferation by human marrow stromal cells: implications in transplantation. Transplantation 2003;75:389-97.

82. Chiu RC-J. MSC Immune Tolerance in Cellular Cardiomyoplasty. Seminars in Thoracic and Cardiovascular Surgery 2008;20:115-8.

83. Wang D, Zhang H, Cao M, et al. Efficacy of allogeneic mesenchymal stem cell transplantation in patients with drug-resistant polymyositis and dermatomyositis. Annals of the rheumatic diseases 2011;70:1285-8.

84. Liang J, Zhang H, Wang D, et al. Allogeneic mesenchymal stem cell transplantation in seven patients with refractory inflammatory bowel disease. Gut 2011.

85. Bonab M, Alimoghaddam K, Talebian F, Ghaffari S, Ghavamzadeh A, Nikbin B. Aging of mesenchymal stem cell in vitro. BMC Cell Biology 2006;7:14.

86. Aguilar S, Nye E, Chan J, et al. Murine but Not Human Mesenchymal Stem Cells Generate Osteosarcoma-Like Lesions in the Lung. Stem Cells 2007;25:1586-94.

87. Tolar J, Nauta AJ, Osborn MJ, et al. Sarcoma Derived from Cultured Mesenchymal Stem Cells. Stem Cells 2007;25:371-9.

88. Breitbach M, Bostani T, Roell W, et al. Potential risks of bone marrow cell transplantation into infarcted hearts. Blood 2007;110:1362-9.

89. Freyman T, Polin G, Osman H, et al. A quantitative, randomized study evaluating three methods of mesenchymal stem cell delivery following myocardial infarction. Eur Heart J 2006;27:1114-22.

90. Ly HQ, Hoshino K, Pomerantseva I, et al. In vivo myocardial distribution of multipotent progenitor cells following intracoronary delivery in a swine model of myocardial infarction. European Heart Journal 2009;30:2861-8.

91. Vulliet PR, Greeley M, Halloran SM, MacDonald KA, Kittleson MD. Intra-coronary arterial injection of mesenchymal stromal cells and microinfarction in dogs. Lancet 2004;363:783-4.

92. Steinmetz M, Nickenig G, Werner N. Endothelial-Regenerating Cells: An Expanding Universe. Hypertension 2010;55:593-9.

93. Caprioli A, Jaffredo T, Gautier R, Dubourg Cc, Dieterlen-LiÃ¨vre Fo. Blood-borne seeding by hematopoietic and endothelial precursors from the allantois. Proceedings of the National Academy of Sciences of the United States of America 1998;95:1641-6.

94. Choi K, Kennedy M, Kazarov A, Papadimitriou JC, Keller G. A common precursor for hematopoietic and endothelial cells. Development 1998;125:725-32.

95. Asahara T, Murohara T, Sullivan A, et al. Isolation of Putative Progenitor Endothelial Cells for Angiogenesis. Science 1997;275:964-6.

96. Shi Q, Rafii S, Wu MH-D, et al. Evidence for Circulating Bone Marrow-Derived Endothelial Cells. Blood 1998;92:362-7.

97. Padfield GJ, Newby DE, Mills NL. Understanding the Role of Endothelial Progenitor Cells in Percutaneous Coronary Intervention. Journal of the American College of Cardiology 2010;55:1553-65.

98. Mills NL, Tura O, Padfield GJ, et al. Dissociation of phenotypic and functional endothelial progenitor cells in patients undergoing percutaneous coronary intervention. Heart 2009;95:2003-8.

99. Prokopi M, Pula G, Mayr U, et al. Proteomic analysis reveals presence of platelet microparticles in endothelial progenitor cell cultures. Blood 2009;114:723-32.

100. Bartunek J, Vanderheyden M, Vandekerckhove B, et al. Intracoronary injection of CD133-positive enriched bone marrow progenitor cells promotes cardiac recovery after recent myocardial infarction: feasibility and safety. Circulation 2005;112:I178-83.

101. Mansour S, Vanderheyden M, De Bruyne B, et al. Intracoronary delivery of hematopoietic bone marrow stem cells and luminal loss of the infarct-related artery in patients with recent myocardial infarction. J Am Coll Cardiol 2006;47:1727-30.

102. Manginas A, Goussetis E, Koutelou M, et al. Pilot study to evaluate the safety and feasibility of intracoronary CD133(+) and CD133(-) CD34(+) cell therapy in patients with nonviable anterior myocardial infarction. Catheter Cardiovasc Interv 2007;69:773-81.

103. Yerebakan C, Kaminski A, Westphal B, et al. Impact of preoperative left ventricular function and time from infarction on the long-term benefits after intramyocardial CD133+ bone marrow stem cell transplant. The Journal of thoracic and cardiovascular surgery 2011;142:1530-9.e3.

104. Beltrami AP, Barlucchi L, Torella D, et al. Adult cardiac stem cells are multipotent and support myocardial regeneration. Cell 2003;114:763-76.

105. Messina E, De Angelis L, Frati G, et al. Isolation and Expansion of Adult Cardiac Stem Cells From Human and Murine Heart. Circ Res 2004;95:911-21.

106. Oh H, Bradfute SB, Gallardo TD, et al. Cardiac progenitor cells from adult myocardium: Homing, differentiation, and fusion after infarction. Proceedings of the National Academy of Sciences of the United States of America 2003;100:12313-8.

107. Matsuura K, Honda A, Nagai T, et al. Transplantation of cardiac progenitor cells ameliorates cardiac dysfunction after myocardial infarction in mice. The Journal of Clinical Investigation 2009;119:2204-17.

108. Tang X-L, Rokosh G, Sanganalmath SK, et al. Intracoronary Administration of Cardiac Progenitor Cells Alleviates Left Ventricular Dysfunction in Rats With a 30-Day-Old Infarction. Circulation 2010;121:293-305.

109. Bolli R, Chugh AR, D'Amario D, et al. Cardiac stem cells in patients with ischaemic cardiomyopathy (SCIPIO): initial results of a randomised phase 1 trial. The Lancet 2011;378:1847-57.

110. Makkar RR, Smith RR, Cheng K, et al. Intracoronary cardiosphere-derived cells for heart regeneration after myocardial infarction (CADUCEUS): a prospective, randomised phase 1 trial. The Lancet 2012;379:895-904.

111. Joggerst SJ, Hatzopoulos AK. Stem cell therapy for cardiac repair: benefits and barriers. Expert Reviews in Molecular Medicine 2009;11:e20.

112. Reinecke H, Minami E, Zhu WZ, Laflamme MA. Cardiogenic differentiation and transdifferentiation of progenitor cells. Circ Res 2008;103:1058-71.

113. Campbell NG, Suzuki K. Cell Delivery Routes for Stem Cell Therapy to the Heart: Current and Future Approaches. J Cardiovasc Transl Res 2012;Epub ahead of print.

114. Williams LR, Leggett RW. Reference values for resting blood flow to organs of man. Clinical Physics and Physiological Measurement 1989;10:187.

115. Hofmann M, Wollert KC, Meyer GP, et al. Monitoring of bone marrow cell homing into the infarcted human myocardium. Circulation 2005;111:2198-202.

116. Aicher A, Brenner W, Zuhayra M, et al. Assessment of the tissue distribution of transplanted human endothelial progenitor cells by radioactive labeling. Circulation 2003;107:2134-9.

117. Hou D, Youssef EA, Brinton TJ, et al. Radiolabeled cell distribution after intramyocardial, intracoronary, and interstitial retrograde coronary venous delivery: implications for current clinical trials. Circulation 2005;112:I150-6.

118. Forest VF, Tirouvanziam AM, Perigaud C, et al. Cell distribution after intracoronary bone marrow stem cell delivery in damaged and undamaged myocardium: implications for clinical trials. Stem Cell Res Ther 2010;1:4.

119. Brenner W, Aicher A, Eckey T, et al. 111In-labeled CD34+ hematopoietic progenitor cells in a rat myocardial infarction model. J Nucl Med 2004;45:512-8.

120. Kang WJ, Kang HJ, Kim HS, Chung JK, Lee MC, Lee DS. Tissue distribution of 18F-FDG-labeled peripheral hematopoietic stem cells after intracoronary administration in patients with myocardial infarction. J Nucl Med 2006;47:1295-301.

121. Hare JM, Traverse JH, Henry TD, et al. A Randomized, Double-Blind, Placebo-Controlled, Dose-Escalation Study of Intravenous Adult Human Mesenchymal Stem Cells (Prochymal) After Acute Myocardial Infarction. Journal of the American College of Cardiology 2009;54:2277-86.

122. Nagaya N, Fujii T, Iwase T, et al. Intravenous administration of mesenchymal stem cells improves cardiac function in rats with acute myocardial infarction through angiogenesis and myogenesis. Am J Physiol Heart Circ Physiol 2004;287:H2670-6.

123. Kraitchman DL, Tatsumi M, Gilson WD, et al. Dynamic imaging of allogeneic mesenchymal stem cells trafficking to myocardial infarction. Circulation 2005;112:1451-61.

124. George JC, Goldberg J, Joseph M, et al. Transvenous intramyocardial cellular delivery increases retention in comparison to intracoronary delivery in a porcine model of acute myocardial infarction. J Interv Cardiol 2008;21:424-31.

125. Perin EC, Silva GV, Assad JAR, et al. Comparison of intracoronary and transendocardial delivery of allogeneic mesenchymal cells in a canine model of acute myocardial infarction. Journal of Molecular and Cellular Cardiology 2008;44:486-95.

126. Nyolczas N, Gyöngyösi M, Beran G, et al. Design and rationale for the Myocardial Stem Cell Administration After Acute Myocardial Infarction (MYSTAR) Study: A multicenter, prospective, randomized, single-blind trial comparing early and late intracoronary or combined (percutaneous intramyocardial and intracoronary) administration of nonselected autologous bone marrow cells to patients after acute myocardial infarction. American Heart Journal 2007;153:212.e1-.e7.

127. Suzuki K, Murtuza B, Beauchamp JR, et al. Role of interleukin-1beta in acute inflammation and graft death after cell transplantation to the heart. Circulation 2004;110:II219-24.

128. Fukushima S, Varela-Carver A, Coppen SR, et al. Direct intramyocardial but not intracoronary injection of bone marrow cells induces ventricular arrhythmias in a rat chronic ischemic heart failure model. Circulation 2007;115:2254-61.

129. Donndorf P, Kundt G, Kaminski A, et al. Intramyocardial bone marrow stem cell transplantation during coronary artery bypass surgery: A meta-analysis. The Journal of thoracic and cardiovascular surgery 2011;142:911-20.

130. Zhao Q, Sun Y, Xia L, Chen A, Wang Z. Randomized Study of Mononuclear Bone Marrow Cell Transplantation in Patients With Coronary Surgery. The Annals of Thoracic Surgery 2008;86:1833-40.

131. Dib N, Michler RE, Pagani FD, et al. Safety and Feasibility of Autologous Myoblast Transplantation in Patients With Ischemic Cardiomyopathy. Circulation 2005;112:1748-55.

132. Fukushima S, Coppen SR, Lee J, et al. Choice of Cell-Delivery Route for Skeletal Myoblast Transplantation for Treating Post-Infarction Chronic Heart Failure in Rat. PLoS ONE 2008;3:e3071.

133. Brasselet C, Morichetti MC, Messas E, et al. Skeletal myoblast transplantation through a catheter-based coronary sinus approach: an effective means of improving function of infarcted myocardium. European Heart Journal 2005;26:1551-6.

134. Thompson CA, Nasseri BA, Makower J, et al. Percutaneous transvenous cellular cardiomyoplasty - A novel nonsurgical approach for myocardial cell transplantation. Journal of the American College of Cardiology 2003;41:1964-71.

135. Ikeno F, Lyons J, Kaneda H, Baluom M, Benet LZ, Rezaee M. Novel percutaneous adventitial drug delivery system for regional vascular treatment. Catheter Cardiovasc Interv 2004;63:222-30.

136. Penn MS, Ellis S, Gandhi S, et al. Adventitial delivery of an allogeneic bone marrow-derived adherent stem cell in acute myocardial infarction: phase I clinical study. Circ Res 2012;110:304-11.

137. Medicetty S, Wiktor D, Lehman N, et al. Percutaneous Adventitial Delivery of Allogeneic Bone Marrow Derived Stem Cells Via Infarct Related Artery Improves Long-term Ventricular Function in Acute Myocardial Infarction. Cell Transplant 2011:Epub ahead of print. First published: 14 Oct 2011.

138. Hristov M, Weber C. The therapeutic potential of progenitor cells in ischemic heart disease. Basic Research in Cardiology 2006;101:1-7.

139. Suzuki K, Brand NJ, Smolenski RT, Jayakumar J, Murtuza B, Yacoub MH. Development of a novel method for cell transplantation through the coronary artery. Circulation 2000;102:III359-64.

140. Strauer BE, Brehm M, Zeus T, et al. [Intracoronary, human autologous stem cell transplantation for myocardial regeneration following myocardial infarction]. Dtsch Med Wochenschr 2001;126:932-8.

141. Tuma J, Fernanadez-Vina R, Carrasco A, et al. Safety and Feasibility of Percutaneous Retrograde Coronary Sinus Delivery of Autologous Bone Marrow Mononuclear Cell Transplantation in Patients with Chronic Refractory Angina. J Transl Med 2011;9:183.

142. Chiu LL, Iyer RK, Reis LA, Nunes SS, Radisic M. Cardiac tissue engineering: current state and perspectives. Frontiers in bioscience : a journal and virtual library 2012;17:1533-50.

143. Elloumi-Hannachi I, Yamato M, Okano T. Cell sheet engineering: a unique nanotechnology for scaffold-free tissue reconstruction with clinical applications in regenerative medicine. Journal of Internal Medicine 2010;267:54-70.

144. Miyagawa S, Saito A, Sakaguchi T, et al. Impaired Myocardium Regeneration With Skeletal Cell Sheets-A Preclinical Trial for Tissue-Engineered Regeneration Therapy. Transplantation 2010;90:364-72 doi:10.1097/TP.0b013e3181e6f201.

145. Konstam MA, Kronenberg MW, Rousseau MF, et al. Effects of the angiotensin converting enzyme inhibitor enalapril on the long-term progression of left ventricular dilatation in patients with asymptomatic systolic dysfunction. SOLVD (Studies of Left Ventricular Dysfunction) Investigators. Circulation 1993;88:2277-83.

146. Assmus B, Rolf A, Erbs S, et al. Clinical Outcome 2 Years After Intracoronary Administration of Bone Marrow-Derived Progenitor Cells in Acute Myocardial Infarction. Circ Heart Fail 2010;3:89-96.

147. Seth S, Bhargava B, Narang R, et al. The ABCD (Autologous Bone Marrow Cells in Dilated Cardiomyopathy) Trial: A Long-Term Follow-Up Study. Journal of the American College of Cardiology 2010;55:1643-4.

148. Jaiswal RK, Jaiswal N, Bruder SP, Mbalaviele G, Marshak DR, Pittenger MF. Adult Human Mesenchymal Stem Cell Differentiation to the Osteogenic or Adipogenic Lineage Is Regulated by Mitogen-activated Protein Kinase. Journal of Biological Chemistry 2000;275:9645-52.

149. Strauer BE, Brehm M, Zeus T, et al. Repair of infarcted myocardium by autologous intracoronary mononuclear bone marrow cell transplantation in humans. Circulation 2002;106:1913-8.

150. Schachinger V, Assmus B, Britten MB, et al. Transplantation of progenitor cells and regeneration enhancement in acute myocardial infarction: final one-year results of the TOPCARE-AMI Trial. J Am Coll Cardiol 2004;44:1690-9.

151. Ruan W, Pan CZ, Huang GQ, Li YL, Ge JB, Shu XH. Assessment of left ventricular segmental function after autologous bone marrow stem cells transplantation in patients with acute myocardial infarction by tissue tracking and strain imaging. Chin Med J (Engl) 2005;118:1175-81.

152. Strauer BE, Brehm M, Zeus T, et al. Regeneration of human infarcted heart muscle by intracoronary autologous bone marrow cell transplantation in chronic coronary artery disease: the IACT Study. J Am Coll Cardiol 2005;46:1651-8.

153. Ge J, Li Y, Qian J, et al. Efficacy of emergent transcatheter transplantation of stem cells for treatment of acute myocardial infarction (TCT-STAMI). Heart2006:1764-7.

154. Lunde K, Solheim S, Aakhus S, et al. Intracoronary injection of mononuclear bone marrow cells in acute myocardial infarction. N Engl J Med 2006;355:1199-209.

155. Assmus B, Honold J, Schachinger V, et al. Transcoronary Transplantation of Progenitor Cells after Myocardial Infarction. N Engl J Med 2006;355:1222-32.

156. Kang H-J, Lee H-Y, Na S-H, et al. Differential Effect of Intracoronary Infusion of Mobilized Peripheral Blood Stem Cells by Granulocyte Colony-Stimulating Factor on Left Ventricular Function and Remodeling in Patients With Acute Myocardial Infarction Versus Old Myocardial Infarction: The MAGIC Cell-3-DES Randomized, Controlled Trial. Circulation 2006;114:I-145-51.

157. Penicka M, Horak J, Kobylka P, et al. Intracoronary injection of autologous bone marrow-derived mononuclear cells in patients with large anterior acute myocardial infarction: a prematurely terminated randomized study. J Am Coll Cardiol 2007;49:2373-4.

158. Li ZQ, Zhang M, Jing YZ, et al. The clinical study of autologous peripheral blood stem cell transplantation by intracoronary infusion in patients with acute myocardial infarction (AMI). Int J Cardiol 2007;115:52-6.

159. Tatsumi T, Ashihara E, Yasui T, et al. Intracoronary Transplantation of Non-Expanded Peripheral Blood-Derived Mononuclear Cells Promotes Improvement of Cardiac Function in Patients With Acute Myocardial Infarction. Circulation Journal 2007;71:1199-207.

160. Suarez de Lezo J, Herrera C, Pan M, et al. [Regenerative therapy in patients with a revascularized acute anterior myocardial infarction and depressed ventricular function]. Rev Esp Cardiol 2007;60:357-65.

161. Ang K-L, Chin D, Leyva F, et al. Randomized, controlled trial of intramuscular or intracoronary injection of autologous bone marrow cells into scarred myocardium during CABG versus CABG alone. Nat Clin Pract Cardiovasc Med 2008;5:663-70.

162. Meluzin J, Janousek S, Mayer J, et al. Three-, 6-, and 12-month results of autologous transplantation of mononuclear bone marrow cells in patients with acute myocardial infarction. Int J Cardiol 2008;128:185-92.

163. Plewka M, Krzeminska-Pakula M, Peruga JZ, et al. The effects of intracoronary delivery of mononuclear bone marrow cells in patients with myocardial infarction: a two year follow-up results. Kardiol Pol 2009;69:1234-40.

164. Cao F, Sun D, Li C, et al. Long-term myocardial functional improvement after autologous bone marrow mononuclear cells transplantation in patients with ST-segment elevation myocardial infarction: 4 years follow-up. Eur Heart J 2009;30:1986-94.

165. Yao K, Huang R, Sun A, et al. Repeated autologous bone marrow mononuclear cell therapy in patients with large myocardial infarction. Eur J Heart Fail 2009;11:691-8.

166. Yousef M, Schannwell CM, Kostering M, Zeus T, Brehm M, Strauer BE. The BALANCE Study: clinical benefit and long-term outcome after intracoronary autologous

bone marrow cell transplantation in patients with acute myocardial infarction. J Am Coll Cardiol 2009;53:2262-9.

167. Grajek S, Popiel M, Gil L, et al. Influence of bone marrow stem cells on left ventricle perfusion and ejection fraction in patients with acute myocardial infarction of anterior wall: randomized clinical trial: Impact of bone marrow stem cell intracoronary infusion on improvement of microcirculation. Eur Heart J 2010;31:691-702.

168. Strauer B-E, Yousef M, Schannwell CM. The acute and long-term effects of intracoronary Stem cell Transplantation in 191 patients with chronic heARt failure: the STAR-heart study. Eur J Heart Fail 2010;12:721-9.

169. Piepoli MF, Vallisa D, Arbasi M, et al. Bone marrow cell transplantation improves cardiac, autonomic, and functional indexes in acute anterior myocardial infarction patients (Cardiac Study). Eur J Heart Fail 2010;12:172-80.

170. Wohrle J, Merkle N, Mailander V, et al. Results of intracoronary stem cell therapy after acute myocardial infarction. Am J Cardiol 2010;105:804-12.

171. Hirsch A, Nijveldt R, van der Vleuten PA, et al. Intracoronary infusion of mononuclear cells from bone marrow or peripheral blood compared with standard therapy in patients after acute myocardial infarction treated by primary percutaneous coronary intervention: results of the randomized controlled HEBE trial. European Heart Journal 2011;32:1736-47.

172. Roncalli J, Mouquet F, Piot C, et al. Intracoronary autologous mononucleated bone marrow cell infusion for acute myocardial infarction: results of the randomized multicenter BONAMI trial. European Heart Journal 2011;32:1748-57.

173. Traverse JH, Henry TD, Ellis SG, et al. Effect of Intracoronary Delivery of Autologous Bone Marrow Mononuclear Cells 2 to 3 Weeks Following Acute Myocardial Infarction on Left Ventricular Function. JAMA: The Journal of the American Medical Association 2011;306:2110-19.

174. Quyyumi AA, Waller EK, Murrow J, et al. CD34+ cell infusion after ST elevation myocardial infarction is associated with improved perfusion and is dose dependent. American Heart Journal 2011;161:98-105.

175. Goussetis E, Manginas A, Koutelou M, et al. Intracoronary Infusion of CD133 Selected Autologous Bone Marrow Progenitor Cells in Patients with Chronic Ischemic Cardiomyopathy: Cell Isolation, Adherence to the Infarcted Area, and Body Distribution. Stem Cells 2006;24:2279-83.

176. Kurpisz M, Czepczynski R, Grygielska B, et al. Bone marrow stem cell imaging after intracoronary administration. International Journal of Cardiology 2007;121:194-5.

177. Schachinger V, Aicher A, Dobert N, et al. Pilot Trial on Determinants of Progenitor Cell Recruitment to the Infarcted Human Myocardium. Circulation 2008;118:1425-32.

178. Penicka M, Lang O, Widimsky P, et al. One-day kinetics of myocardial engraftment after intracoronary injection of bone marrow mononuclear cells in patients with acute and chronic myocardial infarction. Heart 2007;93:837-41.

179. Schots R, De Keulenaer G, Schoors D, et al. Evidence that intracoronary-injected CD133+ peripheral blood progenitor cells home to the myocardium in chronic postinfarction heart failure. Experimental Hematology 2007;35:1884-90.

180. Blocklet D, Toungouz M, Berkenboom G, et al. Myocardial homing of nonmobilized peripheral-blood CD34+ cells after intracoronary injection. Stem Cells 2006;24:333-6.

181. Penicka M, Widimsky P, Kobylka P, Kozak T, Lang O. Early Tissue Distribution of Bone Marrow Mononuclear Cells After Transcoronary Transplantation in a Patient With Acute Myocardial Infarction. Circulation 2005;112:e63-5.

182. Doyle B, Kemp BJ, Chareonthaitawee P, et al. Dynamic Tracking During Intracoronary Injection of 18F-FDG-Labeled Progenitor Cell Therapy for Acute Myocardial Infarction. J Nucl Med 2007;48:1708-14.

183. Tossios P, Krausgrill B, Schmidt M, et al. Role of balloon occlusion for mononuclear bone marrow cell deposition after intracoronary injection in pigs with reperfused myocardial infarction. Eur Heart J 2008;29:1911-21.

184. Terrovitis JV, Smith RR, Marban E. Assessment and optimization of cell engraftment after transplantation into the heart. Circ Res 2010;106:479-94.

185. Fedak PWM, Szmitko PE, Weisel RD, et al. Cell transplantation preserves matrix homeostasis: A novel paracrine mechanism. J Thorac Cardiovasc Surg 2005;130:1430-9.

186. Qian C, Tio RA, Roks AJM, et al. A promising technique for transplantation of bone marrow-derived endothelial progenitor cells into rat heart. Cardiovascular Pathology 2007;16:127-35.

187. Meluzin J, Vlasin M, Groch L, et al. Intracoronary Delivery of Bone Marrow Cells to the Acutely Infarcted Myocardium. Optimization of the Delivery Technique. Cardiology 2008;112:98-106.

188. Rosen AB, Kelly DJ, Schuldt AJ, et al. Finding fluorescent needles in the cardiac haystack: tracking human mesenchymal stem cells labeled with quantum dots for quantitative in vivo three-dimensional fluorescence analysis. Stem Cells 2007;25:2128-38.

189. Suzuki K, Murtuza B, Beauchamp JR, et al. Dynamics and mediators of acute graft attrition after myoblast transplantation to the heart. FASEB J 2004:03-1308fje.

190. Robey TE, Saiget MK, Reinecke H, Murry CE. Systems approaches to preventing transplanted cell death in cardiac repair. Journal of Molecular and Cellular Cardiology 2008;45:567-81.

191. Blackwood KJ, Lewden B, Wells RG, et al. In Vivo SPECT Quantification of Transplanted Cell Survival After Engraftment Using 111In-Tropolone in Infarcted Canine Myocardium. Journal of Nuclear Medicine2009:927-35.

192. Nowak B, Weber C, Schober A, et al. Indium-111 oxine labelling affects the cellular integrity of haematopoietic progenitor cells. European Journal of Nuclear Medicine and Molecular Imaging 2007;34:715-21.

193. Barbash IM, Chouraqui P, Baron J, et al. Systemic delivery of bone marrow-derived mesenchymal stem cells to the infarcted myocardium: feasibility, cell migration, and body distribution. Circulation 2003;108:863-8.

194. Adonai N, Nguyen KN, Walsh J, et al. Ex vivo cell labeling with 64Cu-pyruvaldehyde-bis(N4-methylthiosemicarbazone) for imaging cell trafficking in mice with positron-emission tomography. Proc Natl Acad Sci USA2002:3030-5.

195. Balaban EP, Simon TR, Frenkel EP. Toxicity of indium-111 on the radiolabeled lymphocyte. J Nucl Med 1987;28:229-33.

196. Wu JC, Chen IY, Sundaresan G, et al. Molecular Imaging of Cardiac Cell Transplantation in Living Animals Using Optical Bioluminescence and Positron Emission Tomography. Circulation2003:1302-5.

197. Arbab AS, Bashaw LA, Miller BR, et al. Characterization of biophysical and metabolic properties of cells labeled with superparamagnetic iron oxide nanoparticles and transfection agent for cellular MR imaging. Radiology 2003;229:838-46.

198. Arbab AS, Yocum GT, Rad AM, et al. Labeling of cells with ferumoxides-protamine sulfate complexes does not inhibit function or differentiation capacity of hematopoietic or mesenchymal stem cells. NMR in biomedicine 2005;18:553-9.

199. Amsalem Y, Mardor Y, Feinberg MS, et al. Iron-oxide labeling and outcome of transplanted mesenchymal stem cells in the infarcted myocardium. Circulation 2007;116:I38-45.

200. Terrovitis J, Stuber M, Youssef A, et al. Magnetic resonance imaging overestimates ferumoxide-labeled stem cell survival after transplantation in the heart. Circulation 2008;117:1555-62.

201. Chen IY, Greve JM, Gheysens O, et al. Comparison of optical bioluminescence reporter gene and superparamagnetic iron oxide MR contrast agent as cell markers for noninvasive imaging of cardiac cell transplantation. Mol Imaging Biol 2009;11:178-87.

202. Woodfin A, Voisin MB, Imhof BA, Dejana E, Engelhardt B, Nourshargh S. Endothelial cell activation leads to neutrophil transmigration as supported by the sequential roles of ICAM-2, JAM-A, and PECAM-1. Blood 2009;113:6246-57.

203. Woodfin A, Voisin M-B, Nourshargh S. Recent developments and complexities in neutrophil transmigration. Current Opinion in Hematology 2010;17:9-17.

204. Toma C, Wagner WR, Bowry S, Schwartz A, Villanueva F. Fate Of Culture-Expanded Mesenchymal Stem Cells in The Microvasculature: In Vivo Observations of Cell Kinetics. Circ Res 2009;104:398-402.

205. Scheiermann C, Colom B, Meda P, et al. Junctional adhesion molecule-C mediates leukocyte infiltration in response to ischemia reperfusion injury. Arterioscler Thromb Vasc Biol 2009;29:1509-15.

206. van der Bogt KEA, Schrepfer S, Yu J, et al. Comparison of Transplantation of Adipose Tissue- and Bone Marrow-Derived Mesenchymal Stem Cells in the Infarcted Heart. Transplantation 2009;87:642-52.

207. Gheysens O, Lin S, Cao F, et al. Noninvasive evaluation of immunosuppressive drug efficacy on acute donor cell survival. Mol Imaging Biol 2006;8:163-70.

208. Li SH, Lai TY, Sun Z, et al. Tracking cardiac engraftment and distribution of implanted bone marrow cells: Comparing intra-aortic, intravenous, and intramyocardial delivery. J Thorac Cardiovasc Surg 2009;137:1225-33 e1.

209. Langendorff O. Untersuchungen am überlebenden Säugetierherzen. Pflügers Archiv 1898;61:291-332.

210. Skrzypiec-Spring M, Grotthus B, Szelag A, Schulz R. Isolated heart perfusion according to Langendorff---still viable in the new millennium. J Pharmacol Toxicol Methods 2007;55:113-26.

211. Bailey LE, Ong SD. Krebs-Henseleit solution as a physiological buffer in perfused and superfused preparations. Journal of Pharmacological Methods 1978;1:171-5.

212. Schenkman KA, Beard DA, Ciesielski WA, Feigl EO. Comparison of buffer and red blood cell perfusion of guinea pig heart oxygenation. Am J Physiol Heart Circ Physiol 2003;285:H1819-25.

213. Fukushima S, Campbell NG, Coppen SR, et al. Quantitative assessment of initial retention of bone marrow mononuclear cells injected into the coronary arteries. Journal of Heart and Lung Transplantation 2011;30:227-33.

214. Sutherland FJ, Shattock MJ, Baker KE, Hearse DJ. Mouse isolated perfused heart: characteristics and cautions. Clin Exp Pharmacol Physiol 2003;30:867-78.

215. Reichelt ME, Willems L, Hack BA, Peart JN, Headrick JP. Cardiac and coronary function in the Langendorff-perfused mouse heart model. Exp Physiol 2009;94:54-70.

216. Headrick JP, Peart J, Hack B, Flood A, Matherne GP. Functional properties and responses to ischaemia-reperfusion in Langendorff perfused mouse heart. Exp Physiol 2001;86:703-16.

217. Farago N, Kocsis GF, Feher LZ, et al. Gene and protein expression changes in response to normoxic perfusion in mouse hearts. J Pharmacol Toxicol Methods 2008;57:145-54.

218. Duda M, Czarnowska E, Kurzelewski M, Konior A, Beresewicz A. Ischemic preconditioning prevents endothelial dysfunction, P-selectin expression, and neutrophil adhesion by preventing endothelin and O2- generation in the post-ischemic guinea-pig heart. J Physiol Pharmacol 2006;57:553-69.

219. Jung U, Norman KE, Scharffetter-Kochanek K, Beaudet AL, Ley K. Transit time of leukocytes rolling through venules controls cytokine-induced inflammatory cell recruitment in vivo. The Journal of Clinical Investigation 1998;102:1526-33.

220. Dunne JL, Ballantyne CM, Beaudet AL, Ley K. Control of leukocyte rolling velocity in TNF-alpha -induced inflammation by LFA-1 and Mac-1. Blood 2002;99:336-41.

221. Oh I-Y, Yoon C-H, Hur J, et al. Involvement of E-selectin in recruitment of endothelial progenitor cells and angiogenesis in ischemic muscle. Blood 2007;110:3891-9.

222. Vajkoczy P, Blum S, Lamparter M, et al. Multistep Nature of Microvascular Recruitment of Ex Vivoâ€“expanded Embryonic Endothelial Progenitor Cells during Tumor Angiogenesis. The Journal of Experimental Medicine 2003;197:1755-65.

223. Ryzhov S, Solenkova NV, Goldstein AE, et al. Adenosine Receptor-Mediated Adhesion of Endothelial Progenitors to Cardiac Microvascular Endothelial Cells. Circ Res 2008;102:356-63.

224. Sackstein R, Merzaban JS, Cain DW, et al. Ex vivo glycan engineering of CD44 programs human multipotent mesenchymal stromal cell trafficking to bone. Nat Med 2008;14:181-7.

225. Wu Y, Ip JE, Huang J, et al. Essential role of ICAM-1/CD18 in mediating EPC recruitment, angiogenesis, and repair to the infarcted myocardium. Circ Res 2006;99:315-22.

226. Segers VF, Van Riet I, Andries LJ, et al. Mesenchymal stem cell adhesion to cardiac microvascular endothelium: activators and mechanisms. Am J Physiol Heart Circ Physiol 2006;290:H1370-7.

227. Bevilacqua MP, Nelson RM. Selectins. The Journal of Clinical Investigation 1993;91:379-87.

228. Chukwuemeka AO, Brown KA, Venn GE, Chambers DJ. Changes in P-Selectin Expression on Cardiac Microvessels in Blood-Perfused Rat Hearts Subjected to Ischemia-Reperfusion. Ann Thorac Surg 2005;79:204-11.

229. Ying SQ, Fang L, Xiang MX, Xu G, Shan J, Wang JA. Protective effects of magnesium against ischaemia-reperfusion injury through inhibition of P-selectin in rats. Clin Exp Pharmacol Physiol 2007;34:1234-9.

230. Weyrich AS, Buerke M, Albertine KH, Lefer AM. Time course of coronary vascular endothelial adhesion molecule expression during reperfusion of the ischemic feline myocardium. J Leukoc Biol 1995;57:45-55.

231. Weyrich AS, Ma XY, Lefer DJ, Albertine KH, Lefer AM. In vivo neutralization of P-selectin protects feline heart and endothelium in myocardial ischemia and reperfusion injury. The Journal of Clinical Investigation 1993;91:2620-9.

232. La Bonte LR, Davis-Gorman G, Stahl GL, McDonagh PF. Complement inhibition reduces injury in the type 2 diabetic heart following ischemia and reperfusion. American Journal of Physiology - Heart and Circulatory Physiology 2008;294:H1282-H90.

233. Zingarelli B, Salzman AL, Szabó C. Genetic Disruption of Poly (ADP-Ribose) Synthetase Inhibits the Expression of P-Selectin and Intercellular Adhesion Molecule-1 in Myocardial Ischemia/Reperfusion Injury. Circulation Research 1998;83:85-94.

234. Kukielka GL, Hawkins HK, Michael L, et al. Regulation of intercellular adhesion molecule-1 (ICAM-1) in ischemic and reperfused canine myocardium. The Journal of Clinical Investigation 1993;92:1504-16.

235. Bowden RA, Ding Z-M, Donnachie EM, et al. Role of Î±4 Integrin and VCAM-1 in CD18-Independent Neutrophil Migration Across Mouse Cardiac Endothelium. Circulation Research 2002;90:562-9.

236. Osborn L, Hession C, Tizard R, et al. Direct expression cloning of vascular cell adhesion molecule 1, a cytokine-induced endothelial protein that binds to lymphocytes. Cell 1989;59:1203-11.

237. Woodfin A, Reichel CA, Khandoga A, et al. JAM-A mediates neutrophil transmigration in a stimulus-specific manner in vivo: evidence for sequential roles for JAM-A and PECAM-1 in neutrophil transmigration. Blood 2007;110:1848-56.

238. Thomas R, Cheng Y, Yan J, et al. Upregulation of coronary endothelial P-selectin in a monkey heart ischemia reperfusion model. Journal of Molecular Histology 2010;41:277-87.

239. Frangogiannis NG, Smith CW, Entman ML. The inflammatory response in myocardial infarction. Cardiovascular Research 2002;53:31-47.

240. Sutherland FJ, Hearse DJ. The isolated blood and perfusion fluid perfused heart. Pharmacological Research 2000;41:613-27.

241. Meluzín J, Mayer J, Groch L, et al. Autologous transplantation of mononuclear bone marrow cells in patients with acute myocardial infarction: The effect of the dose of transplanted cells on myocardial function. American Heart Journal 2006;152:975.e9-.e15.

242. Houwen B. Blood Film Preparation and Staining Procedures. Laboratory Haematology 2000;6:1-7.

243. Cohen GM, Sun XM, Snowden RT, Dinsdale D, Skilleter DN. Key morphological features of apoptosis may occur in the absence of internucleosomal DNA fragmentation. Biochem J 1992;286 (Pt 2):331-4.

244. Kleeberger CA, Lyles RH, Margolick JB, Rinaldo CR, Phair JP, Giorgi JV. Viability and recovery of peripheral blood mononuclear cells cryopreserved for up to 12 years in a multicenter study. Clinical and diagnostic laboratory immunology 1999;6:14-9.

245. Shibata T, Naruse K, Kamiya H, et al. Transplantation of Bone Marrow-Derived Mesenchymal Stem Cells Improves Diabetic Polyneuropathy in Rats. Diabetes 2008;57:3099-107.

246. Mylotte LA, Duffy AM, Murphy M, et al. Metabolic Flexibility Permits Mesenchymal Stem Cell Survival in an Ischemic Environment. Stem Cells 2008;26:1325-36.

247. Neuhuber B, Gallo G, Howard L, Kostura L, Mackay A, Fischer I. Reevaluation of in vitro differentiation protocols for bone marrow stromal cells: Disruption of actin cytoskeleton induces rapid morphological changes and mimics neuronal phenotype. Journal of Neuroscience Research 2004;77:192-204.

248. Rodriguez JP, Gonzalez M, Rios S, Cambiazo V. Cytoskeletal organization of human mesenchymal stem cells (MSC) changes during their osteogenic differentiation. J Cell Biochem 2004;93:721-31.

249. Rousselle C, Barbier M, Comte V, et al. Innocuousness and intracellular distribution of PKH67: A fluorescent probe for cell proliferation assessment. In Vitro Cellular & Developmental Biology - Animal 2001;37:646-55.

250. Shujia J, Haider HK, Idris NM, Lu G, Ashraf M. Stable therapeutic effects of mesenchymal stem cell-based multiple gene delivery for cardiac repair. Cardiovascular Research 2008;77:525-33.

251. Funcke F, Hoyer H, Brenig F, et al. Characterisation of the interaction between circulating and in vitro cultivated endothelial progenitor cells and the endothelial barrier. Eur J Cell Biol 2007.

252. Huang RC, Yao K, Zou YZ, et al. [Long term follow-up on emergent intracoronary autologous bone marrow mononuclear cell transplantation for acute inferior-wall myocardial infarction]. Zhonghua Yi Xue Za Zhi 2006;86:1107-10.

253. Meyer GP, Wollert KC, Lotz J, et al. Intracoronary bone marrow cell transfer after myocardial infarction: eighteen months' follow-up data from the randomized, controlled BOOST (BOne marrOw transfer to enhance ST-elevation infarct regeneration) trial. Circulation 2006;113:1287-94.

254. Bell RM, Smith CCT, Yellon DM. Nitric oxide as a mediator of delayed pharmacological (A1 receptor triggered) preconditioning; is eNOS masquerading as iNOS? Cardiovascular Research 2002;53:405-13.

255. Hwang H, Arcidi JM, Hale SL, et al. Ranolazine as a Cardioplegia Additive Improves Recovery of Diastolic Function in Isolated Rat Hearts. Circulation 2009;120:S16-S21.

256. Nolan DJ, Ciarrocchi A, Mellick AS, et al. Bone marrow-derived endothelial progenitor cells are a major determinant of nascent tumor neovascularization. Genes & Development 2007;21:1546-58.

257. Meyer KD, Zhang H, Zhang L. Prenatal cocaine exposure abolished ischemic preconditioning-induced protection in adult male rat hearts: role of PKCÎµ. American Journal of Physiology - Heart and Circulatory Physiology 2009;296:H1566-H76.

258. Tani M, Neely JR. Role of intracellular Na+ in Ca2+ overload and depressed recovery of ventricular function of reperfused ischemic rat hearts. Possible involvement of H+-Na+ and Na+-Ca2+ exchange. Circ Res 1989;65:1045-56.

259. Brown DA, Aon MA, Akar FG, Liu T, Sorarrain N, O'Rourke B. Effects of 4'-chlorodiazepam on cellular excitation-contraction coupling and ischaemia-reperfusion injury in rabbit heart. Cardiovasc Res 2008;79:141-9.

260. Ytrehus K. The ischemic heart--experimental models. Pharmacol Res 2000;42:193-203.

261. Neely, Rovetto M, Whitmer J, Morgan H. Effects of ischemia on function and metabolism of the isolated working rat heart. American Journal of Physiology -- Legacy Content 1973;225:651-8.

262. Neely J, Whitmer J, Rovetto M. Effect of coronary blood flow on glycolytic flux and intracellular pH in isolated rat hearts. Circulation Research 1975;37:733-41.

263. Hu X, Wang J, Chen J, et al. Optimal temporal delivery of bone marrow mesenchymal stem cells in rats with myocardial infarction. Eur J Cardiothorac Surg 2007;31:438-43.

264. Eeckhout E, Kern MJ. The coronary no-reflow phenomenon: a review of mechanisms and therapies. European Heart Journal 2001;22:729-39.

265. Avkiran M, Curtis MJ. Independent dual perfusion of left and right coronary arteries in isolated rat hearts. American Journal of Physiology - Heart and Circulatory Physiology 1991;261:H2082-H90.

266. Assmus B, Tonn T, Seeger FH, et al. Red Blood Cell Contamination of the Final Cell Product Impairs the Efficacy of Autologous Bone Marrow Mononuclear Cell Therapy. Journal of the American College of Cardiology 2010;55:1385-94.

267. Assmus B, Fischer-Rasokat U, Honold J, et al. Transcoronary Transplantation of Functionally Competent BMCs Is Associated With a Decrease in Natriuretic Peptide Serum Levels and Improved Survival of Patients With Chronic Postinfarction Heart Failure: Results of the TOPCARE-CHD Registry. Circ Res 2007;100:1234-41.

268. Assmus B, Schachinger V, Teupe C, et al. Transplantation of Progenitor Cells and Regeneration Enhancement in Acute Myocardial Infarction (TOPCARE-AMI). Circulation 2002;106:3009-17.

269. de Leiris J, Harding DP, Pestre S. The isolated perfused rat heart: A model for studying myocardial hypoxia or ischaemia. Basic Research in Cardiology 1984;79:313-21.

270. Bassingthwaighte JB, Yipintsoi T, Harvey RB. Microvasculature of the dog left ventricular myocardium. Microvasc Res 1974;7:229-49.

271. Ono T, Shimohara Y, Okada K, Irino S. Scanning electron microscopic studies on microvascular architecture of human coronary vessels by corrosion casts: normal and focal necrosis. Scanning electron microscopy 1986:263-70.

272. Goebel S, Kuebler WM, Cornelissen AJ, Kuppe H, Pries AR, Habazettl H. In situ analysis of coronary terminal arteriole diameter responses: technical report of a new experimental model. Journal of vascular research 2003;40:442-8.

273. Woolf N. Animal models of myocardial ischaemia. Journal of clinical pathology Supplement (Royal College of Pathologists) 1977;11:53-8.

274. Bhakta S, Greco NJ, Finney MR, et al. The safety of autologous intracoronary stem cell injections in a porcine model of chronic myocardial ischemia. J Invasive Cardiol 2006;18:212-8.

275. Qi CM, Ma GS, Liu NF, et al. Transplantation of magnetically labeled mesenchymal stem cells improves cardiac function in a swine myocardial infarction model. Chin Med J 2008;121:544-50.

276. Ball RM, Bache RJ, Cobb FR, Greenfield JC, Jr. Regional myocardial blood flow during graded treadmill exercise in the dog. J Clin Invest 1975;55:43-9.

277. Domenech R, Hoffman J, Noble M, Saunders K, Henson J, Subijanto S. Total and Regional Coronary Blood Flow Measured by Radioactive Microspheres in Conscious and Anesthetized Dogs. Circulation Research 1969;25:581-96.

278. Carabello BA. Understanding Coronary Blood Flow. Circulation 2006;113:1721-2.

279. Toyota E, Ogasawara Y, Hiramatsu O, et al. Dynamics of flow velocities in endocardial and epicardial coronary arterioles. American Journal of Physiology - Heart and Circulatory Physiology 2005;288:H1598-H603.

280. Hoffman JIE. Transmural myocardial perfusion. Progress in Cardiovascular Diseases 1987;29:429-64.

281. Ziegelhoeffer T, Fernandez B, Kostin S, et al. Bone marrow-derived cells do not incorporate into the adult growing vasculature. Circulation Research 2004;94:230-8.

282. Prinzmetal M, Simkin B, et al. Studies on the coronary circulation; the collateral circulation of the normal human heart by coronary perfusion with radioactive erythrocytes and glass spheres. Am Heart J 1947;33:420-42.

283. Otsuru S, Hofmann TJ, Olson TS, Dominici M, Horwitz EM. Improved isolation and expansion of bone marrow mesenchymal stromal cells using a novel marrow filter device. Cytotherapy 2013;15:146-53.

284. Eppihimer MJ, Lipowsky HH. The Mean Filtration Pressure of Leukocyte Suspensions and Its Relation to the Passage of Leukocytes through Nuclepore Filters and Capillary Networks. Microcirculation 1994;1:237-50.